

https://dspace.org/

The antimalarial properties of thiosemicarbazone, chalcone, and nucleoside phosphonate derivatives

Moseley, Emma Jane

2013-03-04
http://hdl.handle.net/10539/12482

Downloaded from a DSpace repository. https://dspace.org/

THE ANTIMALARIAL PROPERTIES OF THIOSEMICARBAZONE, CHALCONE, AND NUCLEOSIDE PHOSPHONATE DERIVATIVES

Emma Jane Moseley

A dissertation submitted to the Faculty of Health Sciences, University of the Witwatersrand, Johannesburg, in fulfilment of the requirements for the degree of Master of Science in Medicine (Pharmacology)

Johannesburg, 2012

DECLARATION

I, Emma Jane Moseley, declare that this dissertation is my own work. It is being submitted for the degree of Master of Science in Medicine (Pharmacology) at the University of the Witwatersrand, Johannesburg. It has not been submitted before for any degree or examination at this or any other University.

Signed.....

On this the.....day of....., 2012.

DEDICATION

I dedicate this dissertation to my parents who always encouraged me to further my studies and supported me throughout.

ACKOWLEDGEMENTS

I would like to acknowledge Mr. Z Rogers, I will always be grateful to him for his patience and support throughout my studies. Thank you.

I would like to thank Mr. S-L Moseley for his helpful discussions during the course of my writing.

I am extremely grateful to my supervisor, Prof. R van Zyl, for the knowledge she shared with me and for the time, guidance and advice she contributed. I would like to thank my co-supervisor, Prof. I Havlik, for his help in the chemistry component of this study.

My sincere thanks to Mr. C-T Chen and Mr. H Motau for their assistance in the laboratory, their support, and for many an interesting discussion over a cup of coffee. My thanks also go to the Departmental staff for their advice and helpful discussions throughout my Msc.

I gratefully acknowledge Dr. S Lauterbach and Mr. K Naidoo (Department of Molecular Medicine and Haematology, University of the Witwatersrand) for their help with the flow cytometry.

For the financial support they provided me with I would like to sincerely thank the Belgium Technical Co-operation (Fellowship), the National Research Foundation (Scholarship), as well as the University of the Witwatersrand (Postgraduate scholarship, Postgraduate Merit Award and Faculty Research Committee Grant).

ABSTRACT

Plasmodium falciparum is responsible for ninety percent of malaria infections in sub-Saharan Africa, and the majority of malaria-related deaths, with antimalarial drugs failing at an alarming rate. To combat this deadly disease, not only are novel target-specific antimalarial drugs needed, but also a high-throughput method for the screening of compounds to replace standard methodologies.

A total of 112 novel compounds from three chemical classes were assessed for antimalarial activity against the chloroquine-sensitive 3D7 strain of *P. falciparum* using the [^{3}H]-hypoxanthine incorporation assay, and their haemolytic activity against healthy red blood cells determined. Lead compounds were examined for their effects on parasite morphology and parasitic development; as well as their pharmacological interactions when combined with standard antimalarial drugs. Antimalarial mechanisms of action were examined using the β-haematin inhibitory activity, 2,2-diphenyl-1-picrylhydrazyl (DPPH$^\bullet$) free-radical scavenging, and ferrous iron chelating activity assays. Using the DNA probe dihydroethidium, flow cytometry as a high-throughput drug screening method was validated against the [^{3}H]-hypoxanthine incorporation assay and assessed for its ability to determine the stage-specific activity of the compounds.

Of the three classes of compounds, the metronidazole-thiosemicarbazone analogues were the most active, 75% of the compounds inhibited parasite growth at IC_{50} values below 10 µM, whilst also exhibiting no haemolytic activity. The most active of which, 4-(2-Chlorobenzyl)-1-(4-(2-(1-(2-hydroxyethyl)-5-nitro-1*H*-imidazol-2-yl)vinyl)benzylidene)-thio-semi-carbazide (compound Y-3) (IC_{50} value: 2.83 ± 0.20 µM) was also a potent inhibitor of β-haematin formation (IC_{50} value: 19.08 ± 2.37 µM), proving to be more active than chloroquine (IC_{50} value: 29.64 ± 3.35 µM). Similarly, metronidazole-thiosemicarbazones analogues were potent scavengers of the free-radical of DPPH$^\bullet$, with the activity of 1-(4-(2-(1-(2-Hydroxyethyl)-5-nitro-1*H*-imidazol-2-yl)vinyl)benzylidene)-4-benzyl-4-methyl-thio-semi-carbazide (compound Y-8) (IC_{50} value: 21.98 ± 0.56 µM), comparable to that of the standard, ascorbic acid (IC_{50} value: 19.31 ± 2.62 µM). When combined with quinine and dihydroartemisinin, compound Y-3 produced an additive pharmacological interaction.

Seventy one percent of the chloroquinoline-chalcones tested had IC_{50} values below 100 µM, with (E)-3-(2-chloro-7-methylquinoline-3yl)-1-(pyridine-2yl)prop-2-en-1-one

(compound F-13) the most active (IC_{50} value: 31.31 ± 0.87 µM). None of the compounds displayed any notable activity in the antimalarial mechanisms of action tested for, whilst also resulting in no red blood cell toxicity. When combined with quinine, compound F-13 exhibited an additive interaction.

The nucleoside phosphonates, phosphonic acids and purine/pyrimidine derivatives exhibited disappointing antimalarial activity, with only 21% of the compounds inhibiting parasite growth with IC_{50} values below 100 µM, with compound DR-4850 (currently under patent) the most potent (IC_{50} value: 13.35 ± 0.38 µM). None of the compounds resulted in any red blood cell lysis, with the exception of compound DR-4914B (currently under patent) (50.20 ± 3.35% haemolysis at 100 µM). Some nucleoside derivatives were potent inhibitors of β-haematin formation, with Hexadecyloxypropyl uridin-5'-yl 2-([3*R*,4*R*]-3,4-dihydroxypyrrolidin-1-*N*-yl)ethylphosphonate (compound DR-4137) (IC_{50} value: 8.29 ± 1.11 µM) 3.6-fold more active than chloroquine, although this did not appear to be the primary antimalarial mechanism of action of this class of compounds. Combination studies with quinine produced an additive interaction, whilst combination studies with the nucleoside transporter inhibitor dipyridamole produced additive-antagonistic interactions.

In conclusion, this study examined a wide variety of compounds and identified lead compounds, which following structural modifications may produce potent antimalarial drugs.

CONFERENCES AND PRESENTATIONS

Moseley, E.J., van Zyl, R.L., Abid, M., *et al*. 2009.

The Antimalarial Properties of Metronidazole Thiosemicarbazone Analogues.

Poster presentation: The 5th International Conference On Pharmaceutical And Pharmacological Sciences, North-West University, Potchefstroom, South Africa, 23-26 September 2009 (Abstract in Appendix A1).

Moseley, E.J., van Zyl, R.L., Abid, M., *et al*. 2010.

The Antimalarial Properties of Metronidazole Thiosemicarbazone Analogues.

Basic Clin Pharmacol Toxicol 107 (Suppl 1), 472.

Poster presentation: WorldPharma 2010, the 16th World Congress of Basic and Clinical Pharmacology, Copenhagen, Denmark, 17-23 July 2010 (Abstract in Appendix A2).

Moseley, E.J., van Zyl, R.L., Abid, M., *et al*. 2010.

The Antimalarial Properties of Metronidazole Thiosemicarbazone Analogues II.

Poster presentation: The University of the Witwatersrand Faculty of Health Sciences Research Day, 22 September 2010 (Abstract in Appendix A3).

Moseley, E.J., van Zyl, R.L., Abid, M., *et al*. 2010.

The Antimalarial Properties of Metronidazole Thiosemicarbazone Analogues II.

Poster presentation: The 3rd Cross Faculty Postgraduate Symposium, University of the Witwatersrand, 26-29 October 2010 (Abstract in Appendix A4).

PUBLICATIONS

(Generated from this study)

Hayat, F., Moseley, E., Salahuddin, A., *et al*. 2011. Antiprotozoal activity of chloroquinoline based chalcones. Eur J Med Chem 46(5), 1897-1905 (Publication in Appendix A5).

In preparation:

1) Title: The antimalarial properties of metronidazole-thiosemicarbazone analogues.
   Journal: Bioorg Med Chem Lett.

2) Title: The antimalarial activity of novel nucleoside phosphonates, phosphonic acids and purine/pyrimidine derivatives.
   Journal: Bioorg Med Chem.

TABLE OF CONTENTS

		Page
DECLARATION		II
DEDICATION		III
ACKNOWLEDGEMENTS		IV
ABSTRACT		V
CONFERENCES AND PRESENTATIONS		VII
PUBLICATIONS		VIII
TABLE OF CONTENTS		IX
LIST OF FIGURES		XVII
LIST OF TABLES		XXIII
ABBREVIATIONS, ACRONYMS, AND SYMBOLS		XXVI
CHAPTER 1:	**INTRODUCTION**	**1**
1.1	The global distribution and impact of malaria	1
1.2	Malaria life cycle and transmission	2
1.2.1	The mosquito vector and liver stages	2
1.2.1.1	The mosquito vector	2
1.2.1.2	The liver stage	3
1.2.1.3	The asexual erythrocytic stage of *P. falciparum*	4
1.2.1.4	The sexual erythrocytic stage of *P. falciparum*	9
1.3	Antimalarial prophylaxis and treatment	10

1.3.1 Quinolines..... 12

1.3.1.1 Efficacy and side effects..... 14

1.3.2 Antifolates..... 15

1.3.2.1 Combination therapies..... 16

1.3.3 Napthoquinones..... 17

1.3.4 Antibacterials..... 17

1.3.4.1 Indications and side effects..... 18

1.3.5 Artemisinin and its derivatives (endoperoxides)..... 19

1.3.5.1 Combination therapies and side effects..... 20

1.4 Antimalarial drug resistance..... 21

1.5 The future of malarial prevention and treatment..... 22

1.6 Study objectives..... 25

CHAPTER 2: MATERIALS AND METHODS..... 26

2.1 Protocol for the *in vitro* culturing of *P. falciparum*..... 26

2.1.1 Culture maintenance..... 26

2.1.2 Synchronisation of the culture..... 28

2.1.3 Preparation of incomplete experimental and culture media..... 28

2.1.4 Preparation of sodium bicarbonate and sorbitol solutions..... 28

2.1.5 Preparation of human plasma..... 29

2.1.6 Preparation of complete experimental and culture media..... 29

2.1.7 Preparation of phosphate buffered saline..... 29

2.1.8 Preparation of erythrocytes..... 29

2.2 Antimalarial activity..... 30

2.2.1 Preparation of the test solutions..... 30

2.2.2 The [^{3}H]-hypoxanthine incorporation assay..... 30

2.2.2.1 Experimental protocol..... 30

2.2.2.2 Data analysis..... 32

2.2.2.3 Combination studies..... 33

2.2.3 The use of flow cytometry to assess *in vitro* parasite growth..... 34

2.2.3.1 Method development..... 36

2.2.3.1.1 Thiazole orange as a potential fluorochrome..... 36

2.2.3.1.2 Propidium iodide as a potential fluorochrome..... 42

2.2.3.1.3 Hydroethidine as a potential fluorochrome..... 44

2.2.3.2 Method optimisation..... 49

2.2.3.3 Experimental protocol for the assessment of total parasitaemia..... 51

2.2.3.4 Final experimental protocol used for the assessment of the stage-specific and morphological effects of the compounds on *P. falciparum*..... 54

2.2.3.5 Data analysis..... 55

2.3 Antimalarial mechanisms of action..... 55

2.3.1 β-haematin inhibitory activity assay..... 55

2.3.1.1 Preparation of the solutions..... 56

2.3.1.2 Experimental protocol..... 56

2.3.1.3 Data analysis..... 57

2.3.2 Anti-oxidant activities..... 58

2.3.2.1 The 2,2-diphenyl-1-picrylhydrazyl free-radical scavenging assay..... 58

2.3.2.1.1 Preparation of the solutions..... 59

2.3.2.1.2 Experimental protocol..... 59

2.3.2.1.3 Data analysis..... 60

2.3.2.2 Iron chelating activity..... 60

2.3.2.2.1 Preparation of the solutions..... 60

2.3.2.2.2 Experimental protocol..... 61

2.3.2.2.3 Data analysis..... 61

2.4 Red blood cell toxicity assay..... 62

2.4.1 Preparation of the solutions..... 62

2.4.2 Experimental protocol..... 62

2.4.3 Data analysis..... 63

CHAPTER 3: THE ANTIMALARIAL PROPERTIES OF METRONIDAZOLE-THIOSEMICARBAZONE ANALOGUES..... 65

3.1 Introduction..... 65

3.1.1 Metronidazole..... 65

3.1.2 Thiosemicarbazones..... 66

3.2 Materials and methods..... 67

3.2.1 Chemical synthesis and structural verification..... 67

3.2.2 Pharmacological evaluation..... 68

3.3 Results..... 69

3.3.1 *In vitro* antimalarial and haemolytic activity..... 69

3.3.2 Combination studies..... 72

3.3.3 Morphological and stage-specific effects of compound Y-3..... 73

3.3.4 Antimalarial mechanisms of action..... 76

3.3.4.1 Inhibition of β-haematin formation..... 76

3.3.4.2 Free-radical scavenging activity..... 77

3.3.4.3 Iron chelation activity..... 78

3.4 Discussion..... 79

3.4.1 Antimalarial activity of metronidazole-thiosemicarbazone analogues.. 79

3.4.2 The effect of methodology on antimalarial evaluation..... 81

3.4.3 The antimalarial activity of metronidazole..... 83

3.4.4 Possible mechanisms of action of the metronidazole-thiosemicarbazone analogues..... 84

CHAPTER 4: THE ANTIMALARIAL PROPERTIES OF CHLOROQUINOLINE-CHALCONES..... 95

4.1 Introduction..... 95

4.1.1 Chalcones..... 95

4.1.2 Quinolines..... 96

4.2 Materials and methods..... 100

4.2.1 Chemical synthesis and structural verification..... 100

4.2.2 Pharmacological evaluation..... 102

4.3 Results..... 102

4.3.1 *In vitro* antimalarial and haemolytic activity..... 102

4.3.2 Combination study..... 104

4.3.3 Morphological and stage-specific effects of compound F-13..... 105

4.3.4 Antimalarial mechanisms of action..... 108

4.3.4.1 Inhibition of β-haematin formation..... 108

4.3.4.2 $DPPH^{\bullet}$ free-radical scavenging activity..... 108

4.3.4.3 Iron chelating activity..... 109

4.4 Discussion..... 109

CHAPTER 5: THE ANTIMALARIAL PROPERTIES OF NUCLEOSIDE PHOSPHONATES, PHOSPHONIC ACIDS AND PURINE/PYRIMIDINE DERIVATIVES..... 122

5.1 Introduction..... 122

5.1.1 Purine uptake..... 122

5.1.2 Purine salvage and metabolism..... 124

5.1.3 *De novo* pyrimidine synthesis..... 126

5.1.3.1 The role of the folate pathway in thymidine synthesis..... 128

5.1.4 Therapeutic targets..... 130

5.1.4.1 The parasitic cell division cycle as a drug target..... 133

5.2 Materials and methods..... 132

5.2.1 Test compounds..... 133

5.2.2 Pharmacological evaluation..... 137

5.2.2.1 General methodology..... 137

5.2.2.2 Modified tritiated hypoxanthine incorporation assay..... 138

5.2.2.3 Combination studies with dipyridamole..... 139

5.3 Results..... 140

5.3.1 *In vitro* antimalarial activity..... 140

5.3.1.1 Antimalarial activity over a double parasitic life cycle..... 153

5.3.1.2 The effect of methodology on antimalarial evaluation..... 154

5.3.2 *In vitro* haemolytic activity..... 155

5.3.3 Combination studies..... 156

5.3.4 Morphological and stage-specific effects of compound DR-4463..... 157

5.3.5 Antimalarial mechanisms of action..... 160

5.4 Discussion..... 162

CHAPTER 6: CONCLUSIONS AND RECOMMENDATIONS..... 185

6.1 Conclusions..... 185

6.2 Recommendations..... 188

6.2.1 Metronidazole-thiosemicarbazone analogues..... 188

6.2.2 Chloroquinoline-chalcones..... 188

6.2.3 Nucleoside phosphonates, phosphonic acids and purine/pyrimidine derivatives..... 189

6.2.4 Flow cytometry..... 189

REFERENCES..... 191

APPENDICES..... 218

Appendix A Conference presentations and publications..... 218

Appendix B Biosafety and ethical clearances..... 233

Appendix C Sum of the fractional inhibitory concentrations (FIC_{50}) for combination studies with compounds Y-3 and Y-7..... 235

Appendix D Sum of the fractional inhibitory concentrations (FIC_{50}) for combination studies with compound F-13 and quinine..... 241

Appendix E Sum of the fractional inhibitory concentrations (FIC_{50}) for combination studies with compounds DR-4463 and D1293-S..... 243

LIST OF FIGURES

Page

Figure 1.1 The global distribution and disease control status of malaria..... 1

Figure 1.2 The developmental stages of the malaria parasite, and potential targets for immune system attack..... 3

Figure 1.3 Haemoglobin digestion within the food vacuole of the malaria parasite..... 5

Figure 1.4 Sources of reactive oxygen species and anti-oxidant systems in *P. falciparum*..... 7

Figure 1.5 Internal structure of a *P. falciparum* late schizont, depicting parasite and red blood cell structure..... 9

Figure 1.6 Chemical structures of the quinoline family of antimalarials..... 13

Figure 1.7 Chemical structures of the antifolates..... 15

Figure 1.8 Chemical structure of atovaquone, a napthoquinone..... 17

Figure 1.9 Chemical structures of doxycycline and clindamycin..... 18

Figure 1.10 Chemical structures of artemisinin and its semi-synthetic derivatives..... 19

Figure 1.11 Drug targets within *P. falciparum*..... 24

Figure 2.1 The various intraerythrocytic developmental stages of *P. falciparum*..... 27

Figure 2.2 Microtitre plate layout used for IC_{50} value determination in the [^{3}H]-hypoxanthine incorporation assay..... 31

Figure 2.3 The cut-off points for possible drug interactions between quinine/dihydroartemisinin and a test compound..... 34

Figure 2.4 Flow cytometric analysis of a fixed sample of late rings/early trophozoites at a 5% haematocrit 8% parasitaemia, stained with thiazole orange..... 38

Figure 2.5 Histogram of the maximal fluorescence of thiazole orange (FL1-H) versus cell count of an unfixed sample of uninfected erythrocytes, adjusted to a 5% haematocrit..... 40

Figure 2.6 Flow cytometric analysis of samples of fixed trophozoites (a and b) and unfixed rings and trophozoites (c and d), at a 5% hematocrit 8% parasitaemia, stained with thiazole orange, and read on a BC FC 500 flow cytometer..... 41

Figure 2.7 Flow cytometric analysis of a sample containing ring-, trophozoite- and schizont-stage parasites, at a 5% haematocrit 8% parasitaemia, stained with propidium iodide..... 43

Figure 2.8 The oxidation of hydroethidine by parasitic dehydrogenases to form ethidium which, upon intercalation into parasitic DNA, fluoresces red..... 44

Figure 2.9 Flow cytometric analysis of an unfixed parasite sample of early rings (a-c) and a fixed parasite sample of late rings and early trophozoites (d-f), at a 5% haematocrit 2% parasitaemia, stained with dihydroethidium..... 46

Figure 2.10 Histograms of the maximal fluorescence of dihydroethidium (FL2-H) versus cell count of samples of trophozoites (a) and trophozoites and schizonts (b) at a 5% haematocrit and 2% parasitaemia, stained with dihydroethidium..... 47

Figure 2.11 An overlay of flow cytometric histograms depicting the increasing fluorescent intensity of dihydrethidium (FL2-H) in samples of ring-, trophozoite-, and trophozoite/schizont-staged parasites, at a 5% haematocrit and 2% parasitaemia..... 48

Figure 2.12 An overlay of flow cytometric histograms of samples of uninfected erythrocytes (2% haematocrit), ring-, trophozoite- and schizont-staged parasites prepared to a 2% haematocrit and 2% parasitaemia..... 50

Figure 2.13 The final protocol used for the determination of overall % parasitaemia, as well as parasite stage and % parasites present in each stage, when stained with dihydroethidium..... 50

Figure 2.14 Flow cytometric histogram overlays of the cell count versus the maximal fluorescence of dihydroethidium (FL2-H) of samples treated with varying concentrations of quinine, following a 48 hour incubation period..... 53

Figure 2.15 Formation of β-haematin crystals from haemin..... 57

Figure 2.16 The conversion of $DPPH^{\bullet}$ to DPPH-H by the donation of a hydrogen atom..... 59

Figure 3.1 The chemical structure of metronidazole (a) and the basic thiosemicarbazone structure (b)..... 65

Figure 3.2 The synthesis of metronidazole-thiosemicarbazone analogues..... 68

Figure 3.3 Log sigmoid dose-response curves of compound Y-3 compared to quinine and dihydroartemisinin..... 70

Figure 3.4 The additive pharmacological interactions between compounds Y-3 and Y-7 when combined with quinine and dihydroartemisinin..... 73

Figure 3.5 The effects of compound Y-3 and quinine at their IC_{50} (12μM) and IC_{90} values (200nM), respectively, on parasite morphology and development..... 74

Figure 3.6 The effects of compound Y-3 (black line) and quinine (blue line) at their IC_{50} (12µM; left) and IC_{90} values (200nM; right), respectively, on parasite development compared to the untreated control (red line)..... 75

Figure 3.7 The inhibitory activities of metronidazole-thiosemicarbazone analogues and antimalarial reference agents on parasite growth (lighter blue bar) and β-haematin formation (darker blue bar)..... 77

Figure 3.8 The chemical structures of thiosemicarbazones previously assessed for various pharmacological activities..... 80

Figure 3.9 The activation of metronidazole in the hydrogenosome of the trichomonad protozoa..... 83

Figure 3.10 The correlation between antimalarial and β-haematin inhibitory activity of the metronidazole-thiosemicarbazone analogues..... 85

Figure 3.11 Proposed structure-activity relationships for the antimalarial and β-haematin inhibitory activities of chloroquine..... 86

Figure 3.12 The proposed mechanism of action of chloroquine..... 86

Figure 3.13 The general structure of the metronidazole-thiosemicarbazone analogues, indicating the donor groups capable of chelating metals..... 88

Figure 3.14 The chemical structure of N, N-diethyldithiocarbamate..... 89

Figure 4.1 The basic structure of a) a chalcone and b) a quinoline..... 95

Figure 4.2 Mechanisms of chloroquine-resistance in *P.falciparum*..... 98

Figure 4.3 The synthesis of chloroquinoline-chalcones (1-14)..... 101

Figure 4.4 Log sigmoid dose-response curves of compound F-14, chloroquine and quinine..... 102

Figure 4.5 The additive pharmacological interaction between compound F-13 and quinine..... 105

Figure 4.6 The effects of compound F-13 at its IC_{50} value (70µM) on parasite morphology and development..... 106

Figure 4.7 Flow cytometric analysis depicting the effects of compound F-13 at its IC_{50} value (70µM) on parasite development..... 107

Figure 4.8 The effects of compound F-13 at 200µM (IC_{90} value) on parasite growth and development..... 108

Figure 4.9 Quinoline-chalcones previously assessed for antimalarial activity..... 111

Figure 4.10 The catabolism of haemoglobin in the food vacuole of *P. falciparum*..... 115

Figure 4.11 The proposed interaction of a chalcone with the histidine residue at the active site of a malarial cysteine protease..... 116

Figure 4.12 Proposed mechanisms of action of chloroquine..... 118

Figure 5.1 Purine salvage pathways in *P. falciparum*..... 125

Figure 5.2 The *de novo* synthesis of pyrimidines in *Plasmodium falciparum*..... 127

Figure 5.3 The folate pathway of *P. falciparum* (a) and its role in the thymidylate cycle (b)..... 129

Figure 5.4 One of the reactions catalysed by *Pf*HGXPRT..... 131

Figure 5.5 Antimalarial activity of compounds DR-4850 and DR-4463 compared to quinine..... 141

Figure 5.6 The improved antimalarial activity of compounds DR-4463, DR-3876, DR-4558 and DR-3892 over a double parasitic life cycle..... 154

Figure 5.7 Isobolograms depicting the pharmacological interactions of DR-4463 in combination with quinine (a), as well as DR-4463 (b) and D1293-S (c) in combination with dipyridamole..... 156

Figure 5.8 The effects of compound DR-4463 at the IC_{50} value (20µM) on parasite morphology and development..... 158

Figure 5.9 Flow cytometric analysis depicting the effects of compound DR-4463, at the IC_{50} value (20 µM), on parasite development..... 159

Figure 5.10 Active compounds of the Mickey Mouse, PyrroPME and pyrrolidine nucleotide groups..... 162

Figure 5.11 The general structure of the Lipophosphonoxin group of compounds..... 164

Figure 5.12 The chemical structure of a) N^6-diphenylethyl-5'-phenyl-carboxamidoadenosine and b) compound D1293-S..... 171

Figure 5.13 The invasion of a red blood cell by a merozoite..... 173

Figure 5.14 The chemical structures of tubercidin (a) 9-deazahypoxanthine (b) and immucillin-H (c), showing where the base was modified..... 176

Figure 5.15 The inhibitory activities of compounds from the Lipophosphonate (DR-4137, DR-4458, DR-4459, DR-4463) Nucleoside Lipophosphonate (DR-3621) and Mickey Mouse groups (DR-4598A)..... 179

Figure 5.16 Nucleoside phosphonic acids previously assessed for antimalarial activity..... 181

Figure 5.17 The ideal pharmacophore for inhibition of *Pf*mrk..... 182

Figure 5.18 The ideal pharmacophore of an orotidine-5'-monophosphate decarboxylase inhibitor..... 183

LIST OF TABLES

		Page
Table 2.1:	A comparison of the overall % parasitaemia obtained from flow cytometric and microscopic analysis of samples prepared to an 8, 4 and 2% parasitaemia and stained with dihydroethidium.....	48
Table 3.1:	The metronidazole-thiosemicarbazone analogues evaluated for antimalarial activity.....	69
Table 3.2:	The *in vitro* antimalarial activity, as determined by the [^{3}H]-hypoxanthine incorporation assay (1% haematocrit and 0.5% parasitaemia) and haemolytic effects of metronidazole-thiosemicarbazone analogues and reference agents.....	71
Table 3.3:	Comparison of the IC_{50} values and % inhibition of parasite growth at a 2% haematocrit and 2% parasitaemia, as determined by the [^{3}H]-hypoxanthine incorporation assay and flow cytometric analysis.....	72
Table 3.4:	The free-radical scavenging and iron chelating activity of select metronidazole-thiosemicarbazone analogues.....	78
Table 4.1:	The chloroquinoline-chalcones evaluated for antimalarial activity.....	102
Table 4.2:	The *in vitro* antimalarial (1% haematocrit, 0.5% parasitaemia) and haemolytic activity of chloroquinoline-chalcones and positive control...	104
Table 4.3:	The β-haematin inhibitory, free-radical scavenging, and Fe(II) chelating activity of the compounds.....	110
Table 5.1:	The chemical names and codes of the Phosphonoxin group, as well as the (nucleo)base present.....	134
Table 5.2:	The chemical names and codes of the Nucleoside Lipophosphonate group, as well as the (nucleo)base present.....	134

Table 5.3: The chemical names and codes of the Lipophosphonoxin group, as well as the (nucleo)base present..... 135

Table 5.4: The chemical names and codes of the PyrroPME group, as well as the (nucleo)base present..... 135

Table 5.5: The chemical names and codes of the Mickey Mouse group, as well as the (nucleo)base present..... 136

Table 5.6: The chemical names and codes of the Pyrrolidine nucleotide group, as well as the (nucleo)base present..... 136

Table 5.7: The chemical names and codes of the Piperidine nucleoside (K366-DR-4290B) and nucleotide (K423-K416) groups, as well as the (nucleo)base present..... 137

Table 5.8: The chemical names and codes of the Aza sugars (K568 and K537), U/T miscellaneous nucleosides (K469-K545) and Miscellaneous (DR-3227-K580) groups, as well as the (nucleo)base present..... 138

Table 5.9: Ratios of dipyridamole to the test compounds used to determine pharmacological interactions in the combination study..... 140

Table 5.10: The *in vitro* antimalarial (1% haematocrit, 0.5% parasitaemia) and haemolytic activity of the Nucleoside Lipophosphonate group of compounds..... 142

Table 5.11: The *in vitro* antimalarial (1% haematocrit, 0.5% parasitaemia) and haemolytic activity of the Lipophosphonoxin group of compounds..... 142

Table 5.12: The *in vitro* antimalarial (1% haematocrit, 0.5% parasitaemia) and haemolytic activity of the PyrroPME group of compounds..... 144

Table 5.13: The *in vitro* antimalarial (1% haematocrit, 0.5% parasitaemia) and haemolytic activity of the Mickey Mouse group of compounds..... 145

Table 5.14: The *in vitro* antimalarial (1% haematocrit, 0.5% parasitaemia) and haemolytic activity of the Pyrrolidine nucleotide group of compound.... 147

Table 5.15: The *in vitro* antimalarial (1% haematocrit, 0.5% parasitaemia) and haemolytic activity of the Piperidine nucleoside (K366-DR-4290B) and nucleotide (K423-K416) group of compounds..... 148

Table 5.16: The *in vitro* antimalarial (1% haematocrit, 0.5% parasitaemia) and haemolytic activity of the Aza sugars (K568 and K537), U/T miscellaneous nucleosides (K469-K545) and Miscellaneous (DR-3227-K580) group of compounds..... 150

Table 5.17: The *in vitro* antimalarial (1% haematocrit, 0.5% parasitaemia) and haemolytic activity of the Phosphonoxin group of compounds..... 152

Table 5.18: A comparison of the IC_{50} values and % parasite growth inhibitions, at a 2% haematocrit and 2% parasitaemia, obtained from the [^{3}H]-hypoxanthine incorporation assay and flow cytometry..... 155

Table 5.19: The β-haematin inhibitory, free-radical scavenging, and iron chelating activity of select compounds..... 161

Table 5.20: The compounds tested for cytotoxicity..... 169

ABBREVIATIONS, ACRONYMS AND SYMBOLS

ACTs: artemisinin combination therapies	ADP: adenosine diphosphate
AMP: adenosine monophosphate	ANPs: acyclic nucleoside phosphonates
AT: adenine-thymine	ATP: adenosine triphosphate
AU: adenine-uracil	AZT: 3'-azido-2',3'-deoxythymidine
BC: Beckman Coulter Inc.	BD: Becton, Dickinson and Company
BHIA: β-haematin inhibitory activity assay	CDK: cyclin-dependant kinase
cm^3: centimetre cubed	C^n: refers to a carbon in the n^{th} position of a chemical structure
CNT: concentrative nucleoside transporters	CO_2: carbon dioxide
CTP: cytidine triphosphate	°C: degrees Celsius
DDT: dichlorodiphenyltrichloroethane	DHFR: dihydrofolate reductase
DHPS: dihydropteroate synthase	DMSO: dimethyl sulfoxide
DNA: deoxyribosenucleic acid	$DPPH^{\bullet}$: 2,2-diphenyl-1-picrylhydrazyl free-radical
dTMP: deoxythymidine 5'-monophosphate	dTTP: deoxythymidine 5'-triphosphate
dUMP: deoxyuridine 5'-monophosphate	dUTP: deoxyuridine 5'-triphosphate
E^+: ethidium cation	EDTA: ethylenediaminetetraacetic acid
ENT: equilibrative nucleoside transporter	FIC_{50}: fractional IC_{50} value
FL1-H: maximal fluorescent intensity in the FL1 channel	FL2-H: maximal fluorescent intensity in the FL2 channel
FSC-H: mean forward scatter height	g: gram

GDP: guanosine diphosphate	GMP: guanosine monophosphate
GSH: glutathione	GTP: guanosine triphosphate
HEPES: 4-(2-hydroxyethyl)piperazine-1-ethanesulfonic acid	HGPRT: hypoxanthine-guanine phosphoribosyltransferase
HIV: human immunodeficiency virus	HPLC: high-performance liquid chromatography
IC: inhibitory concentration	IMP: inosine monophosphate
KCl: potassium chloride	kg: kilogram
KH_2PO_4: potassium phosphate monobasic	m^2: meter squared
µl: microliter	µm: micrometer
µM: micromolar	mg: milligram
ml: millilitre	mM: millimolar
mV: millivolt	M: molar
n: number of experimental repeats performed	N_2: nitrogen
NaCl: sodium chloride	$NADP^+$: nicotinamide adenine dinucleotide phosphate
$Na_2HPO_4.2H_2O$: disodium hydrogen phosphate dehydrate	NaOH: sodium hydroxide
NBMPR: 6-[(4-nitrobenzyl)thio]-9-β-D-ribofuranosyl purine	nm: nanometer
nM: nanomolar	N^n: refers to a nitrogen in the n^{th} position on a chemical structure
O_2: oxygen	OMP: orotodine monophosphate

ρABA: ρ-aminobenzoic acid	PBS: phosphate buffered saline
P. falciparum: *Plasmodium falciparum*	*Pf*ATP6*:* calcium-dependant ATPase of *Plasmodium falciparum*
*Pf*CRT: *Plasmodium falciparum* chloroquine resistance transporter	*Pf*ENT1: *Plasmodium falciparum* equilibrative nucleoside transporter 1
*Pf*HGXPRT: *Plasmodium falciparum* hypoxanthine-guanine-xanthine phosphoribosyltransferase	*Pf*HRPII: *Plasmodium falciparum* histidine-rich protein-II
PFO: pyruvate-ferrodoxin oxidoreductase	*pfmdr* 1: *Plasmodium falciparum* multi-drug resistance transporter gene
*Pf*mrk: *Plasmodium falciparum* MO15-related kinase	RNA: ribonucleic acid
ROS: reactive oxygen species	rpm: revolutions per minute
RPMI: Roswell Park Memorial Institute	rRNA: ribosomal ribonucleic acid
((S)-HPMPA): (S)-(3-hydroxy-2-phosphonylmethoxy-propyl)adenine	SODs: superoxide dismutases
SP: sulphadoxine-pyrimethamine	SSC-H: mean side scatter height
ΣFIC: sum of fractional IC_{50} values	TRIS: (hydroxymethyl)aminomethane
TUNEL: terminal deoxynucleotidyl transferase dUTP nick end labelling	UMP: uridine monophosphate
UTP: uridine triphosphate	w/v: weight per volume
WHO: World Health Organisation	XMP: xanthosine monophosphate

CHAPTER 1: INTRODUCTION

1.1 The global distribution and impact of malaria

Malaria continues to be one of the greatest infectious diseases ever known, placing approximately half of the worlds' population, in over 100 countries, at risk of infection (Figure 1.1) (www.rollbackmalaria.org, 2011; WHO, 2011).

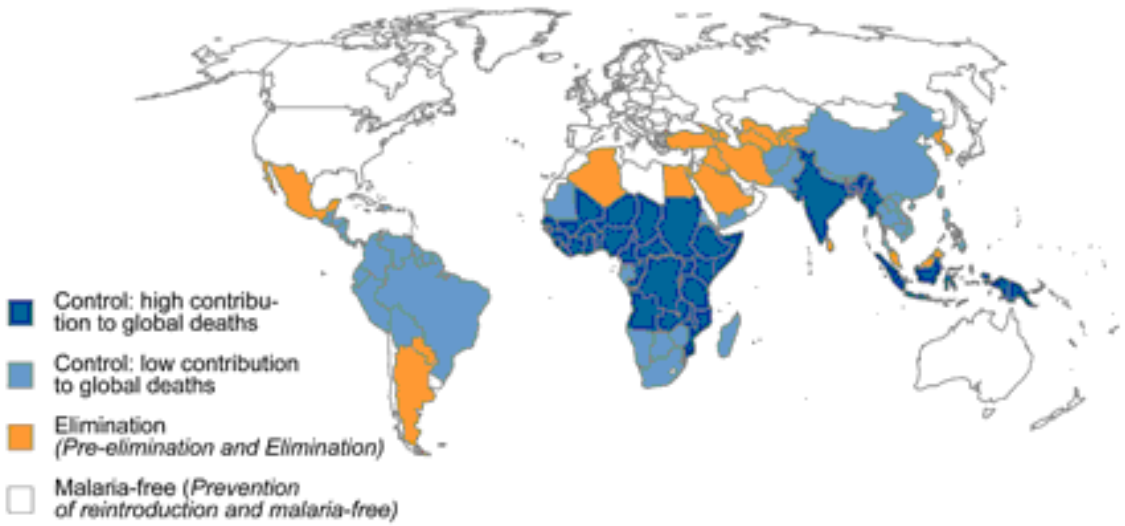


Figure 1.1: The global distribution and disease control status of malaria (www.rollbackmalaria.org, 2009).

The World Health Organisation (WHO) estimated the number of malaria cases to be 216 million in 2010 (WHO, 2011). Africa bears the greatest burden of malaria infections with transmission reported in all sub-Saharan African countries (except Lesotho) (National Department of Health, 2010). Preventative programmes have proven to be highly successful in reducing transmission in South Africa. Once endemic to eastern and low lying northern districts of the country, malaria is now limited to areas of Limpopo, Mpumalanga and northern Kwazulu Natal, with occasional cases reported along the Molopo and Orange rivers in the North West and Northern Cape provinces (National Department of Health, 2009). In spite of control methods being instituted, a general upward trend in mortality and morbidity on the African continent has been observed since the 1970's. This is possibly due to the increased resistance of the mosquito vector to insecticides, as well as the

widespread and improper use of antimalarials (Sanchez *et al*., 2010; WHO, 2010b). Coupled with the enormous humanitarian burden of the disease, is the economic cost of malaria which has resulted in a loss of approximately 12 billion dollars, or 1.3% of the gross domestic product of the African continent per year (www.rollbackmalaria.org, 2008).

1.2 Malaria life cycle and transmission

1.2.1 The mosquito vector and liver stages

Malaria is an infectious disease caused by four species of the *Plasmodium* parasite, namely: *Plasmodium falciparum*, *P. malariae*, *P. ovale* and *P. vivax* (National Department of Health, 2009). Of the four species, *P. falciparum* accounts for over 90% of infections in sub-Saharan Africa and the majority of deaths (White, 2004; Kaur *et al*., 2009). Malaria is transmitted to the human host via the bite of an infected female of the *Anopheles* mosquito. The *Anopheline* family contains all species known to transmit malaria, with at least three species responsible for malaria transmission in Southern Africa (National Department of Health, 2009). The parasite has a complex life cycle which takes place in the mosquito vector and both the liver and red blood cells of the human host (Figure 1.2) (Bozdech *et al*., 2003; WHO, 2010a).

1.2.1.1 The mosquito vector

The sexual phase of the parasite's life cycle is initiated when the female *Anopheles* mosquito ingests a blood meal from an infected person, during which the mosquito ingests both female and male gametocytes (macrogametocytes and microgametocytes, respectively) (Figure 1.2A) (Khan *et al*., 2005; National Department of Health, 2009). In the midgut of the mosquito the microgametocyte emerges from the red blood cell and produces flagella, allowing each microgametocyte to seek out and fertilise a macrogametocyte, forming a zygote or ookinete (Figure 1.2B) (Khan *et al*., 2005). Once attached to the midgut, the oocyst produces thousands of daughter cells, known as sporozoites, which when released migrate to the salivary glands of the mosquito (Figure 1.2C) (Greenwood *et al*., 2008; National Department of Health, 2009; WHO, 2010a). The sexual phase within the mosquito takes between 1-3 weeks and is dependent on the species of *Plasmodia* carried by the mosquito, as well as the humidity and temperature of

the external environment (Greenwood *et al*., 2008; National Department of Health, 2009; WHO, 2010a).

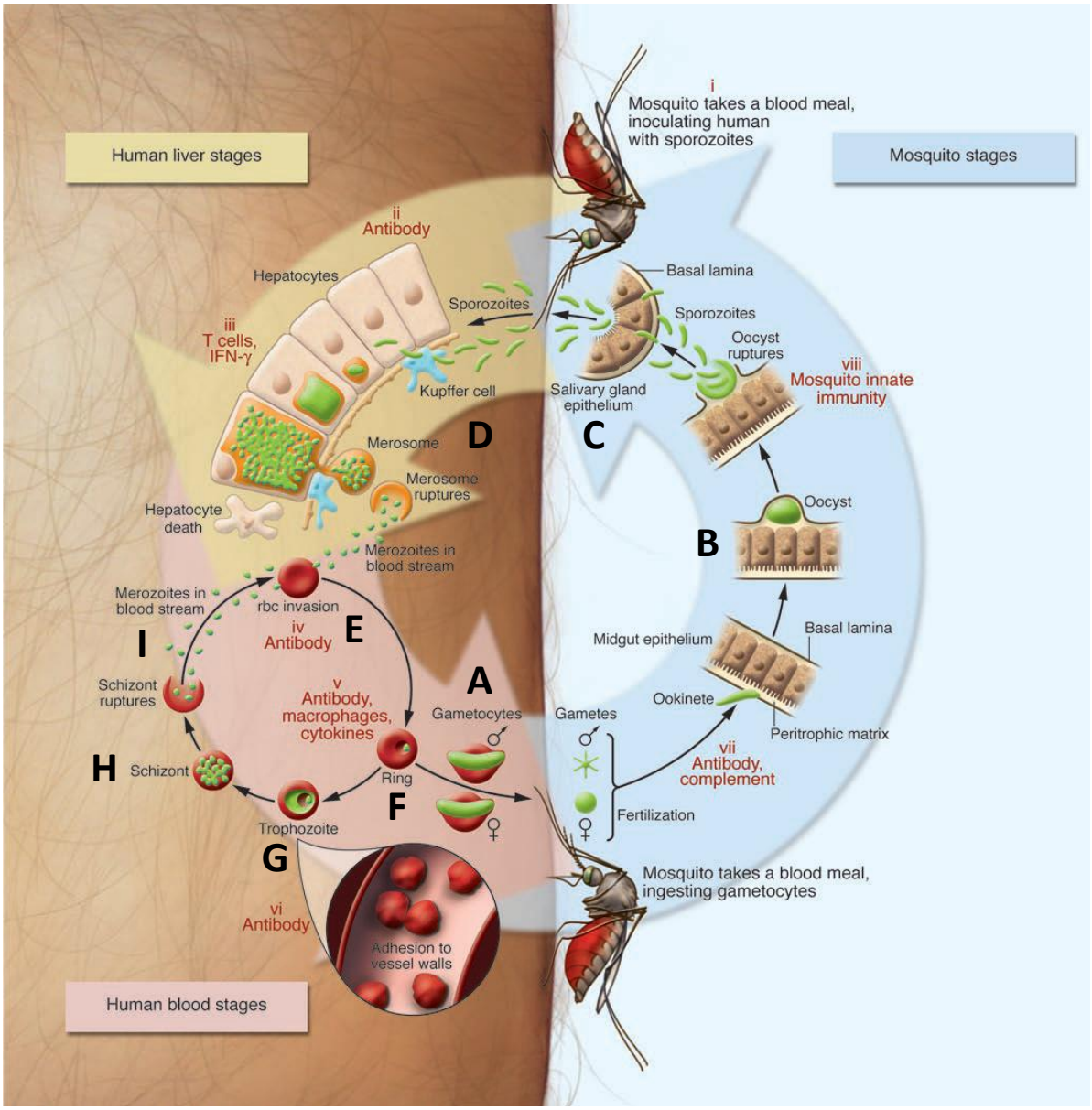


Figure 1.2: The developmental stages of the malaria parasite, and potential targets for immune system attack (adapted from Greenwood *et al*., 2008).
Abbreviation: interferon-γ.

1.2.1.2 The liver stage

The sporozoites, housed within the salivary glands of the mosquito, are released into the human host by the infected mosquito during its next blood meal (Figure 1.2C). Upon

entering the host the sporozoites migrate to the liver, where they invade hepatocytes (Figure 1.2D) (National Department of Health, 2009; WHO, 2010a). In the hepatocyte, the parasite multiplies over 6-21 days, whereupon the ruptured hepatocytes release thousands of merozoites into the blood stream, ending the asymptomatic stage of the disease known as exo-erythrocytic schizogony (National Department of Health, 2009; WHO, 2010a).

1.2.1.3 The asexual erythrocytic stage of *P. falciparum*

Antimalarial drugs target all stages of parasitic development; however the majority of the antimalarials in existence target the intra-erythrocytic stages, thereby reducing the clinical symptoms of the disease (Olliaro, 2001).

The asexual stage begins with merozoite invasion of the red blood cell (Figure 1.2E). Merozoites, although small in size, contain all the organelles needed to exit the ruptured host red blood cell, attach to and invade a healthy red blood cell, and resume the asexual life cycle (Bannister *et al*., 2000; Hanssen *et al*., 2010). Invasion occurs rapidly (within approximately 60 seconds), to decrease the risk of attack by the host's immune system (Cowman *et al*., 2006). Following invasion, dense granules released from merozoite organelles, re-locate to the membrane of the parasitophorous vacuole and release their contents, thereby increasing the surface area of the membrane and possibly initiating the progression of the life cycle into the ring-stage (Figure 1.2F) (Bannister *et al*., 2000; Hanssen *et al*., 2010).

Thereafter, the parasite appears in the red blood cell as a ring-shaped form with a nucleus, apicoplast, mitochondrion, endoplasmic reticulum, golgi apparatus and ribosomes contained in its cytoplasm (Bannister *et al*., 2000; van Dooren *et al*., 2005; Hanssen *et al*., 2010). The ring-stage lasts for approximately 20 hours post invasion, with little change in parasite morphology and low metabolic activity observed during this time (Spielmann *et al*., 2006). However, survival of the parasite and progression into the later stages is dependent on modifications carried out in this stage. In a screening of ring-stage specific genes it was found that most genes code for exported proteins involved in host cell modification. One such protein, the ring-infected erythrocyte surface antigen, is inserted into the red blood cell membrane, allowing it to maintain its biconcave shape and circulate through peripheral blood vessels (Mills *et al*., 2007). Other proteins encoded include: membrane proteins,

which localise to the parasitophorous vacuole membrane and may play a role in parasite and host cell interactions; as well as proteins transported to the red blood cell membrane which affect host cell permeability (Spielmann *et al*., 2003, 2006). Facilitating the sorting, storage and transport of the various parasite proteins to the red blood cell membrane are structures known as Maurer's clefts (Cooke *et al*., 2004; Spycher *et al*., 2006; Tilley *et al*., 2011). Transition from the ring- to trophozoite-stage is marked by the appearance of new permeation pathways, proteins responsible for the cytoadherence of infected red blood cells to microvasculature, as well as haemoglobin ingestion and breakdown (Spycher *et al*., 2006; Coppens *et al*., 2010; Hanssen *et al*., 2010).

In contrast to the low metabolic activity of the ring-stage, parasitic metabolic processes peak in the trophozoite-stage (Figure 1.2G), one of which is host cell haemoglobin degradation (Figure 1.3) (Bozdech *et al*., 2003; Hanssen *et al*., 2010).

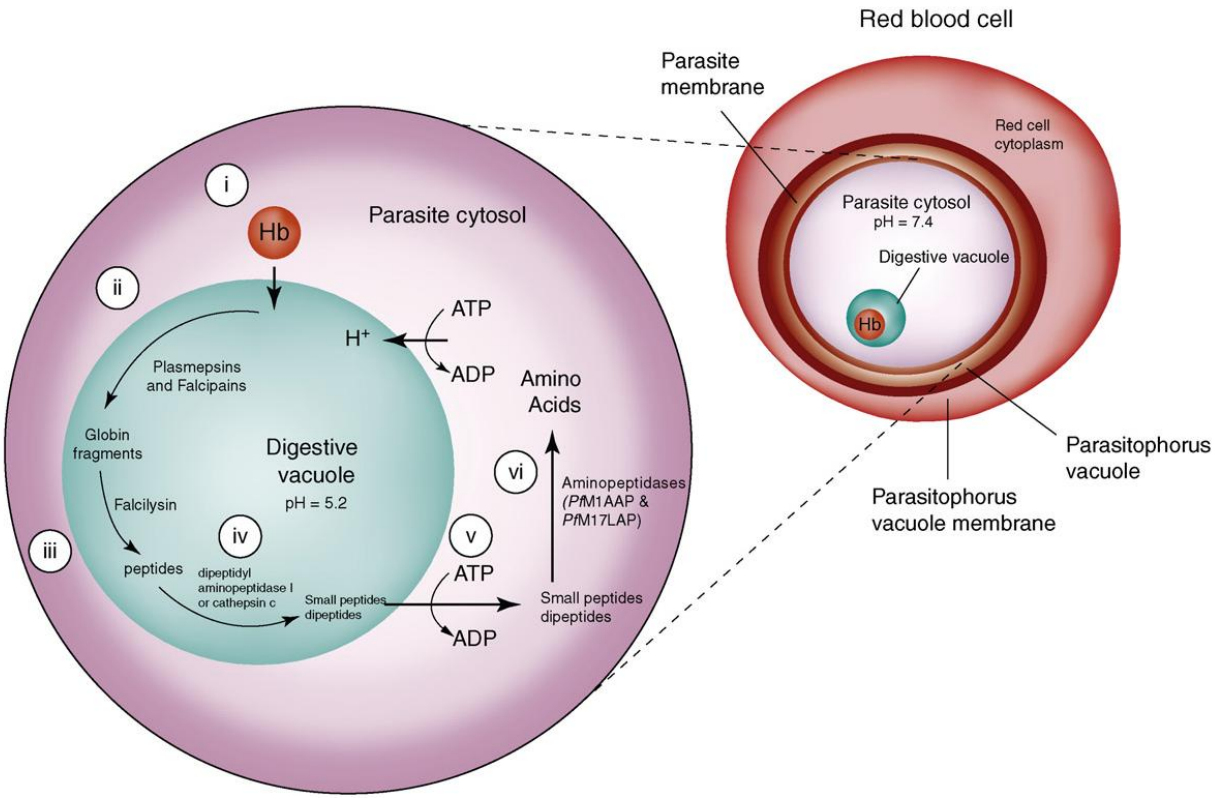


Figure 1.3: Haemoglobin digestion within the food vacuole of the malaria parasite (Skinner-Adams *et al*., 2009). Where: Hb = haemoglobin; *Pf*M1AAP and *Pf*M17LAP = *Plasmodium falciparum* M1-family alanyl aminopeptidase and M17-family leucyl aminopeptidase, respectively.

During the blood phase the parasite digests up to 80% of all haemoglobin present in the red blood cell (Egan, 2008). The process of haemoglobin digestion occurs when portions of haemoglobin-containing erythrocyte cytosol enter the parasite via cytostomes (Hanssen *et al*., 2010; Tilley *et al*., 2011), which are double-membraned invaginations of the parasite plasma and parasitophorous vacuolar membranes (Lazarus *et al*., 2008; Hanssen *et al*., 2010). Following internalisation of the haemoglobin, haemoglobin-containing vesicles bud off from the cytostome and fuse to the food vacuole (Figure 1.3i) (Sullivan, 2002; Lazarus *et al*., 2008; Tilley *et al*., 2011). The food vacuole is a highly acidic compartment with a pH of approximately 5, and contains various parasitic proteases responsible for haemoglobin degradation (Figure 1.3ii-iv) (Banerjee *et al*., 2002; Egan, 2008; Skinner-Adams *et al*., 2009).

The products of the digestion process include haem or Fe(II)-protoporphyrin-IX and peptides (Chemaly *et al*., 2007; Egan, 2008). The host derived peptides are broken down further into small dipeptides (Figure 1.3iv) and then transported into the parasite cytosol, possibly by an ATP-dependant membrane transporter (Figure 1.3v). Whereupon they are further digested into amino acids (Figure 1.3vi), and used for parasite protein synthesis (Skinner-Adams *et al*., 2009).

The haem released by haemoglobin catabolism is highly toxic to the parasite and may move from the food vacuole into the parasite cytoplasm where it undergoes redox reactions to form reactive oxygen species (ROS). The iron present in haem is also capable of reacting with oxygen to form ROS via the Fenton reaction (Figure 1.4). Intracellular ROS attack parasitic macromolecules such as DNA and proteins, and cause lipid peroxidation (Müller, 2004; Zhan *et al*., 2006). The toxic haem must, therefore, be detoxified by the parasite via biomineralisation to form the inert polymer, haemozoin, or degraded by glutathione (GSH) (Figure 1.4) (Müller, 2004; Garavito *et al*., 2007). In addition, the parasite is also under constant oxidative stress from ROS produced by the hosts' immune system (Müller, 2004). In this manner, intracellular ROS levels are controlled via enzymatic and non-enzymatic parasitic defence systems (Müller, 2004; Rasoloson *et al.*, 2004). The first line of enzymatic defence is a family of copper/zinc, iron and manganese metalloproteins, known as the superoxide dismutases (SODs) (Müller, 2004; Rasoloson *et al.*, 2004). SODs catalyse the reaction which forms hydrogen peroxide and oxygen from superoxide anions (Figure 1.4). The reduction of hydrogen peroxide to water and oxygen is catalysed by the second

enzymatic defence system, the peroxidases. The latter include haem-peroxidase catalase, GSH-dependant peroxidises and thioredoxin-dependant peroxidises (Müller, 2004).

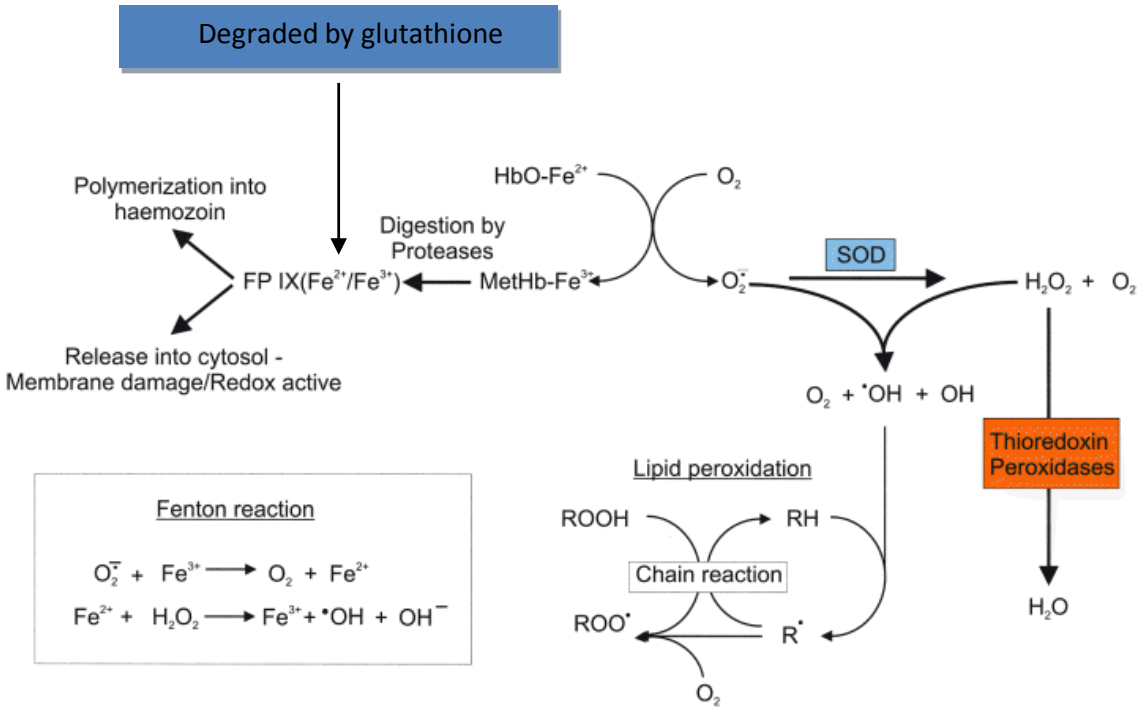


Figure 1.4: Sources of reactive oxygen species and anti-oxidant systems in *P. falciparum* (adapted from Müller, 2004). Abbreviations: FP IX, ferriprotoporphyrin-IX (haem); HbO-Fe^{2+}, oxy-haemoglobin containing haem; MetHb-Fe^{3+}, methaemoglobin containing haem; SOD, superoxide dismutase.

In order to cope with the increased protein synthesis and metabolic processes of the trophozoite- and schizont-stages, various internal changes occur in the parasite. Notably an increase in the number of ribosomes, enlargement of the endoplasmic reticulum and Golgi apparatus and lengthening of the mitochondrion and apicoplast (Bannister *et al*., 2000; Hanssen *et al*., 2010). The apicoplast, an important target in drug development, houses various metabolic processes such as an isoprenoid and a type II fatty acid synthetic pathway, which utilise products of glycolysis imported from the parasite cytosol (Coppens *et al*., 2010; Lim and McFadden, 2010). Enzymes involved in the haem biosynthesis pathway and iron-sulphur cluster biosynthesis have also been localised to the apicoplast (Becker *et al*., 2004; Lim *et al*., 2010). The close association between the mitochondrion and apicoplast during asexual development facilitates the transfer of metabolites between

the two organelles (van Dooren *et al*., 2005; Lim *et al*., 2010). The mitochondrion of *P. falciparum* contains enzymes involved in electron transport, the citric acid cycle as well as ubiquinone biosynthesis (Becker *et al*., 2004; Hyde, 2005). Another key enzyme of the folate pathway, dihydropteroate synthase (DHPS), has been hypothesised to be located in the mitochondrion, apicoplast and nucleus (Hyde, 2005; Müller *et al*., 2010).

The folate pathway is crucial for parasite growth. It involves the conversion of GTP, ρ-aminobenzoic acid (ρABA) and ι-glutamate into cofactors necessary for various metabolic pathways, such as DNA synthesis and amino acid catabolism (Hyde, 2005; Chango and Abdennebi-Najar, 2011). *P. falciparum* is incapable of *de novo* purine synthesis and requires specialised purine transporters located on the parasite plasma membrane, as well as a unique set of purine salvage enzymes to scavenge the host-derived purines (Section 5.1) (El Bissati *et al*., 2006; Downie *et al*., 2008). In contrast to purine salvage, the parasite relies on *de novo* salvage of pyrimidines (Section 5.1) (Hyde, 2007; Jana and Paliwal, 2007).

As the parasite moves from the late trophozoite- into the schizont-stage (Figure 1.2H), the rate of DNA synthesis becomes exponential in anticipation for nuclear division (de Rojas *et al*., 1985). Ingestion of host-derived haemoglobin continues well into the schizont-stage, until virtually all of the available haemoglobin has been digested, forming a large compact haemozoin crystal (Bannister *et al*., 2000; Hanssen *et al*., 2010). Similarly, the expression and export of parasite proteins continues into the schizont-stage. Proteins exported to the red blood cell membrane distort the membrane so that an increase in 'knobs' are visualised at the surface (Figure 1.5). Some proteins, such as the ring-infected erythrocyte surface antigen, are produced in the late schizont-stage and stored in apical organelles following merozoite formation (Bannister *et al*., 2000; Marti *et al*., 2005). The nucleus of *P. falciparum* completes approximately 4 divisions, with the peak in DNA synthesis between 33-45 hours indicating that each newly synthesised DNA molecule is used as a template for the next (de Rojas *et al*., 1985; Bannister *et al*., 2000). From the 4 divisions, approximately 16-20 individual nuclei may be formed, although as many as 32 may be formed (Bannister *et al*., 2000; Hanssen *et al*., 2010). Accompanying nuclear division is multiplication of the mitochondrion and apicoplast, as well as proliferation of the endoplasmic reticulum and ribosomes. As the maturation of the merozoites proceeds, the apical organelles are

assembled and a nucleus, mitochondrion and apicoplast move into each merozoite from the schizont cytoplasm (Figure 1.5) (Bannister *et al*., 2000; Hanssen *et al*., 2010).

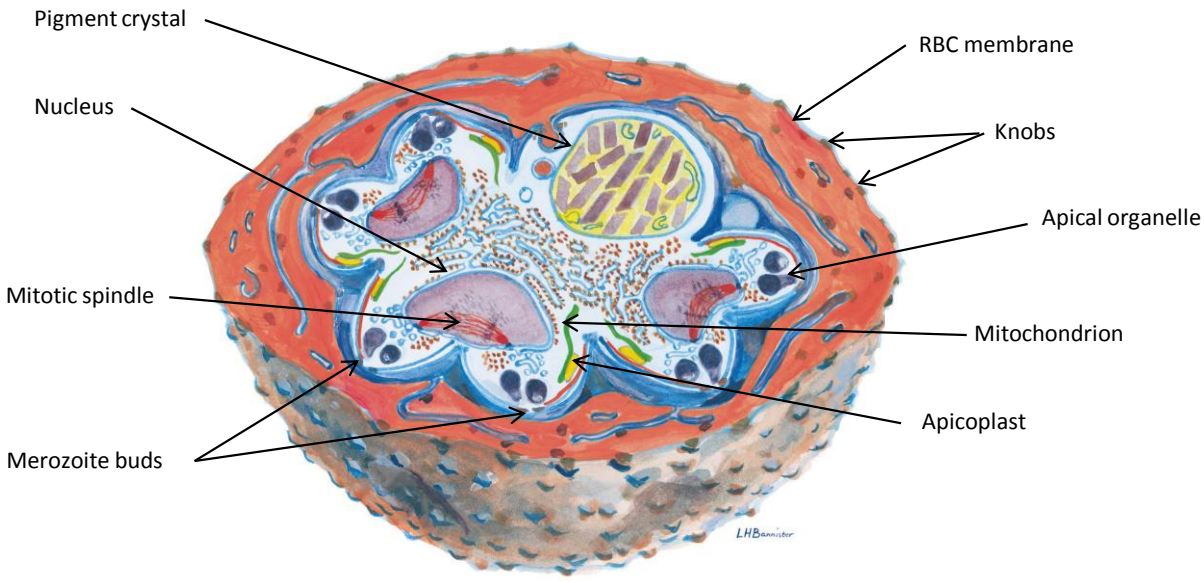


Figure 1.5: Internal structure of a *P. falciparum* late schizont, depicting parasite and red blood cell structure (Bannister *et al*., 2000).

The merozoites are then separated by a constriction ring and primary rupture of red blood cell membrane occurs, releasing parasitophorous vacuole membrane-associated merozoites. Following which, a secondary rupture of the parasitophorous vacuolar membrane, probably due to protease activity, releases the invasive merozoites (Figure 1.2I) which will infect new red blood cells, thereby repeating the life cycle (Figure 1.2E) (Marti *et al*., 2005; Soni *et al*., 2005; Hanssen *et al*., 2010).

1.2.1.4 The sexual erythrocytic stage of *P. falciparum*

Some asexual-staged parasites may also differentiate into gametocytes (Figure 1.2A), a process taking about 12 days in *P. falciparum*. A number of conditions are known to induce gametocytogenesis; certain antimalarial drugs, such as chloroquine and young red blood cells in circulation. Commitment to gametocytogenesis appears to occur in the late schizont- or early ring-stage in the generation preceeding gametocyte formation, indicating some form of signalling pathway must be involved in gametocytogenesis (Gardiner *et al*.,

2005). Gametocytes do not contribute to the symptoms of the disease; however they do persist in the blood stream for weeks, contributing to the spread of the disease as well as antimalarial drug resistance (Wirth, 2002; National Department of Health, 2009; WHO, 2010b).

1.3 Antimalarial prophylaxis and treatment

The WHO aims to reduce the number of malaria cases by 75% by 2015 (WHO, 2011). The control of malaria falls into two classes, prevention and treatment (WHO, 2011). The prevention of malaria has a further two divisions, personal protection methods and prophylaxis. Personal protection methods include reducing exposure to the mosquito vector, such as mosquito repellents applied to the skin, insecticide impregnated bed nets and the spraying of dwellings with insecticides. However, insecticides come with their own health risks, and the mosquito has rapidly developed resistance to insecticides, as is the case with pyrethroid and dichlorodiphenyltrichloroethane (DDT) resistance in parts of Western and Eastern Africa (Abdalla *et al*., 2008; WHO, 2011). Insecticide resistance was also observed in South Africa in the late 1990's/early 2000's, with the worst outbreak of malaria in South Africa in 50 years attributed to the resistance of the *Anopheles fenestus* vector to pyrethroid insecticides used to spray dwellings (Coetzee & Fontenille, 2004). The addition of prophylaxis to personal protection methods is usually recommended in high risk populations such as pregnant women, children, the elderly as well as immune-compromised individuals (National Department of Health, 2009). The choice of prophylaxis must be tailored to the geographical region, as well as to the individual (National Department of Health, 2009).

Subsequent to the failure of preventative measures, the correct and timeous treatment of malaria is vital. The symptoms of malaria generally present within 10-21 days following an infection and are often non-specific and easily confused with other diseases such as influenza, hepatitis and tick bite fever (National Department of Health, 2010). Diagnosis of malaria can therefore not only rely on a clinical assessment, a blood test should be carried out to confirm the diagnosis and percentage parasitaemia, as well the species of malaria, so that an appropriate therapeutic regimen can be implemented (National Department of Health, 2010). Rapid diagnostic tests are also available for *P. falciparum* and *P. vivax*

detection, and are based on their ability to detect parasite antigens such as histidine-rich protein 2 or parasitic lactate dehydrogenase (National Department of Health, 2010).

If promptly detected and appropriately treated, fatality due to uncomplicated *P. falciparum* infection is low. However, if not, there is a rapid progression into severe malaria and at this stage the risk of mortality approaches 100% (WHO, 2010b). Progression from uncomplicated into severe malaria is characterised by a high parasitaemia (3-4% or higher), respiratory distress, lactic acidosis, haemoglobinuria, anaemia, convulsions and coma with resultant organ failure (National Department of Health, 2010; WHO, 2010b). The cause of the clinical features of severe malaria appears to be partly mediated by the release of inflammatory cytokines by the immune system that, when uncontrolled, induce pathology in both the host and parasite; as well as the sequestering of parasites in vital organs such as the brain, resulting in the obstruction of blood flow (Clark and Cowden, 2003; Alonso, 2006; Sauerwein, 2009).

The treatment of *P. falciparum* malaria relies on the use of two or more antimalarial agents, with differing modes of action, in order to combat the risk of treatment failure and drug resistance (WHO, 2010b). Currently, artemether-lumefantrine is the first-line and most widely used treatment for uncomplicated *P. falciparum* malaria in most countries, including South Africa, with a combination of quinine and either doxycycline or clindamycin recommended as a second line treatment (Rosenthal, 2009; National Department of Health, 2010; Vinetz *et al*., 2011). In the case of pregnant women, quinine and clindamycin is used as the first line treatment, with artemether-lumefantrine recommended only in the second and third trimesters due to insufficient safety information (Rosenthal, 2009; National Department of Health, 2010; Vinetz *et al*., 2011).

For severe *P. falciparum* malaria, intravenous quinine is the treatment of choice in South Africa. Parenteral artesunate is recommended by the WHO as the treatment of choice for severe *P. falciparum* malaria, partially due to the fact that it does not require cardiac monitoring or a slow infusion like quinine, but is currently the second-line treatment in South Africa (National Department of Health, 2010; WHO, 2010b). Both treatments should be administered for a minimum of 24 hours, following which, a full course of quinine plus doxycycline/clindamycin or artemether-lumefantrine should be given to ensure total

parasite clearance (National Department of Health, 2010; WHO, 2010b). For mixed *P. falciparum* infections, treatment follows that of *P. falciparum* infections, with the addition of primaquine to clear tissue schizontocides (National Department of Health, 2010).

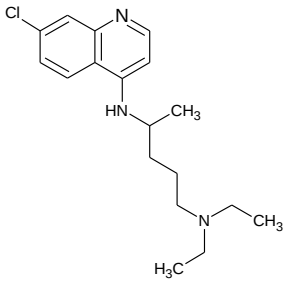
Compounds used for the prophylaxis and treatment of malaria can be classified into 5 groups based on similar mechanisms of action and include: the quinolines, antifolates, napthoquinones, antibacterials and artemisinin-type compounds (Olliaro, 2001). These compounds target various stages of the parasitic life cycle such as: the asexual blood stage (blood schizontocides), the liver or exo-erythrocytic stage (tissue schizontocides), the sexual blood stage (gametocytocides) and the developmental stages within the mosquito vector (sporontocides) (Vangapandu *et al*., 2007; Rosenthal, 2009). With blood schizontocides acting to combat the clinical symptoms of malaria, tissue schizontocides acting to combat development of infection past the liver stage, gametocytocides inhibiting transmission from the host to the mosquito and sporontocides acting to inhibit transmission from the mosquito to the host (Vangapandu *et al*., 2007).

1.3.1 Quinolines

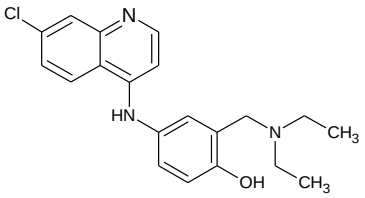
Chloroquine, amodiaquine, quinine, mefloquine and lumefantrine (Figure 1.6) are blood schizontocides, and exhibit no gametocytocidal effects against mature gametocytes. Chloroquine may even increase infectivity in mature gametocytes (Butcher, 1997; WHO, 2010b). Primaquine exhibits little blood schizontocidal activity and is used primarily as a tissue schizontocide, sporontocide and gametocytocidal agent. It is reportedly active against mature gametocytes, whilst also accelerating gametocyte clearance (Butcher, 1997; Vangapandu *et al*., 2007; WHO, 2010b).

The quinolines are a large family of antimalarial drugs comprising the 4-aminoquinolines; chloroquine and amodiaquine, the aryl amino alcohols; quinine, mefloquine and lumefantrine and the 8-aminoquinoline primaquine (Figure 1.6) (Olliaro, 2001; Biagini *et al*., 2003; Vangapandu *et al*., 2007). The 4-aminoquinolines and aryl amino alcohols are both weak bases; however, the 4-aminoquinolines are hydrophilic at neutral pH, whereas the aryl amino alcohols are lipophilic at neutral pH. They exhibit similar antimalarial mechanisms of action, albeit different interactions with their targets (Olliaro, 2001). The predominant antimalarial mechanism of action for these two groups appears to be

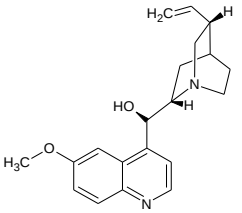
interference in the haem detoxification process, resulting in inhibition of haemozoin formation (Olliaro, 2001; Biagini *et al*., 2003; Vangapandu *et al*., 2007).



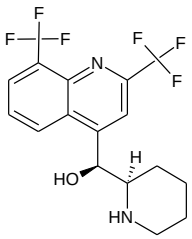
Chloroquine



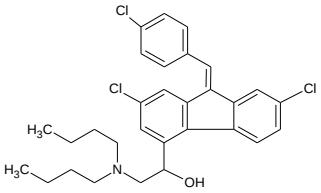
Amodiaquine



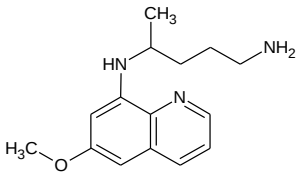
Quinine



Mefloquine



Lumefantrine



Primaquine

Figure 1.6: Chemical structures of the quinoline family of antimalarials (WHO, 2010b).

Other mechanisms of action which have been proposed include: intercalation in to parasitic DNA thereby inhibiting DNA replication, inhibition of protein synthesis; as well as inhibition of lipase and aspartic proteases within the food vacuole. However, these effects may only be achieved at high drug concentrations (Olliaro, 2001). It has been shown that chloroquine is also capable of depleting GSH, a major anti-oxidant defence system of the parasite, resulting in parasite death due to oxidative stress (Müller, 2004). The 8-aminoquinoline, primaquine, does not appear to play a role in inhibiting the formation of haemozoin, as is the case with the other quinolines. In contrast, its mechanism of action appears to lie in its ability to act as a pro-oxidant, generating reactive oxygen species within the red blood cell which attack parasite macromolecules (Vangapandu *et al*., 2007; Basso *et al*., 2011).

1.3.1.1 Efficacy and side effects

Chloroquine has been rendered virtually obsolete against *P. falciparum* due to widespread resistance (White, 2004; Jana and Paliwal, 2007; Vangapandu *et al*., 2007). Whilst amodiaquine usage was initially discouraged due to side effects such as hepatotoxicity and agranulocytosis, it has been reconsidered as a possible antimalarial since the emergence of chloroquine resistance. However, cross resistance in chloroquine-resistant *P. falciparum* strains may occur (Biagini *et al*., 2003; Kerb *et al*., 2009; WHO, 2010b).

Mefloquine remains mostly effective against *P. falciparum*, including strains resistant to chloroquine and sulphadoxine-pyrimethamine, and is used as a prophylactic agent in South Africa. It should be taken weekly, starting one week before exposure, during exposure, and for four weeks afterwards (National Department of Health, 2009). However, mefloquine resistance has emerged in areas where it is widely used, such as South-East Asia, and in such areas it is no longer recommended for prophylaxis or in treatment regimens (Rosenthal, 2009; WHO, 2010b).

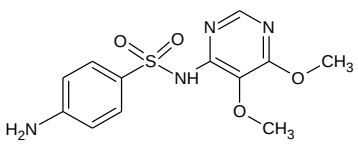
Mefloquine usage may result in various adverse effects such as neuropsychiatric disturbances, and is also known to interfere with the metabolism of anti-epileptics. It is therefore contraindicated for use in persons suffering from central nervous system disorders or epilepsy (Rosenthal, 2009; Rossiter, 2010). The concomitant use of mefloquine and chloroquine is contraindicated, with chloroquine not only used as an antimalarial agent, but also to manage conditions such as rheumatoid arthritis and systemic lupus erythematosus (Rosenthal, 2009; Rossiter, 2010). In addition, quinine and mefloquine are also contraindicated. In both cases, serious adverse effects such as cardio- and neurotoxicity are observed, with quinine also possibly inhibiting mefloquine metabolism (National Department of Health, 2009; Rossiter, 2010).

Quinine remains effective against *P. falciparum*; however, cases of quinine resistance have been reported in South-East Asia (Rosenthal, 2009; National Department of Health, 2010). A common side effect of quinine, affecting up to 70% of patients, is cinchonism (tinnitus, hearing impairment, headache, nausea, giddiness, blurred vision); whilst less common but serious side effects include hypoglycaemia and cardiac arrhythmias (National Department of Health, 2010; Rossiter, 2010; WHO, 2010b). Due to its pro-oxidant properties,

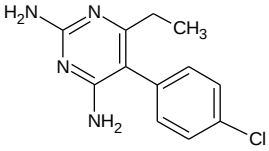
primaquine can cause haemolysis and haemolytic anaemia in patients' deficient in glucose-6-phosphate dehydrogenase (Kerb *et al*., 2009; WHO, 2010b).

1.3.2 Antifolates

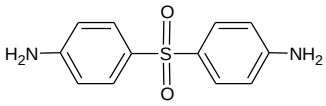
Antifolates (Figure 1.7) act as blood and tissue schizontocides and are active against all asexual and early intra-hepatic stages of the parasite; but appear to have no gametocytocidal activity (Butcher, 1997; Vangapandu *et al*., 2007). Pyrimethamine, proguanil and chlorproguanil act as sporontocides by reducing oocyst numbers in the mosquito vector, either through direct damage to the oocyst or inhibition of development (Butcher, 1997; WHO, 2010b).



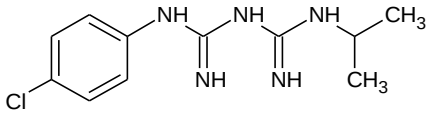
Sulphadoxine



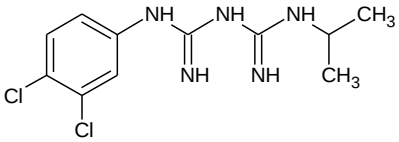
Pyrimethamine



Dapsone



Proguanil



Chlorproguanil

Figure 1.7: Chemical structures of the antifolates (O' Neill and Posner, 2004; WHO, 2010b).

The antifolates have comprised of some of the most extensively used antimalarial drugs (Olliaro 2001). They can be classified into two classes, depending on which enzyme of the folate pathway they inhibit (Olliaro, 2001).

The type-1 antifolates; dapsone and sulphadoxine, inhibit dihydropteroate synthase (DHPS), thereby preventing *de novo* folate synthesis (Rosenthal, 2009; WHO, 2010b). Whereas the type-2 antifolates, pyrimethamine, proguanil and chlorproguanil are competitive inhibitors of dihydrofolate reductase (DHFR), a key enzyme involved in folate salvage, as well as nucleotide and methionine biosynthesis (Vangapandu *et al*., 2007; Rosenthal, 2009). Type 1 and 2 antifolates are used in combination therapies,

predominantly with each other; with one inhibitor synergisticically potentiating the activity of another, resulting in a sequential blockade of the folate pathway (Nzila, 2006; Rosenthal, 2009).

1.3.2.1 Combination therapies

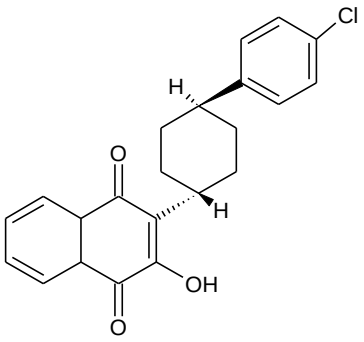
Sulphadoxine in combination with pyrimethamine (SP) was one of the most widely used antimalarial therapies following the emergence of chloroquine-resistance. However, resistance to SP has rapidly emerged, such that the combination is no longer recommended for use in many countries, including South Africa (Rosenthal, 2009; National Department of Health, 2010). In addition, side effects of SP, Stevens-Johnson syndrome, epidermal necrolysis and erythema multiforme, have curatailed its use as a chemoprophlactic agent, even in areas where resistance has not yet developed (Rosenthal, 2009). The combination of dapsone and chlorproguanil (Lapdap®), metabolised in the liver to its active component chlorcycloguanil, was formulated as an alternative to SP (Nzila, 2006; Fanello *et al*., 2008; Rosenthal, 2009). However, SP cross resistance as well as concerns about drug safety, particularly in glucose-6-phosphate dehydrogenase deficient patients has resulted in this combination no longer being used (Kremsner and Krishna, 2004; Rosenthal, 2009; WHO, 2010b).

Prophylaxis with a single folate antagonist is no longer recommended due to antimalarial drug resistance, such that proguanil and its active metabolite, cycloguanil, are no longer used as monotherapy or in combination with chloroquine (Rosenthal, 2009; WHO, 2010b). Proguanil is now used in combination with atovaquone in both prophylaxis and treatment regimens, and is highly effective and well tolerated. However, the regimen is very costly (Kremsner and Krishna, 2004; Rosenthal, 2009; WHO, 2010b). Currently the regimen is only registered for prophylactic use in South Africa, with a daily dose taken one day prior to exposure, during exposure, and for seven days after returning from a malaria area (National Department of Health, 2009; Rossiter, 2010). This regimen has the best safety profile of all antimalarial prophylactics, together with improved compliance due to the shorter dose regimen (National Department of Health, 2009; Rossiter, 2010). Tetracyclines, opiods, paracetamol, laxatives, rifampicin and antidiarrhoeal agents are contraindicated for use

with atovaquone-proguanil as they decrease the plasma concentration of atovaquone (Rossiter, 2010).

1.3.3 Napthoquinones

Atovaquone (Figure 1.8) is a tissue schizontocide, sporontocide and blood schizontocide (Rosenthal, 2009; WHO, 2010b). It is a broad spectrum antiplasmodial drug acting to inhibit the electron transport chain of *P. falciparum*, resulting in the disruption of the regeneration of ubiquonone which is the electron acceptor for dihydroorotate dehydrogenase, a key enzyme of pyrimidine biosynthesis (WHO, 2010b; Hughes *et al*., 2011; Vinetz *et al*., 2011). It is not used as monotherapy due to the rapid spread of resistance, and as such it is used in combination with proguanil (Rosenthal, 2009; WHO, 2010b). Atovaquone is generally well tolerated and is also used to treat pneumonia caused by *Pneumocystis jirovecii,* an opportunistic infection commonly seen in human immunodeficiency virus (HIV) positive persons, as well as *Toxoplasma gondii*, the causative agent of toxoplasmosis (Rosenthal, 2009; Hughes *et al*., 2011).



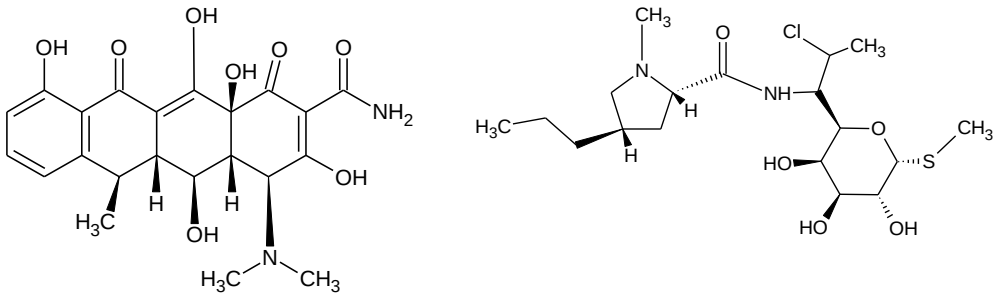
Atovaquone

Figure 1.8: Chemical structure of atovaquone, a napthoquinone (WHO, 2010b).

1.3.4 Antibacterials

Doxycycline and clindamycin (Figure 1.9) are slow-acting blood schizontocides, with no gametocytocidal activity (Dahl *et al*., 2006; Rosenthal, 2009). Doxycycline belongs to the tetracycline group of antibiotics and is commonly used with a fast acting antimalarial as its antimalarial activity only occurs after one asexual cycle or approximately 48 hours (Dahl *et al*., 2006; Greenwood *et al*., 2008; Vinetz *et al*., 2011). Its mechanism of action appears to

lie in its ability to inhibit protein translation in the apicoplast, thereby inhibiting protein synthesis (Rosenthal, 2009; Vinetz *et al*., 2011). Clindamycin acts as a translation blocker in bacteria and appears to target rRNA of the apicoplast in *Plasmodium* and, in a manner similar to doxycycline, results in parasite death only in the second asexual cycle of blood stages of the parasite (Goodman *et al*., 2007; Vinetz *et al*., 2011).



Doxycycline Clindamycin

Figure 1.9: Chemical structures of doxycycline and clindamycin (WHO, 2010b).

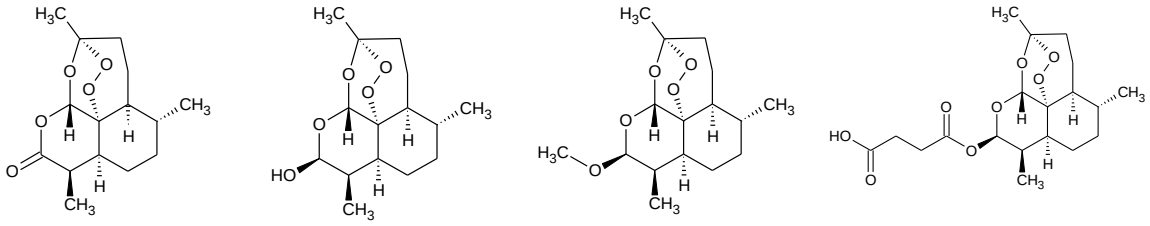
1.3.4.1 Indications and side effects

Doxycycline is recommended by the centres for disease control and prevention as a prophylactic agent and is currently used as a chemoprophylactic agent in South Africa. It is the recommended prophylactic agent for HIV-positive persons on antiretrovirals, as no drug interactions with antiretroviral regimens have been noted (National Department of Health, 2009; Vinetz *et al*., 2011). Doxycycline should be taken daily, starting one day before exposure, during exposure, and for four weeks afterwards (National Department of Health, 2009). In addition, it is also used in combination with quinine for the treatment of *P. falciparum* malaria (Rosenthal, 2009; National Department of Health, 2009). However, doxycycline is contraindicated in pregnant or lactating women and children under the age of eight, as it interferes with bone growth and may cause raised intracranial pressure (National Department of Health, 2009; WHO, 2010b; Vinetz *et al*., 2011).

Clindamycin is safe for use in pregnant women and children, and in these cases is combined with quinine to treat *P. falciparum* malaria. Side effects of clindamycin include mainly gastrointestinal disturbances; however, some fatal cases of pseudomembranous colitis have been reported (WHO, 2010b).

1.3.5 Artemisinin and its derivatives (endoperoxides)

The artemisinins (Figure 1.10) act as blood schizontocides against all asexual stages and also exhibit gametocytocidal activity against young gametocytes, making them invaluable antimalarial drugs (Rosenthal, 2009; WHO, 2010b).



Artemisinin Dihydroartemisinin Artemether Artesunate

Figure 1.10: Chemical structures of artemisinin and its semi-synthetic derivatives (WHO, 2010b).

Artemisinin is an extract of *Artemisia annua* (sweet wormwood) and has been used in China as an anti-pyretic agent for over a thousand years, and was first available for commercial use in the 1980's (Meshnick, 2002). Since the discovery of the potent antimalarial effects of artemisinin, various semi-synthetic derivatives have been made available for use namely; dihydroartemisinin, artemether and artesunate (Olliaro, 2001). The original theories of the antimalarial mechanism of action of artemisinin and its derivatives were that cleavage of the endoperoxide bridge by free intraparasitic haem, as a result of haemoglobin digestion, generated free-radicals which alkylated proteins and damaged membranes; and that artemisinin inhibited haemozoin formation via the formation of adducts with haem (Pandey *et al*., 1999; Meshnick, 2002; Biagini *et al*., 2003).

However, these mechanisms of action were questioned when localisation studies showed that artemisinin accumulated outside of the food vacuole. In addition, artemisinin and its derivatives are active against the early ring-stage of the parasite, where no haemoglobin digestion occurs (Krishna *et al*., 2008). The most recent hypothesis is that artemisinin inhibits a calcium-dependant ATPase of *P. falciparum* (*PfATP6)*, which has been localised to the endoplasmic reticulum (Krishna *et al*., 2010; Vangapandu *et al*., 2007). Calcium

signalling is vital in all stages of the parasitic life cycle and is involved in regulation of invasion of the red blood cell, motility and intracellular development (Krishna *et al*., 2010).

Artemisinin has now largely been replaced by its derivatives dihydroartemisinin, artemether and artesunate (WHO, 2010b). The WHO states that artemisinin derivatives should never be used as monotherapy, in order to reduce the risk of widespread antimalarial drug resistance (WHO, 2010b), with limited cases of resistance to artemisinin and its derivatives recently reported on the Thailand-Cambodia border, and in Myanmar and Vietnam (WHO, 2010b; WHO, 2011). The choice of ACT depends on the tolerability of the combination, as well as levels of resistance to the partner drug (WHO, 2010b). However, as is the case with all ACTs, the short half-life of the artemisinin derivative leaves the partner drug and its metabolites vulnerable to the development of resistance (Kremsner and Krishna, 2004; Kerb *et al*., 2009).

1.3.5.1 Combination therapies and side effects

Artemisinin and its derivatives appear to be generally well tolerated (Kerb *et al*., 2009). Some Type I hypersensitivity reactions have been reported, as well as some neurotoxicity in animal trials; however neurotoxicity was not noted in human trials (Kerb *et al*., 2009; WHO, 2010b). In patients co-infected with HIV there is an increased risk that artemisinin may decrease the efficacy of HIV medication; whilst also increasing the risk of drug reactions (Kerb *et al*., 2009). Four combination therapies are currently in widespread use and recommended by the WHO (Rosenthal, 2009; WHO, 2010b).

Artemether is commonly used in combination with lumefantrine, the short half life of artemisinin derivatives leave residual parasites which are then cleared by a slowly eliminated drug such as lumefantrine, which has a half-life of three days (Kremsner and Krishna, 2004; WHO, 2010b). This combination is highly effective and well tolerated (Kremsner and Krishna, 2004; Rosenthal, 2009).

Artesunate is also commonly used in combination with amodiaquine or mefloquine or SP (WHO, 2010b). However, combination regimens of artesunate plus amodiaquine have shown to cause neutropenia, a side effect attributed to amodiaquine, which is worsened in HIV-infected persons (Kremsner and Krishna, 2004; National Department of Health, 2010;

WHO, 2010b). Additionally, hepatotoxicity has been reported when artesunate plus amodiaquine and efavirenz were taken concomitantly (WHO, 2010b). Clinical trials of artesunate plus SP have shown the combination to be more effective than SP alone and well tolerated; however, it is not recommended in most countries due to widespread SP resistance (Rosenthal, 2009; Kremsner and Krishna, 2004). Artesunate plus mefloquine appears to be safe and highly effective, however as with most ACTs it is costly (Kremsner and Krishna, 2004).

1.4 Antimalarial drug resistance

Owing to stringent malaria control campaigns the disease was virtually eradicated by the early 1960's, however malaria has staged an enormous comeback, and is now emerging as one of the biggest killers in the tropics (Vangapandu *et al*., 2007). Antimalarial drug resistance is particularly worrying due to the massive distribution of malaria worldwide, the degree of mortality attributed to the disease, as well as the time and associated costs of developing replacements drugs (WHO, 2010b). Resistance has been reported to all widely used antimalarials, such as: chloroquine, amodiaquine, mefloquine, quinine, SP, and more recently, artemisinin derivatives (WHO, 2010b; WHO, 2011). Drug resistance may be geographically localised, as is the case with mefloquine, amodiaquine, artemisinin and quinine, or more widespread as with chloroquine and SP (WHO, 2010b). It appears as if drug resistance is perpetuated in two ways. Firstly, by the use of an antimalarial to which partial resistance has already occurred, as it confers an advantage to parasites which are resistant to the drug, with these parasites also shown to produce higher gametocyte numbers. This is compounded by antimalarials which induce gametocytogenesis, such as the antifolates, which further promotes the transmission of drug resistant parasites (Vinetz *et al*., 2011). Secondly, gametocytes which carry drug resistant genes are shown to be more infectious, by producing more oocytes within the mosquito; as well as by infecting a higher percentage of mosquitoes (Butcher, 1997; WHO, 2010b). Genetic mutations on parasitic chromosomes confer antimalarial drug resistance by altering drug transport and accumulation within the parasite, as is the case with chloroquine, amodiaquine, quinine and mefloquine. Or by reducing the affinity of the antimalarial drug to the parasitic target, as is the case with pyrimethamine, cycloguanil, sulphonamides and atovaquone (Kerb *et al*., 2009; Rosenthal, 2009; Vinetz *et al*., 2011). Antimalarial drug resistance provides a major

challenge to the treatment of malaria, with treatment failure resulting in a rapid disease progression and enormous increase in the risk of mortality (WHO, 2010b). This has initiated the urgent development of novel compounds with unique mechanisms of action against the parasite, that, when combined with current antimalarial treatments have a favourable interaction.

1.5 The future of malarial prevention and treatment

Thus far malaria preventative methods include personal protection methods and chemoprophylaxis; a third possible option is an antimalarial vaccine. Owing to the massive resurgence of malaria and the spread of drug resistance, the global fight against malaria has increased to include development of an antimalarial vaccine (The RTS,S clinical trials partnership, 2011). Vaccine development has concentrated on targeting stage-specific antigens present in the sporozoite, tissue and asexual stages, as well as the blockade of transmission of gametocytes and gametes (Figure 1.2) (Greenwood *et al*., 2008; Greenwood and Targett, 2009). In high malaria transmission areas of Africa, children who survive *P. falciparum* infections in early life rarely develop severe malaria in later infections (Sauerwein, 2009). This clinical immunity appears to be as a result of a combination of both naturally acquired immunity mediated by host antibodies targeting parasite proteins, as well as the production of cytokines, such as interferon-γ, which act to inhibit parasite growth mainly in the liver stage (Figure 1.2) (Greenwood and Targett, 2009; Sauerwein, 2009).

Attempts to develop a vaccine against malaria began over 50 years ago, with the Spf66 experimental vaccine showing promising results. Spf66 was a synthetic vaccine composed of amino acid sequences derived from the *P. falciparum* merozoite circumsporozoite protein and was designed to act against the asexual stage of the parasitic life cycle (Amador et al., 1992). Spf66 was shown to be 30% effective in providing immunity against the disease; however, this was not validated in later clinical trials (Greenwood and Targett, 2009). More recently, the RTS,S vaccine, a sub-unit vaccine composed of a polypeptide segment of the circumsporozoite protein fused to the hepatitis B surface antigen, designed to act against the liver stage of the disease, has displayed promising results (Greenwood *et al*., 2008; Vanderberg, 2009). Results from the RTS,S vaccine trials conducted in Africa

showed that the vaccine was approximately 50% effective in reducing the risk of *P. falciparum* infection, whilst also reducing the risk of developing severe malaria by approximately 35% in children aged between 6-12 weeks and 5-17 months (The RTS,S clinical trials partnership, 2011)

Another vaccine trial using the rodent malaria model (*Plasmodium berghei)* examined the ability of genetically modified whole *P. berghei* sporozoites, viable sporozoites administered together with a prophylactic agent such as azithromycin, pyrimethamine, primaquine or chloroquine and over-irradiated sporozoites to provide protective immunity (Friesen and Matuschewski, 2011). Friesen and Matuschewski (2011) found that genetically modified *P. berghei* sporozoites and viable sporozoites administered together with azithomycin provided a high degree of protection (80%), whereas over-irradiated *P. berghei* sporozoites failed to elicit any protection against the disease. Despite the promising results of these trials, vaccine candidates have been unable to re-produce the same effect as the clinical immunity developed from multiple exposures (Vanderberg, 2009).

An alternative therapeutic strategy included intermittent preventative treatment, wherein high-risk populations such as pregnant women and infants are intermittently treated with a prophylactic agent such as SP, has shown to reduce malaria infection by 60% in infants (Alonso, 2006; Greenwood and Targett, 2009). However, a concern with this strategy is that antimalarial drug resistance has limited the number of medications available.

The current lack of a vaccine, as well as the increase in antimalarial drug resistance, has made it imperative to develop new effective antimalarial drugs that are target specific. Drug development may be achieved by re-examining existing antimalarials or by developing new drugs which act on previously exploited or novel parasitic targets (Figure 1.11) (Vangapandu *et al*., 2007; Greenwood *et al*., 2008). The efficacy of existing antimalarials could be improved upon by synthesising derivatives with various side chains substitutions; or by combating drug resistance by the inclusion of a resistance reversal agent (Vangapandu *et al*., 2007). An example of an exploited parasitic target includes the folate pathway. The addition of a third drug, capable of inhibiting other processes in the pathway and acting synergistically with available antifolate combination therapies, may be a possibility to kerb folate resistance (Biagini *et al*., 2003; Greenwood *et al*., 2008).

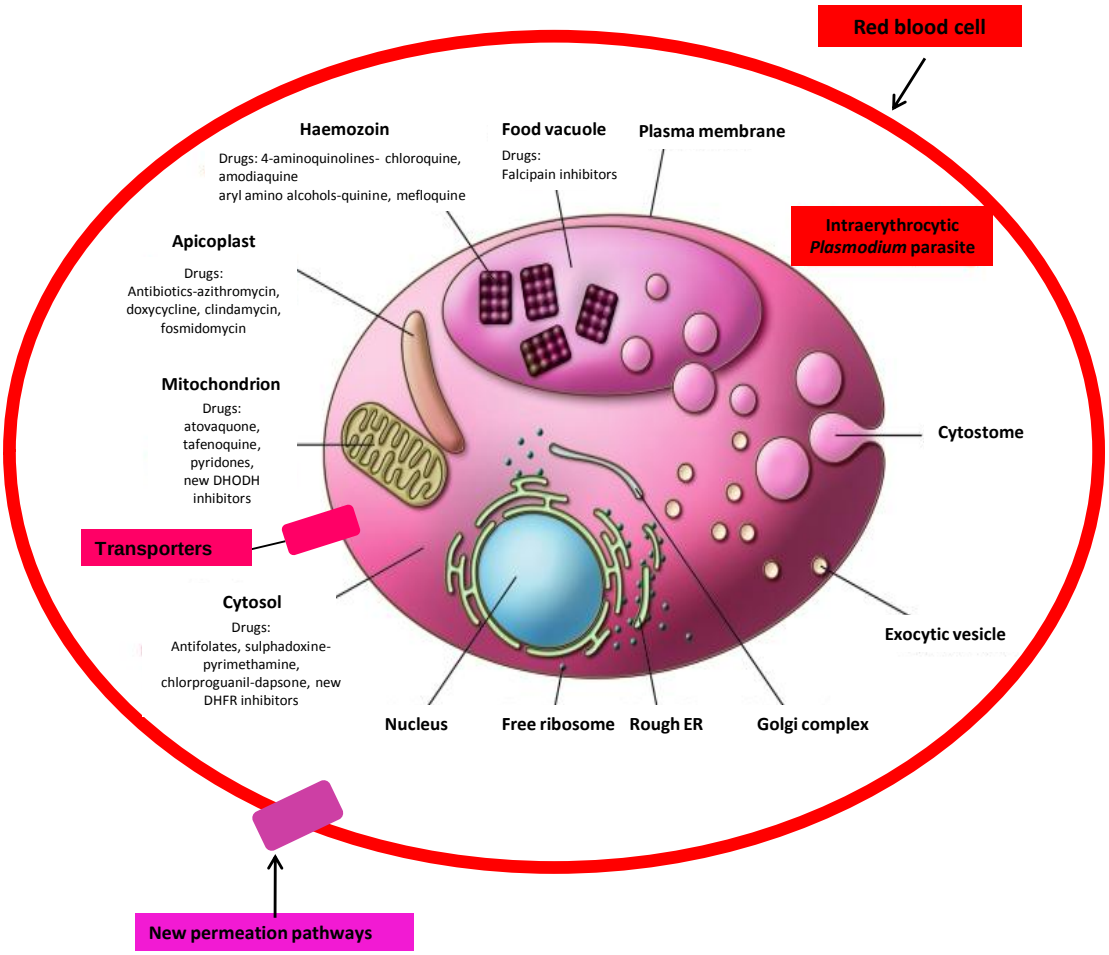


Figure 1.11: Drug targets within *P. falciparum* (adapted from Greenwood *et al*., 2008). Where: DHODH = dihydroorotate dehydrogenase; DHFR = dihydrofolate reductase; ER = endoplasmic reticulum.

Novel parasitic targets include: new permeation pathways, transporters, proteases within the food vacuole, the mitochondrial system, the apicoplast, as well as protein kinases involved in DNA synthesis and replication pathways (Figure 1.11) (Jana and Paliwal, 2007; Greenwood *et al*., 2008; Solyakov *et al*., 2011). In a recent study by Solyakov *et al*. (2011) 36 protein kinases were identified and found to be involved in not only DNA replication processes, but also cyto-adherence and red blood cell invasion, thereby providing additional targets for novel antimalarial drugs.

The benefits of exploiting specific parasitic targets would be to not only decrease the side effect profile of the drug, but also to formulate drug combinations, wherein each drug acts on a different parasitic target increasing the efficacy of the drugs in combination, as well as decreasing the risk of drug resistance (Kremsner and Krishna, 2004; Jana and Paliwal, 2007).

In this respect, the aim of this study was to investigate the exact nature of the effects of three novel classes of compounds on previously exploited and novel parasitic targets; as well as to examine the interactions of select compounds from each class with standard antimalarial drugs, with the goal of elucidating structure-activity relationships.

1.6 Study objectives

To determine the antimalarial activity of metronidazole-thiosemicarbazone derivatives, chloroquinoline-chalcones, as well as nucleoside phosphonates, phosphonic acids and purine/pyrimidine derivatives:

- A total of 112 compounds from the three diverse groups of compounds were tested against *P. falciparum*, using the [^{3}H]-hypoxanthine incorporation assay, from which lead compounds were identified and structure-activity relationships determined.
- A flow cytometric methodology as a high-throughput means of testing the antimalarial activity of compounds against *P. falciparum* was established and validated against the [^{3}H]-hypoxanthine incorporation assay.
- Lead compounds were combined with standard antimalarials to assess pharmacological interactions.
- Morphological and stage-specific effects of the lead compounds were examined in order to elucidate antimalarial mechanisms of action.
- Antimalarial mechanisms of action were further examined by use of assays to examine the effects of the compounds on haemozoin formation, iron chelation and free-radical scavenging.
- The effect of the compounds on healthy red blood cells was examined to give an indication of cytotoxicity.

CHAPTER 2: MATERIALS AND METHODS

2.1 Protocol for the *in vitro* culturing of *P. falciparum*

The first successful attempt at the continuous *in vitro* culturing of the malaria parasite occurred in 1976, with the culture derived from a monkey infected with the Vietnam-Oak Knoll chloroquine-resistant strain of *P. falciparum* (Trager and Jensen, 1976). Following which, Jensen and Trager (1978) showed that parasite cultures derived from individuals infected with *P. falciparum* could also be successfully cultured. These parasite cultures were maintained in RPMI-1640 culture media supplemented with (4-(2-hydroxyethyl)piperazine-1-ethanesulfonic acid) (HEPES) buffer, bicarbonate, and 10 or 15% human serum; to which human AB^+ erythrocytes were added (Jensen and Trager, 1978). The petri dish/candle jar technique was used, wherein the parasite suspension was grown in plastic petri dishes which were incubated in a candle jar maintained at 37 °C (Jensen and Trager, 1978). However, Freese *et al*. (1988) found the candle jar technique unsuitable for the establishment of South African *P. falciparum* isolates, with the survival time of the cultures ranging from 2 to 44 days. Freese *et al*. (1988) then modified the methodology of Jensen and Trager (1978) so that parasite cultures could be maintained in a tissue culture flask gassed with a mixture of 3% O_2, 4% CO_2 and 93% N_2, in addition, the culture media was further supplemented with glucose, hypoxanthine, and gentamicin.

2.1.1 Culture maintanence

The 3D7 (chloroquine-sensitive) strain of *P. falciparum* (Biosafety clearance/protocol number: 20090503, Appendix B1) was continuously maintained, according to the methodology of Jensen and Trager (1978) and Freese *et al*. (1988). On a daily basis thin blood smears were prepared, fixed with methanol, and stained with a rapid diagnostics kit (Global diagnostics), which contained a Giemsa component for detection of the parasite. From the blood smear the % parasitaemia was calculated and the stage of the asexual life cycle (Figure 2.1) determined. The culture was maintained at a 5% haematocrit and parasitaemia below 10%, with nutrient-depleted culture media (Section 2.1.6) aspirated and replaced daily with fresh complete culture media. During the trophozoite- and schizont-stages, uninfected eythrocytes (Section 2.1.8) were added to the culture. Prior to

incubation, at 37 °C, the culture was gassed with a mixture of 92% N_2, 5% CO_2 and 3% O_2 (Afrox).

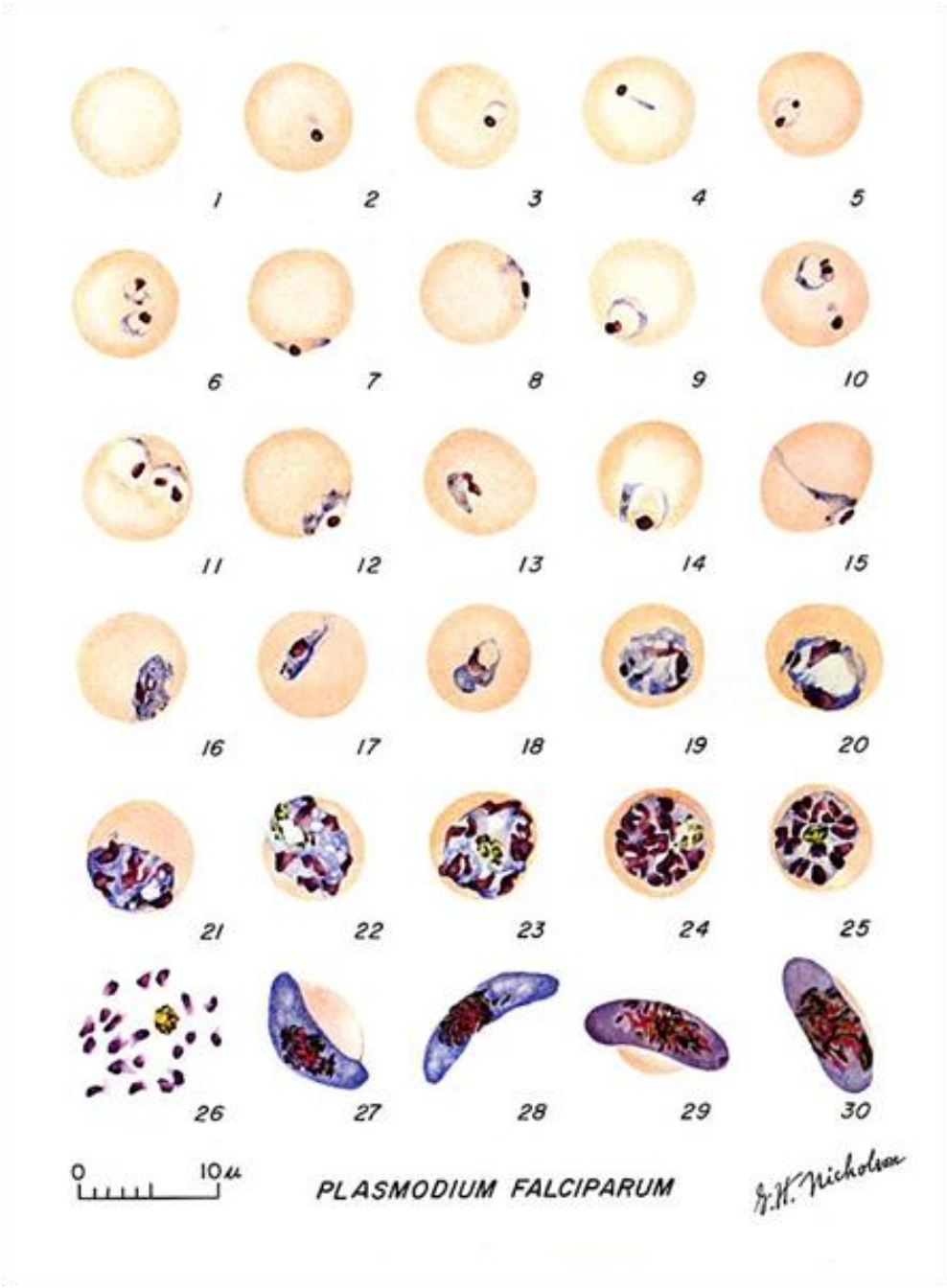


Figure 2.1: The various intraerythrocytic developmental stages of *P. falciparum*. With number 1 depicting an uninfected red blood cell, and numbers 2-10, 11-18, 19-26, 27-10 representative of the ring-, trophozoite-, schizont- and sexual stages, respectively (Centres for Disease Control and Prevention, 2009).

2.1.2 Synchronisation of the culture

P. falciparum maintained *in vitro* loses its natural synchronisity seen *in vivo* (Lambros *et al*., 1979). In order to establish a synchronised culture, for experimental purposes, the culture was treated with 5% (w/v) D-sorbitol (Section 2.1.4) when predominantly in the early ring-stage (Figure 2.1, numbers 2-5). Sorbitol enters red blood cells via new permeation pathways inserted into the red blood cell membrane at the end of the ring/early trophozoite-stage (Wagner *et al*., 2003). In this respect, negligible amounts of sorbitol will enter a ring-infected red blood cell, whereas sorbitol readily enters trophozoite and schizont infected red blood cells resulting in osmotic lysis (Wagner *et al*., 2003).

Culture synchronisation was carried out by transferring the parasite suspension to a 50 ml centrifuge tube and centrifuging it at 1500 rpm for 5 minutes, following which the supernatant was aspirated and replaced with 20 ml of D-sorbitol (Section 2.1.4). Subsequent to a 20 minute incubation period at room temperature, the suspension was centrifuged at 1500 rpm for 5 minutes and the supernatant aspirated. Complete culture media (Section 2.1.6) was added, the culture transferred back to a culture flask, gassed, and incubated at 37 °C.

2.1.3 Preparation of incomplete experimental and culture media

The incomplete experimental media was prepared as follows: 10.4 g RPMI-1640 (Gibco), 5.9 g HEPES buffer (Sigma), 4.0 g D-glucose (Merck) were dissolved in 1 litre of MilliQ™ water and sterile filtered through a 0.22 µm Millipore™ filter unit. The media was stored at 4 °C until needed. Incomplete culture media was prepared as above, with the addition of 100 µl 50 mg/ml gentamicin sulphate (Sigma) and 44 mg hypoxanthine (Sigma).

2.1.4 Preparation of sodium bicarbonate and sorbitol solutions

The 5% (w/v) solutions of sodium bicarbonate and D-sorbitol were prepared by dissolving 50 g sodium bicarbonate (Saarchem) and 50 g D-sorbitol (Sigma), respectively, in 1 litre MilliQ™. The solutions were then sterile filtered through a 0.22 µm Millipore™ filter unit and stored at 4 °C until needed.

2.1.5 Preparation of human plasma

Six bags of human plasma (South African National Blood Services) were thawed at 4 °C and heat inactivated at 56 °C for 2 hours. The plasma was then centrifuged at 3000 revolutions per minute (rpm) for 10 minutes. Following which, the supernatant was aliquoted into sterile 50 ml tubes and stored at -20 °C until required.

2.1.6 Preparation of complete experimental and culture media

To prepare complete experimental and culture media, 10 ml of heat-inactivated human plasma and 4.2 ml of the 5% (w/v) sodium bicarbonate stock solution were added to either incomplete experimental or culture media (Section 2.1.3) up to a final volume of 100 ml.

2.1.7 Preparation of phosphate buffered saline

To prepare phosphate buffered saline (PBS, pH 7.5); 8.0 g NaCl (Saarchem), 0.3 g KCl (Sigma), 0.73 g $Na_2HPO_4.2H_2O$ (Merck) and 0.2 g KH_2PO_4 (Fluka) were dissolved in 1 litre of MilliQ™ water and autoclaved at 120 °C for 20 minutes. The solution was stored at 4 °C until needed.

2.1.8 Preparation of erythrocytes

Whole blood, collected from volunteers (Ethical clearance number: M090532, Appendix B2), was stored in anticoagulant tubes (BD) containing acid citrate dextrose-B and centrifuged at 2000 rpm for 5 minutes to separate it into its components. The supernatant and buffy coat were aspirated and the erythrocyte-containing pellet re-suspended in sterile PBS (Section 2.1.7), this was repeated a total of three times. Following this, the pellet was re-suspended in an equal volume of incomplete experimental media and stored at 4 °C for a maximum of a week. Although the pellet would have contained a small percentage of reticulocytes (0.5-1.4%) (d'Onofrio *et al*., 1995), reticulocytes mature into erythrocytes in approximately 2-3 days *in vitro*, with the reticulocyte population halving after only 12 hours in culture (Gronowicz *et al*., 1984; Koury *et al*., 2004). In this respect, the term 'erythrocytes' will be used in this study, with the exception of the red blood cell toxicity assay (Section 2.4.2) in which blood no older than two days was utilised, as the term 'red blood cells' encompasses both erythrocytes and reticulocytes.

2.2 Antimalarial activity

2.2.1 Preparation of the test solutions

The novel test compounds were prepared to 10 mM stock concentrations in either autoclaved MilliQ™ water or dimethyl sulfoxide (DMSO; Merck), depending on the polarity of the compounds, as determined by examining the individual chemical structures. In the case of compounds soluble in water, a small volume of DMSO (< 10% final concentration of DMSO) was added to ensure sterility. In some instances, the solutions were heated for approximately 30 seconds in boiling water and vortexed vigorously as they did not go into solution initially. Positive controls included quinine hydrochloride (Sigma) and chloroquine diphosphate (Sigma), solubilised in autoclaved MilliQ™ water and sterilised through a 0.22 µm Acrodisc™ filter; as well as artemisinin (Sigma) and dihydroartemisinin (Sigma) solubilised in DMSO, all prepared to 10 mM stock concentrations. Both the test compounds and positive controls were stored at -20 °C until needed.

2.2.2 The [^{3}H]-hypoxanthine incorporation assay

P. falciparum is incapable of *de novo* purine synthesis, and through specialised transporters and enzymes the parasite scavenges and metabolises host-derived purines (Desjardins *et al*., 1979; Smeijsters *et al*., 1999; El Bissati *et al*., 2006). The major route of purine salvage is the conversion of adenosine into hypoxanthine, which is then incorporated into parasitic DNA during the trophozoite- and schizont-stages (Chulay *et al*., 1983; Smeijsters *et al*., 1999; El Bissati *et al*., 2006). Incorporation of the [^{3}H]-hypoxanthine isotope into parasitic DNA provides a direct measure of the number of parasitised red blood cells in the culture, thereby providing a way to quantify parasite growth (Desjardins *et al*., 1979; Chulay *et al*., 1983).

2.2.2.1 Experimental protocol

For the initial drug screenings, 1 mM and 10 µM working solutions of the test compounds and positive controls, respectively, were prepared in incomplete experimental media. Therafter, the working solutions were serially diluted in a 1:10 ratio, in incomplete experimental media, to achieve final screening concentrations of 100 µM, 10 µM, 1 µM, 0.1 µM and 0.01 µM for the test compounds and 1000 nM, 100 nM, 10 nM, 1 nM and 0.1 nM

for the positive controls (taking into account the 10 times dilution factor of the experiment). All dilutions were plated out in triplicate in a sterile 96-well microtitre plate (Techno Plastic Products), so that each well contained 25 µl of the test compound/positive control, with the exception of the parasite and erythrocyte control wells, to which 25 µl incomplete experimental media was added. Following the initial screening, the concentrations were adjusted so as to achieve an optimal sigmoid dose-response curve. Synchronised ring-stage parasites, adjusted to a final parasitaemia of 0.5% and haematocrit of 1% in complete experimental media were added (200 µl) to each well of the 96-well plate; with the exception of four wells that received non-parasitised erythrocytes (1% haematocrit), which served as a negative erythrocyte control (Figure 2.2) (Desjardines *et al*., 1979).

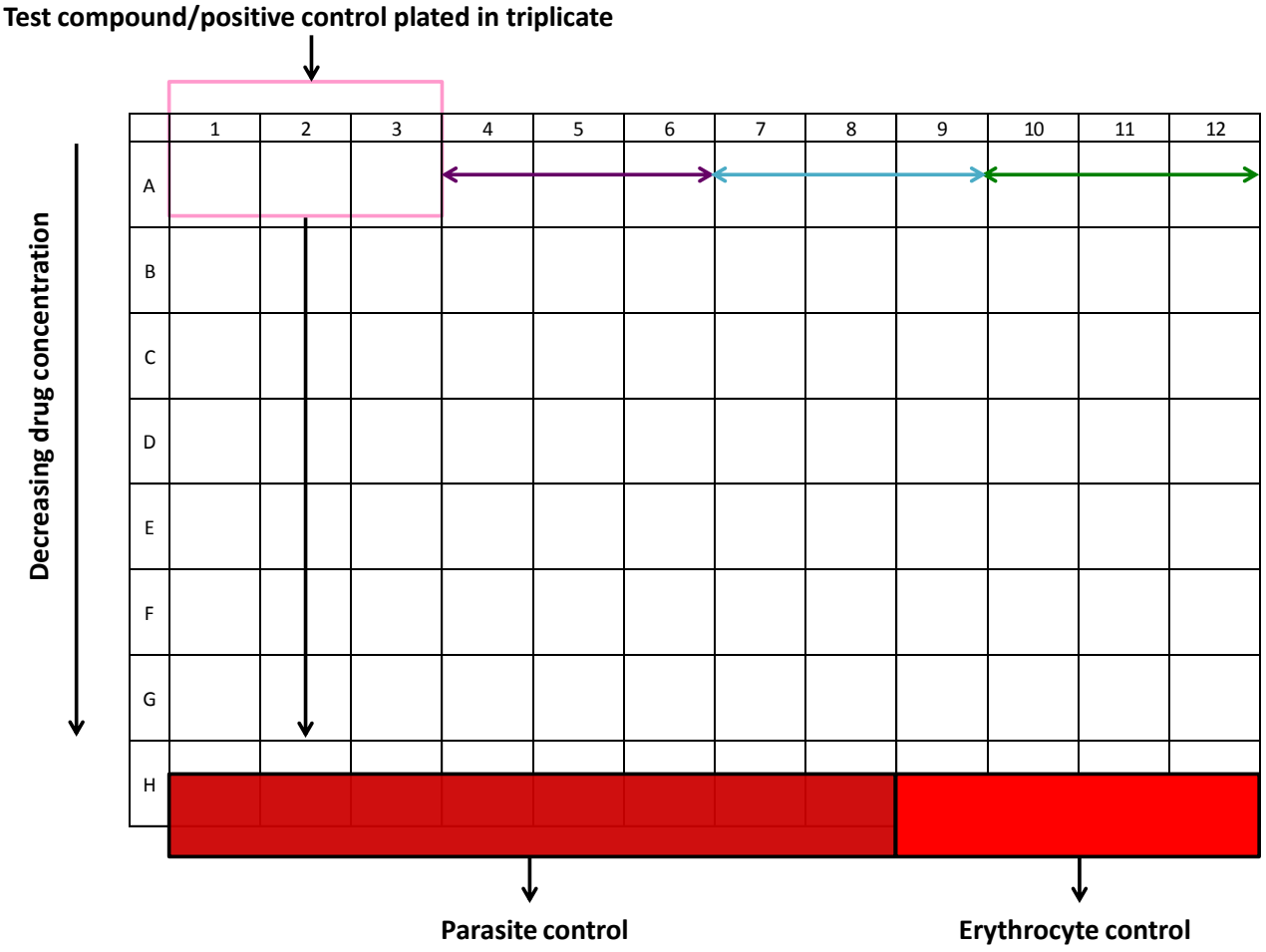


Figure 2.2: Microtitre plate layout used for IC_{50} value determination in the [^{3}H]-hypoxanthine incorporation assay.

The plate was then incubated for 24 hours at 37 °C in a humidifed glass dessicator, to which a lit candle was added, in order to produce an oxygen-deficient (approximately 3% O_2) environment (Jensen and Trager, 1977). Thereafter, 25 µl of the radiolabeled [^{3}H]-hypoxanthine isotope (185 MBq/5 mCi, Amersham), diluted in incomplete experimental media (10 µl:2.7 ml), was added to each well, and the plate returned to the candle jar for a further 24 hour incubation period. The parasitic [^{3}H]-DNA was then harvested onto glass fibre filter mats (Wallac™) using a Titertek® semi-automatic cell harvester. The filter mats, left to air dry overnight were transferred to sample bags to which 10 ml liquid beta scintillation fluid (Wallac™) was added. Incorporation of the [^{3}H]-hypoxanthine isotope into the parasitic DNA was quantified using a Wallac™ beta scintillation counter, and expressed as counts per minute (cpm).

The percentage parasite growth was calculated using the formula below:

$$\% \text{ Parasite growth} = \frac{\text{Compound (cpm)} - \text{mean erythrocyte control (cpm)}}{\text{Mean parasite control (cpm)} - \text{mean erythrocyte control (cpm)}} \quad (\times 100\%)$$

2.2.2.2 Data analysis

Log sigmoid dose response curves were constructed by plotting the % parasite growth versus the log of the drug concentration, using the Enzfitter® (version 1.05) software, from which IC_{50} values (concentration required to inhibit parasite growth by 50%) were determined. For compounds exhibiting little or no antimalarial activity, the % inhibition of parasite growth at 100 µM was calculated. All experiments were repeated at least in triplicate to produce a mean ± standard deviation. In order to determine if there was a statistically significant difference between a test compound and positive control, an unpaired Students T-test was executed using the Graphpad Prism® (version 5) software, with a p value of less than 0.05 considered statistically significant. In the case of some compounds, a correlation between antimalarial activity and antimalarial mechanisms of action (Section 2.3) was determined using linear regression, with a 95% confidence interval.

2.2.2.3 Combination studies

The use of combination therapies to curb the emergence of resistant organisms and ensure successful treatment, has long been applied to the treatment of many diseases such as tuberculosis and HIV/AIDS, and has also become pivotal in antimalarial chemotherapy (Nosten and Brasseur, 2002; Kremsner and Krishna, 2004). An ideal antimalarial combination would be one where there is a synergistic interaction between the two drugs, so that the doses of the individual drugs needed to produce the same overall effect may be reduced. Conversely, an antagonistic interaction is regarded as unfavourable as it would result in treatment failure (Nosten and Brasseur, 2002; Bell, 2005).

The most active compound(s) from each drug class were combined with quinine or dihydroartemisinin, and by means of the tritiated hypoxanthine incorporation assay (Section 2.2.2.1) their pharmacological interactions assessed. Solutions of the test compound and quinine/dihydroartemisinin were prepared at concentrations 20 times higher than the final concentration required in the experiment, in order to account for the 10 times dilution factor of the tritiated hypoxanthine assay (Section 2.2.2.1) and 2 times dilution factor generated by combining equal volumes of the test compound and quinine/dihydroartemisinin.

The two drugs were combined in various ratios (10:0, 9:1, 8:2, 7:3, 6:4, 5:5, 4:6, 3:7, 2:8, 1:9, 0:10) and serially diluted seven times, from which log sigmoid dose response curves were constructed. From the dose response curves, IC_{50} values (Section 2.2.2.2) for the drug alone and the drug in combination were obtained and relative ratios or fractional IC_{50} values (FIC_{50}) calculated using the formula below:

$$FIC_{50}\text{ value} = \frac{IC_{50}\text{ value of compound in combination}}{IC_{50}\text{ value of compound alone}}$$

The FIC_{50} values were plotted, from which an isobologram was generated. The degree of the interaction, which is equivalent to the sum of the FIC_{50} values (ΣFIC_{50}) for the test compound and quinine/dihydroartemisinin at each combination ratio, was then calculated (Berenbaum, 1978). The cut-off points used to define the possible interactions differ amongst authors, therefore, for the purpose of this study a $\Sigma FIC_{50} < 0.5$ indicates synergism,

a 0.5 < ΣFIC_{50} < 2 indicates an additive relationship, and a ΣFIC_{50} > 2 indicates antagonism (Figure 2.3) (Fidock *et al*., 2004).

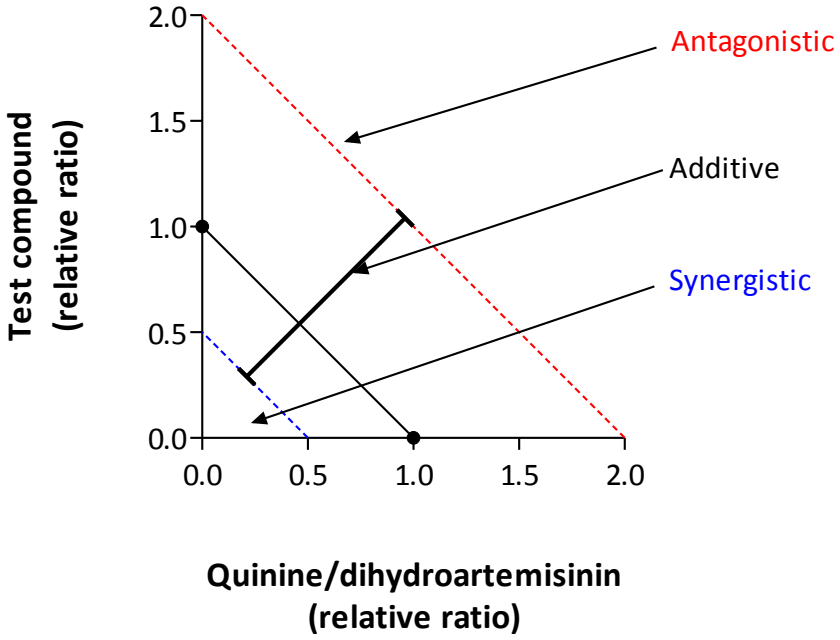


Figure 2.3: The cut-off points for possible drug interactions between quinine/dihydroartemisinin and a test compound.

2.2.3 The use of flow cytometry to assess *in vitro* parasite growth

Widely-used techniques for the assessment of parasite growth include microscopic examination of Giemsa-stained blood smears, as well as the tritiated hypoxanthine incorporation and parasite lactate dehydrogenase assays (Scott *et al*., 2002; Bennett *et al*., 2004; Grimberg *et al*., 2008). There are limitations to all three methodologies. Microscopic examination of blood smears is time consuming and prone to human error; the tritiated hypoxanthine incorporation assay requires the use of costly radioactive material and provides no information on the stage-specific activity of drugs; and lastly, the lactate dehydrogenase assay requires multiple processing steps and only measures metabolic activity in the latter half of the parasitic asexual life cycle (Bennett *et al*., 2004; Grimberg *et al*., 2008). A rapid, sensitive and stage-specific technique for the screening of potential antimalarial drugs would be invaluable in antimalarial drug development.

Flow cytometry technology was developed during the Second World War as a means to detect anthrax spores (Grimberg, 2011). Since then, there has been a rapid technological progression to include a wide range of applications such as drug screening, receptor pharmacology, protein expression systems and signalling pathways, together with improved instrument sensitivity (Nolan *et al*., 1999; Waller *et al*., 2004; Sklar *et al*., 2007). The modern flow cytometer is capable of analysing up to 50 000 cells per second, based on size, morphology and fluorescence of the probe or dye (Nolan *et al*., 1999; Waller *et al*., 2004; Sklar *et al*., 2007). Flow cytometric probes extend beyond conjugated antibody's to include dyes which show increased fluorescence upon interaction with a target, such as DNA (Nolan *et al*., 1999; Waller *et al*., 2004; Sklar *et al*., 2007).

The use of flow cytometry and fluorescent DNA dyes has been well documented in the analysis of the cell cycle of mammalian cells, and has since extended into the study of the intra-erythrocytic growth of the malaria parasite (Whaun *et al*., 1983; Hare and Bahler, 1986). The use of DNA dyes to study intra-erythrocytic parasite growth works on the principle that uninfected erythrocytes do not contain DNA, whereas parasitised erythrocytes do, and upon addition of a DNA dye will fluoresce upon exposure to a certain wavelength of light (Whaun *et al*., 1983; Waki *et al*., 1986; Grimberg *et al*., 2008). The intensity of fluorescence equates to the amount of DNA present, and therefore the stage of the erythrocytic life cycle (Whaun *et al*., 1983; Waki *et al*., 1986; Grimberg *et al*., 2008). The ratio of erythrocytes staining positive for DNA to the total number of erythrocytes in the sample provides a percentage parasitaemia (Grimberg, 2011). Thereby providing a means in which both quantitative and qualitative results may be obtained (Whaun *et al*., 1983).

Several DNA dyes have been examined for use in the detection of the malaria parasite, including: Hoechst 33258, acridine orange, thiazole orange, propidium iodide, and hydroethidine (Wyatt *et al*., 1991; van Vianen *et al*., 1993; Grimberg *et al*., 2011). Hoechst 33258 is a DNA binding dye with selectivity for AT regions, making it ideal for the detection of the AT rich malaria parasite (Grimberg, 2011). However, it requires excitation by an ultraviolet laser (van Vianen *et al*., 1993; Grimberg, 2011), which is not standard in most flow cytometers available for use. Acridine orange is capable of binding to both DNA and RNA, emitting green and red fluorescence, respectively, thereby permitting two-colour analysis (Whaun *et al*., 1983; Hare and Bahler, 1986; Grimberg, 2011). It was excluded as a

potential fluorochrome on the basis that it quenches upon nucleic acid binding and accumulates in acidic compartments due to its weak base properties, forming aggregates which fluoresce red, thereby interfering with RNA detection (Wissing *et al*., 2002; Grimberg, 2011). Furthermore, single-stranded and denatured DNA also fluoresce red following staining with acridine orange, all of which provide difficulty in quantifying DNA and RNA (Grimberg, 2011).

As no flow cytometric protocol was available in the department, a method was developed, and validated, to assess overall percentage parasitaemia, identify the various asexual intraerythrocytic parasitic stages, as well as the percentage of parasites in each stage.

2.2.3.1 Method development

2.2.3.1.1 Thiazole orange as a potential fluorochrome

Thiazole orange is a membrane-permeable nucleic acid dye which primarily stains RNA, by intercalating into AU doublets, and has been used primarily to detect reticulocytes in blood samples (Makler *et al.*, 1987; Grimberg, 2011). A methodology for fixing the samples prior to staining with thiazole orange has been previously described (Schulze *et al*., 1997). This methodology was selected for this study, thus allowing for samples to be analysed in large batches and at a more convenient time, according to the availability of the flow cytometer.

In order to set up a protocol wherein the various stages of the parasitic life cycle and percentage parasitaemia could be detected, samples of ring-, trophozoite- and schizont-staged parasites were initially prepared to a stock culture of a 10% haematocrit and 8% parasitaemia. With a 10% haematocrit uninfected erythrocyte solution also being prepared to act as a diluent, as well as the uninfected erythrocyte control. Both solutions were prepared in complete experimental media (Section 2.1.6). The stock culture was then serially diluted with the uninfected erythrocyte suspension, in order to maintain the 10% haematocrit, and achieve parasitaemias of 4, 2 and 1%. Duplicate samples were prepared so that the flow cytometry results could be verified from Giemsa-stained blood smears and parasite counts, wherein the overall % parasitaemia was determined by counting 1000 erythrocytes or 10 microscope fields.

The samples were then fixed in the following solution: a Tris-saline buffer consisting of 10 mM (hydroxymethyl)aminomethane (TRIS; Saarchem), 150 mM NaCl (Saarchem) and 10 mM sodium azide (Sigma); to which 37.23% formaldehyde (Calbiochem) and D-glucose (Saarchem) were added, in order to achieve a 10% formaldehyde and 4% D-glucose fixing solution (Schulze *et al*., 1997). The pH of the solution was then adjusted to 7.3, in order to prevent lysis of the erythrocytes, before being filtered through a 0.22 µm Millipore™ filter, and stored at 4 °C until needed. Fixing solution (100 µl) was added to 100 µl of the sample, so that the final haematocrit was reduced to 5%, whilst the percentage parasitaemia of the samples remained unchanged. The samples were then stored at 4 °C for 18 hours or longer, before being analysed.

The 10 mM thiazole orange (Sigma) stock solution was prepared in DMSO and kept wrapped in foil at -20 °C until needed. For the flow cytometric analysis, a working solution of 1 µM thiazole orange in sterile PBS (Section 2.1.7) was prepared. A 50 µl sample was added to 1 ml working solution and incubated at room temperature in the dark, for an hour. Thereafter, the samples were transferred to flow cytometric tubes (Becton, Dickinson and Company) and read on a Becton, Dickinson and Company (BD) FACSCalibur™ flow cytometer, with argon laser excitation at 488 nm and detection at 533 nm, located in the Department of Surgery, 9th Floor of the University of the Witwatersrand Medical School. A total of 50 000 cells per sample were counted and analysed using BD CellQuest Pro™ and FlowJo software (Version 7.6.1, under licence from Tree Star Inc, serial numbers: gQQ3Gy1i&8-TgZ0E, d5T@C1sMWM34tU01, validity: 07/10/2010-07/10/2012) (Figure 2.4).

❖ **Troubleshooting**

However, upon analysis of the samples several problems were identified, with the following steps taken to correct them:

A large amount of erythrocyte lysis was noted in the supernatant of the samples following a 24 hour incubation period in the fixative solution. Therefore, the percentage of formaldehyde in the fixing solution was reduced to 5%, whereupon cell lysis, although to a lesser degree, was still observed. To determine if the sodium azide present in the fixing solution was the causative factor of the lysis, the Tris-saline buffer was replaced with sterile PBS; however lysis was still observed. As an alternative, a fixing solution of 2%

formaldehyde was prepared, whereupon no lysis was observed. However, examination of the blood smears showed that the parasites in the sample had progressed into the next stage of the life cycle, despite the samples being stored at 4 °C. To determine whether a reduction in the amount of cells to fixing solution would decrease the amount of lysis, samples were then prepared to a final haematocrit of 1%, whilst the % parasitaemias remained as previously described. The degree of lysis in a 5% formaldehyde fixing solution decreased. However, upon flow cytometric analysis of the samples, a lack of discrimination between the unparasitised and parasitised erythrocyte populations was noted, exhibiting similar results to samples prepared to a 5% haematocrit. Furthermore, the acquisition time per sample was approximately three minutes, making a 1% haematocrit parasite solution unsuitable for high-throughput screening.

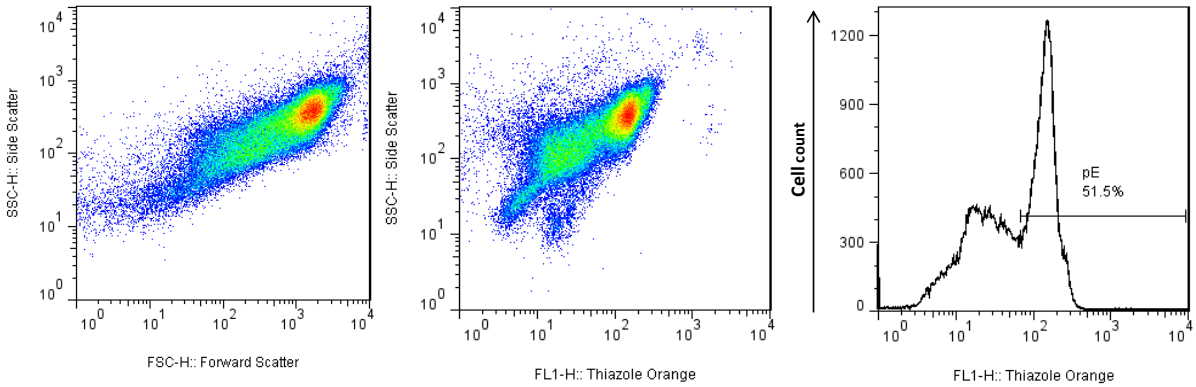


Figure 2.4: Flow cytometric analysis of a fixed sample of late rings/early trophozoites at a 5% haematocrit and 8% parasitaemia, stained with thiazole orange. Where: a = a dot-plot of the size (forward scatter) versus the granularity (side scatter) of the erythrocytes; b = dot-plot of the maximal fluorescence of thiazole orange (FL1-H) versus the granularity of the erythrocytes; c = histogram of maximal fluorescence of thiazole orange versus the cell count, where pE = % parasitised erythrocytes.

The wide distribution of cells in the forward scatter axis (Figure 2.4a), indicated a range of different sized cells, which could have been due to cell aggregation, as a result of formaldehyde treatment (Deitch *et al*., 1982). The lack of discrimination between

unparasitised and parasitised erythrocyte populations (Figure 2.4b), wherein the parasitaemia as determined by flow cytometry and microscopic analysis were 51.5% (Figure 2.4c) and 7.57%, respectively, may be attributed to the indiscriminate staining of cell debris and parasitic DNA remnants or the induction of auto-fluorescence in fixed erythrocytes (Deitch *et al*., 1982; Grimberg, 2011). Furthermore, formaldehyde treatment may have interfered with the uptake of the thiazole orange or altered the emission spectra of the dye, as observed with the antibody-conjugated fluorochrome, allophycocyanin (APC) (Deitch *et al*., 1982; BD, 2011).

A study conducted by Apte *et al*. (2011), wherein *Plasmodium*-infected blood was fixed in various concentrations of paraformaldehyde and stained with the DNA dye, 4', 6-diamidino-2-phenylindole (DAPI), found that fixation resulted in a loss of side and forward scatter properties of unparasitised red blood cells, when compared to unfixed samples, and attributed it to a loss of cytosolic components and haem. The study concluded that a reliable method for parasite detection would require a one-step fixation and lysis. However, cell lysis was not an option in this study, as it could result in inaccurate determination of overall % parasitaemia, with the calculation of % parasitaemia reliant on the ratio of infected to uninfected erythrocytes.

As a result, the fixing step was then disregarded and unfixed samples were stained with thiazole orange, whereupon two separate populations could be visualised. However, the % parasitaemia as per flow cytometric analysis was higher than those ascertained from microscopic analysis, especially at low % parasitaemias, where the overall % parasitaemia as determined by flow cytometry and microscopic analysis was 2.95% and 0.87%, respectively. This could not be attributed to the co-staining of the RNA in reticulocytes, which have been shown to degrade after approximately 20 hours in cultured mammalian reticulocytes (Koury *et al*., 2005), or any whole blood remnants present in the sample. The effect may have been attributed to the indiscriminate staining of other cellular components containing DNA or RNA (Scott *et al*., 2002). Alternatively, it may have been due to the staining of the erythrocyte membrane upon standing of the sample (S. Lauterbach; personal communication). With a sample of uninfected erythrocytes exhibiting thiazole orange fluorescence and erroneously reflecting a parasitaemia of 1.77% (Figure 2.5), which

would result in over-estimated overall % parasitaemias, particularly in large batches of samples.

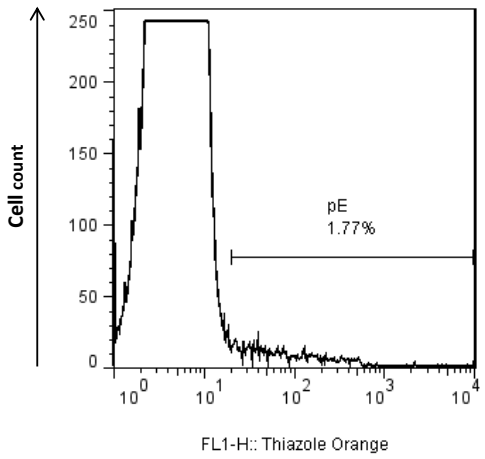


Figure 2.5: Histogram of the maximal fluorescence of thiazole orange (FL1-H) versus cell count of an unfixed sample of uninfected erythrocytes, adjusted to a 5% haematocrit.

To compare instrument sensitivity, both fixed and unfixed samples (Figure 2.6) were then analysed on a Beckman Coulter Inc. (BC) FC 500 flow cytometer using CXP (version 2.2) software, located in the Department of Molecular Medicine and Haematology, 7th Floor, University of the Witwatersrand Medical School.

Although two cell populations were visible in a dot-plot of complexity versus size in the samples fixed with a 5% formaldehyde solution (Figure 2.6a), the larger population appeared to be cell debris, and gating of the smaller population (Figure 2.6, Region A) produced no cells staining positive for thiazole orange (Figure 2.6b, Region E).

In contrast, the unfixed samples exhibited a uniform distribution of cells in a dot-plot of complexity versus size (Figure 2.6c); as well as complete separation of the unparasitised and parasitised erythrocyte populations (Figure 2.6d, Region E). Furthermore, the overall % parasitaemia and % of parasites in each stage as determined by flow cytometric and microscopic analysis were similar; 8.68%, composed of 53% rings and 47% trophozoites, compared to 8.20%, composed of 46% rings and 54% trophozoites, respectively.

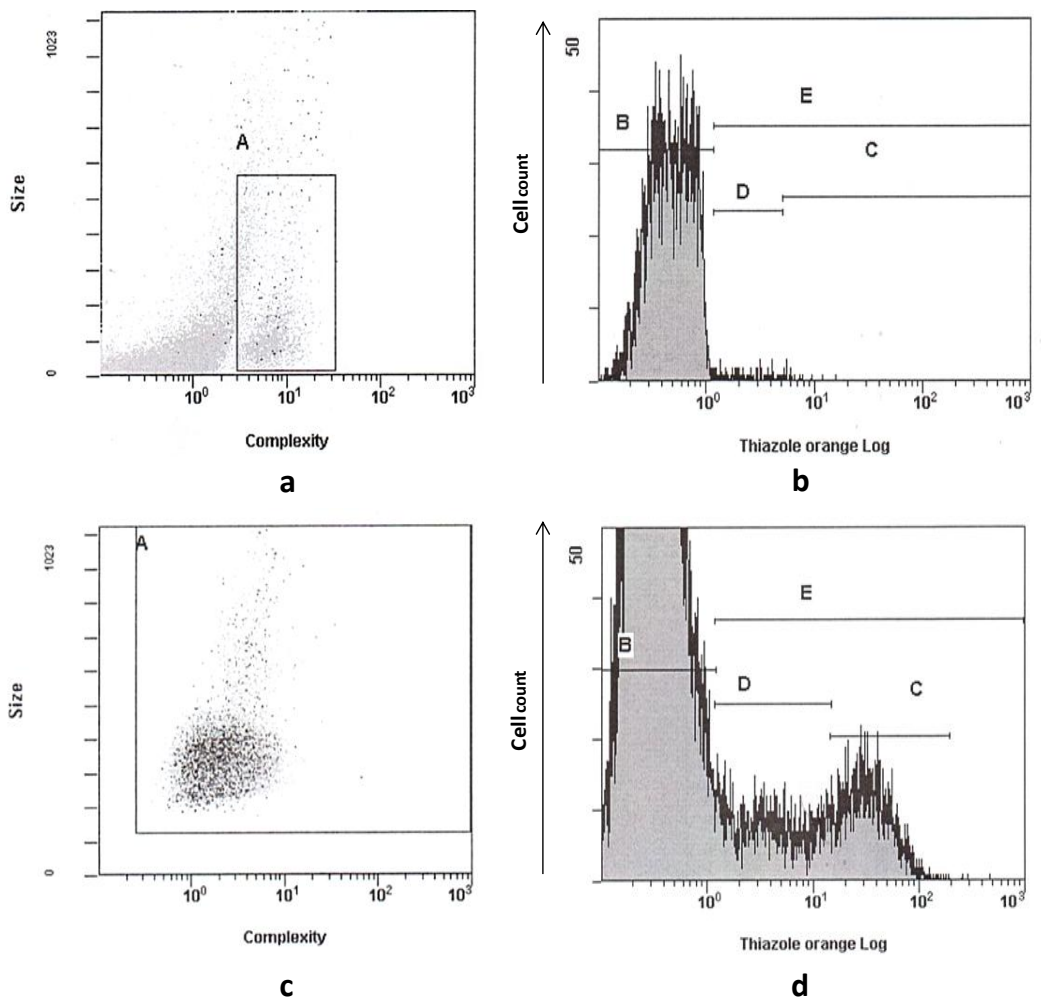


Figure 2.6: Flow cytometric analysis of samples consisting of fixed trophozoites (a and b) and unfixed rings and trophozoites (c and d), at a 5% haematocrit and 8% parasitaemia, stained with thiazole orange, and read on a BC FC 500 flow cytometer. Where: a and c are dot-plots of the granularity (side scatter) versus the size (forward scatter) of the erythrocytes; b and d are histograms of thiazole orange fluorescence versus cell count, wherein gate E = overall % parasitaemia, D = ring-stage parasites and C = trophozoite- and schizont-stage parasites.

However, the availability of the BC FC 500 flow cytometer was highly limited, and due to the fact that the fixing of samples was not a viable option, another nucleic acid dye was identified for the assessment of parasite growth using the BD FACSCalibur™ flow cytometer.

2.2.3.1.2 Propidium iodide as a potential fluorochrome

Propidium iodide is a membrane-impermeable nucleic acid dye used primarily in flow cytometric cell viability and apoptosis studies to distinguish dead from live cells and necrotic from apoptotic cells, respectively (Jouin *et al*., 2004) and has been previously used to assess *in vitro* drug sensitivity on *P. falciparum* (Pattanapanyasat *et al.*, 1997).

Flow cytometric samples of a 5% haematocrit and 8, 4, 2 and 1% ring-, trophozoite- and schizont-staged parasites were prepared (Section 2.2.3.1.1), with a duplicate sample for microscopic analysis. To ensure that the dye could penetrate infected erythrocytes, the erythrocyte membrane was made permeable by fixing the samples in a 1% formaldehyde sterile PBS solution. A 10 mM stock solution of propidium iodide (Sigma) was prepared in autoclaved MilliQ™ water, wrapped in foil and stored at -20 °C until required. The staining methodology utilised was that as described by Pattanapanyasat *et al*. (1997), wherein the samples were washed with sterile PBS prior to the transfer of 50 µl of each sample to a 1 ml working solution of propidium iodide in sterile PBS (14 µM). The samples were left to stand in the dark at room temperature for an hour, before being transferred to flow cytometric tubes (BD). The samples were then read on a BD FACSCalibur™ flow cytometer, with argon laser excitation at 488 nm and detection at 617 nm, with a total of 50 000 cells per sample counted and analysed using BD CellQuest Pro™ and FlowJo (version 7.6.1) software (Figure 2.7).

❖ **Troubleshooting**

The wide range of cells of different sizes observed in Figure 2.7a was similar to Figure 2.4a, reflecting the effect of formaldehyde treatment on cells, even at a concentration as low as 1%. A slight separation between unparasitised and parasitised erythrocyte populations was visible in Figure 2.7b, as opposed to Figure 2.4b. However, the % overall parasitaemia as determined by flow cytometry (Figure 2.7c) and microscopic analysis was 10.4% and 6.68%, respectively.

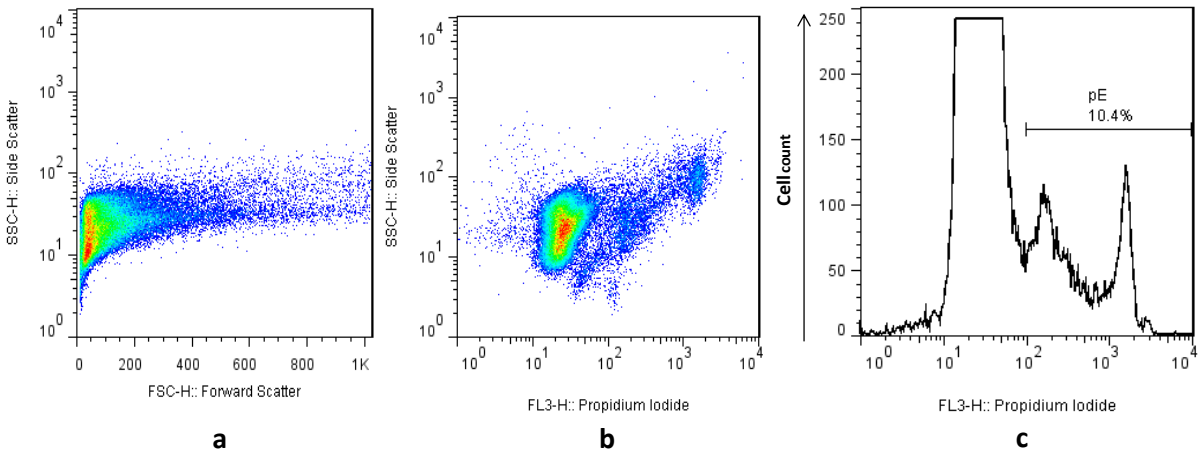


Figure 2.7: Flow cytometric analysis of a sample containing ring-, trophozoite- and schizont-stage parasites, at a 5% haematocrit and 8% parasitaemia, stained with propidium iodide. Where: a = dot-plot of the size (forward scatter) versus the granularity (side scatter) of the erythrocytes; b = dot-plot of the maximal fluorescence of propidium iodide (FL3-H) versus the granularity of the erythrocytes (side scatter); c = histogram of maximal fluorescence of propidium iodide versus cell count.

Discrepancies between % parasitaemias as determined by flow cytometric and microscopic analysis have been previously reported, with flow cytometric analysis generally producing an assessment that is 1.2-fold higher than that determined microscopically (Apte *et al*., 2011). With this effect possibly due to haemolysis of uninfected erythrocytes during flow cytometric sample preparation or the loss of infected erythrocytes during blood smear preparation (Apte *et al*., 2011).

However, the overall % parasitaemia as determined by flow cytometric analysis was far greater than 1.2-fold as determined microscopically, and could not be solely attributed to these factors. Yet it may be as a result of formaldehyde treatment in the permeabilisation step. Propidium iodide has shown to lack the fluorescent intensity needed to overcome auto fluorescence induced by formaldehyde treatment, resulting in an incomplete separation of uninfected and infected populations, particularly in samples of ring-stage parasites, which contain small amounts of DNA and at low parasitaemias (Grimberg, 2011).

The discrepancy may also have been as a result of indiscriminate staining of cell debris due to over-staining. However, the same effect was observed when the incubation time was reduced to 30 minutes and 5 minutes. Furthermore, the methodology proved to be unreproducible, with parameters having to be re-adjusted for each experiment.

Propidium iodide is useful in the detection of dead versus live cells, in the absence of fixatives or membrane permeabilisation. However, in this context, its use is hampered by the fact that permeabilisation of membranes by fixatives such as formaldehyde, glutaraldehyde, ethanol, or methanol results in the induction of auto fluorescence and cell aggregation (Grimberg, 2011), and also allows for the indiscriminate staining of DNA of both live and dead parasites, which may skew results when using this stain for IC_{50} value determination.

2.2.3.1.3 Hydroethidine as a potential fluorochrome

Hydroethidine is a membrane permeable dye that is oxidised by dehydrogenase enzymes into ethidium, only in viable cells. The cationic nature of ethidium results in it being trapped intracellularly where it intercalates into DNA and fluoresces red upon excitation (Figure 2.8) (Olive, 1989; Grimberg, 2011).

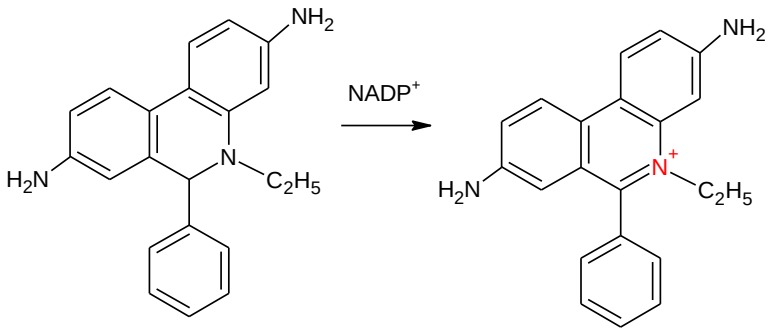


Figure 2.8: The oxidation of hydroethidine by parasitic dehydrogenases to form ethidium which, upon intercalation into parasitic DNA, fluoresces red (Olive, 1989).

The initial use of hydroethidine, to detect superoxide anions has extended into the assessment of the *in vitro* growth of intraerythrocytic parasites, including *P. falciparum* (Wyatt *et al*., 1991; van der Heyde *et al*., 1995; Grimberg, 2011). The selectivity of this

fluorochrome for only viable parasites is highly beneficial in that erythrocytes containing viable parasites can not only be distinguished from unparasitised erythrocytes, but also from erythrocytes containing dead parasites (Wyatt *et al*., 1991).

Three separate suspensions containing predominantly ring-, trophozoite-, and schizont-staged parasites were prepared (Section 2.2.3.1.1), in duplicate, to achieve samples of a 5% haematocrit and parasitaemias of 8, 4 and 2%. A 1% parasitaemia sample was not prepared, as counting of parasitised erythrocytes in blood smears proved to be time consuming, making a protocol based on a 1% parasitaemia impractical.

The stock solution (10 mM) of dihydroethidium (Sigma) was prepared in DMSO, wrapped in foil and stored at -20 °C until needed. The staining methodology of Wyatt *et al*. (1991) was followed. The samples were centrifuged at 1500 rpm for 5 minutes, the supernatant removed and replaced with 1 ml dihydroethidium in PBS (159 µM), and the pellet resuspended. The samples were left to incubate in the dark, at 37 °C for 20 minutes; thereafter the samples were washed three times in sterile PBS and resuspended in 1 ml sterile PBS for analysis. The samples were transferred to flow cytometric tubes (BD) and read on a BD FACSCalibur™ flow cytometer, with argon laser excitation at 488 nm and detection at 610 nm, a total of 50 000 cells per sample were counted and analysed using BD CellQuest Pro™ and FlowJo (version 7.6.1) software (Figure 2.9a-c).

For comparative purposes, fixed samples were also prepared and stained with dihydroethidium prior to fixation in a 5% formaldehyde Tris-saline buffer solution (Section 2.2.3.1.1). Following a 24 hour incubation period at 4 °C, the samples were washed and resuspended in 1 ml sterile PBS for analysis (Figure 2.9d-f).

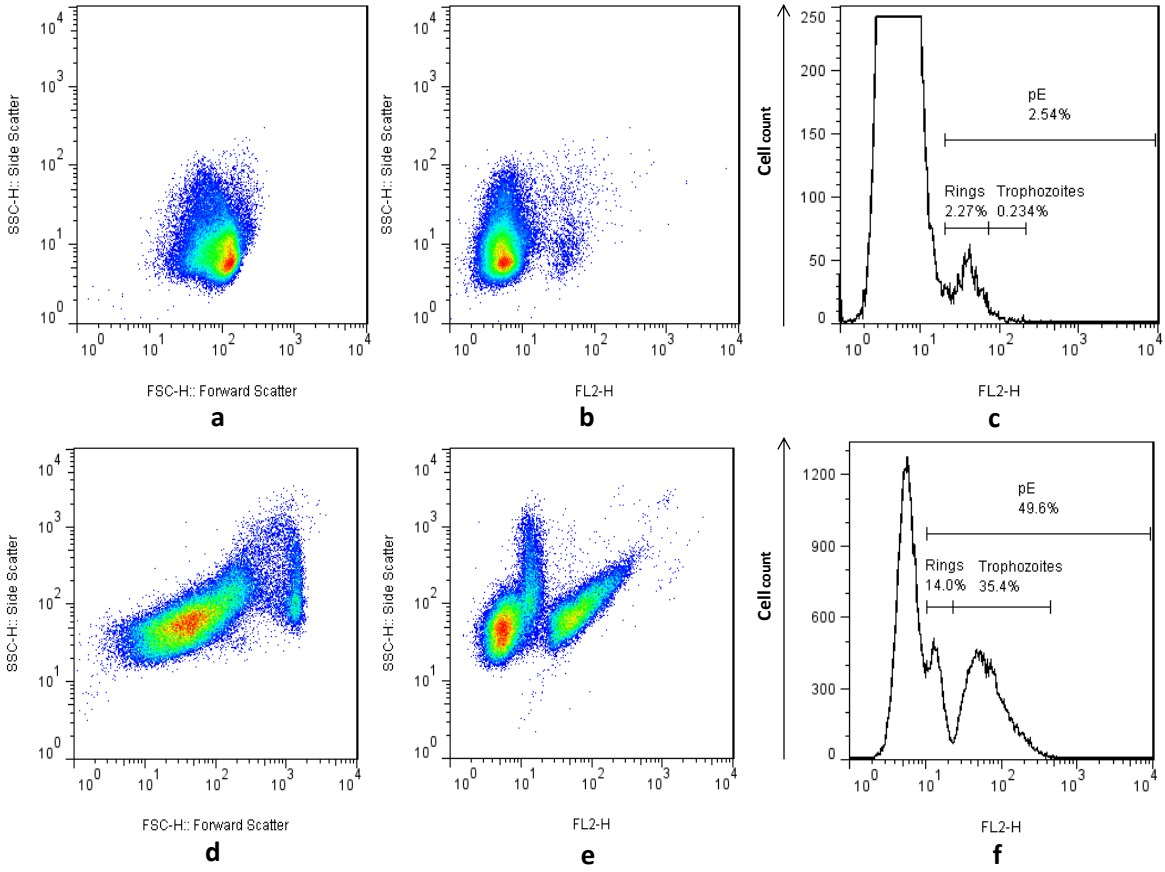


Figure 2.9: Flow cytometric analysis of an unfixed parasite sample of early rings (a-c) and a fixed parasite sample of late rings and early trophozoites (d-f), at a 5% haematocrit and 2% parasitaemia, stained with dihydroethidium. Where: a and d are dot-plots of the size (forward scatter) versus the granularity (side scatter) of the erythrocytes; b and e are dot-plots of the maximal fluorescence of dihydroethidium (FL2-H) versus side scatter, and c and f are histograms of maximal fluorescence of dihydroethidium versus cell count.

The dot-plot of forward versus side scatter of the fixed parasite sample (Figure 2.9d) is similar to those of Figures 2.4a and 2.7a, indicating definitively that formaldehyde treatment results in the change of the scatter properties of erythrocytes, and is not a result of the fluorochrome used. The dot-plot and histogram of Figures 2.9e and f, respectively, showed two separate populations; however this did not correspond to unparasitised and parasitised populations, nor represent parasite stage. The overall % parasitaemia, as determined by flow cytometric analysis, was 49.6% (Figure 2.9f) composed of 28% rings and 71% trophozoites; whereas the overall % parasitaemia as determined by microscopic

analysis was 1.95%, composed of 55% rings and 45% trophozoites. The massively inflated parasitaemia, as determined by flow cytometric analysis, was similar to that noted in fixed parasite samples stained with thiazole orange (Figure 2.4c), ruling out fixation post-staining as a viable option.

In contrast, unfixed samples of early rings stained with dihydroethidium showed a higher degree of uniformity in their forward scatter characteristics (Figure 2.9a), as well as discrimination between unparasitised and parasitised erythrocyte populations, as seen in the dot-plot and histogram (Figures 2.9b and c). The overall % parasitaemia as determined by flow cytometric and microscopic analysis was 2.54%, composed of 89% rings and 9% trophozoites (Figure 2.9c), and 2.20%, composed of 88% rings and 12% trophozoites, respectively.

Samples of trophozoite- (Figure 2.10a) and trophozoite- and schizont-staged parasites (Figure 2.10b) exhibited the same level of discrimination from the unparasitised erythrocyte population and, when compared to ring-stage parasites, an increase in dihydroethidium fluorescence (Figure 2.11).

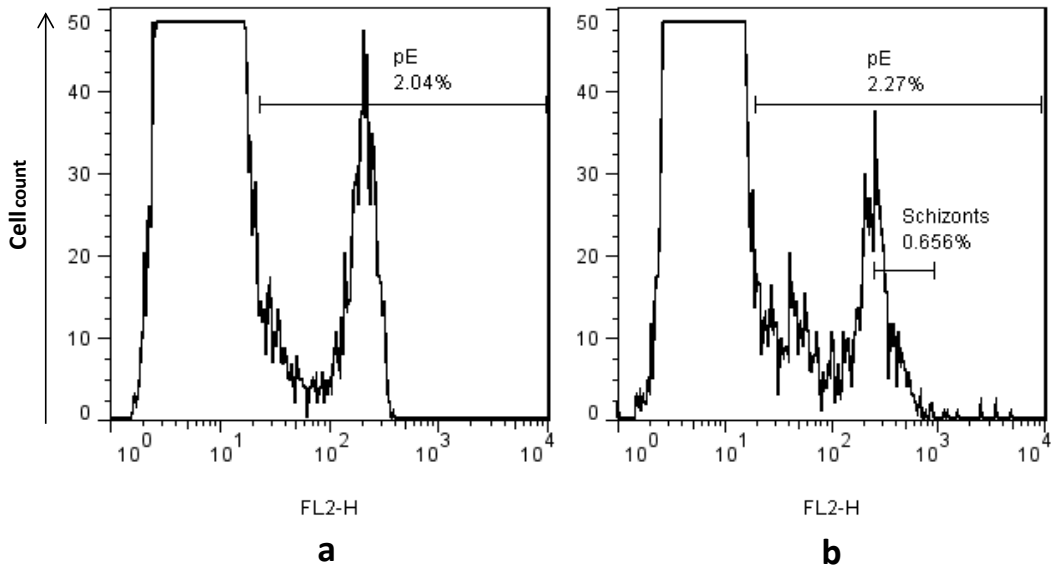


Figure 2.10: Histograms of the maximal fluorescence of dihydroethidium (FL2-H) versus cell count of samples of trophozoites (a) and trophozoites and schizonts (b) at a 5% haematocrit and 2% parasitaemia, stained with dihydroethidium.

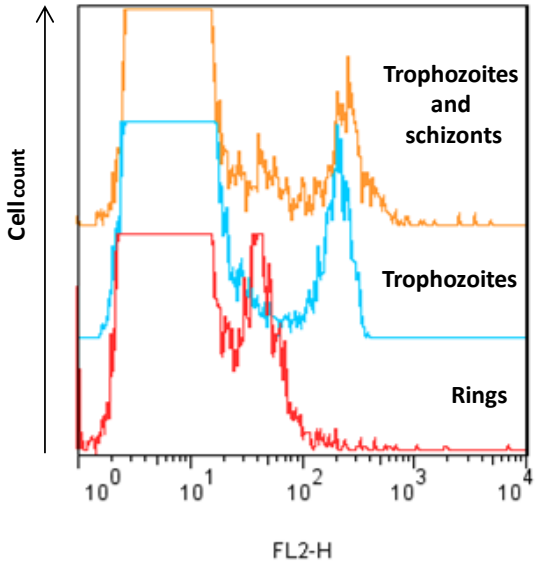


Figure 2.11: An overlay of flow cytometric histograms depicting the increasing fluorescent intensity of dihydroethidium (FL2-H) in samples of ring-, trophozoite-, and trophozoite/schizont-staged parasites, at a 5% haematocrit and 2% parasitaemia.

The overall % parasitaemias as determined from flow cytometric analysis correlated with those as determined from blood smears; 2.04%, 2.27%, and 1.98%, 1.93%, respectively. Furthermore, schizont-stage parasites could be distinguished from trophozoites in a sample of trophozoite and schizont-staged parasites based on increased dihydroethidium fluorescence (Figure 2.11); wherein 28.9% and 29.2% of the sample was composed of schizonts, as determined by flow cytometric and microscopic analysis, respectively. A similar correlation between the overall % parasitaemia as determined by flow cytometric and microscopic analysis was observed at parasitaemias prepared to 8% and 4% (Table 2.1).

Table 2.1: A comparison of the overall % parasitaemia obtained from flow cytometric and microscopic analysis of samples prepared to an 8, 4 and 2% parasitaemia and stained with dihydroethidium (n = 4).

Overall parasitaemia (%)		
Prepared	**Flow cytometry**	**Microscopic analysis**
8	7.42 ± 0.81	7.96 ± 0.23
4	4.48 ± 0.55	4.71 ± 0.33
2	2.30 ± 0.38	2.03 ± 0.17

2.2.3.2 Method optimisation

After establishing that dihydroethidium proved to be a viable fluorochrome, and provided a means in which total parasitaemia and parasite stages could be determined, the protocol was tailored to decrease the amount of stock parasite culture required.

A 5% haematocrit parasite solution was deemed unfeasible for drug screening, as it not only required a large amount of parasite stock, even at lower parasitaemias, but also affected parasite viability during a 48 hour incubation period in a 96-well plate. A haematocrit solution of 1%, with a parasitaemia of 0.5% would have been ideal, as this would have correlated with that used in the [^{3}H]-hypoxanthine incorporation assay (Section 2.2.2.1). However, a 1% haematocrit solution was previously assessed in samples stained with thiazole orange (Section 2.2.3.1.1), and ruled out for high-throughput screening on the basis of the lengthy sample acquisition time (approximately 3 minutes per sample). Furthermore, microscopic analysis of a 0.5% parasite solution would be an unviable option; particularly with the decreased number of erythrocytes per field at a 1% haematocrit.

To overcome this, a 2% haematocrit and 2% parasitaemia suspension, as used in the methodology of Verhaeghe *et al*. (2009), was then assessed. This proved to be acceptable in terms of sample acquisition time, i.e. 30-45 seconds to acquire 50 000 cells, as well as the volume of parasite stock required for the duplicate samples for comparative analysis of flow cytometric and microscopic results. Following optimisation of the % haematocrit and % parasitaemia suspension suitable for analysis, three separate suspensions of predominantly ring-, trophozoite- and schizont-staged parasites were prepared. The ring-, trophozoite-, and schizont-staged samples prepared to a 2% parasitaemia, exhibited overall % parasitaemias of 1.66%, 2.83%, 2.14% and 1.68%, 2.45%, 2.17%, in the two methodologies, respectively.

Thereafter, the parasites stages were determined by optimal gating of each stage of the parasitic life cycle (Figure 2.12) and, finally, a protocol constructed wherein % overall parasitaemia, parasite stage, and % of parasites in each stage could be assessed (Figure 2.13).

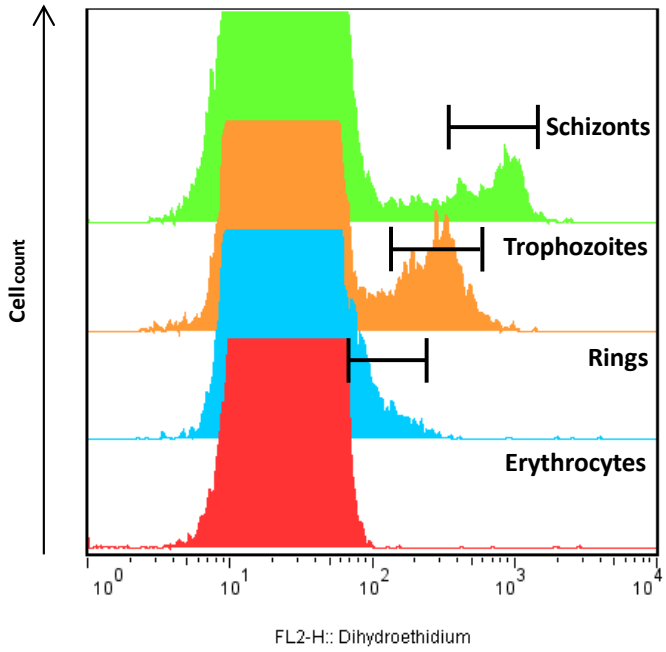


Figure 2.12: An overlay of flow cytometric histograms of samples of uninfected erythrocytes (2% haematocrit), ring-, trophozoite- and schizont-staged parasites prepared to a 2% haematocrit and 2% parasitaemia.

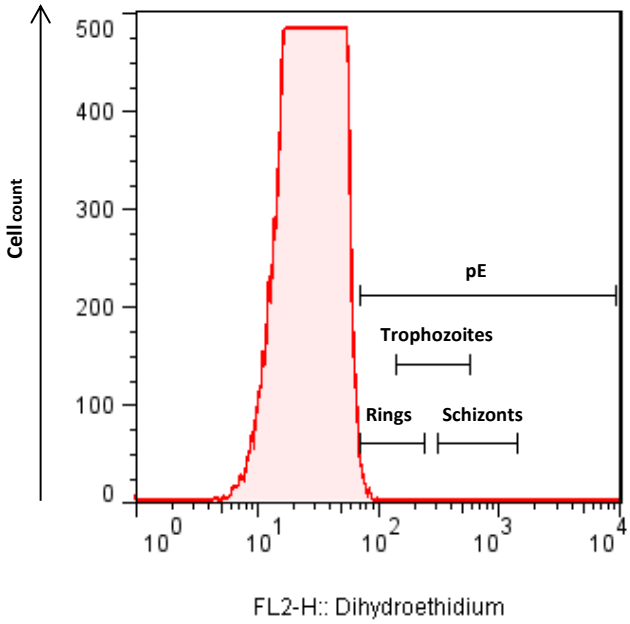


Figure 2.13: The final protocol used for the determination of overall % parasitaemia, as well as parasite stage and % parasites present in each stage, when stained with dihydroethidium.

The overlap between the ring- and trophozoite-stages may have been due to the fact that ring- and early trophozoite-stage parasites have a single nucleus, and would exhibit similar dihydroethidium fluorescence. Whereas in the mid and late trophozoite-stage DNA synthesis begins, resulting in increased dihydroethidium fluorescence (Arnot *et al*., 2011). Similarly, the overlap between the trophozoite- and schizont-stages may have been attributed to an overlap between the late trophozoite- and early schizont-stages, with this transition being undetectable by blood smear analysis (Arnot *et al*., 2011). The overlap between the stages made it imperative to prepare a duplicate sample for blood smear analysis, in order to correlate it with the % of parasites present in each stage as obtained from flow cytometric analysis.

Following method optimisation, the staining methodology was adapted for use in a 96-well plate, so that parallel [^{3}H]-hypoxanthine incorporation assays and flow cytometric analysis of samples could be performed, in order to compare the results obtained from the two methodologies.

2.2.3.3 Experimental protocol for the assessment of total parasitaemia

Positive controls, chloroquine and quinine, as well as compounds from each drug class were selected for drug screening and IC_{50} value determination by flow cytometric analysis, based on [^{3}H]-hypoxanthine incorporation assays performed at a 1% haematocrit and 0.5% parasitaemia. As the previous drug screenings and IC_{50} value determinations were carried out at this lower % haematocrit and % parasitaemia, and the optimal haematocrit and parasitaemia for flow cytometric analysis was determined to be at 2% for both haematocrit and parasitaemia, the [^{3}H]-hypoxanthine incorporation assay (Section 2.2.2.1) was performed concurrently, at this optimal higher % haematocrit and % parasitaemia, for comparative purposes.

Working solutions for IC_{50} value determination was calculated from the previous [^{3}H]-hypoxanthine incorporation assays, whilst compensating for the higher haematocrit and parasitaemia. Those compounds that showed little or no activity at a final drug concentration of 100 µM were re-screened at 100 µM to confirm lack of antimalarial activity.

The preparation of 96-well plates for flow cytometric analysis paralleled those prepared for the [^{3}H]-hypoxanthine incorporation assay (Section 2.2.2.1), with a few alterations in methodology. Working solutions of the positive controls and test compounds were prepared and serially diluted in incomplete experimental media; however, dilutions were carried out in duplicate, to allow for one sample to be used for flow cytometric analysis and one for blood smear analysis. Control wells included three wells: one erythrocyte control well and one parasite control well to be used for flow cytometric analysis; as well as one parasite control well to be used for blood smear analysis. The 2% haematocrit erythrocyte and 2% haematocrit and 2% parasitaemia solutions were prepared in complete culture media, as the interference of hypoxanthine present in culture media with isotope uptake was not a concern. Duplicate plates were prepared simultaneously for the [^{3}H]-hypoxanthine incorporation assay, according to the methodology described in Section 2.2.2.1, to which 2% haematocrit erythrocyte and 2% haematocrit/2% parasitaemia suspensions prepared in complete experimental media were added.

The plates were then incubated at 37 °C in a humidified candle jar. Following a 24 hour incubation period, 25 µl of incomplete culture media was added to each well of the plates for flow cytometric analysis, whereas the plates for the [^{3}H]-hypoxanthine incorporation assay received 25 µl of the [^{3}H]-hypoxanthine isotope, prepared (Section 2.2.2.1). The plates were then returned to the candle jar for a further 24 hour incubation period. Thereafter, the parasitic [^{3}H]-DNA was harvested and quantified from the plates for the [^{3}H]-hypoxanthine incorporation assay (Section 2.2.2.1).

Whereas, from the plates for flow cytometric analysis, the wells reserved for blood smear analysis were removed and thin blood smears prepared, from which the overall % parasitaemia was obtained by counting 10 microscope fields, or the equivalent of 1000 erythrocytes. These plates were then centrifuged at 1500 rpm for 5 minutes, the supernatant (200 µl) removed and replaced with dihydroethidium in sterile PBS (159 µM), before being gently shaken at 1500 rpm for 2 minutes, and incubated in a candle jar for 20 minutes at 37 °C.

The plates were centrifuged at 1500 rpm for 5 minutes, following the incubation period, and the supernatant removed and replaced with the same volume of sterile PBS (200 µl),

this was repeated three times. The samples were then transferred to flow cytometric tubes (BD) containing 1 ml of sterile PBS, as such, the final volume was 1.2 ml. The samples were acquired on a BD FACSCalibur™ flow cytometer, with argon laser excitation at 488 nm and detection at 610 nm, a total of 50 000 cells per sample were counted and analysed using BD CellQuest Pro™ and FlowJo (version 7.6.1) software (Figure 2.14).

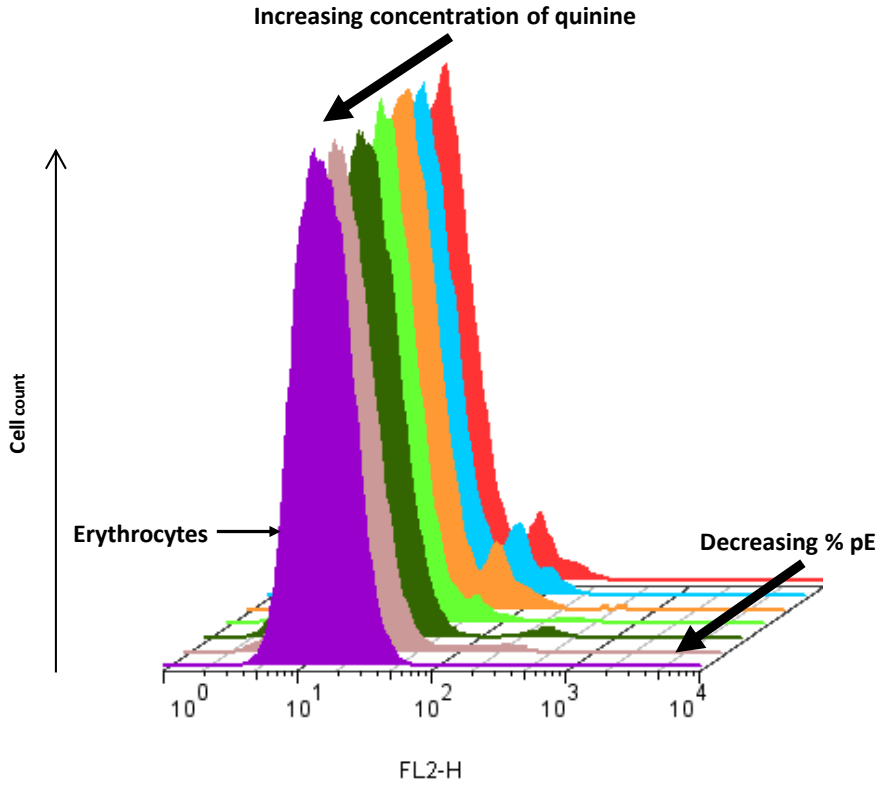


Figure 2.14: Flow cytometric histogram overlays of the cell count versus the maximal fluorescence of dihydroethidium (FL2-H) of samples treated with varying concentrations of quinine, following a 48 hour incubation period.

Thereafter, the overall % parasitaemia (pE) for each sample was obtained from the flow cytometric protocol (Figure 2.13), and % parasite growth calculated using the following equation:

$$\% \text{ Parasite growth} = \frac{\% \text{ pE of test sample or positive control}}{\% \text{ pE of parasite control}} \ (\text{x}100\%)$$

2.2.3.4 Final experimental protocol used for the assessment of the stage-specific and morphological effects of the compounds on *P. falciparum*

Working solutions of a compound from each drug class and a positive control, quinine, were prepared in incomplete experimental media so that their final concentrations were representative of their IC_{90}, IC_{50} and IC_{25} values (concentrations required to inhibit parasite growth by 90%, 50% and 25%, respectively), as determined by construction of log sigmoid dose response curves of data generated by flow cytometric analysis (Section 2.2.3.3). IC_{90}, IC_{50} and IC_{25} values were chosen in order to assess if the compounds exhibited any concentration-dependant effects, as well to ensure the optimal concentration was achieved at which their stage-specific and morphology effects were most evident.

The study was carried out in 25 cm^3 culture flasks (BD), to provide an adequate volume for the frequent removal of samples for flow cytometric and blood smear analysis. Separate culture flasks were reserved for each drug concentration, as well as for erythrocyte and parasite controls, such that 600 µl of the test compound, positive control or incomplete experimental media was placed in the flask. To which, 5.4 ml of synchronised ring-stage parasites (2% haematocrit and 2% parasitaemia), or, in the case of the erythrocyte control, a 2% haematocrit solution was added.

The flasks were then gassed (Section 2.1.1), sealed, and incubated at 37 °C. Prior to removal of the samples, the flasks were gently agitated to resuspend the erythrocytes. Samples (250 µl) for flow cytometric and blood smear analysis were taken eight hourly during the ring-stage, and five hourly during the trophozoite- and schizont-stages, with the last sample taken approximately four hours post-invasion, or four hours into the next asexual cycle. Following removal of the samples, the flasks were gassed, sealed, and placed back in the incubator. The samples were then centrifuged at 1500 rpm for 5 minutes; thereafter, thin blood smears were prepared (Section 2.1.1) to determine the overall % parasitaemia, the % of parasites present in each stage, as well as any changes in parasite morphology.

The staining procedure and flow cytometric acquisition and analysis of the samples was performed as described in Section 2.2.3.1.3. From the final flow cytometric protocol (Figure 2.13), the % overall parasitaemia as well as the stage of parasites present in the sample could be determined, and confirmed with the results of the blood smear analysis.

2.2.3.5 Data analysis

A total of 50 000 cells per sample were acquired using a BD FACSCalibur™ flow cytometer, with the following instrument settings: Forward Scatter (FSC-H), voltage E-1, amp gain 2, mode log; side scatter (SSC-H), voltage 263, amp gain 1, mode log; fluorescence 2 (FL-2), voltage 527, amp gain 1, mode log. The % overall parasitaemia was calculated using BD CellQuest Pro™ and FlowJo (version 7.6.1) software, based on gates constructed using unparasitised and parasitised erythrocyte samples. Gates were constructed to be representative of each stage of the parasitic life cycle, based on maximum dihydroethidium fluorescence (FL2-H) levels, from which the % of parasites in each stage could be determined, using the above software.

Log sigmoid dose response curves were constructed, from which IC_{50} values were determined, using the Enzfitter® (version 1.05) software. For compounds exhibiting little or no antimalarial activity the % inhibition of parasite growth at 100 µM was obtained. All experiments were repeated, at least, in triplicate to produce a mean ± standard deviation. In order to determine if there were statistically significant differences between IC_{50} values determined from flow cytometric analysis and the [^{3}H]-hypoxanthine incorporation assay, an unpaired Students T-test, with $p < 0.05$ considered statistically significant was performed using Graphpad Prism® (version 5) software.

2.3 Antimalarial mechanisms of action

Elucidating antimalarial mechanisms of actions is imperative, as target identification not only provides a means in which structure-activity relationships may be performed and the activity of the drug optimised, but also provides an indication as to how a novel compound may interact with another antimalarial drug with a known mechanism of action (Olliaro, 2001).

2.3.1. β-haematin inhibitory activity assay

Inhibition of haemozoin formation is a validated antimalarial target, with antimalarial drugs such as chloroquine known to act in this manner (Section 1.3.1). The assay works on the principle that the synthetic molecule, β-haematin, retains the biological and chemical properties of the native malaria pigment, haemozoin, thereby providing a means of

quantifying the β-haematin inhibitory activity (BHIA) of compounds (Basilico *et al*., 1998; Egan *et al*., 2000).

A modified BHIA assay was used (Chemaly *et al*., 2007), wherein β-haematin was synthesised from haem under acidic conditions, similar to that in the parasitic food vacuole.

2.3.1.1. Preparation of the solutions

The test compounds, positive controls (chloroquine and quinine) and antimalarial reference agent (dihydroartemisinin) were prepared in either DMSO or MilliQ™ water to a concentration of 3.2 mM, in order to account for the eight times dilution factor of the experiment. A freshly made 1 mg/ml (1.53 mM) stock solution of haemin (Sigma) dissolved in DMSO, was used for each experiment and stored in the dark until needed. A 0.5 M acetate buffer (pH 4.4) was utilised in order to mimic the acidic conditions of the parasitic food vacuole and to initiate the reaction (Chemaly *et al*., 2007). The 0.5 M acetate buffer was prepared by adding 19.5 ml of a 0.5M sodium acetate solution to 30.5 ml of a 0.5 M glacial acetic acid solution, and the pH determined with a Beckman pH meter. The 0.5 M stock solutions of sodium acetate and glacial acetic acid were prepared as follows: 41.015 g of anhydrous sodium acetate (Sigma) was dissolved in 1 litre of MilliQ™ water and 14.3 ml of undiluted glacial acetic acid (specific gravity 1.05 kg/l; BDH) was added to MilliQ™ water to achieve a final volume of 500 ml. Prior to each experiment the buffer was diluted in a 1:1 ratio in MilliQ™ water. A 10 M sodium hydroxide stock solution was prepared by dissolving 40 g NaOH pellets (Merck) in 100 ml MilliQ™ water, 2 M and 1 M solutions were prepared by diluting the stock solution in MilliQ™ water.

2.3.1.2 Experimental protocol

Non-sterile 96-well plates (Greiner Bio-one) were prepared in a specific order: 25 µl of the test compound or positive control (400 µM) were plated in triplicate in the first row of the test plate and serially diluted, three times, in a 1:2 ratio in either MilliQ™ water or DMSO, so that the final volume of drug in each well was 12.5 µl. The last row of the test plate was set aside to act as the untreated β-haematin control and contained 12.5 µl of DMSO or MilliQ™ water was added. Thereafter, 12.5 µl haem (192 µM) was added to each well, followed by 25 µl MilliQ™ water and finally, 50 µl 0.5 M acetate buffer, to achieve a final pH

of 4.6-4.8 (Chemaly *et al*., 2007). The plates were then incubated at 37 °C in a humidified environment for 24 hours. Thereafter, 100 µl of DMSO was added to each well, and the plate centrifuged at 3000 rpm for 10 minutes. Following centrifugation, 100-150 µl was removed and replaced with the same volume DMSO, a process that was repeated three times to ensure removal of any unreacted haemin (Figure 2.15). The wells were then washed twice with MilliQ™ water.

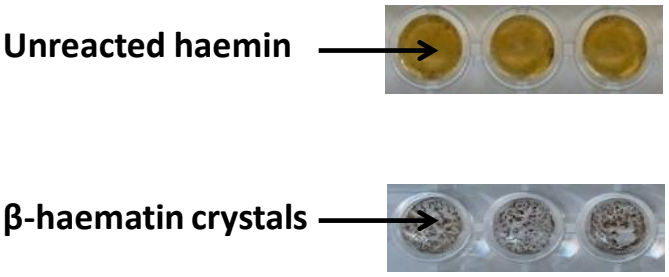


Figure 2.15: Formation of β-haematin crystals from haemin. Unreacted haemin is soluble in DMSO, whereas β-haematin crystals do not dissolve in DMSO and remain intact.

Finally, 100 µl was removed and substituted with the same volume of 2 M NaOH in order to dissolve the β-haematin crystals. The solution was then diluted in a 1:2 or 1:4 ratio in 1 M NaOH, so that the absorbance was < 1, and the absorbance read at 405 nm in a Labsystems iEMS microplate Reader MF, using Ascent software (version 2.4).

The inhibitory activities of the compounds, relative to the untreated control, were calculated using the formula below:

$$\% \text{ Inhibition of β-haematin formation} = \frac{ABS_{Control} - ABS_{Compound}}{ABS_{Control}} \quad (x100\%)$$

2.3.1.3 Data analysis

This constituted the methodology for the initial screening of compounds. For compounds exhibiting strong inhibitory activity at 100 µM, seven 1:2 serial dilutions were prepared, and log sigmoid dose response curves constructed using the Enzfitter® (version 1.05) software,

from which IC_{50} values (concentration required to inhibit the formation of β-haematin formation by 50%) were determined. For compounds exhibiting little or no inhibitory activity, the % inhibition of β-haematin formation at 400 µM was recorded. All experiments were repeated at least in triplicate to produce a mean ± standard deviation. In order to determine if there was a statistically significant difference between a test compound and positive control, an unpaired Students T-test with $p < 0.05$ was performed using the Graphpad Prism® (version 5) software.

2.3.2. Anti-oxidant activities

The effects of ROS in malaria can be both harmful and beneficial depending on the amount and site of ROS production. Pro-oxidants acting directed against the parasite are highly effective in combating the infection. However, excessive ROS production outside of the infected red blood cell overcomes the hosts' anti-oxidant defence systems and results in altered red blood cell deformability and lipid peroxidation of both parasitised and healthy red blood cells, contributing towards anaemia and vascular damage seen in *P. falciparum* malaria (Delmas-Beauvieuz *et al*., 1995; Postma *et al*., 1996; Griffiths *et al*., 2001). Anti-oxidants such as ascorbic acid and tocopherol have been shown to have protective effects by reinforcing the hosts defence systems, scavenging ROS and maintaining redox homeostasis, even in severe malaria (Postma *et al*., 1996; Gülçin *et al*., 2004; Quaye, 2008). Iron chelators may also act as anti-oxidants by chelating iron, thereby preventing the formation of ROS (Postma *et al*., 1996; Gülçin *et al*., 2004). Iron chelators also act to withhold iron from the parasite, thereby inhibiting the activity of enzymes to which iron is essential, including; enzymes involved in DNA synthesis, pyrimidine synthesis, glycolysis and haem synthesis amongst others (Postma *et al*., 1996; Mabeza *et al*., 1999).

2.3.2.1 The 2,2-diphenyl-1-picrylhydrazyl free-radical scavenging assay

The 2,2-diphenyl-1-picrylhydrazyl ($DPPH^{\bullet}$) free-radical scavenging assay measures the ability of an anti-oxidant to scavenge the free-radical of $DPPH^{\bullet}$, converting it to the stable molecule, 2,2'-diphenyl-1-picrylhydrazine (DPPH-H). A decrease in absorbance at 540 nm corresponds to the colour change from purple ($DPPH^{\bullet}$) to yellow (DPPH-H), as the free-radical is scavenged (Figure 2.16) (von Gadow *et al*., 1997; Jagetia *et al*., 2003; Gülçin *et al*., 2004).

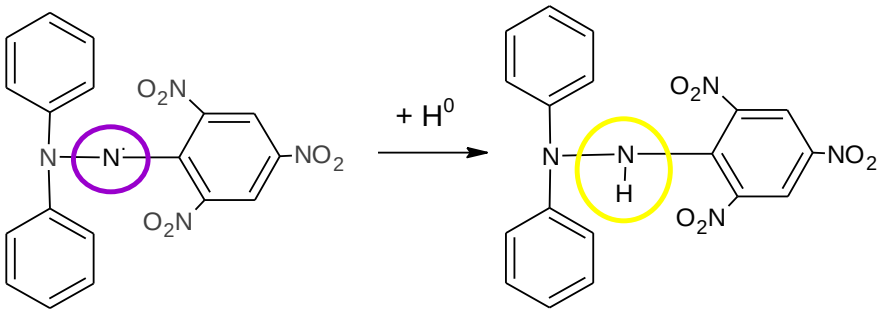


Figure 2.16: The conversion of DPPH$^{\bullet}$ to DPPH-H by the donation of a hydrogen atom (Jagetia *et al.*, 2003).

2.3.2.1.1 Preparation of the solutions

A 96.16 µM stock solution of DPPH$^{\bullet}$ (Sigma) was prepared in HPLC grade methanol (Rochelle Chemicals), and stored in the dark at 4 °C for a maximum period of a week.

The test solutions, antimalarial reference agents (chloroquine, quinine and dihydroartemsinin); as well as the positive control, ascorbic acid (Riedel de Haen), were prepared in either DMSO or MilliQ™ water to a starting concentration of 1.2 mM, in order to account for the five times dilution factor of the experiment.

2.3.2.1.2 Experimental protocol

Test compounds, antimalarial reference agents, and ascorbic acid were initially screened at a concentration of 240 µM or a 3:1 ratio of drug: DPPH$^{\bullet}$. This was achieved by pipetting 25 µl of the 1.2 mM solution into triplicate wells of a non-sterile 96-well plate and adding DPPH$^{\bullet}$ (100 µl) to the test wells, or HPLC grade methanol (100 µl) to colour control wells in order to negate the effects of colour interference by the compounds. Wells containing DMSO or MilliQ™ water (25 µl) and DPPH$^{\bullet}$ (100 µl) were included as a 100% DPPH$^{\bullet}$ control; whereas wells containing 25 µl DMSO or MilliQ™ water and 100 µl HPLC grade methanol were included as blanks. The plates were then incubated at room temperature, in the dark for 30 minutes. Thereafter, the absorbance was read at 540 nm in a Labsystems iEMS microplate Reader MF, using Ascent software (version 2.4). The free-radical scavenging

activities of the compounds were expressed as the percent decrease in the absorbance (scavenging activity) when compared to the DPPH$^{\bullet}$ control, using the formula below:

$$\% \text{ Scavenging activity} = \frac{(ABS_{DPPH^{\bullet}\ control} - ABS_{Blank}) - (ABS_{Compound} - ABS_{Colour\ control/Blank})}{(ABS_{DPPH^{\bullet}\ control} - ABS_{Blank})} \quad (x100\%)$$

2.3.2.1.3 Data analysis

Compounds that exhibited over 50% DPPH$^{\bullet}$ free-radical scavenging activity in the initial screening were serially diluted seven times, in either DMSO or MilliQ™ water. Following the above protocol, IC_{50} values (concentrated at which 50% of the free-radical of DPPH$^{\bullet}$ was scavenged) were calculated using the Enzfitter® software. In the case of compounds exhibiting activity of less than 50% at 240 µM, the % free-radical scavenging activity at 240 µM was recorded. All experiments were repeated, at least, in triplicate to produce a mean ± standard deviation. In order to determine if there was a statistically significant difference between a test compound, antimalarial reference agent and the positive control an unpaired Students T-test with $p < 0.05$ was performed, using the Graphpad Prism® (version 5) software.

2.3.2.2 Iron chelating activity

The iron chelating activity assay works on the principle that the test compound was capable of binding ferrous iron, thereby preventing ferrozine-Fe^{2+} complex formation, with a resultant decrease in the red colour of the complex corresponding to a decreased absorbance at 550 nm (Gülçin *et al*., 2004; Zhan *et al*., 2006). The decrease in absorbance thereby provides a manner in which the iron chelating activity of the compound may be determined.

2.3.2.2.1 Preparation of the solutions

The test solutions, antimalarial reference agents, chloroquine, quinine and dihydroartemsinin, as well as the positive control, ethylenediaminetetraacetic acid (EDTA; Rochelle Chemicals), were prepared in either DMSO or MilliQ™ water to a concentration of 1.5 mM, in order to account for the 7.5 times dilution factor of the experiment.

A 649 µM ammonium acetate (Fluka) solution was prepared in MilliQ™ water, and stored at room temperature until needed. A 1.2 mM ferrozine (3-[2-pyridyl]-5,6-diphenyl-1,2,4-triazine; Fluka) solution was prepared in MilliQ™ water and stored in the dark, at room temperature until needed. A 0.48 mM ferrous chloride solution ($FeCl_2.4H_2O$; Fluka) was freshly prepared in the ammonium acetate solution, for each experiment, and stored in the dark until just before use.

2.3.2.2.2 Experimental protocol

Test compounds, antimalarial reference agents, and EDTA were plated out (20 µl), in triplicate wells in a non-sterile 96-well plate. To which ferrous chloride (30 µl) and ferrozine (100 µl) were added, providing a drug concentration of 200 µM/well or a 2:1 ratio of drug: ferrous chloride. In the case of compounds possessing a background colour, additional wells were plated, to which ferrous chloride (30 µl) and MilliQ™ water (100 µl) were added. Experimental controls included: eight 100% ferrozine-Fe^{2+} complex formation wells, which contained DMSO or MilliQ™ water (20 µl), ferrous chloride (30 µl) and ferrozine (100 µl); as well as four blank wells, which contained DMSO or MilliQ™ water (20 µl), ferrous chloride (30 µl) and MilliQ™ water (100 µl). The test plate was left to incubate at room temperature in the dark for 30 minutes. Thereafter, the absorbance was read at 540 nm in a Labsystems iEMS microplate Reader MF with Ascent software (version 2.4).

The percentage iron chelating activity of the test compounds, antimalarial reference agents and EDTA were calculated using the following equation:

$$\%\ \text{Iron chelating activity} = \frac{(ABS_{Control} - ABS_{Blank}) - (ABS_{Compound} - ABS_{Colour\ control/Blank})}{(ABS_{Control} - ABS_{Blank})} \quad (x100\%)$$

2.3.2.2.3 Data analysis

Compounds exhibiting over 50% metal chelating activity in the initial screening at 200 µM were serially diluted in a 1:2 ratio, seven times, in either DMSO or MilliQ™ water, and the IC_{50} value (concentration at which 50% of Fe(II) was chelated) calculated using the Enzfitter® software. In the case of compounds exhibiting activity of less than 50% at 200 µM, the % chelating activity at 200 µM was recorded. All experiments were repeated, at least, in triplicate to produce a mean ± standard deviation. In order to determine if there

was a statistically significant difference between a test compound, antimalarial reference agent and the positive control, an unpaired Students T-test with $p < 0.05$ was performed using the Graphpad Prism® (version 5) software.

2.4 Red blood cell toxicity assay

Distinct morphological changes in the red blood cell membrane, such as membrane internalisation or externalisation occur during the process of haemolysis, with compounds exhibiting differing effects on the rate and severity of the haemolysis (Aki and Yamamoto, 1991). In this respect, the effects on the stability of the red blood cell membrane provide an indication of the ability of a drug to cause drug-induced haemolysis (Aki and Yamamoto, 1991; Sharma and Sharma, 2001). The haemolytic activity of compounds may be assessed by an *in vitro* method, wherein healthy red blood cells are treated with differing concentrations of a drug, with the amount of haemoglobin released by the red blood cell indicating the degree of haemolysis (Sharma and Sharma, 2001).

2.4.1 Preparation of the solutions

Solutions of the test compounds, antimalarial reference agents (chloroquine, quinine and dihydroartemisinin); as well as the positive haemolytic control, Triton™ X-100 (Sigma), were all prepared in incomplete experimental media to concentrations 10 times higher than that of the final concentration, in order to account for the dilution factor of the experiment. A 1% haematocrit of red blood cells was prepared in complete experimental media (Section 2.2.2.1) with red blood cells no older than two days utilised to ensure that the red blood cell membrane was not compromised.

2.4.2 Experimental protocol

A modified *in vitro* haemolytic assay was followed, wherein the experimental set up was that of the [^{3}H]-hypoxanthine incorporation assay (Section 2.2.2.1).

The 1 mM and 500 µM solutions of test compounds and antimalarial reference agents were plated out (25 µl) in duplicate, in a sterile 96-well plate, with extra wells plated for compounds with a background colour. Experimental controls included: a positive Triton™ X-100-induced haemolysis control; as well as negative haemolysis and media controls, to

which incomplete experimental media (25 µl) was added. Complete experimental media (200 µl) was added to the background and media control wells; whereas the red blood cell suspension (200 µl) was added to the experimental wells, as well as the positive and negative haemolysis control wells.

The plate was then incubated at 37 °C in a humidified candle jar for 24 hours, thereafter, 25 µl of incomplete experimental media was added to each well, and the plate returned to the candle jar for a further 24 hour incubation period. Following the 48 hour exposure period, the plate was sealed with a microplate sealer (Nunc), and shaken at 1500 rpm for 5 minutes to disrupt the red blood cell pellet. Thereafter, the plate was centrifuged at 1500 rpm for 5 minutes. The supernatant (100 µl) was then removed and plated out into a non-sterile 96-well plate. In the case of the positive Triton™ X-100-induced haemolysis control and compounds exhibiting haemolytic activity, the supernatant was diluted in PBS (pH 7.5) at a 1:2 or 1:4 ratio, to a final volume of 100 µl, in order to ensure the that absorbance was < 1. Finally, the latter plate was left to stand at room temperature for 10 minutes, before being gently shaken at 1000 rpm for 2 minutes, and the absorbance read at 412 nm in a Labsystems iEMS microplate Reader MF, with Ascent software (version 2.4). The percentage haemolysis was calculated using the formula below:

$$\% \text{ Haemolysis} = \frac{(ABS_{Compounds} - ABS_{CC/MC}) - (ABS_{NC} - ABC_{MC})}{(ABS_{PC} - ABS_{NC})} \quad (x100\%)$$

Where:

$ABS_{CC/MC}$ = mean absorbance of the colour control or media control wells

ABS_{NC} = mean absorbance of the negative red blood cell lysis control wells

ABS_{PC} = mean absorbance of the Triton™ X-100-induced haemolysis control

2.4.3 Data analysis

For each experiment, two replicates of each concentration (100 µM and 50 µM/well) were obtained. Experiments were repeated, at least, in quadruplicate to produce a mean ± standard deviation. For compounds exhibiting haemolytic activity of < 50% at 100 µM, the % haemolysis was recorded. For compounds exhibiting haemolytic activity of > 50% at 50

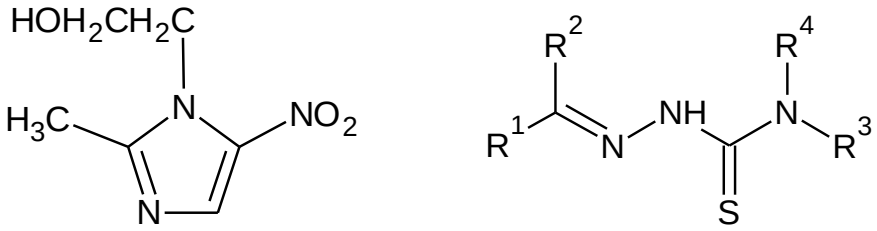
μM, IC_{50} values (concentration at which 50% haemolysis occurred) were calculated using the Enzfitter® software.

CHAPTER 3: THE ANTIMALARIAL PROPERTIES OF METRONIDAZOLE-THIOSEMICARBAZONE ANALOGUES

3.1 Introduction

3.1.1 Metronidazole

Metronidazole, 1-(2-hydroxyethyl)-2-methyl-5-nitroimidazole, (Figure 3.1a) is used to treat a variety of bacterial and protozoal infections, such as bacterial vaginosis, amoebic dysentery, trichomoniasis and giardiasis (Rossiter, 2010). It exhibits good oral availability, is widely distributed in body fluids and tissues and has a favourable side effect profile; exhibiting selective toxicity against microorganisms due to a lack of conversion to its cytotoxic form in mammalian cells (Jenks and Edwards, 2002; Mendz and Mégraud, 2002). However, sensory disturbances and peripheral neuropathies have been reported at high doses and following prolonged administration (Athar *et al*., 2005). Metronidazole exerts its effects via the inhibition of nucleic acid synthesis, by causing DNA oxidation resulting in strand breakages and cell death (Edwards, 1993; Mendz and Mégraud, 2002). Following diffusion into the cell, the 5-nitro group of metronidazole is reduced, via interactions with redox systems such as ferrodoxins or flavodoxins, to form the cytotoxic nitro radical and other reduction products which cause single and double-strand DNA breakage and DNA helix destabilisation (Edwards, 1993; Hoffman *et al*., 1996; Mendz and Mégraud, 2002).



a) b)

Figure 3.1: The chemical structure of metronidazole (a) and the basic thiosemicarbazone structure (b). Where: R^1 = aryl, alkyl or heterocyclic group; R^2 = H, aryl, alkyl group; R^3 and R^4 = H, alkyl, aryl or heterocyclic group (Chellan *et al*., 2010).

3.1.2 Thiosemicarbazones

Thiosemicarbazones (Figure 3.1b) are of considerable clinical interest, with compounds of the thiosemicarbazone structure possessing antidepressant, psychoanaleptic and hypnotic properties; whilst also displaying antibacterial, anticancer, antifungal and antimalarial activity (Greenbaum *et al*., 2004; Khan *et al*., 2008; Chellan *et al*., 2010). It appears as if they exert their biological activity through their thiourea moiety, which contains donor atoms that are capable of forming complexes with transition metals such as iron, copper and zinc (Dilović *et al*., 2008; Chellan *et al*., 2010; Hancock *et al*., 2011). The presence of iron in the active sites of enzymes involved in a wide variety of metabolic processes has propelled the search for compounds capable of acting as iron chelators (Rodriguez-Lucena *et al*., 2011).

Triapine®, 3-aminopyridine-2-carboxaldehyde thiosemicarbazone, is one such compound currently in Phase II clinical trials as an anticancer agent, with its efficacy attributed to its strong binding affinity for Fe^{3+} (Mackenzie *et al*., 2007; Rodriguez-Lucena *et al*., 2011). One such metabolic process relying heavily on iron-containing enzymes is cell division. Ribonucleotide reductase is an enzyme involved in DNA synthesis, with the inhibition of this enzyme resulting in the depletion of nucleotides needed for cell division and DNA repair (Mackenzie *et al*., 2007; Dilović *et al*., 2008).

Another possible mechanism of the anticancer properties of thiosemicarbazones is the alkylation of thiol residues of topoisomerase-II-DNA complexes, leading to stabilisation of these cleavage complexes (Dilović *et al*., 2008). Recent evidence has also pointed to the redox effects of the Triapine®-Fe^{3+} complex. Studies with copper-chelated thiosemicarbazones have shown that these complexes were capable of depleting GSH and forming reactive oxygen species, thereby inducing cell death (Hancock *et al*., 2011).

Nitroaromatic compounds have shown activity against *P. falciparum* via the formation of ROS, mediated by flavoenzyme redox cycling (Grellier *et al*., 2001). The parasite is particularly vulnerable to attack by free-radicals and is under constant oxidative stress from the hosts' immune system and haemoglobin breakdown; but possesses limited anti-oxidant capabilities (Müller, 2004). In this manner, a compound such as metronidazole, which may be activated within the microaerobic environment of the parasite and capable of forming

DNA damaging intermediates with an affinity for AT rich regions (Edwards, 1993) may be an effective antimalarial agent. The purpose of synthesising metronidazole-thiosemicarbazone analogues was to examine if hybridisation of metronidazole with the thiosemicarbazone scaffold could produce compounds acting in a synergistic manner to inhibit parasite growth by inducing DNA damage, as well as inhibit other crucial metabolic processes such as haem degradation and biosynthesis pathways.

The objectives of this chapter were to:

- Determine the antimalarial properties of metronidazole-thiosemicarbazones analogues
- Determine the pharmacological interactions of lead compounds when combined with quinine or dihydroartemisinin.
- Examine the stage-specific and morphological effects of a lead compound on parasite development.
- Elucidate possible antimalarial mechanisms of action of the compounds.
- Test for haemolytic activity as an indication of toxicity.

3.2 Materials and methods

3.2.1 Chemical synthesis and structural verification

The compounds were acquired from Professor A. Azam, Department of Chemistry, Jamia Millia Islamia, New Delhi, India. The analogues (**1-8**) were synthesised as depicted in Figure 3.2. Intermediate **A** was formed by the reaction of metronidazole with terepthaldialdehyde-monodiethylacetal, following which it was dissolved in tetrahydrofuran and recrystallised in ethanol to form intermediate **B** (Figure 3.2) (Abid *et al*., 2008)**.** Thereafter, intermediate **B** was condensed with various N^4 cyclic and aromatic-substituted thiosemicarbazides to produce the metronidazole-thiosemicarbazone analogues (Table 3.1) (Abid *et al*., 2008).

The compounds were found to be stable both in solution as well as in their solid form, with structural analysis carried out by infrared, electronic, ^{1}H and ^{13}C nuclear magnetic

resonance and purity determined by thin layer chromatography and elemental analysis (Abid *et al*., 2008).

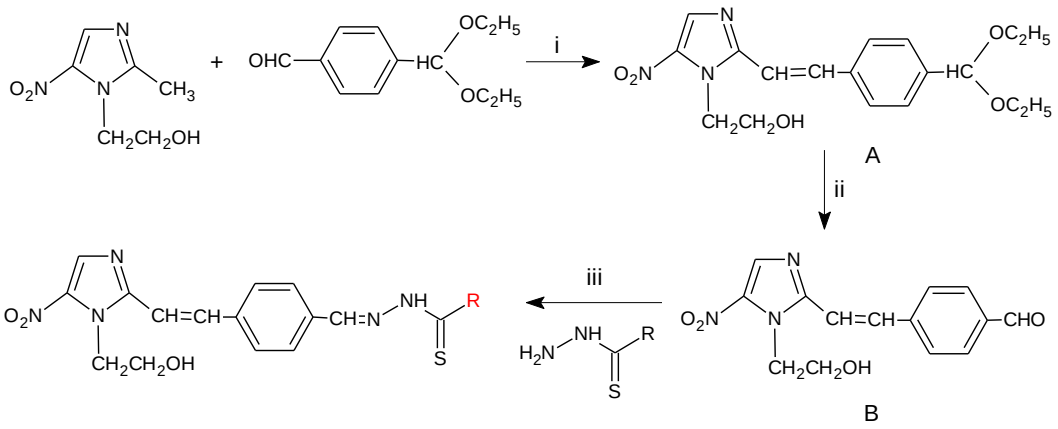


Figure 3.2: The synthesis of metronidazole-thiosemicarbazone analogues. (i) Sodium methoxide, DMSO, methanol, room temperature; (ii) HCl, tetrahydrofuran, 50 °C; (iii) ethanol, 80 °C, reflux (Abid *et al*., 2008).

3.2.2 Pharmacological evaluation

The *in vitro* antimalarial activity of the analogues (Table 3.1), metronidazole and positive controls were assessed using the tritiated hypoxanthine incorporation (Section 2.2.2.1) and flow cytometry (Section 2.2.3.3) methodologies. The most active compounds were selected for combination studies with quinine and dihydroartemisinin (Section 2.2.2.3), as well as for stage sensitivity and parasite morphology studies (Section 2.2.3.4). The β-haematin inhibitory activity (Section 2.3.1.2), $DPPH^{\bullet}$ free-radical scavenging (Section 2.3.2.1.2) and iron chelation assays (Section 2.3.2.2.2) were carried out to identify possible antimalarial mechanisms of action of the analogues. The red blood cell toxicity assay was performed to give an indication of the toxicity of the analogues (Section 2.4.2). Due to the fact that only small amounts of the analogues were received and no more could be made available, some studies could not be completed on all analogues and, in some cases, lead compounds had to be substituted with the next most active analogue available.

Table 3.1: The metronidazole-thiosemicarbazone analogues evaluated for antimalarial activity.

Chemical name	Chemical code	N^4 (R-group) substitution (Figure 3.2)
1-(4-(2-(1-(2-Hydroxyethyl)-5-nitro-1*H*-imidazol-2-yl)vinyl) benzylidene)-4-cyclooctylthiosemicarbazide	**Y-1**	Cyclooctyl amine
1-(4-(2-(1-(2-Hydroxyethyl)-5-nitro-1*H*-imidazol-2-yl)vinyl) benzylidene)-4-*p*-tolylthiosemicarbazide	**Y-2**	*p*-Toluidine
4-(2-Chlorobenzyl)-1-(4-(2-(1-(2-hydroxyethyl)-5-nitro-1*H*-imidazol-2-yl)vinyl)benzylidene)-thiosemi-carbazide	**Y-3**	2-Chloro-benzyl amine
1-(4-(2-(1-(2-Hydroxyethyl)-5-nitro-1*H*-imidazol-2-yl)vinyl) benzylidene)-4-cyclohexylthiosemicarbazide	**Y-4**	Cyclohexyl amine
N'-(4-(2-(1-(2-Hydroxyethyl)-5-nitro-1*H*-imidazol-2-yl)vinyl) benzylidene)pyrrolidine-1-carbo-thio-hydrazide	**Y-5**	Pyrrolidine
N'-(4-(2-(1-(2-Hydroxyethyl)-5-nitro-1*H*-imidazol-2-yl)vinyl) benzylidene)-4-methylpiperidine-1-carbo-thio-hydrazide	**Y-6**	4-Methyl piperidine
N'-(4-(2-(1-(2-Hydroxyethyl)-5-nitro-1*H*-imidazol-2-yl)vinyl) benzylidene)-3,4-dihydroquinoline-1(2*H*)-carbothiohydrazide	**Y-7**	1,2,3,4-Tetra-hydroquinoline
1-(4-(2-(1-(2-Hydroxyethyl)-5-nitro-1*H*-imidazol-2-yl)vinyl) benzylidene)-4-benzyl-4-methylthiosemi-carbazide	**Y-8**	*N*-Methyl benzyl amine

3.3 Results

3.3.1 *In vitro* antimalarial and haemolytic activity

The criteria for the classification of a compound as being active against *P. falciparum* depend on the study design and the class of compounds. Generally, compounds exhibiting activity in the order of less than 1-5 µM in initial drug screenings necessitate further study, with compounds exhibiting activity similar to existing antimalarial drugs such as quinine, or compounds active in the low nanomolar range considered potent (Fidock *et al*., 2004). For the purpose of this study; compounds with an IC_{50} value ≤ 5 µM were considered active, compounds with an IC_{50} value of between 5 and 10 µM were considered promising, compounds with an IC_{50} value of between 10 and 50 µM considered moderately active,

compounds with an IC_{50} value of between 50 and 100 µM considered to have low activity, and finally, compounds with an IC_{50} value ≥ 100 µM were considered to be inactive.

As seen in Table 3.2, the compounds exhibited promising antimalarial activity against *P. falciparum*, with six compounds inhibiting parasite growth in a dose-dependant manner, with IC_{50} values below 10 µM (Figure 3.3). Compounds Y-1 and Y-3 were the most active (IC_{50} values: 2.99 ± 0.16 µM and 2.83 ± 0.20 µM, respectively); however they were 19.9- and 18.9-fold less active than quinine (IC_{50} value: 0.15 ± 0.012 µM). Compounds Y-5 and Y-6 showed weak antimalarial activity, with parasitic growth inhibition of 51.91 ± 6.03% at 100µM and an IC_{50} value of 71.07 ± 8.97 µM, respectively (Table 3.2). Metronidazole showed very little antimalarial activity, and was only capable of inhibiting parasite growth by 22.94 ± 5.61% at 100 µM.

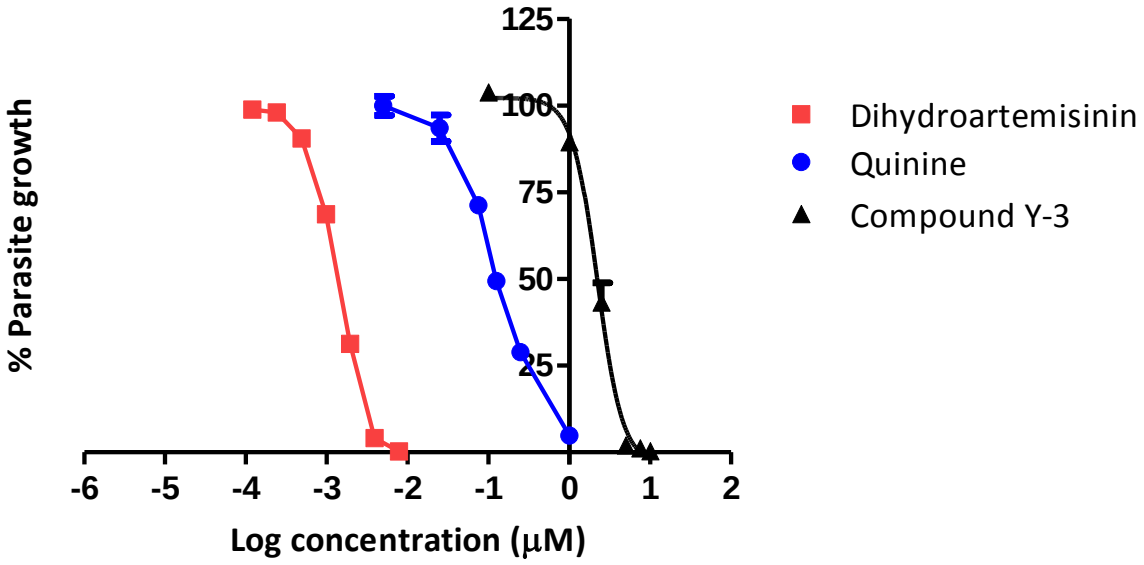


Figure 3.3: Log sigmoid dose-response curves of compound Y-3 compared to quinine and dihydroartemisinin.

The haemolytic activity of the derivatives were negligible (Table 3.2), ranging from 0.55 ± 0.18% to 1.97 ± 0.56% at 100 µM and were comparable to that of quinine (1.22 ± 0.98% at 100µM). Dihydroartemisin proved to be highly haemolytic at 100 µM (100.00 ± 5.29%), however, at 50 µM only 1.13 ± 0.51% haemolysis was observed. Furthermore, due to its potent antimalarial activity (IC_{50} value: 0.0014 ± 0.00020 µM), the dosage at which

haemolysis would be observed would be well in excess of that required to inhibit parasite growth.

Table 3.2: The *in vitro* antimalarial activity, as determined by the [^{3}H]-hypoxanthine incorporation assay (1% haematocrit and 0.5% parasitaemia) and haemolytic effects of metronidazole-thiosemicarbazone analogues and reference agents (n = 5).

Compound	Antimalarial activity		% Haemolytic activity
	IC_{50} value (µM ± s.d.)	% inhibition (100µM ± s.d.)	(100µM ± s.d.)
Y-1	2.99 ± 0.16		1.12 ± 0.97
Y-2	7.55 ± 0.49		1.15 ± 0.60
Y-3	2.83 ± 0.20		1.49 ± 1.13
Y-4	6.92 ± 0.68		1.97 ± 0.56
Y-5	> 100	51.91 ± 6.03	0.72 ± 0.92
Y-6	71.07 ± 8.97		0.99 ± 0.63
Y-7	3.79 ± 0.72		0.80 ± 0.79
Y-8	8.74 ± 0.30		0.55 ± 0.18
Metronidazole	> 100	22.94 ± 5.61	0.78 ± 0.32
Chloroquine	0.0064 ± 0.00019		0.72 ± 0.32
Quinine	0.15 ± 0.012		1.22 ± 0.98
Dihydroartemisinin	0.0014 ± 0.00020		100.00 ± 5.29

In order to confirm if antimalarial activity as determined by flow cytometric analysis produced results similar to that of the [^{3}H]-hypoxanthine incorporation assay; compounds Y-3, Y-7 and Y-5 as well as reference agents were selected for comparison, wherein the % haematocrit and % parasitaemia were 2-fold and 4-fold, respectively, higher than that utilised to obtain the values in Table 3.2. On comparison of the IC_{50} values obtained by the two methodologies (Table 3.3), all show statistically significant differences ($p < 0.05$), with the exception of chloroquine. The greatest discrepancy occurred between the IC_{50} values of quinine as determined by flow cytometric analysis (IC_{50} value: 0.058 ± 0.0026 µM) and the [^{3}H]-hypoxanthine incorporation assay (IC_{50} value: 0.15 ± 0.0014 µM) (Table 3.3). The IC_{50} values for compounds Y-3 and Y-7 as obtained by flow cytometry (IC_{50} values: 12.35 ± 0.84 µM and 10.35 ± 0.41 µM, respectively) were 1.7- and 1.4-fold higher than those obtained from the tritiated hypoxanthine assay (IC_{50} values: 7.46 ± 0.41µM and 7.45 ± 0.21 µM, respectively). The % growth inhibition of compound Y-5 in the two methodologies was

similar, 36.10 ± 5.28% and 39.60 ± 3.39% (Table 3.3). The % growth inhibition of metronidazole showed a slight difference, exhibiting 6.00 ± 2.21% inhibition in the [^{3}H]-hypoxanthine incorporation assay and 12.74 ± 4.53% inhibition in the flow cytometric analysis.

Table 3.3: Comparison of the IC_{50} values and % inhibition of parasite growth at a 2% haematocrit and 2% parasitaemia, as determined by the [^{3}H]-hypoxanthine incorporation assay and flow cytometric analysis. Values in parenthesis indicate the % inhibition of parasite growth at 100 µM (n = 7).

Compound	**Antimalarial activity**	
	[^{3}H]-hypoxanthine incorporation assay	**Flow cytometric analysis**
	IC_{50} value: µM ± s.d. (% inhibition at 100 µM)	**IC_{50} value: µM ± s.d. (% inhibition at 100 µM)**
Y-3	7.46 ± 0.41	12.35 ± 0.84
Y-7	7.45 ± 0.21	10.35 ± 0.41
Y-5	> 100 (36.10 ± 5.28%)	> 100 (39.60 ± 3.39%)
Metronidazole	> 100 (6.00 ± 2.21%)	> 100 (12.74 ± 4.53%)
Chloroquine	0.012 ± 0.0013	0.014 ± 0.00068
Quinine	0.15 ± 0.0014	0.058 ± 0.0026

3.3.2 Combination studies

The isobolograms of Figure 3.4 depict the additive interactions of Y-3 and Y-7 in combination with quinine and dihydroartemisin. The ΣFIC for each experiment was calculated from FIC values generated for each data point (Appendix C). The ΣFIC values for compound Y-3 and quinine (1.14 ± 0.09), compound Y-3 and dihydroartemisinin (1.29 ± 0.075), compound Y-7 and quinine (1.21 ± 0.14) and compound Y-7 and dihydroartemisinin (1.14 ± 0.057) were calculated over three experiments. The ΣFIC values confirm the additive interaction depicted in the isobolograms, falling well within the guidelines of an additive interaction, wherein the ΣFIC_{50} range lies between 0.5 and 2 (Section 2.2.2.3).

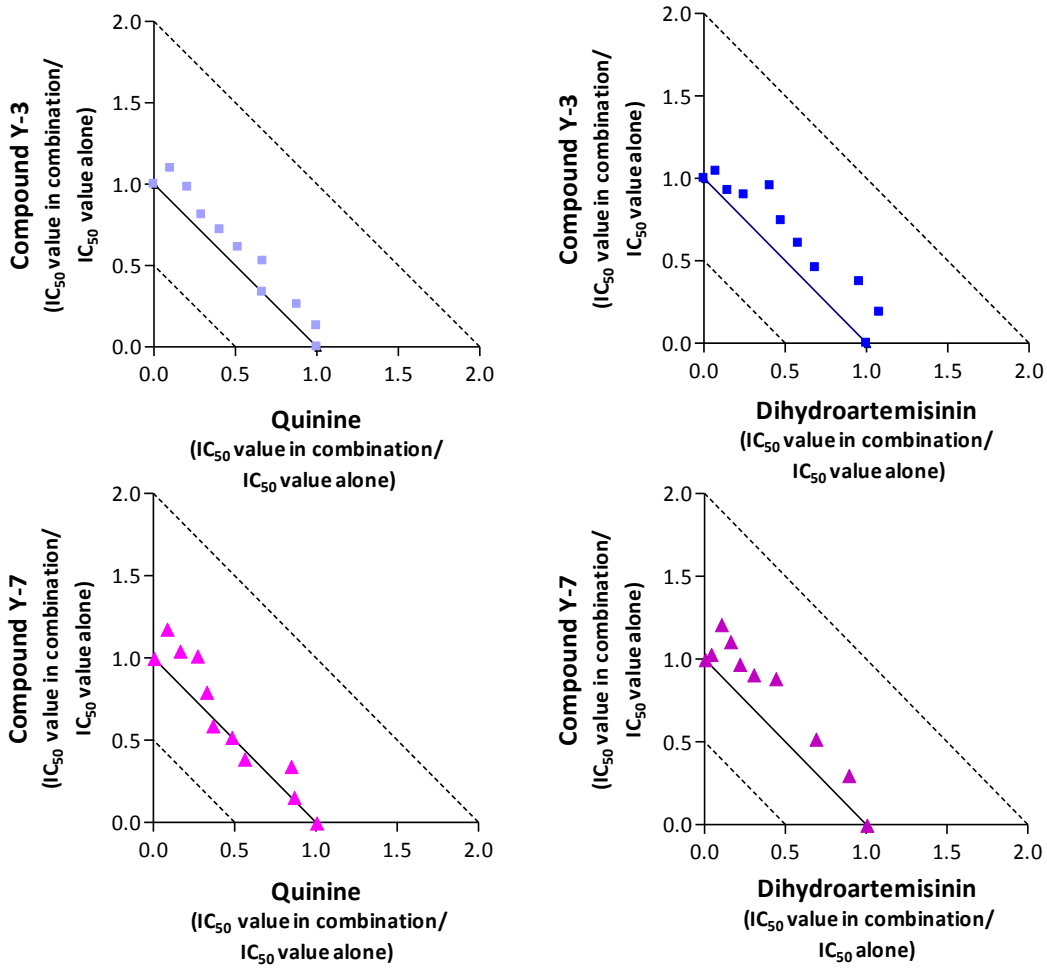


Figure 3.4: The additive pharmacological interactions between compounds Y-3 and Y-7 when combined with quinine and dihydroartemisinin (n = 3).

3.3.3 Morphological and stage-specific effects of compound Y-3

The morphological and stage-specific effects of compound Y-3 were assessed at its IC_{90} (30 µM), IC_{50} (12 µM) and IC_{25} (7 µM) values, and compared to that of quinine. When treated with compound Y-3 at its IC_{90} value, parasites showed no progression past the late ring-stage, appeared to be smaller (pyknotic) than the untreated control, and exhibited intense staining, similar to so-called 'crisis forms', which may be an indication of chromatin condensation and cell shrinkage (Deponte and Becker, 2004; Lopez *et al*., 2010).

Compound Y-3 at its IC_{25} value produced little stage-specific or morphological effects. However, a slight lag in parasite development was noted, with most of the treated parasites appearing as late trophozoites when the untreated control was in the early to mid

schizont-stage, and most treated parasites appearing as early-mid schizonts when the parasite control was in the late schizont- and early ring-stages. An examination of the blood smears four hours post-invasion or four hours into the next parasitic showed that the early-mid schizonts had progressed through the cycle, with early rings evident.

The stage-specific and morphological effects of compound Y-3 at its IC_{50} value were similar to those of its IC_{90} value, and are depicted in Figures 3.5 and 3.6.

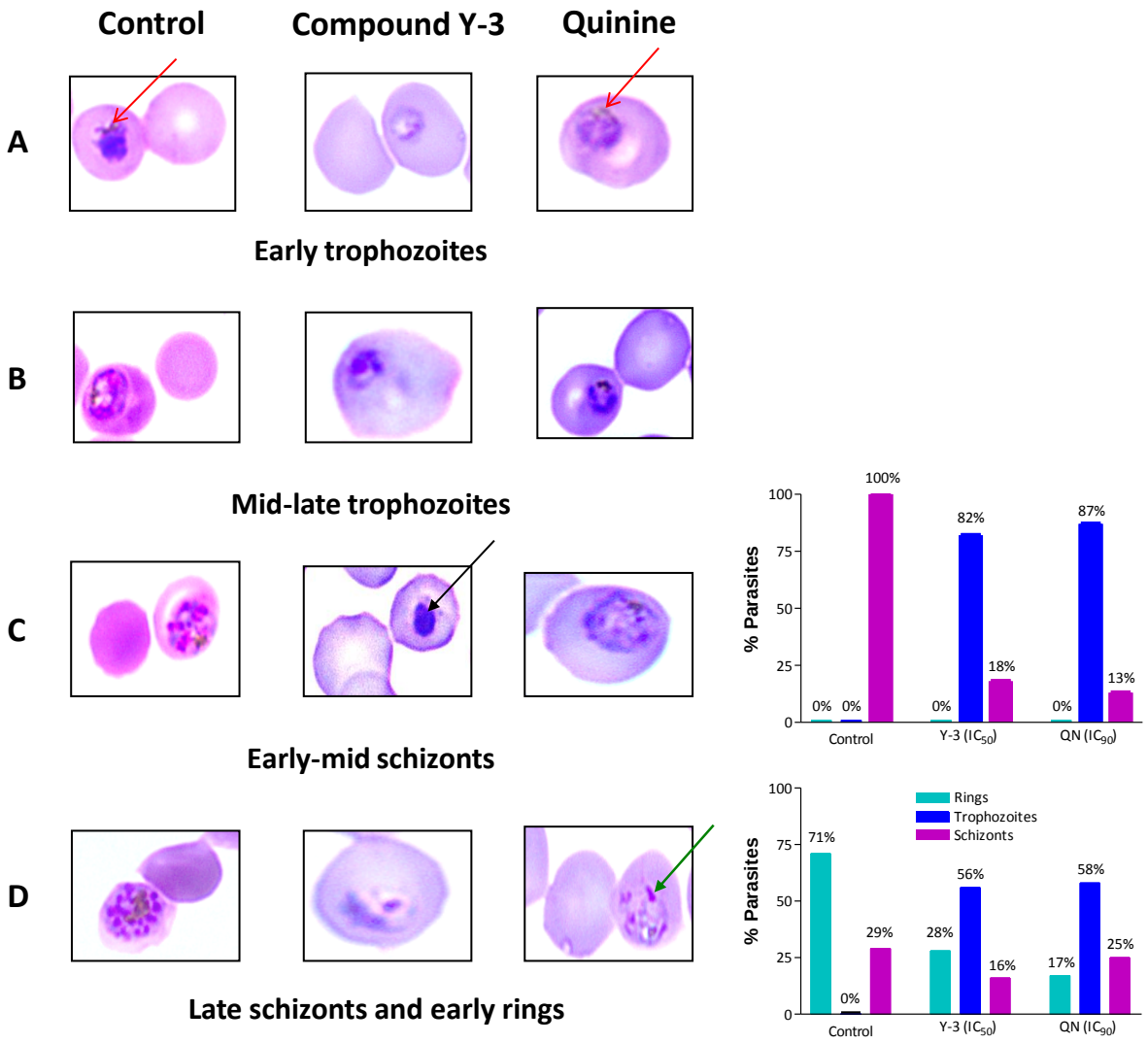


Figure 3.5: The effects of compound Y-3 and quinine at their IC_{50} (12 µM) and IC_{90} (200 nM) values, respectively, on parasite morphology and development. Indicating morphological changes: Haemozoin (red arrows), 'crisis forms' (black arrows), possible DNA fragmentation (green arrows) (n = 1).

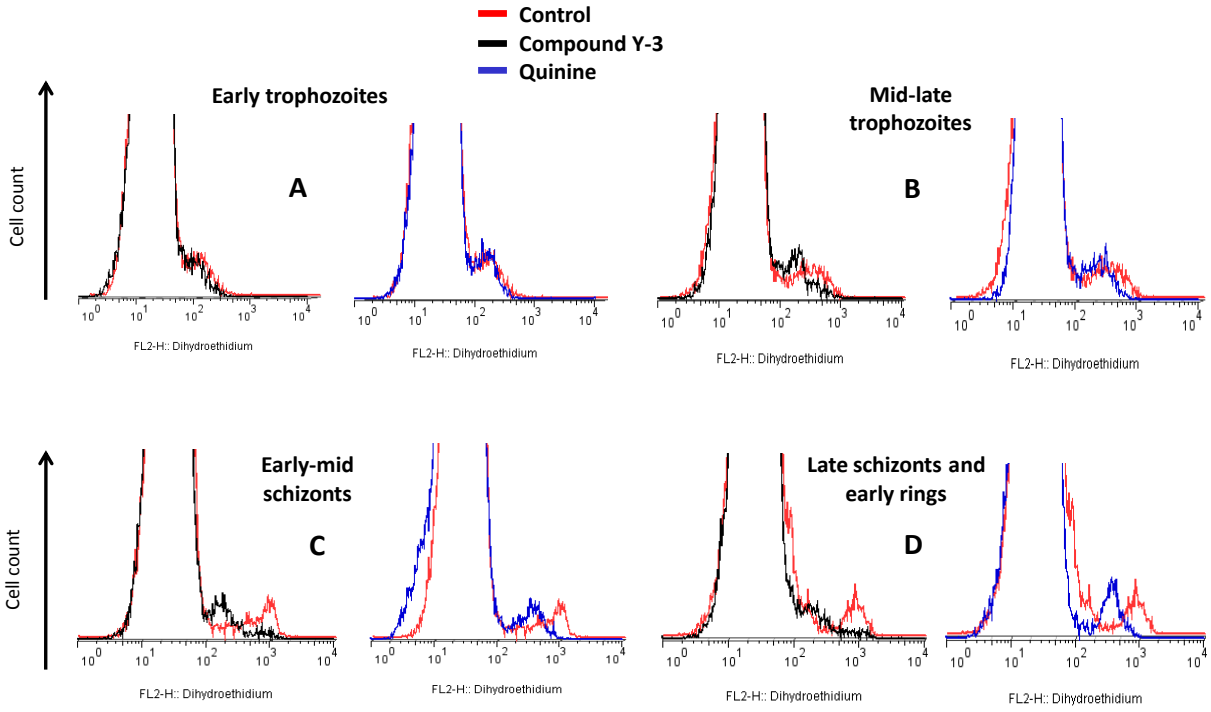


Figure 3.6: The effects of compound Y-3 (black line) and quinine (blue line) at their IC_{50} (12 µM; left) and IC_{90} values (200 nM; right), respectively, on parasite development compared to the untreated control (red line) (n = 1).

No notable changes in parasite morphology occurred during the ring-stage. However, upon progression from the late ring- to trophozoite-stage, a distinct lack of haemozoin formation was visible when compared to the control (Figure 3.5a). When compared to parasite controls of mid to late trophozoites, early to mid schizonts, and late schizonts and early rings, the treated parasites appeared smaller (pyknotic) (Deponte and Becker, 2004; Lopez *et al*., 2010) and exhibited intense staining. A parasite count revealed that when the untreated control was in the early to mid schizont-stage, 82% of the compound Y-3-treated parasites remained in the early trophozoite-stage (Figure 3.5c), and when the untreated control proceeded into the late schizont- (29%) and early ring-stages (71%), 28% of compound Y-3 treated parasites were in the ring-stage, 56% were halted in the early trophozoite-stage, and 16% were present as mid to late schizonts (Figure 3.5d). When examining the histogram overlays (Figures 3.6a,b,c,d) of compound Y-3 at its IC_{50} value along with the parasite control, it can be seen that parasitic development past the early trophozoite-stage (Figure 3.6a) was affected.

The stage-specific and morphological effects of quinine were most visible at its IC_{90} value (200 nM) and are depicted in Figures 3.5 and 3.6. The treated parasites progressed through the ring-stage into the early trophozoite-stage with no notable morphological changes; haemozoin crystals were clearly visible in the early trophozoite-stage (Figure 3.5a). When compared to the mid-late trophozoite parasite control, it appeared as if parasitic development was stalled in the mid trophozoite-stage (Figures 3.5b and 3.6b). When comparing treated parasites to the early-mid schizont control, a lag in parasitic development was evident, with 87% of the quinine treated parasites present in the mid to late trophozoite-stage (Figures 3.5c and 3.6c). Finally, as the parasite control progressed into the late schizont- (29%) and early ring-stages (71%), 58% of the quinine treated parasites remained in the trophozoite-stage with 17% and 25% of parasites in the early ring- and late schizont-stages, respectively (Figure 3.6d). Additionally, quinine treated parasites exhibited signs of possible DNA fragmentation (Figure 3.5d) (Deponte and Becker, 2004), although this would need to be confirmed by DNA gel electrophoresis or the TUNEL assay. When examining blood smears of treated parasites four hours post invasion, or four hours into the next parasitic cycle, the treated parasites resembled that of Figure 3.5d, and did not progress into the ring-stage. In contrast, no distinct morphological and stage-specific effects were noted at quinine's IC_{50} (60 nM) or IC_{25} value (30 nM), with treated parasites progressing through the trophozoite-stage, where haemozoin formation was comparable to that of the untreated control. A slight lag in parasite development was evident, with treated parasites appearing mainly as late trophozoites when the untreated control was in the early-mid schizont stage. However, four hours into the next parasitic cycle early rings were evident indicating that the treated parasites had progressed through the cycle.

3.3.4 Antimalarial mechanisms of action

3.3.4.1 Inhibition of β-haematin formation

All the analogues, with the exception of two (compounds Y-5 and Y-6), inhibited β-haematin formation with IC_{50} values ranging from 19.08 ± 2.37 µM to 64.80 ± 6.61 µM (Figure 3.7). Compounds Y-5 and Y-6 only inhibited the formation of β-haematin by 26.46 ± 5.72% and 61.73 ± 5.50% at 400 µM, respectively. When compared to chloroquine (IC_{50} value: 29.64 ± 3.35 µM), all analogues were statistically less effective ($p < 0.05$) with the

exception of compound Y-3 (IC_{50} value: 19.08 ± 2.37 µM), which was more effective in inhibiting β-haematin formation ($p > 0.05$). When compared to quinine (IC_{50} value: 63.00 ± 3.27 µM), all analogues, with the exception of compound Y-2, Y-5 and Y-6 were more potent inhibitors of β-haematin formation. Metronidazole and dihydroartemisinin did not inhibit the formation of β-haematin, where 100 µM inhibited 14.76 ± 2.94% and 7.46 ± 2.27% of β-haematin formation, respectively.

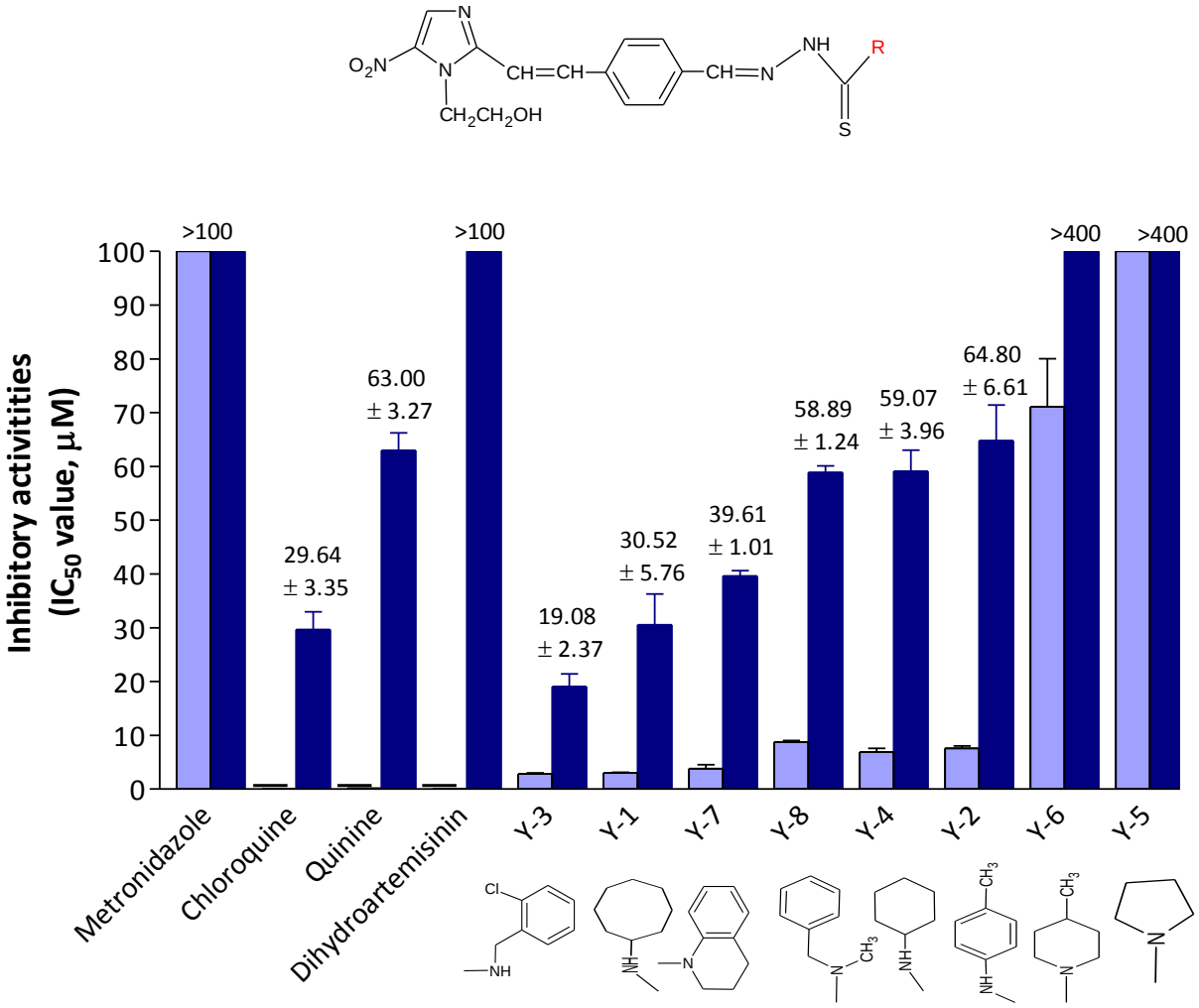


Figure 3.7: The inhibitory activities of metronidazole-thiosemicarbazone analogues and antimalarial reference agents on parasite growth (lighter blue bar) and β-haematin formation (darker blue bar) (n = 6).

3.3.4.2 Free-radical scavenging activity

Of the five analogues tested for free-radical scavenging activity, all but one (compound Y-4) exhibited the ability to scavenge $DPPH^{\bullet}$ with IC_{50} values below 100 µM (Table 3.4). The only

statistical difference between the analogues and ascorbic acid (IC_{50} value: 19.31 ± 2.62 µM) was with compound Y-3 (IC_{50} value: 80.00 ± 2.22 µM) (p value < 0.0001). Compounds Y-5, Y-7 and Y-8 exhibited potent free-radical scavenging activity, with IC_{50} values less than 30 µM. Compound Y-4 as well as the controls, metronidazole, chloroquine, quinine and dihydroartemisinin exhibited poor free-radical scavenging activity at 240 µM (Table 3.4).

Table 3.4: The free-radical scavenging and iron chelating activity of select metronidazole-thiosemicarbazone analogues (n = 4). Values in parenthesis depict the % free-radical scavenging activity at 240 µM and % iron chelating activity at 200 µM. N.D = not determined.

Compound	**$DPPH^{\bullet}$ free-radical scavenging IC_{50} value: µM ± s.d. (% Activity at 240 µM)**	**Fe^{2+} chelation IC_{50} value: µM ± s.d. (% Activity at 200 µM)**
Y-2	N.D.	> 100 (0.01 ± 7.84%)
Y-3	80.00 ± 2.22	> 100 (10.29 ± 4.16%)
Y-4	> 100 (8.70 ± 2.48%)	> 100 (0.01 ± 0.83%)
Y-5	26.90 ± 4.18	> 100 (9.49 ± 2.98%)
Y-7	26.06 ± 4.02	> 100 (13.46 ± 2.51%)
Y-8	21.98 ± 0.56	> 100 (55.64 ± 9.31)
Metronidazole	> 100 (0.01 ± 1.38%)	> 100 (0.01 ± 6.14%)
Chloroquine	> 100 (0.31 ± 3.28%)	> 100 (70.68 ± 0.97%)
Quinine	> 100 (2.53 ± 1.17%)	> 100 (0.01 ± 6.08%)
Dihydroartemisinin	> 100 (0.01 ± 2.70%)	> 100 (0.01 ± 2.44%)
EDTA	N.D.	23.90 ± 1.83
Ascorbic acid	19.31 ± 2.62	N.D.

3.3.4.3 Iron chelation activity

None of the analogues tested exhibited any significant iron chelating properties when compared to EDTA (IC_{50} value: 23.90 ± 1.83 µM) (Table 3.4).

Compound Y-8 showed the greatest activity, chelating 55.64 ± 9.31% Fe(II) at 200 µM, whilst the remainder of the analogues exhibited no more than 13.46 ± 2.51% chelating activity at 200 µM. Metronidazole, quinine and dihydroartemisinin exhibited no iron chelation properties at 200 µM, whilst chloroquine was capable of chelating 70.68 ± 0.97% Fe(II) at 200 µM (Table 3.4).

3.4 Discussion

3.4.1 Antimalarial activity of metronidazole-thiosemicarbazone analogues

The various side chains attached to the imidazole ring of metronidazole provided an opportunity to carry out various structural modifications, as well as to determine if metronidazole contributed to the overall pharmacological activity of the metronidazole-thiosemicarbazone analogues. Considering the substitutions at the N^4 position of the metronidazole-thiosemicarbazone analogues, the most active compounds were those possessing a 2-chloro-benzyl amine (compound Y-3), cyclooctyl amine (compound Y-1) or a 1,2,3,4-tetrahydroquinoline (compound Y-7) substitution (Tables 3.1 and 3.2). None of the metronidazole-thiosemicarbazone derivatives exhibited any toxicity towards the host red blood cell, with % haemolysis ranging from 0.55 to 1.97% at 100 µM (Table 3.2). Thus indicating that the antimalarial activity of the derivatives was as a result of a direct effect on the parasite, with the above substitutions conferring the greatest antimalarial activity.

Thiosemicarbazones have elicited great interest due to their numerous biological activities and generally favourable toxicity profile; in this respect many studies have been conducted to investigate the antimalarial properties of thiosemicarbazones. One of the first studies showed that from a wide variety of compounds screened, only 2-acetylpyridine-4-phenyl-3-thiosemicarbazone (Figure 3.8a) exhibited any antimalarial activity against *Plasmodium berghei* in mice (Klayman *et al*., 1979). Stucture-activity relationships based on this compound indicated that a 2-pyridylethylidene moiety on N^4 was pivotal to the antimalarial activity, with antimalarial activity abolished when this moiety was replaced by another aromatic ring system (Klayman *et al*., 1979). The same study also found that an unsubstituted phenyl ring on N^4 conferred increased antimalarial activity, whereas a substituted phenyl ring or linear aliphatic conferred little or no antimalarial activity (Klayman *et al*., 1979).

A recent study conducted by de Oliveira *et al*. (2008) on the chloroquine-resistant W2 strain of *P. falciparum,* wherein the thiourea moiety was replaced by a carbonyl moiety, showed that the thiourea moiety was imperative to antimalarial activity. The same study also showed that substitution with an aliphatic moiety on N^1 (Figure 3.8b) was also critical for

antimalarial activity, and that the substitution of an aromatic derivative on N^1 proved to diminish activity (de Oliveira *et al*., 2008).

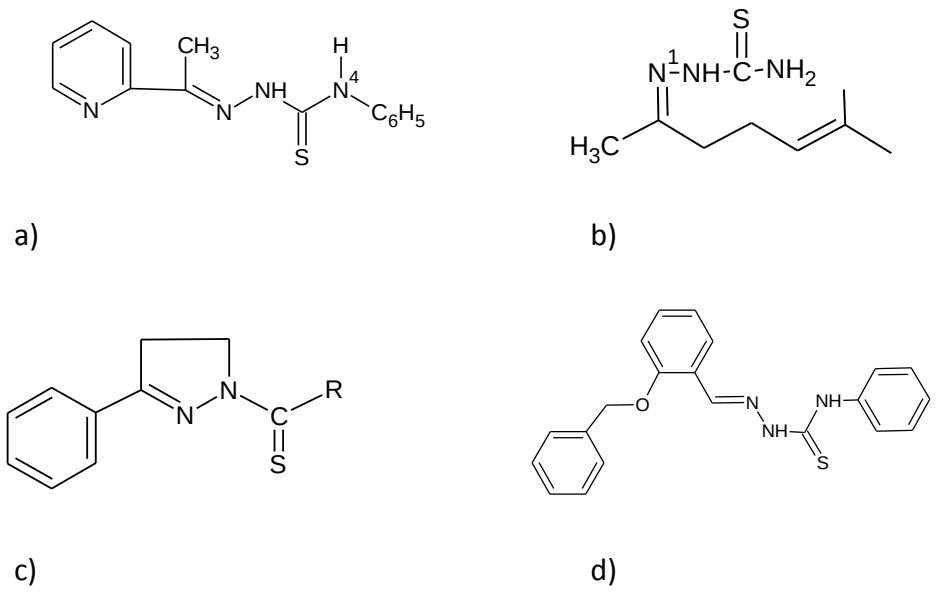


Figure 3.8: The chemical structures of thiosemicarbazones previously assessed for various pharmacological activities. a = Klayman *et al*. (1979); b = de Oliveira *et al*. (2008); c = Abid and Azam (2005), Abid *et al*. (2009).

In contrast to the findings of Klayman *et al*. (1979) and de Oliveira *et al*. (2008), none of the compounds tested in this study were 2-pyridylethylidene substituted on N^4, with the most active analogue, compound Y-3, containing a chloro-substituted phenyl ring. Similarly, none of the compounds in this study possessed aliphatic substitutions on N^3, the equivalent of N^1 in the de Oliveira *et al*. (2008) study, yet displayed antimalarial activity. The antimicrobial activity linked to substitution on N^4 was verified when steroidal thiosemicarbazones were tested against various strains of bacteria, with acetoxy- and chloro-substituted cyclopentyl and cyclohexyl derivatives proving to be the most active (Khan *et al*., 2008). This was similar to the findings of this study wherein compound Y-3, a chloro-substituted cyclohexyl thiosemicarbazone derivative proved to be the most active.

Previous studies on cyclised thiosemicarbazones (Figure 3.8c) possessing the same side chain substitutions as compounds Y-1, Y-2, Y-3, Y-5, Y-6 and Y-8 (Table 3.1; Figure 3.7) exhibited poor antimalarial activity against the chloroquine-resistant FCR-3 strain of *P. falciparum*, with IC_{50} values ranging from 26 µM to greater than 50 µM (C-T Chen; personal

communication). The decrease in antimalarial activity may be as a result of the different strain of *P. falciparum* used; however, the cyclised thiosemicarbazones exhibited no β-haematin inhibitory activity in comparison to the metronidazole-thiosemicarbazone analogues, indicating the importance of the acyclic thiosemicarbazone moiety in antimalarial and β-haematin inhibitory activity.

3.4.2 The effect of methodology on antimalarial evaluation

A comparison of the IC_{50} values obtained by flow cytometric analysis and the [^{3}H]-hypoxanthine incorporation assay (Table 3.3), at a 2% haematocrit and 2% parasitaemia revealed statistically significant differences ($p < 0.05$), with the exception of chloroquine. All compounds, with the exception of quinine, exhibited higher IC_{50} values in flow cytometric analysis when compared to those obtained by the [^{3}H]-hypoxanthine incorporation assay (Table 3.3).

A study conducted by Saito-Ito *et al*. (2001) comparing IC_{50} values obtained using the [^{3}H]-hypoxanthine incorporation assay, microscopic examination and flow cytometric analysis, wherein acridine orange was used as a probe, also found no statistically significant different in the IC_{50} value of chloroquine in all methodologies. However, the IC_{50} value of pyrimethamine was greater as determined by flow cytometry and microscopic examination than by the [^{3}H]-hypoxanthine incorporation assay. They attributed the differences to the fact that microscopic examination and flow cytometric analysis both take a direct measure of parasite number, with non-viable parasites counted in blood smears also reflected in the flow cytometric analysis, whereas the [^{3}H]-hypoxanthine incorporation assay does not directly reflect parasite number, but parasite growth (Saito-Ito *et al*., 2001).

The probe utilised in this study, dihydroethidium (hydroethidine) is oxidised into the DNA intercalating ethidium cation (E^+) by dehydrogenase enzymes present only in viable cells, therefore hydroethidine fluorescence should only be attributed to viable parasites (Olive, 1989; Grimberg, 2011). However, it has been shown that hydroethidine can react with H_2O_2 to form E^+, and can also react with coordinated Fe(III) as well as mitochondrial cytochromes to form an oxidation product with a similar excitation and emission profile to that of E^+ (Papapostolou *et al*., 2004; Zielonka and Kalyanaraman, 2010).

The discrepancies between the IC_{50} values obtained by flow cytometric analysis and the [^{3}H]-hypoxanthine incorporation assay (Table 3.3) may, therefore, be attributed to the spontaneous conversion of hydroethidine into E^+ within the parasite, and subsequent intercalation of E^+ into residual DNA of non-viable parasites, or to fluorescent interference by the hydroethidine-coordinated Fe(III) or hydroethidine-cytochrome oxidation products. However, in the presence of DNA, the hydroethidine-coordinated Fe(III)/cytochrome oxidation products only produce a 7-fold increase in fluorescent intensity, whereas binding of E^+ to DNA produces a 40-fold increase in fluorescent intensity, when compared to the unbound form (Papapostolou *et al*., 2004; Zielonka and Kalyanaraman, 2010).

Therefore, the correlation between parasite growth as determined by microscopic and flow cytometric analysis and discrepancies between flow cytometric analysis and the [^{3}H]-hypoxanthine incorporation assay may be due to that fact that non-viable parasites counted in microscopic analysis were also reflected in flow cytometric analysis. Thereby producing IC_{50} values that were inflated when compared to those obtained by the [^{3}H]-hypoxanthine incorporation assay; where the [^{3}H]-hypoxanthine incorporation assay only measured the incorporation of [^{3}H]-hypoxanthine into the DNA of viable parasites.

In the case of quinine, the IC_{50} value obtained by flow cytometric analysis was far less than that obtained by the [^{3}H]-hypoxanthine incorporation assay (Table 3.3). Quinine itself exhibits fluorescence and may have resulted in fluorescent interference. With a solution of quinine sulphate or quinine hydrochloride in dilute sulphuric acid used as a fluorescence standard for calibrating spectrofluorometers (Chen, 1967; Fletcher *et al*., 1973). However, samples of quinine hydrochloride prepared to concentrations of 1 µM, 100 nM and 10 nM, exhibited excitation and emission spectra of 200-250 nm and 370-500 nm, respectively, when read on a Perkin Elmer LS50 luminescence spectrophotometer, differing from the excitation and emission spectra of dihydroethidium (Ex = 488 nm, Em = 610 nm).

The discrepancy may be as a result of quinine, due to its weak base properties, altering the pH of the parasite cytosol, resulting in decreased fluorescence of dihydroethidium. With decreased fluorescence of ethidium bromide, the oxidised form of hydroethidine, noted at both acidic and alkaline pH values as a result of denaturation of double-stranded DNA and subsequent lack of intercalation of the probe (LePecq and Paoleti, 1967).

3.4.3 The antimalarial activity of metronidazole

In contrast to the promising antimalarial activity of the metronidazole-thiosemicarbazone analogues, metronidazole exhibited disappointing antimalarial activity (Table 3.2), despite the fact that all indications pointed to the fact that metronidazole should act as an effective antimalarial agent. Metronidazole is activated under microaerobic oxygen concentrations, generating superoxide radicals that in the presence of transition metals form the DNA damaging hydroxyl free-radical, which attack DNA in AT rich regions. All of which is enhanced at an acidic pH (Edwards, 1993; Hoffman *et al*., 1996; Jenks and Edwards, 2002). Similarly, metronidazole exhibited no activity against the W2 and FCR-3 chloroquine-resistant strains of *P. falciparum* (IC_{50} values greater than 800 µM and 1mM, respectively) (Pradines *et al*., 2001; R van Zyl; personal communication).

The inactivity of metronidazole against *P. falciparum* may lie in fundamental differences of the fermentation processes used by metronidazole-sensitive organisms and the malaria parasite (Figure 3.9) (Ginsburg, 2011).

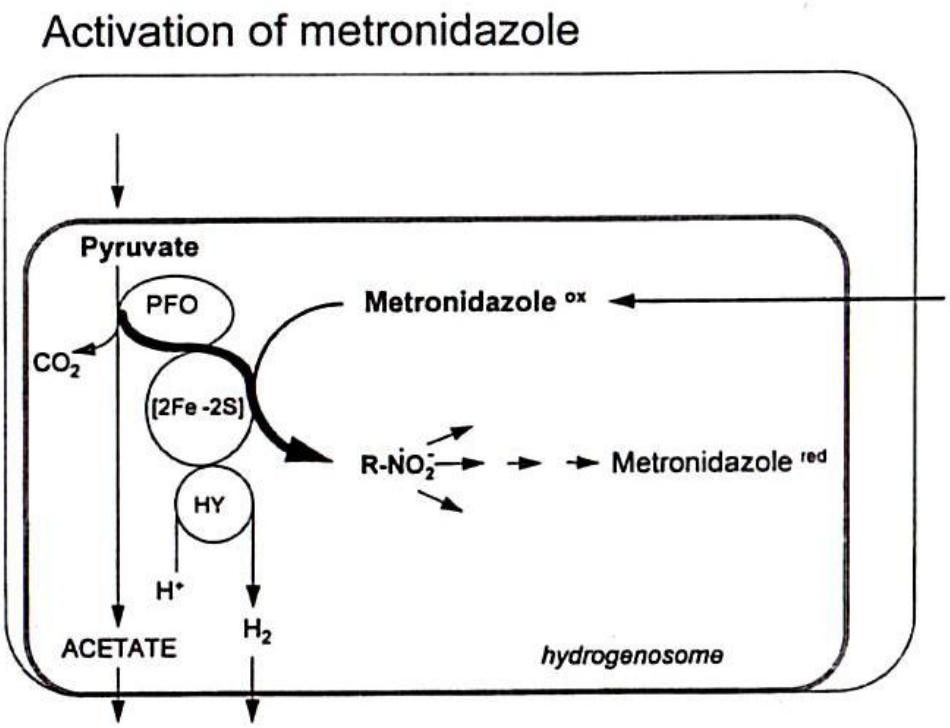


Figure 3.9: The activation of metronidazole in the hydrogenosome of the trichomonad protozoa (Kulda, 1999). PFO: pyruvate:ferrodoxin oxidoreductase; HY: hydrogenase; 2Fe-2S: ferrodoxin.

The nitro group of metronidazole requires activation by accepting electrons from the electron carrier ferrodoxin, with the electrons originating from the decarboxylation of pyruvate by pyruvate:ferrodoxin oxidoreductase (PFO), the complex responsible for the fermentation of pyruvate to ethanol or acetate (Figure 3.9) (Samuelson, 1999; Jenks and Edwards, 2002; Land *et al*., 2002).

Furthermore, the reduction of the nitro group establishes a transmembrane concentration gradient, facilitating the entry of metronidazole into the cell (Samuelson, 1999; Jenks and Edwards, 2002). In this manner, the lack of activity against *P. falciparum* may be due to the fact that metronidazole requires activation by a redox system with a lower reduction potential than that of the drug (-486 mV), with a lack of activation resulting in the decreased accumulation of metronidazole in the parasite (Kulda, 1999; Mendz and Mégraud, 2002).

Although *P. falciparum* possesses a strong reducing environment, as well as an apicoplast-located ferrodoxin and ferrodoxin-$NADP^+$ reductase which form a short electron chain for the production of isoprenoid precursors, it lacks the PFO complex, which may be necessary in producing a sufficient reduction potential for metronidazole activation (Balconi *et al*., 2009; Ginsburg, 2011). With metronidazole resistance in trichomonads partially attributed to a decrease in PFO activity, and subsequent lack of activation of the drug (Kulda, 1999; Land *et al*., 2002).

P. falciparum lacks the PFO complex possibly due to the fact that, in contrast to metronidazole-sensitive organisms, pyruvate produced by glycolysis is converted into lactate, through the action of lactate dehydrogenase enzymes, and transported out of the parasite into the host cell (Samuelson, 1999; Olszewski *et al*., 2010). The resultant acetyl-CoA produced through the action of the pyruvate dehydrogenase complex is used for fatty acid elongation instead of acetate or ethanol production (Samuelson, 1999; Olszewski *et al*., 2010; Ginsburg, 2011).

3.4.4 Possible mechanisms of action of the metronidazole-thiosemicarbazone analogues

Although the latter proved not to be a possible mechanism of action of the metronidazole-thiosemicarbazone analogues, the unique biochemical pathway in which haemoglobin is

digested by the parasite to form haemozoin and amino acids, is a viable antimalarial drug target (Biot and Chibale, 2006). With this in mind, the ability of the metronidazole-thiosemicarbazone analogues to inhibit the formation of synthetic haemozoin (β-haematin) in a manner similar to chloroquine was tested.

The ability of the analogues to inhibit the formation of β-haematin correlated ($r^2 = 0.868$) to their antimalarial activity (Figure 3.10), with compounds incapable of inhibiting β-haematin formation exhibiting low or no antimalarial activity. Thus indicating a possible mechanism of action of the metronidazole-thiosemicarbazones under investigation.

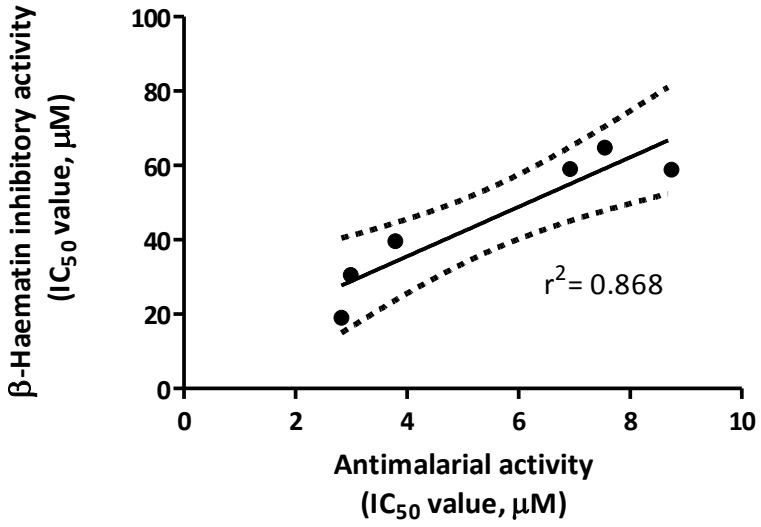


Figure 3.10: The correlation between antimalarial and β-haematin inhibitory activity of the metronidazole-thiosemicarbazone analogues. Plotted with a 95% confidence interval.

On examination of the structure-activity relationship of the aminoquinolones, whose primary mechanism of action is inhibition of haemozoin formation, three criteria were established for antimalarial activity: 1) The compound must contain basic side chains so as to allow accumulation in the food vacuole due to pH trapping; 2) the compound must be able to form complexes with Fe(III) protoporphyrin IX and, 3) the compound must be capable of inhibiting β-haematin formation (Figure 3.11) (Egan *et al*., 2000).

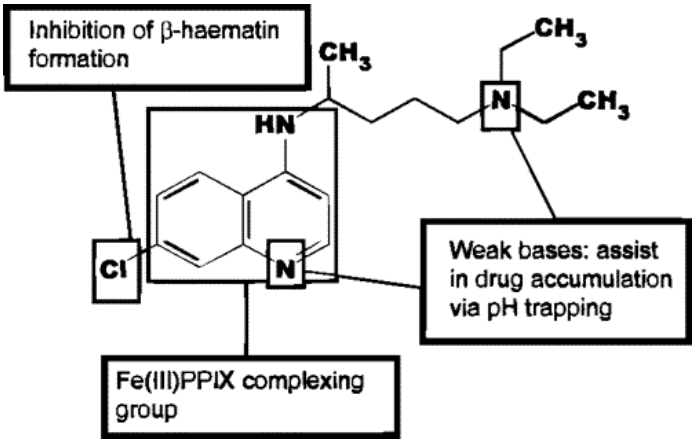


Figure 3.11: Proposed structure-activity relationships for the antimalarial and β-haematin inhibitory activities of chloroquine (Egan *et al*., 2000).

The proposed mechanism by which chloroquine exerts its effects on β-haematin formation involves the following: the weak base diffuses into the food vacuole along the pH gradient, where it is trapped due to protonation at the low pH of the food vacuole (Figure 3.12).

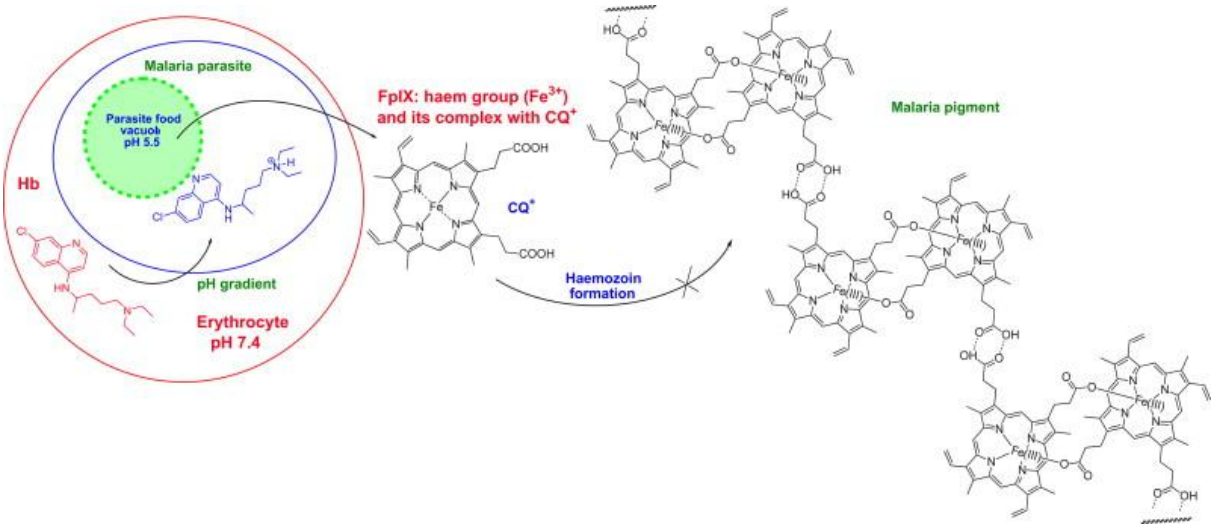


Figure 3.12: The proposed mechanism of action of chloroquine (Kouznetsov and Gómez-Barrio, 2009).

Increased protonation of the drug results in more compound entering the food vacuole, where it forms a complex with Fe(III) protoporphyrin IX (Figure 3.12), possibly through the interaction of the nitrogen atom of the quinoline ring and Fe(III) or through the interaction

with haem propionate groups, thereby inhibiting the formation of haemozoin (Sullivan, 2002; de Dios *et al*., 2003; Egan, 2008).

When examining the structures of the metronidazole-thiosemicarbazone analogues, it can be hypothesised that the nitrogenous groups may act as weak bases, trapping the drug in the acidic food vacuole of the parasite, in a manner similar to chloroquine (Figure 3.11), and that the N^4 substitutions confer the β-haematin inhibitory activity of the analogues. Upon examining the N^4 substitutions of the compounds, it can be seen that substitutions which do not contain an amine group lack antimalarial activity, as observed in compounds Y-5 and Y-6 (Table 3.2). Thus indicating that the thiourea moiety appears to be essential for β-haematin inhibitory and subsequent antimalarial activity, possibly through complex formation with haem propionate groups or with Fe(III) directly (Egan *et al*., 2000; de Dios *et al*., 2003). The exception is compound Y-7 which does not contain an amine group, yet still exhibits strong β-haematin inhibitory and antimalarial activity (Figure 3.7). However, compound Y-7 has a quinoline ring structure, similar to that of chloroquine (Figure 3.11), wherein the nitrogen atom of the quinoline ring may act to complex Fe(III) protoporphyrin IX (Egan *et al*., 2000; de Dios *et al*., 2003).

Metronidazole-thiosemicarbazone analogues may, therefore, act in a similar manner to chloroquine, by accumulating in the food vacuole and forming drug-haemin complexes via interaction with haem propionate groups or with Fe(III), thereby sequestering haem and preventing its polymerisation into haemozoin (Sullivan, 2002; Egan, 2008). Particularly in the case of compound Y-3 (IC_{50} value: 19.08 ± 2.37 μM) (Figure 3.7) which contains a chloro-atom, known to be involved in the inhibition of haemozoin formation (Figure 3.11) (Sullivan, 2002; Egan, 2008).

Various mechanisms of antimalarial action have been proposed for thiosemicarbazones, with the majority pointing towards processes affecting haemoglobin digestion such as the formation of complexes with iron via amine and thiocarbonyl moieties (Figure 3.13). With the iron-thiosemicarbazone complexes inhibiting cysteine protease activity; where the nucleophilic attack of the thiosemicarbazone moiety on the electrophilic centres of the cysteine protease enzymes inhibit activity (Chellan *et al*., 2010; Zhong *et al*., 2010; Rodriguez-Lucena *et al*., 2011).

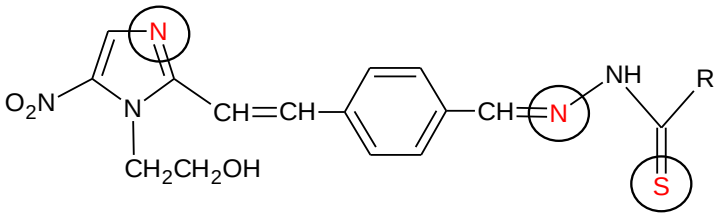


Figure 3.13: The general structure of the metronidazole-thiosemicarbazone analogues, indicating the donor groups capable of chelating metals (Liberta & West, 1992; Athar *et al*., 2005).

The ability of thiosemicarbazones to chelate iron has been well documented, with the resultant effect of not only the inhibition of haemoglobin digestion and haem biosynthesis, but also withholding iron from vital enzymes such as ribonucleotide reductase, thereby interfering with DNA synthesis and division (Chipeleme *et al*., 2007; Chellan *et al*., 2010; Rodiquez-Lucena *et al*., 2011). In this study, the analogues exhibited no Fe(II) chelation properties (Table 3.4), with compound Y-8 only capable of chelating 55.64 ± 9.31% of Fe(II) at 200 µM. This may be explained by the fact that the iron atom has six coordination sites; the thiosemicarbazone moiety of the metronidazole-thiosemicarbazone analogues provides two donor groups, whilst the metronidazole moiety contributes one donor group shown to be capable of chelating transition metals (Figure 3.13) (Athar *et al*., 2005).

In this manner, the compounds may act as tridentate chelators, chelating iron in a 2:1 ratio of drug to iron (200 µM). However at this drug concentration all, with the exception of compound Y-8, exhibited little activity, possibly indicating that the structure of the compounds does not allow for the optimal conformation for the chelation of Fe(II). Additionally, this group of analogues may preferentially bind Fe(III). In studies conducted with derivatives of desferrioxamine (DFO), a potent iron chelator, it was shown that the derivatives maintained the ability to bind Fe(III), but exhibited a reduced affinity to bind Fe(II). Whilst still maintaining their activity against *P. falciparum,* possibly due to the fact that the parasite's iron pool is in the form of Fe(III) (Mabeza, 1999; Chipeleme *et al*., 2007; Chellan *et al*., 2010).

Thiosemicarbazones are known to chelate a wide variety of transition metals and as such this set of analogues may preferentially chelate other transition metals, such as copper. Copper ions have five coordination sites and exist in two oxidation states, as the reduced cuprous form, Cu(I), and the oxidised cupric form, Cu(II), with both forms favouring different donor groups (Ding *et al*., 2011). The cuprous form is capable of adopting geometries which are not usually favoured by other metals, forming complexes with thiolates and thioethers, whereas the cupric form favours complex formation with amines (Ding *et al*., 2011). Depending on the geometry of the bond formed between the ligand and the copper ion, a chelator may not only favour Cu(I) over Cu(II), but may also result in the reduction of Cu(II) to Cu(I), as is the case with the nitrogen-heterocyclic, neocuprine (2,9-dimethyl-1,10-phenanthroline), a bidentate copper ion chelator (Ding *et al*., 2011).

Copper is a co-factor of many malarial enzymes, such as Cu/Zn superoxide dismutase, which is ingested from the erythrocyte cytoplasm together with haemoglobin (Rasoloson *et al*., 2004). Cu/Zn superoxide dismutases act as part of the enzymatic anti-oxidant defence systems, such that chelation of copper would not only impair these defence systems, but the partial dissociation of a drug-copper complex may result in ROS formation. This may deplete GSH, thereby inhibiting haem detoxification (Müller, 2004; Rasoloson *et al.*, 2004; Hancock *et al*., 2011). One such sulphur based compound, N, N-diethyldithiocarbamate (Figure 3.14) has been shown to inactivate Cu/Zn superoxide dismutases in erythrocytes by reacting with oxyhaemoglobin, resulting in the production of free-radicals and oxidised N, N-diethyldithiocarbamate, which in turn reacts with thiols resulting in GSH depletion and enzyme inactivation (Ding *et al*., 2011).

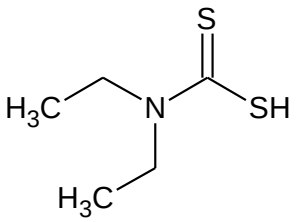


Figure 3.14: The chemical structure of N, N-diethyldithiocarbamate (Ding *et al*., 2011).

Although the analogues did not act as secondary anti-oxidants by chelating iron, thereby preventing ROS formation, they did exhibit strong free-radical scavenging activity, proving

highly effective in scavenging the free-radical of DPPH$^{\bullet}$ (Table 3.4). Compounds Y-8, Y-5 and Y-7 exhibited the most promising anti-oxidant ability, and were comparable ($p > 0.05$) to the anti-oxidant capabilities of ascorbic acid (Table 3.4). Compound Y-3 exhibited poor free-radical scavenging activity, whereas compound Y-6 and metronidazole proved to be inactive (Table 3.4), indicating that the *N*-methyl benzyl amine, 1,2,3,4-tetrahydroquinoline and pyrrolidine side chain substitutions appeared to confer increased anti-oxidant activity. A study conducted on benzyloxybenzaldehyde-4-phenyl-3-thiosemicarbazone (Figure 3.8d), a thiosemicarbazone exhibiting strong structural similarities with this set of analogues, showed that it exhibited similar DPPH$^{\bullet}$ free-radical scavenging activities (42% scavenging at 100 µM) to the standard anti-oxidant, α-tocopherol (53% scavenging at 100 µM) (Prathima *et al*., 2011).

The anti-oxidant capabilities of the analogues may be due to the nitrogen-containing moieties of the analogues, where amine groups have been shown to act as anti-oxidants through the dissociation of the N-H bond, and in this way donate a hydrogen atom to the DPPH$^{\bullet}$ free-radical (Saito and Ishihara, 1997; Nishiyama *et al*., 2002). Compounds that exhibit both antimalarial and anti-oxidant capabilities are highly beneficial, in that not only do they cause parasite death, but they also neutralise the ROS which cause lipid peroxidation and the consequent vascular damage seen in patients infected with *P. falciparum* malaria (Postma *et al*., 1996; Quaye, 2008).

Combinations of compounds Y-3 or Y-7 with quinine or dihydroartemisinin exhibited additive interactions at most tested ratio of analogue:quinine or dihydroartemisinin (Figure 3.4; Appendix C). In order to improve treatment outcome and decrease the risk of antimalarial drug resistance, the WHO advocates the use of combination therapy in the treatment of malaria, specifically the use of quinine or artemisinin derivatives (Section 1.3) (WHO, 2010b). It is, therefore, imperative to understand the interaction of compounds in combination, as ultimately their interaction could indicate their efficacy in a clinical setting.

The pharmacological interaction of two drugs in combination is said to be synergistic when the activity of the combination is higher than that of the activities of the individual drugs added together, additive when the combination produces the same effect as the activity of

the individual drugs added together, and antagonistic when the activity of the combination is lower than the activities of the individual drugs added together (Bell, 2005).

A synergistic interaction may result from: 1) The binding of drug X to a target enhancing the binding of drug Y to the same target, 2) the binding of drug X to a transporter resulting in an influx of drug Y, 3) the formation of a toxic complex by drugs X and Y or 4) the conversion of drug X into its active form by the activity of drug Y (Bell, 2005). With synergism regarded as favourable due to that fact that the doses of the individual drugs may be reduced thereby not only minimising side effects, but also the cost of the treatment regimen (Fidock *et al*., 2004; Bell, 2005). However, a synergistic drug combination wherein both drugs act on the same metabolic pathway, wherein the development of resistance to either component results in loss of efficacy of the combination is not beneficial, as is the case of sulphadoxine-pyrimethamine (Fidock *et al*., 2004). Sulphadoxine-pyrimethamine is a fixed-dose combination of 20 parts sulphadoxine to 1 part pyrimethamine, wherein both drugs act to inhibit enzymes of the folate pathway, resulting in a sequential blockade of folate metabolism (Nzila, 2006; WHO, 2010b). The long elimination half lives of sulphadoxine and pyrimethamine (80 hours and 120 hours, respectively) allows for prolonged exposure of any residual parasites to the combination, and subsequent selection for drug-resistant parasites, which has resulted in high levels of resistance to the combination such that it is no longer recommended for the treatment of malaria in South Africa (Kremsner and Krishna, 2004; National Department of Health, 2010; WHO, 2010b).

Conversely, an antagonistic interaction is unfavourable as the decreased efficacy of the two drugs results in treatment failure, increasing the likelihood of mortality and the spread of drug-resistant organisms (Berenbaum, 1978; Bell, 2005). Antagonism may occur when two drugs act on the same target, as is the case with chloroquine and mefloquine, with the antagonistic interaction possibly due to the inhibition of chloroquine uptake by mefloquine, or the inhibition of haemoglobin uptake into the food vacuole, resulting in reduced haem concentrations (Bell, 2005).

An appropriate combination regimen would be one where an additive or synergistic relationship exists, with the separate components active against different parasitic metabolic targets in different stages of the asexual parasitic life cycle (Fidock *et al*., 2004;

WHO, 2010b). Furthermore, it should be composed of one fast-acting drug, as well as a slowly-eliminated partner drug to clear residual parasites, an example of which is the combination of artemether and lumefantrine (WHO, 2010b).

The additive interaction between the analogues and quinine (Figure 3.4; Appendix C) appears to be as a result of the two groups of drugs acting on different targets. The analogues inhibit parasitic growth past the late ring/early trophozoite-stage. Following the inhibition of haemozoin formation the parasites exhibit intense staining (Figures 3.5b,c) similar to so-called 'crisis forms' observed in *P. falciparum* cultures treated with chloroquine or hydrogen peroxide (Deponte and Becker, 2004). Some authors claim that the nuclear condensation is a hallmark of apoptosis, and others claim that parasitic death occurs via autophagy (Deponte and Becker, 2004; Lopez *et al*., 2010). Residual parasites are then inhibited at the mid to late trophozoite-stage through the action of quinine.

The proposed antimalarial mechanism of action of the quinolines is the inhibition of haemozoin formation (Olliaro, 2001; Biagini *et al*., 2003; Vangapandu *et al*., 2007). Although quinine was capable of inhibiting the formation of β-haematin *ex vivo* (Figure 3.7), an examination of its stage-specific and morphological effects showed no effect on haemozoin formation at all concentrations tested (Figure 3.5), indicating that inhibition of haemozoin formation is not the primary mechanism of action of quinine. Instead, quinine appeared to exert its effects in the mid to late trophozoite-stage, possibly through effects on protein synthesis or parasitic DNA replication; as it has been shown to inhibit parasitic DNA gyrase and intercalate between base pairs in double-stranded DNA (Frayha *et al*., 1997; Padmanaban *et al*., 2007). In this manner, neither drug enhances the activity of the other, but rather act to inhibit parasitic growth through their activity on different targets in different stages of the parasitic life cycle. As seen with the additive interaction noted between chloroquine and quinine in the 3D7 strain of *P. falciparum* (Bell, 2005).

In a similar manner, the interaction between the analogues and dihydroartemisinin also produced an additive effect (Figure 3.4; Appendix C). Artemisinin and its derivatives are active against all stages of the erythrocytic parasitic life cycle, including the ring stage (Vangapandu *et al*., 2007; Krishna *et al*., 2010). The most recently accepted hypothesis of the antimalarial mechanism of action of this class of antimalarials involves the inhibition of

*Pf*ATP6, a Ca^{2+}-ATPase localised to the endoplasmic reticulum and possibly the plasma membrane (Vangapandu *et al*., 2007; Krishna *et al*., 2010). *Pf*ATP6 maintains cytosolic calcium levels, inhibition of which leads to increased cytosolic calcium levels causing dysregulation of various parasitic processes such as parasite invasion and egress, as well as progression through the life cycle (Vangapandu *et al*., 2007; Krishna *et al*., 2010).

Studies conducted combining FR 160, a dicatecholate Fe(II) and Fe(III) chelator, with artesunate and dihydroartemisinin showed antagonistic interactions (Pradines *et al*., 2002; Bell, 2005). The antagonistic interaction may be explained by the fact that Fe(II) is required for the activity of artemisinin and its derivatives on *PfATP6* or that FR 160 acts to induce free-radical generation, thereby interfering with the mechanism of action of the artemisinin derivatives (Pradines *et al*., 2002; Bell, 2005). The fact that iron chelators appear to antagonise the activity of the artemisinin derivatives, whereas the thiosemicarbazone analogues interacted in an additive manner (Figure 3.4; Appendix C), points to the fact that the mechanism of action of the analogues does not lie in their ability to chelate iron and generate free-radicals. If this were their mechanism of action, an antagonistic interaction should have been observed.

Similarly to that observed with the quinine combination studies, it appears as if the metronidazole-thiosemicarbazone analogues and dihydroartemisinin act on different targets within the parasite, with dihydroartemisinin inhibiting the activity of *PfATP6* throughout the parasitic life cycle, and the analogues inhibiting haemozoin formation in the late ring/early trophozoite-stages (Figure 3.5).

Previous studies have hypothesised that the artemisinin derivatives act by inhibiting haemozoin formation (Pandey *et al*., 1999; Kannan *et al*., 2005), however when screened for β-haematin inhibitory activity, dihydroartemisinin was only capable of 7.46 ± 2.27% inhibition at 100 µM (Section 3.3.4.1). In accordance with this observation, no inhibition was observed by other investigators when using the β-haematin inhibitory activity (BHIA) assay, indicating that these compounds do not form π-π interactions with haematin (Haynes *et al*., 2003; Feng *et al*., 2011).

Thiosemicarbazones may attack various biological targets within the malaria parasite, such as DNA synthesis, haemoglobin digestion, and haem biosynthesis (Chellan *et al*., 2010;

Hancock *et al*., 2011). This study has included an extra possible antimalarial mechanism of action, in their ability to inhibit haemozoin formation. The fact that the strong β-haematin inhibitory activity of some analogues, one of which exceeded the activity of chloroquine, did not equate to antimalarial activity in the nanomolar range of chloroquine indicated that perhaps the lipophilicity of the analogues needs to be enhanced, to facilitate the movement of the analogues through membranes so as to enhance their accumulation in the food vacuole of the parasite. The addition of aminoalkyl side chains in the place of metronidazole may also prove beneficial, in order to enhance pH trapping of the compounds within the food vacuole. A study conducted by Egan *et al*. (2000), showed that aminoquinoline derivatives lacking an aminoalkyl side chain showed strong Fe(III) protoporphyrin IX complexing activity and β-haematin inhibitory activity. However, their antimalarial activity lay between 3.8 and 5 μM when compared to chloroquine, which had an IC_{50} value of 38 nM (Egan *et al*., 2000).

It can be concluded that the thiosemicarbazone class of compounds show promising antimalarial activity; however, the addition of metronidazole to the thiosemicarbazone backbone may in fact hamper the iron chelation abilities of thiosemicarbazones by hindering the rotation of the analogues. The additive interaction between compounds Y-3 and Y-7 when combined with currently used antimalarials, as well as their ability to act as anti-oxidants would prove beneficial in the treatment of *P. falciparum* infected individuals. However, a concern would be the pharmacokinetic profile of thiosemicarbazone analogues. It has been shown that Triapine®, a thiosemicarbazone derivative, although generally well tolerated at doses of up to 160 mg/m^2 daily (intravenously), possessed an elimination half-life ranging from 1.67 to 2.30 hours (Giles *et al*., 2003; Murren *et al*., 2003). In this respect, a combination of a thiosemicarbazone analogue with an artemisinin derivative; wherein both drugs have short half-lives may result in recrudescence or require the patient to be on an intravenous drip. Synthesis of derivatives and further investigation into these compounds to include a more favourable pharmacokinetic profile, and an examination of their toxicity on mammalian cells lines may in time provide a new class of potent antimalarials.

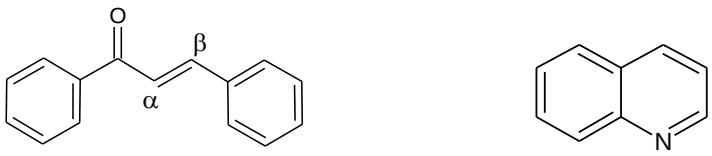
CHAPTER 4: THE ANTIMALARIAL PROPERTIES OF CHLOROQUINOLINE-CHALCONES

4.1 Introduction

Strategies for antimalarial drug discovery include: combination therapies, drug-resistance reversers, analogues of existing antimalarials, the development of target-specific compounds, and the mass screenings of plant-derived compounds (Biagini *et al*., 2003; Muregi and Ishih, 2010). Another drug discovery strategy is the hybridisation of two validated antimalarial drug scaffolds. The principle behind molecular hybridisation is that two compounds, with differing antimalarial mechanisms of action, are fused to produce a single compound with antimalarial activity exceeding that of its components in singularity (Guantai *et al*., 2010; Muregi and Ishih, 2010). Hybridisation is an attractive strategy when applied to compounds to which resistance has developed, such as chloroquine, as the addition of the second compound may act to circumvent or reverse drug resistance (Guantai *et al*., 2010; Muregi and Ishih, 2010).

4.1.1 Chalcones

Chalcone or 1,3-diaryl-2-propen-1-ones (Figure 4.1a) act as key intermediates for the assembly of various heterocyclic scaffolds (Ren *et al*., 2003; Nowakowska, 2007; Bhattacharya *et al*., 2009). They typically consist of two aromatic rings, linked by a three carbon α, β-unsaturated ketone bridge (Figure 4.1a), with many naturally occurring chalcones capable of acting as anti-oxidants, due to polyhydroxylation of their aromatic rings (Go, 2003; Ren *et al*., 2003; Nowakowska, 2007).



a) b)

Figure 4.1: The basic structure of a) a chalcone (Bandgar *et al*., 2010) and b) a quinoline (Guantai *et al*., 2010).

Chalcones are the precursors to a large family of compounds known collectively as flavonoids, which encompass more than 4000 natural polyphenolic compounds abundant in fruits, spices and vegetables (Go, 2003; Ren *et al*., 2003; Nowakowska, 2007), and possess a wide range of biological activities, including anti-inflammatory, anticancer, antiprotozoal and antibacterial effects (Nowakowska, 2007; Mishra *et al*., 2008). One such chalcone is isoliquiritigenin, a component of *Glycyrrhiza glabra L.* (liquorice root), which is currently used as a vasorelaxant, exerting its effects through inhibition of phosphodiesterase III; whilst also possessing antiplatelet aggregation, anti-allergy and anti-cancer properties (Wegener and Nawrath, 1997; Takahashi *et al*., 2004).

The antimalarial properties of chalcones was discovered during a routine screening, where it was found that licochalcone A, an oxygenated chalcone also extracted from *Glycyrrhiza glabra L.,* exhibited antimalarial activity (Chen *et al*., 1994; Go *et al*., 2004). The antimalarial effects of licochalcone A was similar in both chloroquine-sensitive (3D7) and chloroquine-resistant (Dd2) strains of *P. falciparum*, with licochalcone A inhibiting parasite growth by 50% at 0.6 µg/ml, compared to chloroquine which inhibited 50% of parasite growth by 50 ng/ml and 86 ng/ml in the two strains, respectively (Chen *et al*., 1994). In addition, licochalcone A has shown to act as a potent *in vitro* inhibitor of pro-inflammatory responses, which would be beneficial in the treatment of malaria (Kolbe *et al*., 2006).

This discovery prompted an interest in chalcones as antimalarial agents, with various alkoxylated and hydroxylated chalcones; as well as sulphonamide and phenylurea-chalcone derivatives shown to exhibit variable activity against *P*. *falciparum in vitro* (Go *et al*., 2004; Nowakowska, 2007; Mishra *et al*., 2008).

4.1.2 Quinolines

Quinolines (Figure 4.1b), quinine and cinchonine, isolated from the bark of the cinchona tree in the 18th century constituted the first successful treatment of malaria (Wozniacka *et al*., 2002; Sharma, 2005; Solomon and Lee, 2009). During the Second World War, due to the difficulty in the chemical synthesis of quinine, the synthetic quinoline derivative, chloroquine, replaced quinine as the primary prophylactic and antimalarial agent (Wozniacka *et al*., 2002; Sharma, 2005; Solomon and Lee, 2009). For decades chloroquine has been the primary antimalarial chemotherapy due to its low cost, clinical efficiency, and

favourable pharmacokinetic profile (Fidock *et al*., 2004; Sharma, 2005). Chloroquine is absorbed rapidly following oral, intramuscular, or subcutaneous administration and is largely bound to plasma proteins, exhibiting a terminal elimination half-life of one to two months (WHO, 2010b). Metabolism occurs in the liver to form monodesethylchloroquine, which exhibits similar activity against *P. falciparum* (WHO, 2010b). However, decades of use has contributed to the widespread resistance of *P. falciparum*, rendering the drug ineffective in most parts of the world, including South Africa (Fidock *et al*., 2004; National Department of Health, 2009).

Chloroquine is a diprotic weak base, existing as unprotonated, mono-protonated and di-protonated forms (Sanchez *et al*., 2010). Chloroquine, in its unprotonated form, is capable of crossing the membrane of the food vacuole where, upon exposure to the acidic pH, it becomes protonated making it membrane impermeable (Sanchez *et al*., 2010). It exerts its effects in the food vacuole by binding to haem, thereby inhibiting the formation of haemozoin (Figure 3.12), resulting in parasite death due to oxidative stress (Olliaro, 2001; Vangapandu *et al*., 2007; Sanchez *et al*., 2010). Under physiological conditions, the pH of the food vacuole of the malaria parasite is maintained by a H^+-ATPase pump moving H^+ ions into the food vacuole to counter the outward leak of H^+ by an as-yet uncharacterised pathway (van Schalkwyk and Egan, 2006; Lehane *et al*., 2008). It has been previously hypothesised that chloroquine-resistance may be attributed to an increase in the pH of the food vacuoles of chloroquine-resistant parasites, compared to those of sensitive strains (Ginsburg, 1988), which would result in decreased chloroquine accumulation due to weak base trapping (Ginsburg, 1988). However, recent publications have shown that there is no significant difference between the pH of the food vacuoles of chloroquine-resistant and sensitive strains (van Schalkwyk and Egan, 2006; Lehane *et al*., 2008; Sanchez *et al*., 2010).

A more likely hypothesis is that chloroquine-resistance is attributed to mutations in parasitic chromosomes, resulting in the decreased accumulation of chloroquine in the food vacuole (Vangapandu *et al*., 2007; Sanchez *et al*., 2010; WHO 2010b). *Plasmodium falciparum* chloroquine resistance transporter (*Pf*CRT), localised to the food vacuole membrane, mediates the transport of drugs in and out of the food vacuole, both directly and indirectly by transporting drugs and by contributing to the generation of the pH gradient (Figure 4.2) (Vangapandu *et al*., 2007; van Schalkwyk and Egan, 2006; Sanchez *et*

al., 2010). *Pf*CRT mutations confer chloroquine-resistance by resulting in the efflux of chloroquine from the food vacuole at rates 40 times higher than that observed in chloroquine-sensitive strains of *P. falciparum* (Vangapandu *et al*., 2007; Fidock *et al*., 2008).

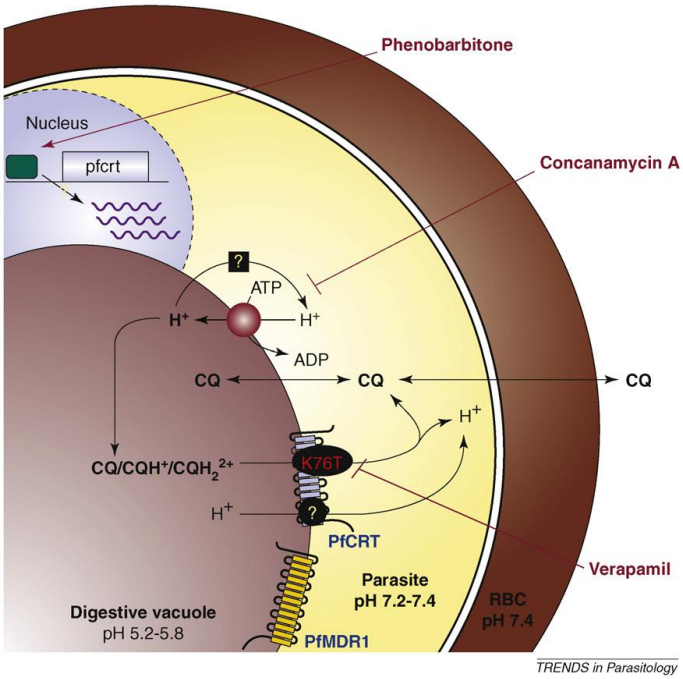


Figure 4.2: Mechanisms of chloroquine-resistance in *P. falciparum* (Fidock *et al*., 2008). With the circled question mark referring to the hypothesis that the efflux of chloroquine from the food vacuole might be H^+-coupled and the black boxed question mark referring to the outward leak of H^+ by an as-yet uncharacterised pathway. Where: $CQ/CQH^+/CQH_2^{2+}$ = chloroquine/monoprotonated chloroquine/diprotonated chloroquine; RBC = red blood cell; PfMDR1 = *Plasmodium falciparum* multi-drug resistance transporter; *Pf*CRT = *Plasmodium falciparum* chloroquine resistance transporter.

Chloroquine-resistance has been attributed to numerous polymorphisms within the *pfcrt* gene, however, conserved amongst the mutant alleles is the replacement of the charged amino acid lysine with the neutral amino acid threonine (K76T) (Fidock *et al*., 2008; Sanchez *et al*., 2010). With the loss of positive charge resulting in the efflux of the protonated form of chloroquine back into the parasite cytoplasm (Figure 4.2) (Fidock *et al*., 2008). Lehane *et al*. (2008) showed that upon inhibition of parasitic H^+-ATPase pumps with concanamycin A, a macrolide antibiotic which inhibits vacuolar H^+-ATPase pumps, alkalinisation of the food

vacuoles of chloroquine-resistant strains were up to 4-fold higher than that observed in chloroquine-sensitive strains. The same study also showed that in the presence of chloroquine a rapid alkalinisation of the food vacuole was noted in chloroquine-resistant strains, with chloroquine-sensitive strains exhibiting a decreased rate of food vacuole alkalinisation (Lehane *et al*., 2008). A process that was inhibited by verapamil, a calcium channel blocker, possibly due to the fact that the positively charged amino group of verapamil compensates for the loss of positive charge in mutated *Pf*CRT's (van Schalkwyk and Egan, 2006; Lehane *et al*., 2008). All of which favours the hypothesis that *Pf*CRT transports chloroquine in symport with H^+ ions, with *Pf*CRT mutations resulting in the efflux of chloroquine and H^+, and subsequently increased rate of alkalinisation of the food vacuole (Lehane *et al*., 2008; Sanchez *et al*., 2010).

Furthermore, mutations within the *Plasmodium falciparum* multi-drug resistance transporter (*pfmdr* 1) gene, implicated in mefloquine and halofantrine resistance, have also been implicated in chloroquine-resistance in certain strains (Vangapandu *et al*., 2007; Johnson *et al*., 2008). It has been shown that the anticonvulsant, phenobarbitone, increased the expression of the gene product of *pfmdr* 1, P-glycoprotein homologue protein 1 (Pgh1), resulting in decreased sensitivity to chloroquine in both chloroquine-resistant and -sensitive strains *in vitro* (Figure 4.2) (Johnson *et al*., 2008).

A possible means of potentiating the effects chloroquine is through the synthesis of modified chloroquine analogues. Sulphonamide-analogues have shown promising antimalarial activity, with one analogue exhibiting 100-fold higher activity and different mechanism of action to that of chloroquine (Vangapandu *et al*., 2007). Various other analogues, in which the alkyl side chain of chloroquine was modified, also exhibited promising antimalarial activity against chloroquine-resistant strains, providing an indication that the aminoalkyl side chain is an important determinant in chloroquine resistance (Vangapandu *et al*., 2007; van Schalkwyk and Egan, 2006).

The rationale behind the synthesis of a series of chloroquinoline-chalcones was that the molecular hybridisation of the active chloroquinoline and chalcone groups may produce a more potent compound capable of evading chloroquine-resistance.

The objectives of this chapter were to:

- Evaluate the efficacy of the chloroquinoline-chalcone derivatives against a chloroquine-sensitive strain of *P. falciparum* and, pending antimalarial activity similar to or more potent than that of chloroquine, examine the activity of the compounds against a chloroquine-resistant strain.

- Determine possible pharmacological interactions between a lead compound and quinine.

- Examine the stage-specific and morphological effects of a lead compound on parasite development.

- Elucidate possible antimalarial mechanisms of action of the compounds.

- Test for haemolytic activity as an indication of toxicity.

4.2 Materials and methods

4.2.1 Chemical synthesis and structural verification

The chloroquinoline-chalcones (**1-14**) were acquired from Professor A. Azam, Department of Chemistry, Jamia Millia Islamia, New Delhi, India. The compounds were synthesised as depicted in Figure 4.3. A series of 2-chloro-3-formylquinolines were prepared by the condensation of different anilines with acetic acid in the presence of acetic anhydride (Figure 4.3a). Following which the 2-chloro-3-formylquinolines were condensed with various aromatic ketones in the presence of aqueous NaOH in ethanol (Figure 4.3b), to produce the chloroquinoline-chalcones (Table 4.1) (Hayat *et al*., 2011). The chemical structures of the 14 chloroquinoline-chalcones were verified by infrared, ^{1}H, ^{13}C nuclear magnetic resonance and mass spectrophotometry, and purity confirmed by elemental analysis (Hayat *et al*., 2011).

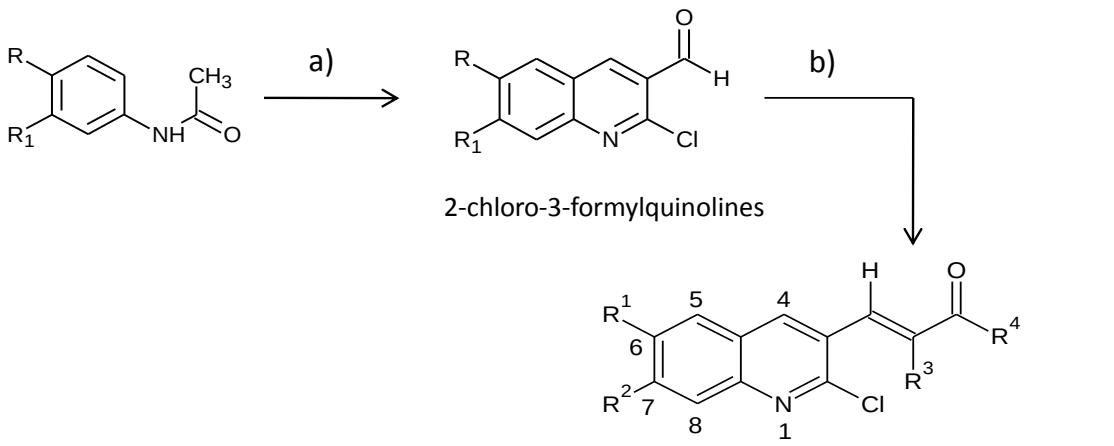


Figure 4.3: The synthesis of chloroquinoline-chalcones (**1-14**). Reagents and conditions: a) dimethylformamide/phosphoryl chloride, 75 °C reflux 17 hours, b) aqueous sodium hydroxide, ethanol, various aromatic ketones (Hayat *et al*., 2011).

Table 4.1: The chloroquinoline-chalcones evaluated for antimalarial activity.

Chemical name	Chemical code
(E)-3-(2-Chloroquinoline-3yl)-1-(pyridine-2yl)prop-2-en-1-one	**F-1**
(E)-1-(3-Bromophenyl)-3-(2-chloroquinoline-3yl)-2-methylprop-2-en-1-one	**F-2**
(E)-1-(4-Chlorophenyl)-3-(2-chloroquinoline-3yl)prop-2-en-1-one	**F-3**
(E)-1-(3-Bromophenyl)-3-(2-chloroquinoline-3yl)prop-2-en-1-one	**F-4**
(E)-1-(4-Bromophenyl)-3-(2-chloroquinoline-3yl)prop-2-en-1-one	**F-5**
(E)-1-(3-Bromophenyl)-3-(2-chloro-6-methylquinolin-3-yl)-2-methylprop-2-en-1-one	**F-6**
(E)-3-(2-Chloro-6-methylquinolin-3-yl)-1-(3-chlorophenyl)-2-methylprop-2-en-1-one	**F-7**
(E)-1-(4-Bromophenyl)-3-(2-chloro-6-methylquinoline-3yl)prop-2-en-1-one	**F-8**
(E)-1-(3-Bromophenyl)-3-(2-chloro-6-methylquinolin-3-yl)prop-2-en-1-one	**F-9**
(E)-3-(2-Chloro-6-methylquinoline-3yl)-1-(pyridine-2yl)prop-2-en-1-one	**F-10**
(E)-3-(2-Chloro-7-methylquinoline-3yl)-1-(3-chlorophenyl)-2-methylprop-2-en-1-one	**F-11**
(E)-1-(3-Bromophenyl)-3-(2-chloro-7-methylquinoline-3yl)-2-methylprop-2-en-1-one	**F-12**
(E)-3-(2-Chloro-7-methylquinoline-3yl)-1-(pyridine-2yl)prop-2-en-1-one	**F-13**
(E)-1-(3-Bromophenyl)-3-(2-chloro-7-methylquinoline-3yl)prop-2-en-1-one	**F-14**

4.2.2 Pharmacological evaluation

The *in vitro* antimalarial activity of the compounds and positive controls were assessed using the [^{3}H]-hypoxanthine incorporation (Section 2.2.2.1) and flow cytometry (Section 2.2.3.3) methodologies. The most active compound was selected for a combination study with quinine (Section 2.2.2.3), as well as for stage sensitivity and parasite morphology studies (Section 2.2.3.4). To elucidate possible antimalarial mechanisms of action; β-haematin inhibitory activity (Section 2.3.1.2), DPPH$^{\bullet}$ free-radical scavenging (Section 2.3.2.1.2) and iron chelation assays (Section 2.3.2.2.2) were carried out. In order to provide an indication of the toxicity of the compounds, a red blood cell toxicity assay was performed (Section 2.4.2). Statistically significant differences were determined by means of an unpaired Students T-test, with $p < 0.05$, using the Graphpad Prism® (version 5) software.

4.3 Results

4.3.1 *In vitro* antimalarial and haemolytic activity

Of the 14 compounds tested for activity against *P. falciparum*, 10 inhibited parasite growth in a dose-dependent manner (Figure 4.4). Of the 10 active compounds, six inhibited parasite growth with IC_{50} values below 50 µM, four between 50 µM and 100 µM, and the remaining four were ineffective at inhibiting parasite growth below 100 µM (Table 4.2).

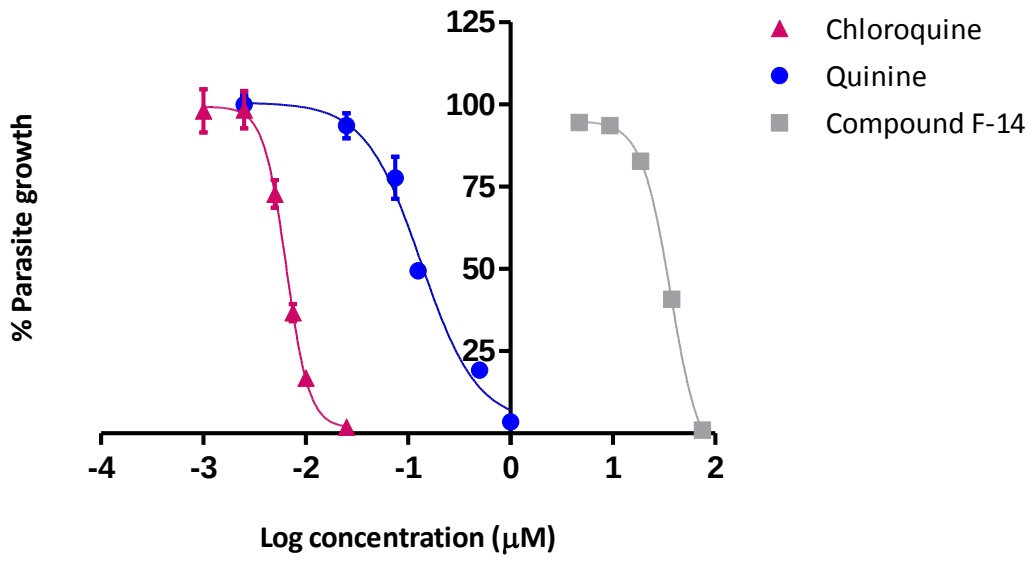
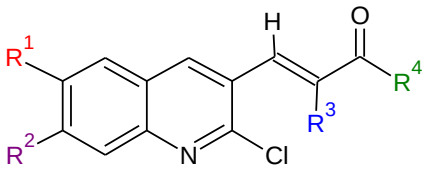
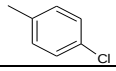
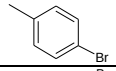
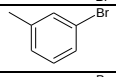
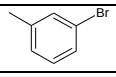
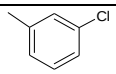
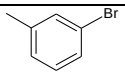
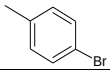
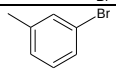
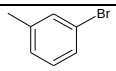
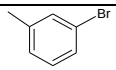
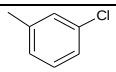


Figure 4.4: Log sigmoid dose-response curves of compound F-14, chloroquine and quinine.

Table 4.2: The *in vitro* antimalarial (1% haematocrit, 0.5% parasitaemia) and haemolytic activity of chloroquinoline-chalcones and positive controls (n = 4). Percentage inhibition of parasite growth at 100 µM is shown in parenthesis.



Compound	R^1	R^2	R^3	R^4	Antimalarial Activity	Haemolytic activity
					IC_{50} value: µM ± s.d. (% growth inhibition at 100 µM)	% Haemolysis at 100 µM (± s.d.)
F-13	H	CH_3	H		31.31 ± 0.87	0.47 ± 0.77
F-10	CH_3	H	H		31.54 ± 3.03	1.55 ± 1.15
F-1	H	H	H		31.98 ± 1.27	1.10 ± 1.04
F-3	H	H	H		39.17 ± 2.05	1.74 ± 0.67
F-5	H	H	H		44.56 ± 1.75	2.20 ± 0.54
F-12	H	CH_3	CH_3		47.06 ± 2.76	1.04 ± 0.64
F-9	CH_3	H	H		50.11 ± 3.58	1.68 ± 0.66
F-11	H	CH_3	CH_3		50.44 ± 3.22	1.44 ± 0.66
F-14	H	CH_3	H		59.73 ± 1.19	1.09 ± 0.55
F-8	CH_3	H	H		74.84 ± 3.39	1.40 ± 0.96
F-4	H	H	H		> 100 (61.22 ± 13.09%)	1.38 ± 0.67
F-6	CH_3	H	CH_3		> 100 (51.15 ± 8.10%)	1.53 ± 0.34
F-2	H	H	CH_3		> 100 (34.30 ± 8.93%)	2.17 ± 0.59
F-7	CH_3	H	CH_3		> 100 (8.74 ± 13.66%)	1.24 ± 0.78
Chloroquine					0.0065 ± 0.0002	0.72 ± 0.32
Quinine					0.14 ± 0.0007	1.22 ± 0.98

Compounds F-13, F-10 and F-1 proved to be the most active; with IC_{50} values of approximately 31 µM (Table 4.2). However, when compared to the antimalarial activity of chloroquine and quinine their activity was statistically less effective ($p < 0.05$).

The haemolytic activity of the compounds was low with percentage haemolysis at 100 µM ranging from 0.47 ± 0.77% to 2.20 ± 0.54%, and were comparable to chloroquine and quinine (0.72 ± 0.32% and 1.22 ± 0.98% haemolysis at 100 µM, respectively) (Table 4.2).

In order to compare results obtained using flow cytometry and the [^{3}H]-hypoxanthine incorporation assay, six compounds were selected for comparison, wherein the % haematocrit and % parasitaemia were 2- and 4-fold higher than that used to obtain the results shown in Table 4.2.

Generally, the IC_{50} values and % parasite growth inhibition at 100 µM exhibited a similar trend in the two methodologies. When comparing the IC_{50} values obtained for compound F-13 using flow cytometric analysis (IC_{50} value: 70.39 ± 0.38 µM) and the [^{3}H]-hypoxanthine incorporation assay (IC_{50} value: 59.48 ± 3.38 µM), no statistically significant difference was noted ($p > 0.05$). A statistically significant difference was apparent ($p < 0.05$) when comparing the IC_{50} values of compound F-1 in the two methodologies, 54.19 ± 3.08 µM and 33.15 ± 1.35 µM as determined by flow cytometric analysis and the [^{3}H]-hypoxanthine incorporation assay, respectively. The % growth inhibition at 100 µM of compounds F-2, F-4, F-6 and F-7 exhibited a similar trend in the [^{3}H]-hypoxanthine incorporation assay and flow cytometric methodologies, although the % growth inhibition as determined by flow cytometry (25.20 ± 1.06% to 34.54 ± 5.39%) was higher than that as determined by the [^{3}H]-hypoxanthine incorporation assay (10.08 ± 4.40 to 12.68 ± 2.32%).

4.3.2 Combination study

The isobologram (Figure 4.5) depicts an additive interaction when compound F-13 was combined with quinine in various ratios. The ΣFIC (1.35 ± 0.11), generated from four experiments (Appendix D), verified the additive interaction shown in Figure 4.5. Falling well within the guidelines of an additive interaction, wherein the ΣFIC_{50} range lies between 0.5 and 2 (Section 2.2.2.3).

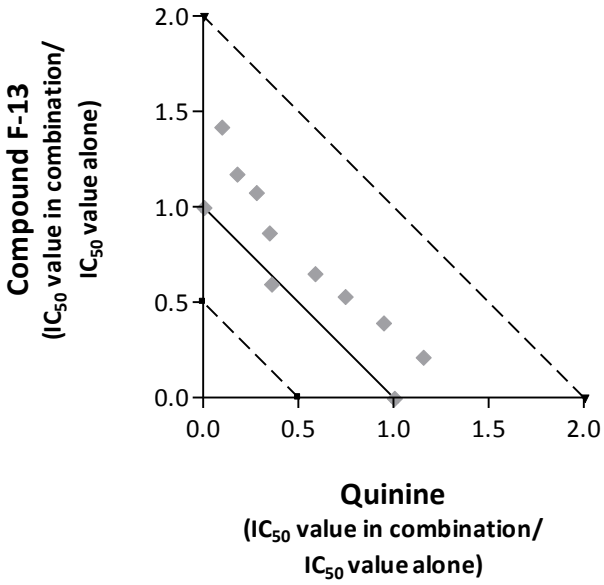


Figure 4.5: The additive pharmacological interaction between compound F-13 and quinine (n = 4).

4.3.3 Morphological and stage-specific effects of compound F-13

The morphological and stage-specific effects of compound F-13 were best visualised using the IC_{50} value (70 µM) (Figures 4.6 and 4.7). No notable changes in parasite morphology or shape occurred during the ring-stage. However, when the untreated parasite control progressed into the early trophozoite-stage, the treated parasites exhibited altered morphology. The treated parasites appeared smaller, with reduced haemozoin formation (Figure 4.6A), and appeared to be in the ring-stage rather than early trophozoite-stage (Figures 4.7A). When compared to the untreated control of parasites in the mid-late trophozoite stage, the treated parasites appeared smaller in size (Figure 4.6B), were primarily in the early trophozoite-stage (Figure 4.7B), and although haemozoin formation was visible, the crystals were not as compact as noted in the untreated control (Figures 4.6B). Thereafter, the parasite control progressed into the early to mid schizont-stage, where merozoite formation was evident (Figure 4.6C). In contrast, treated parasites remained primarily in the trophozoite-stage (Figure 4.7C), with 86% of the treated parasites appearing to be in the early to mid trophozoite-stage, and only 14% of the treated parasites progressing into the schizont-stage (Figure 4.6C). Finally, the parasite control progressed into the late schizont- and early ring-stages (Figures 4.6 and 4.7D), with 71% of parasites in

the early ring-stage, and 29% in the late schizont-stage, equating to an increased parasitaemia of 4.81% (Figure 4.6D). Of the treated parasites, no early ring-stage parasites were present and 48% of parasites were in the early to mid trophozoite-stage (Figure 4.6D). The remaining 52% had progressed into the mid schizont-stage, with the schizonts appearing condensed and the number of merozoites formed reduced (Figure 4.6D), when compared to the early-mid schizont parasite control (Figure 4.6C). An examination of blood smears of the treated parasites four hours post-invasion, or four hours into the next cycle, showed that the schizonts had progressed through the cycle to form merozoites and consequently early rings. However, none of the mid trophozoites had progressed into the schizont-stage, and appeared condensed and intensely stained (data not shown).

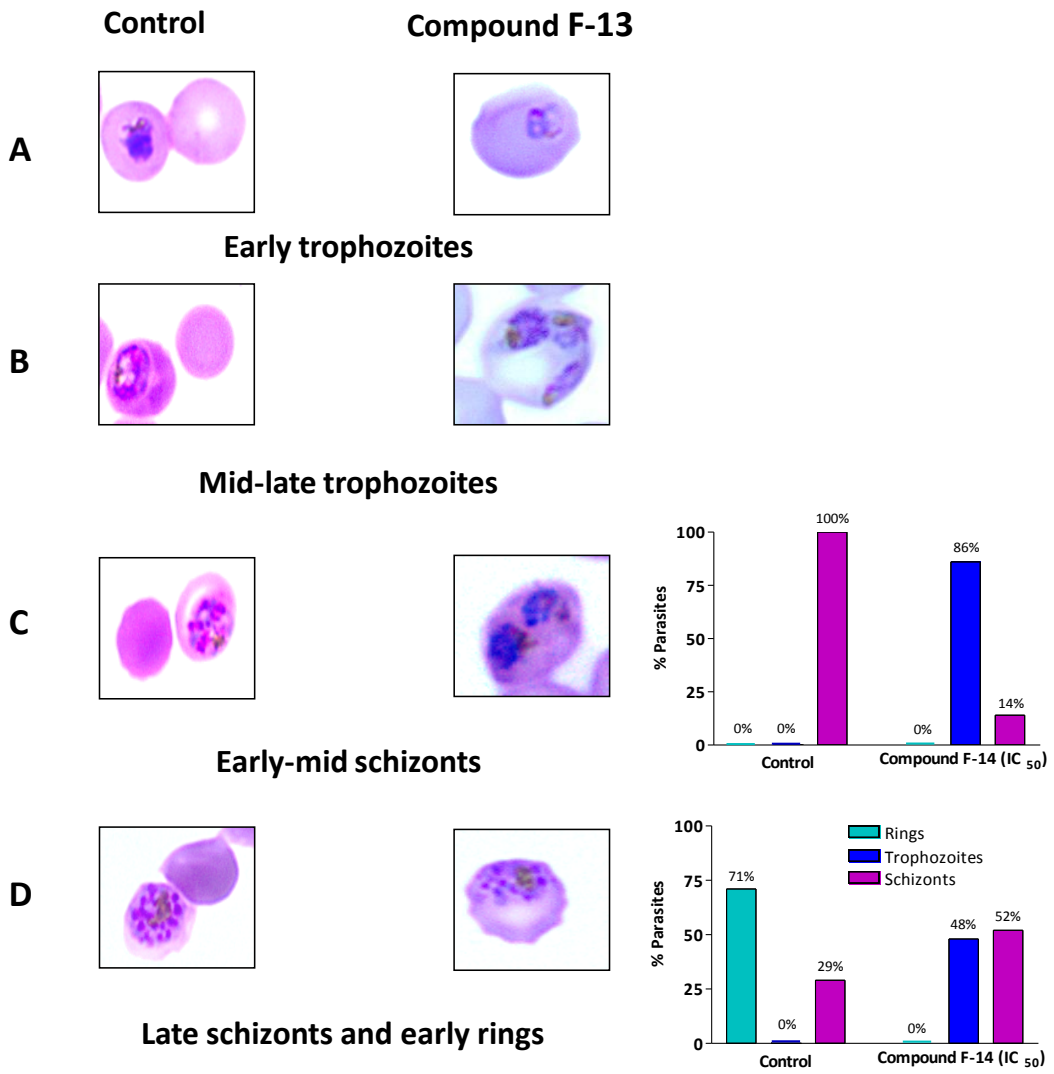


Figure 4.6: The effects of compound F-13 at its IC_{50} value (70 µM) on parasite morphology and development (n = 1).

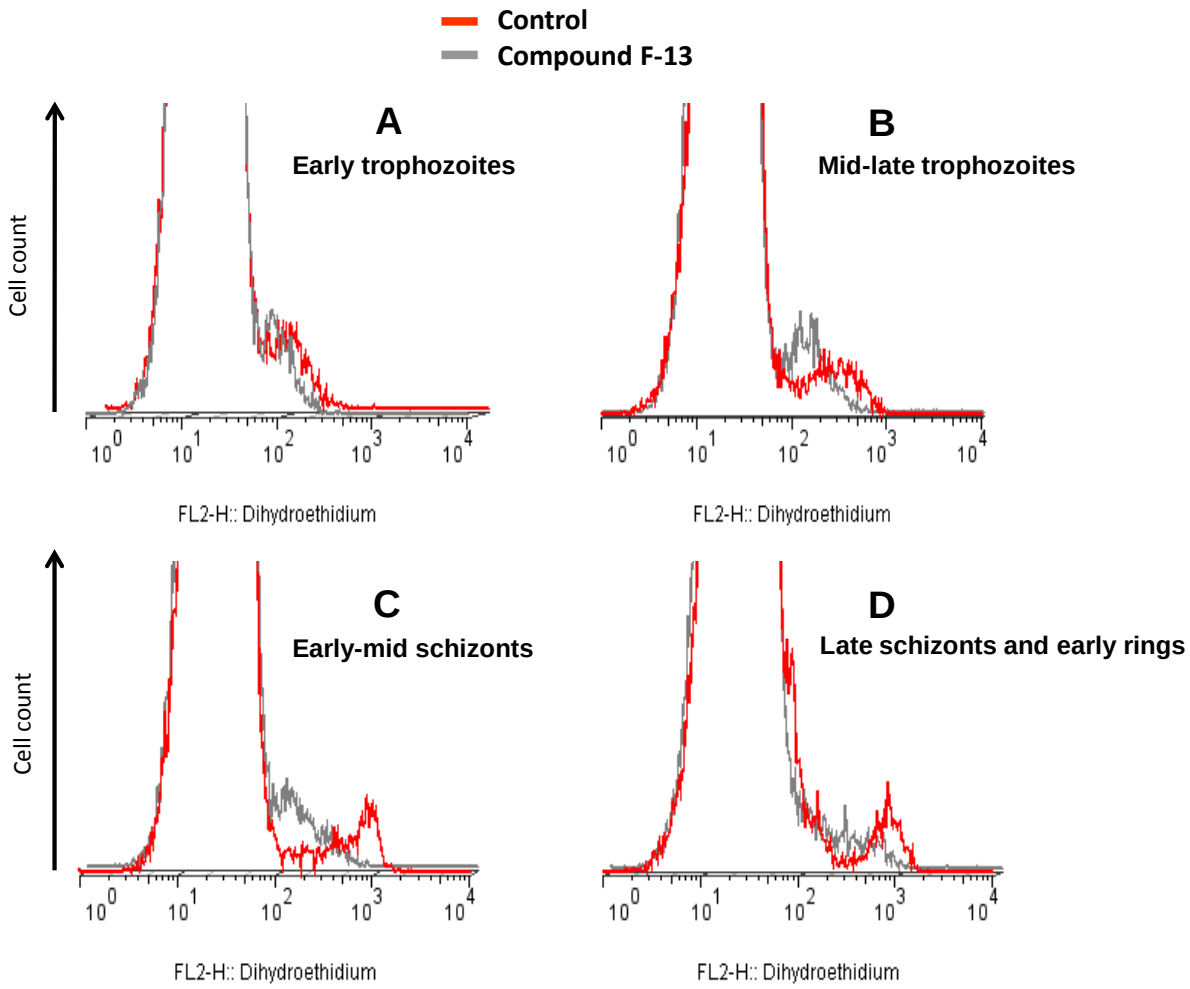
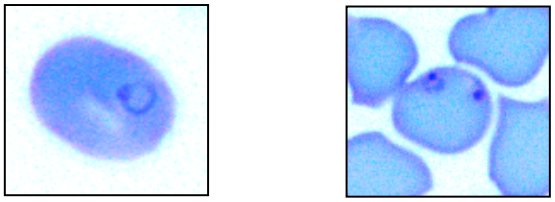


Figure 4.7: Flow cytometric analysis depicting the effects of compound F-13 at its IC_{50} value (70 µM) on parasite development (n = 1). Where: FL2-H represents the maximum fluorescent intensity of dihydroethidium.

An examination of the morphological and stage-specific effects of compound F-13 at 200 µM (IC_{90} value) indicated that treated parasites were able to progress through the ring-stage with no distinct morphological changes (Figure 4.8A). However, there was no progression past the late ring-stage, with treated parasites appearing condensed and exhibiting a distinct lack of haemozoin formation (Figure 4.8B), when compared to the untreated parasite control sample that was in the early to mid schizont-stage (Figure 4.6C). In contrast, the morphological and stage-specific effects of compound F-13 at 25 µM (IC_{25} value) provided little stage-specific or morphological information, with the exception that a slight lag in parasite development was noted. Treated parasites were mainly present in the

late trophozoite-stage compared to the early to mid schizont-stage of the untreated control.



A B

Figure 4.8: The effects of compound F-13 at 200 µM (IC_{90} value) on parasite growth and development (n = 1). Where A = compound F-13 treated parasite that was in the late ring-stage when the parasite control was in the early trophozoite-stage; B = compound F-13 treated parasite's that were in the late ring-stage when the parasite control was in the early to mid schizont-stage.

4.3.4 Antimalarial mechanisms of action

4.3.4.1 Inhibition of β-haematin formation

None of the compounds were capable of inhibiting the formation of β-haematin as effectively as chloroquine or quinine, with the β-haematin inhibitory activity of the compounds ranging from 12.57 ± 8.30% to 92.73 ± 4.11% at 400 µM (Table 4.3). Compounds F-14, F-8 and F-3 were the most active, with inhibitory activities of 92.73 ± 4.11%, 91.97 ± 8.10%, and 89.46 ± 10.00% at 400 µM, respectively (Table 4.3). However, at 100 µM they were only capable of inhibiting the formation of β-haematin by 22.56 ± 6.53%, 9.68 ± 3.20% and 21.34 ± 7.60%, respectively.

4.3.4.2 DPPH$^{\bullet}$ free-radical scavenging activity

When compared to ascorbic acid (IC_{50} value: 19.31 ± 2.62 µM), the compounds proved to be poor scavengers of the free-radical of DPPH$^{\bullet}$, with activity ranging from 0.01 ± 0.65% to 11.34 ± 8.91% at 240 µM (Table 4.3).

4.3.4.3 Iron chelating activity

None of the compounds exhibited any iron chelating activity comparable to that of EDTA (IC_{50} value: 23.90 ± 1.83 μM) (Table 4.3), with % Fe(II) chelation ranging from 0.01 ± 1.28% to 7.57 ± 4.13% at 200 μM. In contrast, chloroquine was capable of chelating 70.68 ± 0.97% Fe(II) at 200 μM (Table 4.3).

Table 4.3: The β-haematin inhibitory, free-radical scavenging, and Fe(II) chelating activity of the compounds (n = 4). Values in parenthesis indicate where IC_{50} values (< 100 μM) were obtained.

Compound	% Inhibition of β-haematin formation at 400 μM (± s.d.)	% DPPH$^{\bullet}$ free-radical scavenging activity at 240 μM (± s.d.)	% Fe(II) chelation at 200 μM (± s.d.)
F-14	92.73 ± 4.11	0.01 ± 1.97	7.57 ± 4.13
F-8	91.97 ± 8.10	0.01 ± 0.70	0.01 ± 3.42
F-3	89.46 ± 10.00	0.01 ± 0.65	3.00 ± 1.82
F-11	41.95 ± 4.19	0.01 ± 1.39	0.01 ± 5.77
F-6	40.77 ± 13.63	0.01 ± 2.80	0.01 ± 3.42
F-7	32.89 ± 5.21	0.01 ± 2.18	0.01 ± 6.96
F-9	32.20 ± 13.42	2.39 ± 2.25	0.01 ± 8.73
F-10	31.71 ± 10.77	2.27 ± 1.21	0.01 ± 5.24
F-13	30.56 ± 5.00	0.78 ± 1.90	0.01 ± 6.72
F-5	26.83 ± 10.39	0.01 ± 0.95	0.01 ± 1.28
F-12	22.60 ± 12.24	1.43 ± 1.18	0.01 ± 5.60
F-1	20.86 ± 6.06	11.34 ± 8.91	0.01 ± 2.23
F-4	14.56 ± 6.46	0.01 ± 1.17	0.01 ± 7.60
F-2	12.57 ± 8.30	0.01 ± 0.87	0.01 ± 5.95
Chloroquine	(29.64 ± 3.35 μM)	0.31 ± 3.28	70.68 ± 0.97
Quinine	(63.00 ± 3.27 μM)	2.53 ± 1.17	0.01 ± 6.08
EDTA	N.D.	N.D.	(23.90 ± 1.83 μM)
Ascorbic acid	N.D.	(19.31 ± 2.62 μM)	N.D.

4.4 Discussion

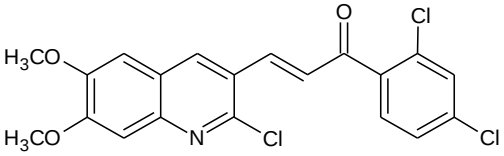
The antimalarial activity of the compounds ranged with IC_{50} values of 31.31 ± 0.87 μM to 8.74 ± 13.66% inhibition of parasite growth at 100 μM (Table 4.2), indicating that the hybridisation of the chloroquinoline and chalcone moieties did not act in a synergistic manner to produce highly potent compounds, and did not warrant further screening against a chloroquine-resistant strain of *P. falciparum.* None of the compounds exhibited

any notable haemolytic activity, with % haemolysis ranging from 0.47 ± 0.77% to 2.20 ± 0.54% at 100µM (Table 4.2), indicating that the variable antimalarial activity of the compounds was not due to a direct effect on the erythrocyte itself, but rather due to the structural differences of the compounds.

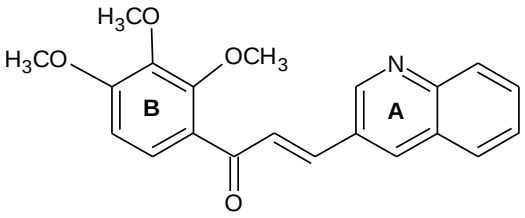
Compounds F-13 (IC_{50} value: 31.31 ± 0.87 µM), F-10 (IC_{50} value: 31.54 ± 3.03 µM), F-1 (IC_{50} value: 31.98 ± 1.27µM) and F-3 (IC_{50} value: 39.17 ± 2.05µM) exhibited the best antimalarial activity (Table 4.2). Structure-activity relationship of the compounds revealed that compounds F-13, F-10 and F-1 all had pyridine ring substitutions at R^4 and a hydrogen group at R^3, with either hydrogen or methyl groups at R^1 and R^2. Whilst compound F-3, which had the highest IC_{50} value of the four, had hydrogen groups at R^1, R^2 and R^3, with a 4-chloro phenyl ring at R^4. The antimalarial activity conferred by the pyridine ring substitution at R^4 become evident when comparing compounds F-13 and F-14, which had identical groups at R^1, R^2 and R^3, yet differed with respect to R^4 (Table 4.2), resulting in the 1.9-fold decrease in antimalarial activity observed in compound F-14 (Table 4.2).

The substitution of either a chloro- or bromo- group on the phenyl ring appeared to have no influence on antimalarial activity, as revealed by a comparison of compounds F-11 and F-12, which had identical groups at R^1, R^2, and R^3, but differed with respect to a chloro- and bromo- substitution at C^3 on the phenyl ring of R^4 (Table 4.2). Structure-activity relationships of the C^3 and C^4 bromo-substituted compounds revealed that the main determinant of antimalarial activity appeared to be the positioning of the methyl and hydrogen substitutions at R^1, R^2 and R^3, rather the positioning of the bromo-group on C^3 or C^4 (Table 4.2).

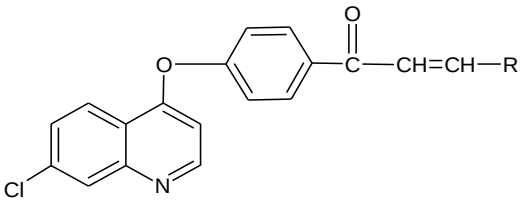
A study conducted by Domínquez *et al*. (2001) testing the activity of a similar series of quinolinyl chalcones against the FCB1 chloroquine-resistant strain of *P. falciparum,* showed that a single bromo- or chloro-substitution on C^4 of the phenyl ring displayed no antimalarial activity, with IC_{50} values > 200 µM. However, di-chloro substitutions at the C^2 and C^4 (Figure 4.9a) and C^2 and C^5 positions produced compounds with IC_{50} values of 19 µM and 48.6 µM, respectively; whilst di-substitution at C^3 and C^4 abolished antimalarial activity.



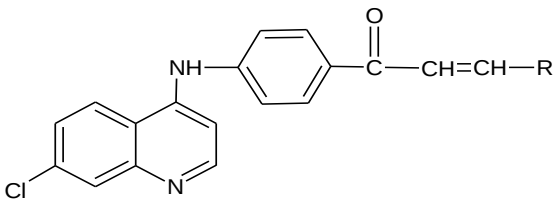
a) 1-(2,4-Dichlorophenyl)-3-[3-(2-chloro-6, 7-dimethoxyquinolinyl)]-2-propen-1-one



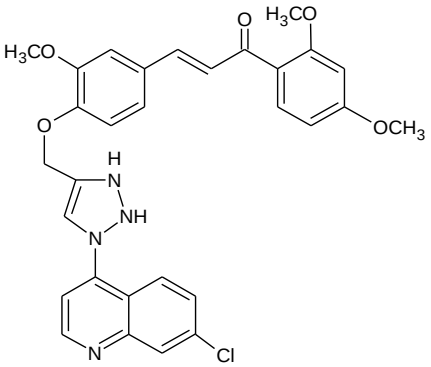
b) 1-(2',3',4'-Trimethoxyphenyl)-3-(3-quinolinyl)-2-prop-1-one



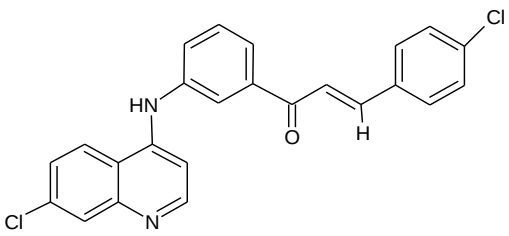
c) 4-Oxo linked quinolinyl-chalcone



d) 4-Amino linked quinolinyl-chalcone



e) 3-{4-[1-(7-Chloro-quinolin-4-yl)-1H-[1,2,3]triazol -4-ylmethoxy]-3-methoxy-phenyl}-1-(2,4-dimethoxy-phenyl) -propenone



f) (2E)-3-(4-Chlorophenyl)-1-3-[7-chloroquinolin-4-yl)amino] phenyl}prop-2-en-1-one

Figure 4.9: Quinoline-chalcones previously assessed for antimalarial activity. a: Domínquez *et al*. (2001); b: Liu *et al*. (2001); c,d: Sharma *et al*. (2009); e: Guantai *et al*. (2010); f: Ferrer *et al*. (2009).

Differences between the results obtained by Domínquez *et al*. (2001) and this study may have been attributed to the different strains of *P. falciparum* used. Domínquez *et al*. (2001) found the IC_{50} value of chloroquine to be 80nM in the FCB1 strain, as opposed to the IC_{50} value of 6.5 ± 0.2 nM as obtained in the 3D7 strain (Table 4.2). Furthermore, the compounds tested by Domínquez *et al*. (2001) had methoxy groups at R^1 and R^2 (Figure 4.9a), instead of hydrogen and methyl groups as in this study (Table 4.2).

In a large structure-activity analysis performed against the chloroquine-resistant K1 strain of *P. falciparum*, Liu *et al*. (2001) identified 1-(2',3',4'-trimethoxyphenyl)-3-(3-quinolinyl)-2-prop-1-one (Figure 4.9b) as a promising inhibitor of parasite growth, with an IC_{50} value of 2 µM (Liu *et al*., 2001). Structural analysis pointed to the fact that 3-quinolinyl derivatives were more active than 4-quinolinyl derivatives, regardless of ring substitutions. Whilst also pointing to the fact that electron-acceptor groups, such as difluoro- or dichloro- at C^2, C^3 or C^2, C^4 positions on ring A were not necessarily contributors to antimalarial activity (Figure 4.9b) (Liu *et al*., 2001).

In general, structure-activity relationships of quinoline and chloroquinoline-chalcones paint a complicated and sometimes contradictory picture. Sharma *et al*. (2009) demonstrated that 4-oxo and 4-amino linked quinoline-chalcones (Figure 4.9c and d, respectively) displayed no activity against the NF-54 chloroquine-sensitive strain of *P. falciparum,* when the R group was a pyridine ring, or a chloro-, bromo-, nitro-, methyl- or methoxy-substituted phenyl ring (Sharma *et al*., 2009).

A recent study conducted by Guantai *et al*. (2010) examined the antimalarial activity of triazole-linked chalcones against the chloroquine-sensitive D10 strain and the chloroquine-resistant Dd2 and W2 strains of *P. falciparum.* Three compounds exhibited IC_{50} values in the sub-micromolar range. The most active, 3-{4-[1-(7-chloro-quinolin-4-yl)-1H-[1,2,3]triazol-4-ylmethoxy]-3-methoxy-phenyl}-1-(2,4-dimethoxy-phenyl)-propenone, which was dimethoxylated at positions C^2 and C^4 on the phenyl ring (Figure 4.9e), inhibited all three strains with IC_{50} values of 0.04 µM, 0.07 µM and 0.09 µM, respectively (Guantai *et al*., 2010). However, it was only 0.7-fold more active than chloroquine in the Dd2 (chloroquine-resistant) strain, whereas in the D10 (chloroquine-sensitive) and W2 (chloroquine-resistant) strains, it was 2.4- and 1.3-fold less active, respectively.

The same study found that none of the compounds containing halogen substitutions on the phenyl ring exhibited sub-micromolar IC_{50} values, and pointed to the 7-chloroquinoline moiety as a possible contributing factor for the activity of the compounds, through the inhibition of haemozoin formation (Guantai *et al*., 2010). However, when tested for β-haematin inhibitory activity, no correlation was observed between the β-haematin inhibitory activity and the antimalarial activity of the compounds (Guantai *et al*., 2010).

Similarly, in this study, compounds F-13, F-10 and F-1, which exhibited the best antimalarial activity (Table 4.2) were only capable of inhibiting the formation of β-haematin by between 21 and 32% at 400 µM (Table 4.3). Whilst compounds F-14 and F-8, which exhibited the best β-haematin inhibitory activity at 400 µM (Table 4.3), had the highest IC_{50} values when tested against the parasite (Table 4.2). The only compound in which the antimalarial and β-haematin inhibitory activity appeared to correlate was compound F-3, which had a chloro-substitution at C^4 on the phenyl ring of R^4, with an IC_{50} value of 39.17 ± 2.05 µM (Table 4.2) and % inhibition of β-haematin formation of 89.46 ± 10.00% at 400 µM (Table 4.3), respectively.

Ferrer *et al*. (2009) also found that a chloro-substitution on C^4 of the phenyl ring (Figure 4.9f) in a series of chloroquinoline-chalcones conferred β-haematin inhibitory activity, whereas a chloro-substitution at C^3 abolished β-haematin inhibitory activity. This was similar to that observed in compounds F-11 and F-7 (Table 4.3). The inverse was noted when the phenyl ring was substituted with a different halogen. The substitution of a fluoro-group at position C^4 abolished β-haematin inhibitory activity, whereas a substitution at C^3 conferred β-haematin inhibitory activity (Ferrer *et al*., 2009). A comparison of compounds F-8 and F-9, which both had a methyl group at R^1 and hydrogen at R^2 and R^3, revealed that positioning of the bromo-substitution at C^4 (compound F-8) instead of C^3 (compound F-9) (Table 4.2) resulted in a 2.9-fold increase in β-haematin inhibitory activity (Table 4.3). However, when comparing compounds F-14 and F-8, both of which exhibited β-haematin inhibitory activity at 400 µM (Table 4.3), compound F-14 had a bromo- substitution at C^3, whereas compound F-8 had a bromo-substitution at C^4 (Table 4.2). Indicating that, as was observed with antimalarial activity, the positioning of the methyl and hydrogen substitutions at R^1, R^2 and R^3 may also play a role in β-haematin inhibitory activity.

However, in the Ferrer *et al*. (2009) study, active compounds exhibited β-haematin inhibitory activity similar to that of chloroquine (96.61 ± 0.26% inhibition of β-haematin formation at 25 µM). Ferrer *et al*. (2009) concluded that the β-haematin inhibitory activity observed was as a result of the 4-amino-7-chloroquinoline moiety; with hydrogen, halogen or N,N-dimethylamino substitutions on the phenyl ring of the chalcone moiety resulting in secondary interactions with haem (Ferrer *et al*., 2009). In this respect, the lack of similar β-haematin inhibitory activity of this series of compounds may be attributed to the positioning of the chloro-group at the C^2 position of the quinoline ring, as opposed to the C^7 position of chloroquine (Egan *et al*., 2000). Structure-activity relationships have pointed to the fact that although compounds possessing the quinoline ring structure are capable of forming a complex with Fe(III) protoporphyrin-IX, the chloro-substitution on C^7 of the quinoline ring results in the actual β-haematin inhibitory activity of the compound (Egan *et al*., 2000; Kumar *et al*., 2007).

Although the antimalarial activity of compounds F-13, F-10 and F-1 may not be attributed to the inhibition of haemozoin formation, their mechanisms of action may lie in their ability to inhibit haemoglobin digestion and alternative pathways of haem detoxification. The pyridine substitution at R^4 (Table 4.2) may have facilitated the accumulation of these compounds in the food vacuole; with nitrogen-containing heterocyclic compounds shown to concentrate in the acidic environment of the food vacuole due to their low pKa values (Mishra *et al*., 2008).

Haemoglobin endocytosed from the erythrocyte is catabolised by proteases in a semi-ordered fashion, to provide amino acids for parasitic protein synthesis (Figure 4.10) (Sharma, 2005; Mishra *et al*., 2008). Several malarial proteases are involved in haemoglobin catabolism, namely; the aspartic proteases (plasmepsins I, II, IV and the histoaspartic protease, plasmepsin III), the cysteine proteases (falcipains), the metalloprotease (falcilysin) (Figure 4.10) and aminopeptidases (Banerjee *et al*., 2002; Sharma, 2005; Naughton *et al*., 2010). The plasmepsins initiate the process of haemoglobin catabolism by cleaving the haemoglobin molecule in a highly conserved hinge region, thereby separating the haemoglobin tetramer (Banerjee *et al*., 2002; Sharma, 2005; Naughton *et al*., 2010). Thereafter, the globin chains are processed into smaller peptides by falcipains and

falcilysin, and finally these peptides are hydrolysed to free amino acids by aminopeptidases (Gavigan *et al*., 2001; Sharma, 2005; Naughton *et al*., 2010).

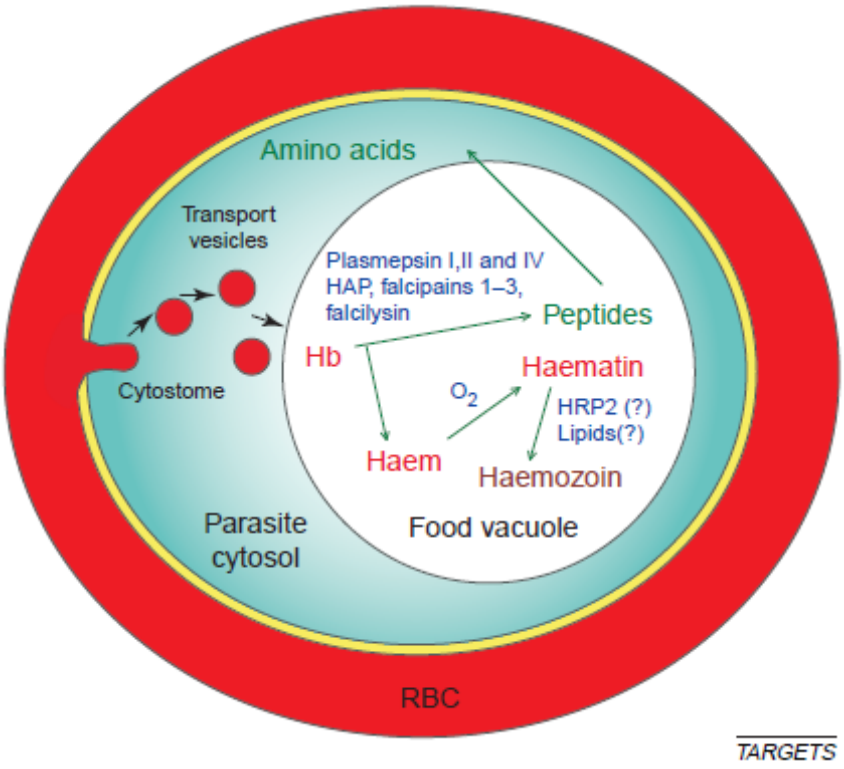


Figure 4.10: The catabolism of haemoglobin in the food vacuole of *P. falciparum* (Egan, 2003). Where: RBC = red blood cell; Hb =haemoglobin; HAP = histo-aspartic protease; HRP2 = histidine-rich protein.

Four falcipains have been identified, namely; falcipain-1, falcipain-2, falcipain-2', and falcipain-3 (Dahl and Rosenthal, 2005; Naughton *et al*., 2010). Falcipain-2 has been shown to localise primarily in the food vacuole, appearing first in the early trophozoite-stage, and persisting into the late schizont-stage, where it is also involved in the rupture of the red blood cell membrane during merozoite egress; whereas falcipain-3 synthesis peaks in the late trophozoite stage (Dahl and Rosenthal, 2005; Dasaradhi *et al*., 2005).

The exact mechanism of the antimalarial activity of chalcones has yet to be described, but homology models have shown that the chalcone structure assumes a linear or planar conformation, and is capable of fitting into the active site of the malarial cysteine protease enzyme, thereby inhibiting its functioning (Mishra *et al*., 2008). Mishra *et al*. (2008)

proposed that the antimalarial activity of a triazolyl-substituted chalcone (IC_{50} value of 1.52 ± 0.04 µM against the 3D7 strain of *P. falciparum*) was as a result of the protonation of the nitro- groups in the triazolyl moiety, at the acidic pH of the food vacuole, thereby enhancing the interaction of the compound with the histidine residue of the enzyme (Figure 4.11).

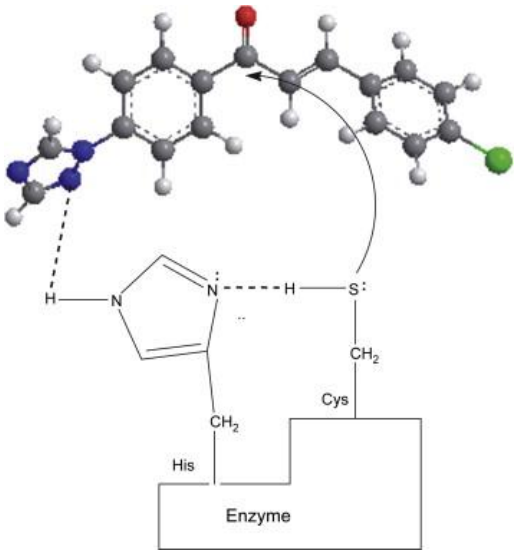


Figure 4.11: The proposed interaction of a chalcone with the histidine residue at the active site of a malarial cysteine protease (Mishra *et al*., 2008). Where: green = chloride; red = oxygen; blue = nitrogen.

Previous studies examining the effects of cysteine protease inhibitors on *P. falciparum* have shown that they inhibit parasite growth in the trophozoite stage, resulting in morphological effects such as swollen dark-staining food vacuoles due to the accumulation of undegraded haemoglobin (Rosenthal, 1995; Rosenthal and Meshnick, 1996; Domínquez *et al*., 1997). Although compound F-13 inhibited parasite growth in the early-mid trophozoite-stage at the IC_{50} value (Section 4.3.3), swollen dark-staining food vacuoles were not observed in treated parasites; with haemozoin formation also visible (Figures 4.6B). However, Naughton *et al*. (2010) showed that early trophozoite-stage parasites of the chloroquine-sensitive 3D7 strain incubated with the cysteine protease inhibitor, *ι-trans*-epoxy-succinyl-leucylamido-(4-guanidino)-butane (E-64) at its IC_{50} value (3 µM) showed no reduction in haemozoin formation. Whereas parasites incubated with plasmepsin inhibitor I (PM-I) at its

IC_{50} value (0.8 µM) exhibited an approximate reduction of 70% in haemozoin formation (Naughton *et al*., 2010).

Thus, based on the morphological and stage-specific effects of compound F-13 at the IC_{50} value; it can be proposed that its antimalarial activity may be attributed to possible cysteine protease inhibition. Most likely inhibition of falcipain-2, since parasite growth was halted in the early-mid trophozoite-stage, with haemozoin formation attributed to the fact that falcipain-2 inhibition would not act to inhibit haemozoin formation, but would inhibit protein degradation, resulting in parasite death (Naughton *et al*., 2010). The inhibition of falcipain-2 by compound F-13 may have possibly been as a result of the interaction of the protonated nitro- group of the pyridine substitution and the carbonyl moiety with the histidine residue of the enzyme, in a manner similar to the inhibition of the enzyme by a triazolyl-substituted chalcone, as proposed by Mishra *et al*. (2008) (Figure 4.11).

However, parasites treated with compound F-13 at the IC_{90} value showed a lack of haemozoin formation and did not develop past the late ring-stage (Figure 4.8), possibly as a result of the induction of additional antimalarial mechanisms of action attributed to chalcones.

Alternative mechanisms for the detoxification of haem by the parasite have been described, namely GSH-mediated degradation of Fe(III) protoporphyrin-IX and haemozoin formation mediated by proteins (Papalexis *et al*., 2001; Kumar *et al*., 2007). In the first mechanism, it is proposed that the amphipathic nature of Fe(III) protoporphyrin-IX allows it to pass through the food vacuole membrane into the parasite cytosol, where it is degraded by host-derived GSH which is endocytosed from the red blood cell cytosol together with haemoglobin in the late ring-stage (Gavigan *et al*., 2001; Frölich *et al*., 2005; Kumar *et al*., 2007).

Compounds possessing the α, β-unsaturated carbonyl group (Figure 4.1a) are capable of forming conjugates with GSH by an enzyme catalysed addition of GSH to the double bond. Some chalcones have been shown to form a conjugate with GSH, thereby inhibiting the degradation of Fe(III) protoporphyrin-IX (Nadelmann *et al*., 1997; Go, 2003; Frölich *et al*., 2005). In this respect, the compounds may have inhibited the GSH-mediated degradation of Fe(III) protoporphyrin-IX, resulting in parasite death due to oxidative stress, thus mimicking

the proposed mechanism of action of chloroquine (Figure 4.12) (Müller, 2004; Kumar *et al*., 2007).

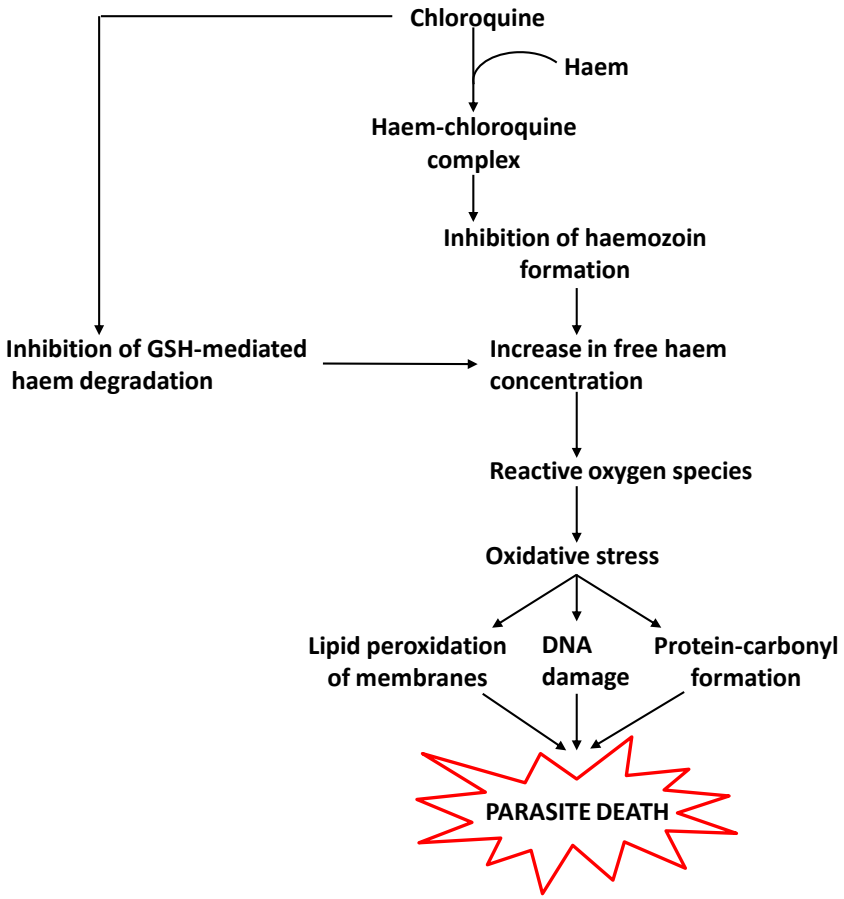


Figure 4.12: Proposed mechanisms of action of chloroquine (adapted from Kumar *et al*., 2007).

In the case of the mechanism involving proteins, the *in vitro* polymerisation of Fe(III) protoporphyrin-IX is proposed to be promoted by histidine-rich proteins produced by *P. falciparum*, specifically histidine-rich protein-II (*Pf*HRP-II) (Papalexis *et al*., 2001; Sharma, 2005; Kumar *et al*., 2007). *Pf*HRP-II is produced throughout the ring-, trophozoite- and schizont-stages, and has been shown to bind between 17 and 50 Fe(III) protoporphyrin-IX molecules, possibly acting as a catalyst of β-haematin formation by facilitating dimer formation in the biocrystallisation process (Papalexis *et al*., 2001). The role of *Pf*HRP-II in haemozoin formation is contentious, with some authors claiming that the inhibition of *Pf*HRP-II results in parasite death; whilst others have shown that parasites carrying a *Pf*HRP-II knock-out gene are still capable of haemozoin formation, and remain viable (Sharma,

2005; Egan, 2008). Chalcones have shown to alkylate proteins, and may inhibit the HRP-II mediated-formation of haemozoin, although the majority of chalcone-mediated protein alkylation appears to occur in sulphur-based nucleophiles (O' Neill and Posner, 2004).

Protein alkylation by chalcones may be a concern if it is not specific to the parasite, and results in host toxicity. When screened for cytotoxicity against a breast cancer cell-line (MCF-7), compounds F-9, F-3, F-12, and F-7 inhibited cell growth by less than 20% at 100 µM, whereas compound F-13 inhibited cell growth by 66% and 36% at 100 µM and 50 µM, respectively (Hayat *et al*., 2011). However, in the red blood cell toxicity assay the compounds showed low levels of toxicity, only causing between 0.47 and 2.20% haemolysis at 100 µM (Table 4.2). It has been shown that quinolines have antitumour activity and suppress the growth of various cancer cell-lines, including the MCF-7 cell-line; where chloroquine and quinine inhibited cell growth with IC_{50} values of 33 µM and 40 µM, respectively, following a 48 hour incubation period (Martirosyan *et al*., 2004; Ferrer *et al*., 2009). In this respect, the toxicity of the compounds may be selective to cancer cells only; however, the compounds should be screened against a normal cell-line and their safety indices compared to that of chloroquine and quinine.

Despite their abilities to induce oxidative stress, chalcones have shown to exhibit anti-oxidant properties (Go, 2003; Ren *et al*., 2003; Nowakowska, 2007). However, in this study, none of the compounds were capable of acting as anti-oxidants by scavenging the free-radical of $DPPH^{\bullet}$ or by chelating Fe(II) (Table 4.3). With compounds F-1 and F-14 exhibiting the best $DPPH^{\bullet}$ free-radical scavenging and Fe(II) chelating activity, respectively, and only been capable of scavenging 11.34 ± 8.91% of $DPPH^{\bullet}$ at 240 µM, and chelating 7.57 ± 4.13% of Fe(II) at 200 µM, respectively (Table 4.3). However, the iron chelating and anti-oxidant capabilities of chalcones has largely been attributed to polyhydroxylation of the phenyl ring (Cheng *et al*., 1998; Ren *et al*., 2003; Grazul and Budzisz, 2009), with none of the test compounds containing hydroxyl- substitutions at R^1, R^2 or R^4 (Table 4.2). Chloroquine was capable of chelating 70.68 ± 0.97% Fe(II) at 200 µM (Table 4.3), most likely through the interaction of Fe(II) with the nitro- donor groups of chloroquine; with removal of the aminoalkyl side chain possibly resulting in the loss of Fe(II) chelating activity observed in the compounds.

Numerous other antimalarial mechanisms of action of chalcones have been proposed. However, these mechanisms of action were not correlated with the antimalarial activity, indicating that chalcone derivatives may act on different parasitic metabolic pathways depending on their side-chain substitutions. For example, Go *et al*. (2004) proposed that chalcones were capable of inhibiting the parasite-induced new permeation pathways formed in the erythrocyte membrane at the end of ring-stage, concluding that dimethoxy- and methoxychalcones were capable of inhibiting sorbitol-induced haemolysis. However, this did not necessarily correlate with their antimalarial activity (Go *et al*., 2004). A subsequent study by Bhattacharya *et al*. (2009) testing three chalcone derivatives with IC_{50} values below 10 µM against *P. falciparum*, found that only a triazole-substituted chalcone, and not a pyrrole or benzotriazole-substituted chalcone, inhibited sorbitol-induced haemolysis (Bhattacharya *et al*., 2009).

The general chalcone structure was identified as a pharmacophore capable of inhibiting *Plasmodium falciparum* MO15-related kinase (*Pf*mrk), a plasmodial CDK expressed throughout the trophozoite- and schizont-stages, responsible for activating other CDK/cyclin complexes (Geyer *et al*., 2005; Keenan *et al*., 2005). Geyer *et al*. (2009) showed that from a series of structurally related chalcone derivatives, the most potent *Pf*mrk inhibitors also displayed the best antimalarial activity. However, they also found that some chalcone derivatives that exhibited no *Pf*mrk inhibitory activity (IC_{50} value > 100 µM) inhibited parasite growth with IC_{50} values < 10 µM, concluding that *Pf*mrk and antimalarial activity was weakly correlated (Geyer *et al*., 2009).

It is evident from the antimalarial activity of the compounds that the hybridisation of the chloroquinoline and chalcone moieties produced compounds with antimalarial activity similar to that of chalcones, which generally exhibit IC_{50} values against *P. falciparum* in the micromolar concentration range (Chen, 2003; Nowakowska, 2007). However, this unsuccessful hybridisation could be improved if a synergistic or additive interaction could be achieved when combined with a standard antimalarial, such as quinine. When compound F-13 was combined with quinine an additive interaction was noted (Figure 4.5; Appendix D). It is proposed that the activity of the two components in the combination acted on different parasitic targets, with compound F-13 inhibiting growth in the early-mid

trophozoite-stage (Figure 4.6) and quinine appearing to act mainly in the late trophozoite-stage (Figure 3.5).

Interestingly, hybrid compounds in which an endoperoxide-like compound was linked to a chalcone were active against the chloroquine-resistant K1 strain of *P. falciparum* in the nanomolar concentration range, similar to the antimalarial activity of endoperoxides (Jefford, 2007). It was proposed that the endoperoxide component would target haem in the food vacuole, resulting in decomposition of the carbon-centred radical to release the chalcone, which would inhibit malarial cysteine proteases in the food vacuole (Jefford, 2007; Walsh and Bell, 2009). Similarly, in combination studies with triazole, pyrrole, and benzotriazole-substituted chalcones and the endoperoxide, artemisinin, an additive interaction was also noted. This interaction was attributed to the chalcone derivatives inhibiting parasite growth in the trophozoite-stage, and artemisinin inhibiting all stages of asexual growth (Bhattacharya *et al*., 2009).

Although the antimalarial activity of the compounds was not as promising as expected, factors such as the additive interaction when combined with quinine, and that chalcones provide an excellent antimalarial drug scaffold, warrant further investigation into a second generation of these compounds. Structural improvements which may produce a potent compound capable of inhibiting parasite growth by various mechanisms of action include the following: a) substitution of a chloro- group on C^7 instead of C^2 of the quinoline ring to improve β-haematin inhibitory activity; b) increasing the compound lipophilicity and c) substitution of nitrogen-containing heterocyclics or groups at R^4 to not only facilitate the accumulation of the compounds in the food vacuole, but also the formation of hydrogen bonds with the histidine residues of falcipain-2.

CHAPTER 5: THE ANTIMALARIAL PROPERTIES OF NUCLEOSIDE PHOSPHONATES, PHOSPHONIC ACIDS AND PURINE/PYRIMIDINE DERIVATIVES

5.1 Introduction

Various discrepancies exist in the processes of nucleic acid metabolism and the overall base composition in the malaria parasite and human host. Purine and pyrimidine metabolism in *P. falciparum* occur via salvage and *de novo* pathways, respectively, to replicate a parasitic genome that is highly AT skewed (81%) (Hyde, 2007). In contrast, purine and pyrimidine metabolism in the human host occur via *de novo* synthesis and both *de novo* and salvage pathways, respectively (Jana and Paliwal, 2007; Hyde, 2007).

5.1.1 Purine uptake

The malaria parasite lacks the necessary enzymes to synthesise the purine scaffold *de novo*. Instead, a wide variety of parasite-derived purine transporters and salvage enzymes, together with host-derived enzymes allow the parasite to transport and metabolise salvaged purines (Jana and Paliwal, 2007; Hyde, 2007). *P. falciparum* scavenges purines in the form of bases or nucleosides, as purine nucleotides are unlikely to cross lipophilic membranes due to their deprotonation at a physiological pH (Carter *et al*., 2001; Downie *et al*., 2008; Hocková *et al*., 2009).

The erythrocytic purine pool is not sufficient to maintain growth of the parasite, with parasitic growth depending on an exo-erythrocytic supply of purines. The salvage pathway begins with the translocation of purines across the host cell, parasitophorous vacuole, and the parasite plasma membranes (Carter *et al*., 2001; Downie *et al*., 2008). The transport of nucleosides into the infected red blood cell is mediated by both the host cells nucleoside transporters, as well as new permeation pathways (Gero *et al*., 2003). The new permeation pathways induced during the trophozoite-stage, transport substances that ordinarily would not be able to penetrate the red blood cell membrane. These transporters are polyspecific, non-saturable, preferential transporters of hydrophobic solutes and anions (Gero *et al*., 2003; Biagini *et al.*, 2005; Jana and Paliwal, 2007). Nucleoside transporters in mammalian cells are high-affinity integral membrane glycoproteins that mediate the uptake of both

purine and pyrimidine bases and nucleosides, as well as synthetic analogues. The transporters may be divided into two classes, namely; equilibrative nucleoside transporters (ENTs) and concentrative nucleoside transporters (CNTs) (Carter *et al*., 2001; Lin and Buolamwini, 2007). CNTs are sodium-dependant transporters which transport nucleosides against a concentration gradient, whereas ENTs transport nucleosides down their concentration gradient (Carter *et al*., 2001; Lin and Buolamwini, 2007). The nucleoside transporters located in the red blood cell membrane are transporters of the ENT type, specifically equilibrative sensitive (ENT1). It is a high-affinity nucleoside transporter that is sensitive to inhibition by both the nucleoside transport inhibitor 6-[(4-nitrobenzyl)thio]-9-β-D-ribofuranosyl purine (NBMPR), and the coronary vasodilator, dipyridamole (Gupte and Buolamwini, 2004; Lin and Buolamwini, 2007).

Once inside the red blood cell cytosol, the salvaged purines cross the parasitophorous vacuole membrane via large pores present on the membrane, and are then transported across the parasite plasma membrane by the *Plasmodium falciparum* equilibrative nucleoside transporter 1 (*Pf*ENT1) (El Bissati *et al*., 2006; Downie *et al*., 2008). *Pf*ENT1 is localised to the parasite plasma membrane, and although it shares some similarities with the human ENT family, it differs with respect to its substrate specificity, kinetics and lack of sensitivity to NBMPR. However, it retains sensitivity to inhibition by dipyridamole (El Bissati *et al*., 2006; Lin and Buolamwini, 2007). *Pf*ENT1 is a low-affinity rapid transporter that has a broad-specificity for both D- and L-nucleosides and bases, and transports purines with a much higher affinity than pyrimidines (El Bissati *et al*., 2006; Downie *et al*., 2008; Riegelhaupt *et al*., 2010). In contrast to human ENT1, a variety of purines are transported by *Pf*ENT1, including adenosine, inosine, hypoxanthine, guanine, guanosine and xanthine (Downie *et al*., 2008; Riegelhaupt *et al*., 2010). Although *Pf*ENT1 is the primary mechanism of uptake of adenosine, hypoxanthine and inosine, parasites carrying a deletion of the *Pf*ENT1 gene are capable of transporting these purines, at supraphysiological concentrations, indicating that perhaps a secondary transport mechanism exists (El Bissati *et al*., 2006; Downie *et al*., 2008; Riegelhaupt *et al*., 2010).

5.1.2 Purine salvage and metabolism

Purine metabolism begins in the cytosol of the infected red blood cell. Adenosine is converted into inosine by human adenosine deamininase enzymes and then into hypoxanthine by purine nucleoside phosphorylase enzymes (Figure 5.1) (Hyde, 2007; Downie *et al*., 2008). Inosine and hypoxanthine are then transported into the parasite by *Pf*ENT1 (Hyde, 2007; Downie *et al*., 2008). Alternatively, adenosine and inosine may be transported directly into the parasite (Figure 5.1) (Downie *et al*., 2008). Hypoxanthine, guanosine, guanine and xanthine require no further metabolism, and are transported into the parasite cytosol by *Pf*ENT1. Whereas adenine, which may be metabolised to other bases or nucleosides within the red blood cell cytosol, enters the parasite via both *Pf*ENT1 and non-*Pf*ENT1 mechanisms (Figure 5.1) (Hyde, 2007; Downie *et al*., 2008).

P. falciparum lacks an adenosine kinase gene, and is therefore incapable of converting adenosine to adenosine monophosphate (AMP) (Riegelhaupt *et al*., 2010). For this reason, upon entry into the parasite cytosol, adenosine is converted into hypoxanthine, via *Plasmodium falciparum* adenosine deaminase and nucleoside phosphorylase enzymes (Hyde, 2007; Downie *et al*., 2008; Riegelhaupt *et al*., 2010). The ability of the *Plasmodium falciparum* adenosine deaminase and nucleoside phosphorylase enzymes to utilise methylthiopurines such as methylthioadenosine and methylthioinosine, respectively, to form hypoxanthine, allows for the salvage of purines from the polyamine biosynthesis pathway, as well as from traditional purine salvage pathways (Downie *et al*., 2008).

Given the central role for hypoxanthine in the purine salvage pathway of *P. falciparum*, the *Plasmodium falciparum* hypoxanthine-guanine-xanthine phosphoribosyltransferase (*Pf*HGXPRT) enzyme proves crucial for parasite survival (Hyde, 2007; Hocková *et al*., 2009; Riegelhaupt *et al*., 2010). *Pf*HGXPRT provides an ideal drug target, as it shares only partial homology with its mammalian counterpart, hypoxanthine-guanine phosphorribosyl-transferase (HGPRT), with the human host not solely dependant on the activity of HGPRT, due to the ability of mammalian cells to synthesise purines *de novo* (Jana and Paliwal, 2007; Hocková *et al*., 2009).

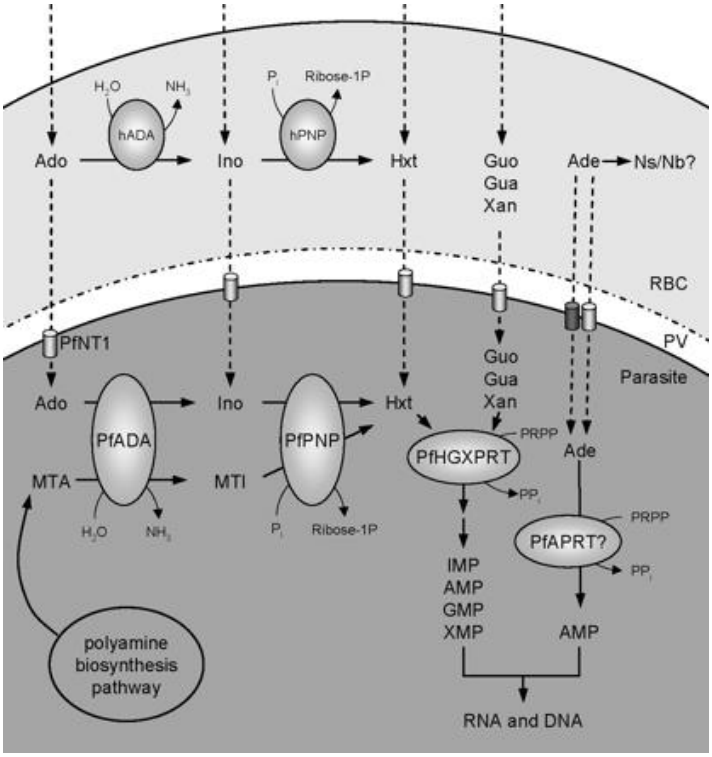


Figure 5.1: Purine salvage pathways in *P. falciparum* (Downie *et al*., 2008). Abbreviations: Ado, adenosine; hADA, human adenosine deaminase; Ino, inosine; hPNP, human purine nucleoside phosphorylase; Hxt, hypoxanthine; Guo, guanosine; Gua, guanine; Xan, xanthine; Ade, adenine; Ns/Nb, nucleoside/nucleobase; RBC, red blood cell; PV, parasitophorous vacuole; *Pf*NT1, *Plasmodium falciparum* equilibrative nucleoside transporter 1; *Pf*ADA, *Plasmodium falciparum* adenosine deaminase; MTA, methylthioadenosine; MTI, methylthioinosine; *Pf*PNP, *Plasmodium falciparum* purine nucleoside phosphorylase; PRPP, phosphoribosylpyrophosphare; *Pf*HGXPRT, *Plasmodium falciparum* hypoxanthine-guanine-xanthine phosphoribosyltransferase; *Pf*APRT, *Plasmodium falciparum* adenine phosphoribosyltransferase; IMP, inosine monophosphate; AMP, adenosine monophosphate; GMP, guanosine monophosphate; XMP, xanthosine monophosphate.

*Pf*HGXPRT catalyses the ribophosphorylation of the nucleo(bases), hypoxanthine, guanine, and xanthine into their nucleoside monophosphate forms, inosine monophosphate (IMP), guanosine monophosphate (GMP), and xanthosine monophosphate (XMP), respectively (Hyde, 2007; Downie *et al*., 2008). A proposed second enzyme, *Plasmodium falciparum*

adenine phosphoribosyltransferase has been suggested for the conversion of adenine to AMP. However, the existence of this enzyme remains contentious, with evidence pointing to the fact that the conversion of adenine occurs in the red blood cell cytosol, or that adenine is not metabolised by the parasite (Downie *et al*., 2008).

The majority of salvaged purines results in the formation of IMP from hypoxanthine, with IMP acting as the precursor for the formation of other purine nucleotides (Riegelhaupt *et al*., 2010). In order to form AMP, IMP is converted to adenylsuccinate and then AMP by adenylsuccinate synthetase and adenylsuccinate lyase, respectively (Downie *et al*., 2008; Bulusu *et al*., 2011). In the case of GMP formation, IMP dehydrogenase converts IMP to XMP, which is then converted to GMP by the activity of the GMP synthetase enzyme (Downie *et al*., 2008; Bulusu *et al*., 2011). AMP and GMP are then phosphorylated by adenylate kinase and guanylate kinase, respectively, to form adenosine diphosphate (ADP) and guanosine diphosphate (GDP), which are then processed further to be used for nucleic acid synthesis, adenosine triphosphate (ATP) generation and cell signalling (Hyde, 2007; Downie *et al*., 2008; Riegelhaupt *et al*., 2010).

5.1.3 *De novo* pyrimidine synthesis

In contrast to purine salvage, pyrimidine nucleotide synthesis in *P. falciparum* occurs through a *de novo* pathway due to the fact that the parasite lacks the uridine kinase and thymidine kinase enzymes necessary for pyrimidine salvage (Hyde, 2007). Consequently exogenous pyrimidines are not incorporated into nucleic acids, with the exception of orotic acid (Hyde, 2007; Jana and Paliwal, 2007; Parker *et al*., 2000). Cytidine triphosphate (CTP) and uridine triphosphate (UTP) are synthesised (Figure 5.2) from the amino acid precursors' glutamine and aspartate (Hyde, 2007; Ginsburg, 2011). Synthesis occurs via a multi-step process, whereby orotic acid and a ribose-5-phosphate moiety result in the formation of orotodine 5'-monophosphate, which is decarboxylated to form uridine 5'-monophosphate (UMP) (Hyde, 2007; Ginsburg, 2011). UMP is then twice phosphorylated to form UTP, and finally converted into CTP via the action of CTP synthase (Hyde, 2007; Jana and Paliwal, 2007; Ginsburg, 2011). Regulation of CTP formation occurs via the first enzyme in the pathway, carbamoyl phosphate synthetase, which is activated by the 5-phosphoribosyl pyrophosphate enzyme, and inhibited by UTP (Hyde, 2007).

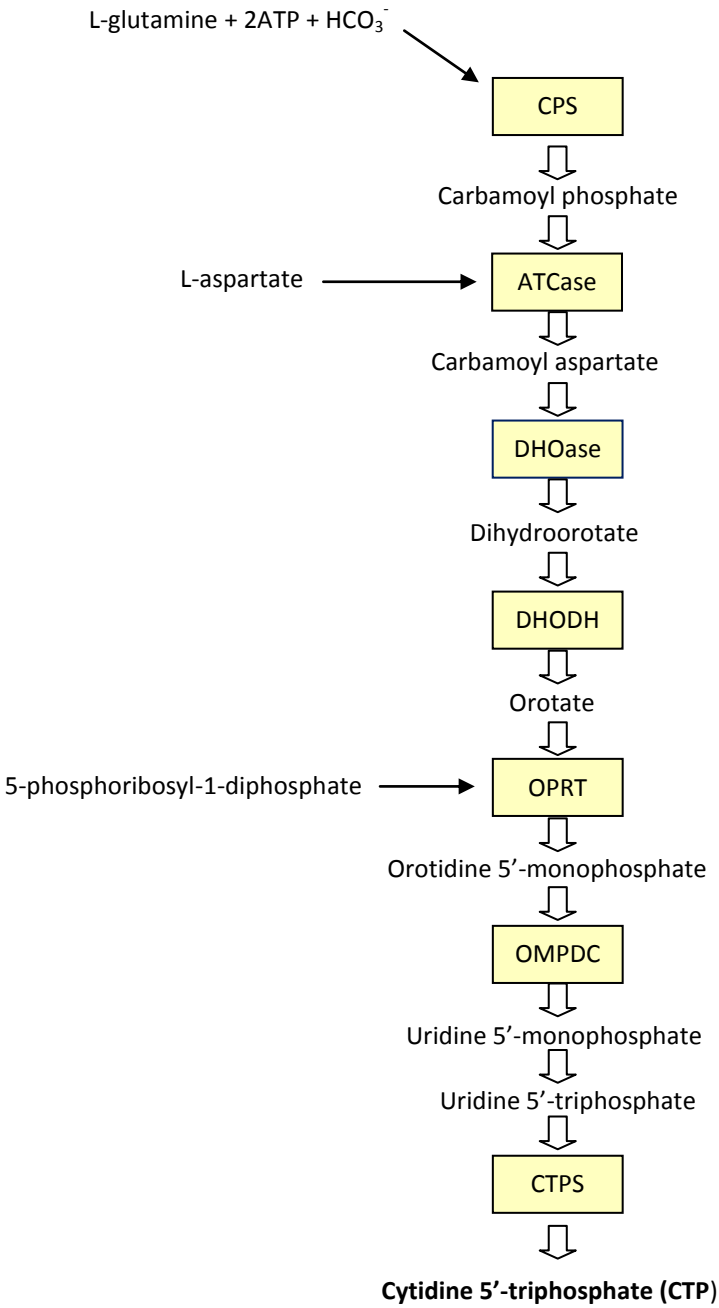


Figure 5.2: The *de novo* synthesis of pyrimidines in *Plasmodium falciparum* (adapted from Hyde, 2007). Yellow shaded boxes represent enzymes of the pathway. Abbreviations: CPS, carbamoyl phosphate synthase; ATCase, aspartate carbamoyltransferase; DHOase, dihydroorotase; DHODH, dihydrorotate dehydrogenase; OPRT, orotate phosphoribosyltransferase; OMPDC, orotidine 5'-monophosphate decarboxylase; CTPS, CTP synthase.

5.1.3.1 The role of the folate pathway in thymidine synthesis

Thymidine synthesis in *P. falciparum* requires the conversion of deoxyuridine 5'-monophosphate (dUMP) into deoxythymidine 5'-monophosphate (dTMP) and is dependent upon cofactors of the folate pathway (Hyde, 2005, 2007; Chango and Abdennebi-Najar, 2011). The most important of which, 5,10-methylenetetrahydrofolate, provides the methyl group that converts dUMP into dTMP, from which dTTP is formed, and consequently incorporated into parasitic DNA (Hyde, 2005, 2007; Chango and Abdennebi-Najar, 2011). Blockade of the folate pathway, by either blocking the synthesis of molecules or salvage from the host, results in the death of the parasite due to thymidine starvation, as the parasite lacks the ability to salvage host thymidine (Hyde, 2005, 2007). The *de novo* folate pathway (Figure 5.3) initiates with the purine precursor, GTP, and requires a source of either salvaged para-aminobenzoic acid (ρABA) or *de novo* ρABA (Hyde 2005, 2007).

The first reaction in the *de novo* folate pathway involves the rearrangement of the purine ring of GTP by GTP cyclohydrolase I to form a pterin; which is linked to ρABA by the dihydropteroate synthase enzyme to form a pteroate derivative (Hyde, 2007; Nzila, 2006). The final step in the *de novo* folate pathway is catalysed by dihydrofolate synthase, and involves the conversion of the pteroate derivative to dihydrofolate via the addition of an L-glutamate moiety (Nzila, 2006; Hyde, 2007; Müller *et al*., 2010). At this stage, dihydrofolate may also be polyglutamated by folylpolyglutamate synthase (Figure 5.3) (Nzila, 2006; Hyde, 2007; Müller *et al*., 2010).

The thymidylate cycle comprises a component of the folate pathway and utilises either folates salvaged from the host, or the 7,8-dihydrofolate product of the *de novo* pathway (Figure 5.3) (Hyde, 2005, 2007; Müller *et al*., 2010). Three enzymes, namely, dihydrofolate reductase, thymidylate synthase and serine hydroxymethyltransferase are involved in the formation of dTMP and recycling of tetrahydrofolate (Hyde, 2007; Müller *et al.*, 2010). Serine hydroxymethyltransferase is involved in the acquisition of an one-carbon (C_1) unit from serine to form methylenetetrahydrofolate, which in turns transfers the C_1 unit to dUMP, through the activity of the thymidylate synthase enzyme, forming dTMP (Figure 5.3) (Hyde, 2007; Müller *et al.*, 2010). For each molecule of dTMP formed, one molecule of

tetrahydrofolate is oxidised to dihydrofolate, which is then recycled by dihydrofolate reductase to form tetrahydrofolate (Hyde, 2005).

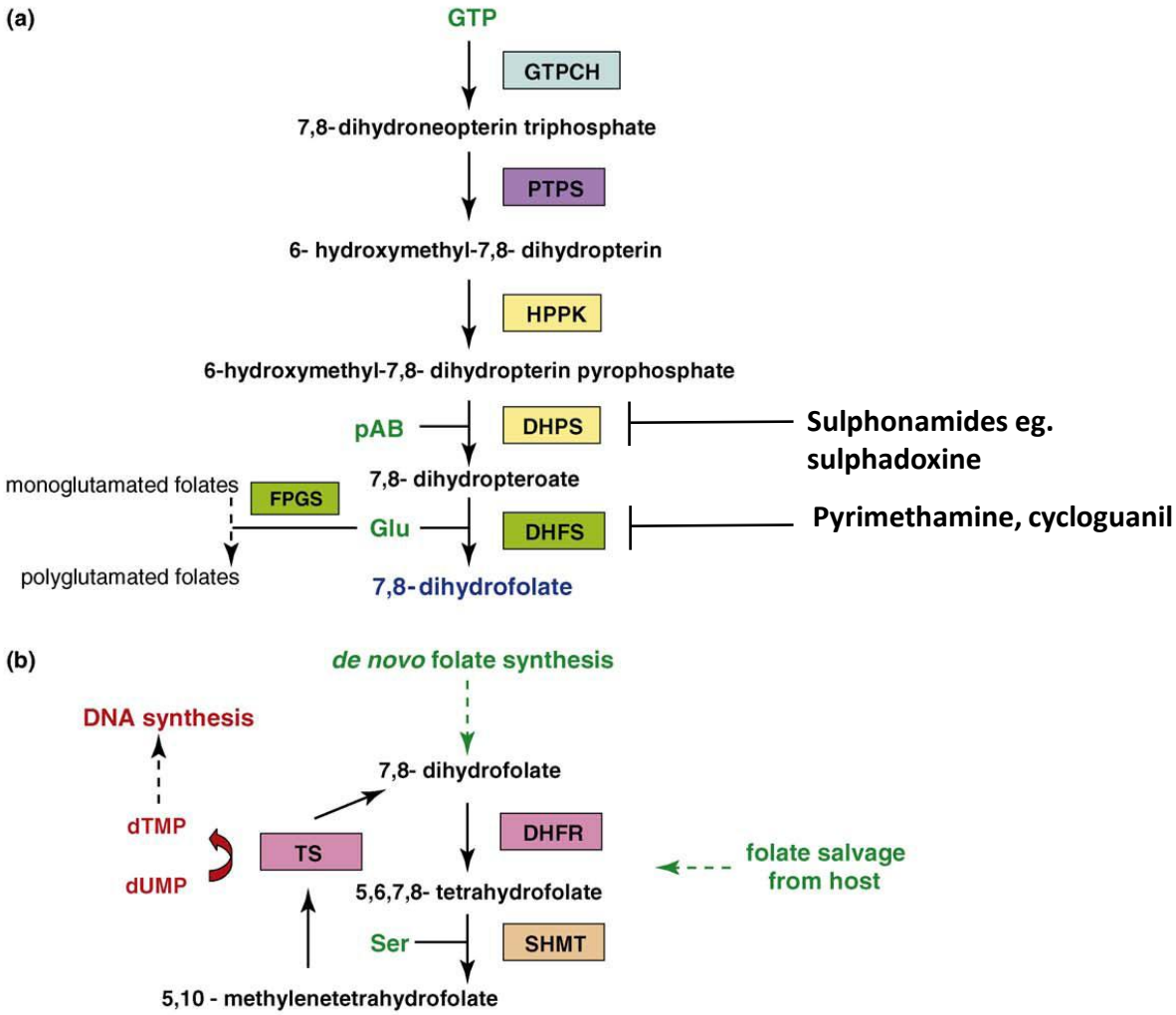


Figure 5.3: The folate pathway of *P. falciparum* (a) and its role in the thymidylate cycle (b) (adapted from Müller *et al*., 2010). Abbreviations: GTP, guanosine triphosphate; GTPCH, GTP cyclohydrolase I; PTPS, 6-pyruvoyltetrahydropterin synthase; HPPK, 6-hydroxy-methyldihydropterin pyrophosphokinase; DHPS, dihydropteroate synthase; DHFS, dihydrofolate synthase; FPGS, folylpolyglutamate synthase; DHFR, dihydrofolate reductase; SHMT, serine hydroxymethyltransferase; TS, thymidylate synthase; dUMP, deoxyuridine monophosphate, dUMP; deoxythymidine monophosphate, dTMP.

Following its synthesis in the thymidylate cycle, dTMP is phosphorylated by the enzyme thymidylate kinase to form dTDP which is subsequently converted by nucleoside diphosphate kinases to its triphosphate form, dTTP, which is then utilised for nucleic acid synthesis (Cui *et al*., 2010).

5.1.4 Therapeutic targets

The essential role of DNA synthesis in the survival of malaria parasite, as well as the striking differences in purine and pyrimidine metabolic pathways to that of the human host, provides promising targets for antimalarial chemotherapy. Inhibition of nucleoside transport via inhibition of NPPs or *Pf*ENT1, the major route of purine entry into the parasite, would result in purine starvation and parasite death (Parker *et al*., 2000). Alternatively, *Pf*ENT1 may be exploited to transport cytotoxic nucleoside derivatives into the parasite, where they would interfere with nucleic acid synthesis (Parker *et al*., 2000; Gero *et al*., 2003).

Cytotoxic nucleoside and nucleobase derivatives such as 5-fluoro-2'-deoxyuridine, 6-thioguanosine, 6-mercaptopurine riboside, 5-fluorouracil, 3'-azido-2',3'-deoxythymidine (AZT), dideoxyinosine, and dideoxycytidine are validated anticancer and antiviral agents (Gero *et al*., 2003; Hyde, 2007; Cui *et al*., 2010). The use of cytotoxic nucleoside derivatives against *P. falciparum* has exhibited promising results. The pyrimidine analogue, 5-fluorouracil, when used as an anticancer agent, acts as an inhibitor of the thymidylate synthase enzyme, however, it was not found to be transported into *P. falciparum* (Hyde, 2007). Upon substitution of the uracil moiety with orotic acid, to form 5-fluoroorotic acid, the compound was readily taken up by the parasite and once incorporated into the pyrimidine biosynthesis pathway, it inactivated parasitic thymidylate synthase, killing the parasite at nanomolar concentrations (Hyde, 2007; Muregi *et al*., 2009). However, thymidylate synthase is highly conserved among *P. falciparum* and the human host, in this manner an effective thymidylate synthase inhibitor would be a combination of a cytotoxic nucleoside and a nucleoside such as uridine, which can be salvaged by the host to bypass host cell toxicity (Biagini *et al*., 2003; Hyde, 2007; Jana and Paliwal, 2007).

Following entry into the target cell/organism, pro-drugs of nucleoside analogues are phosphorylated into their active triphosphate forms and exert their activity by acting as

DNA chain terminators. A study testing the antimalarial activity of AZT hypothesised that the plasmodial enzyme thymidylate kinase would be capable of converting the AZT monophosphate (AZTMP) pro-drug to AZT diphosphate (AZTDP). The latter would subsequently be converted to its triphosphate form (AZTTP) by nucleoside diphosphate kinase enzymes and incorporated into parasitic DNA, thereby arresting DNA replication (Cui *et al*., 2010). The results obtained showed that the monophosphate pro-drug was more active than the AZT parent compound; however they lacked potent antimalarial activity (Cui *et al*., 2010).

In contrast, acyclic nucleoside phosphonates (ANPs), which are currently in use as antiviral treatments, showed potent antimalarial activity; with an adenine derivative, (S)-(3-hydroxy-2-phosphonylmethoxy-propyl)adenine ((S)-HPMPA) exhibiting activity at sub-micromolar concentrations (Smeijsters *et al*., 1999). Other non-adenine ANP derivatives have also shown promising antimalarial activity, inhibiting growth of *P. falciparum* with IC_{50} values of 1 µM; as well as exhibiting low toxicity towards mammalian cells (Hocková *et al*., 2009). The antimalarial activity of these ANP derivatives appears to lie in their ability to inhibit the *Pf*HGXPRT enzyme in the purine salvage pathway (Figure 5.1), and thereby the production of nucleoside monophosphates (Hocková *et al*., 2009; Keough *et al*., 2010). ANPs, wherein selected purine bases are linked to the phosphate moiety via a stable phosphorous-carbon bond, act as analogues of the purine nucleoside monophosphate product of the *Pf*HGXPRT-mediated reaction (Figure 5.4) (Hocková *et al*., 2009; Keough *et al*., 2010).

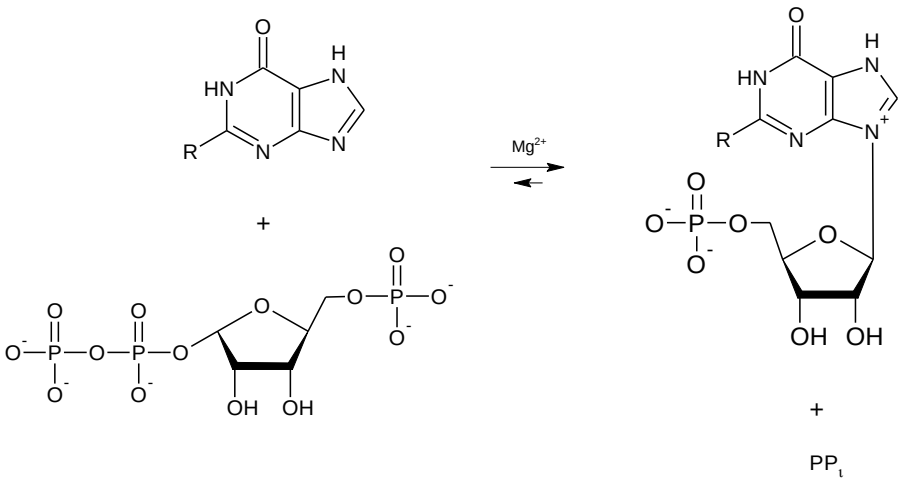


Figure 5.4: One of the reactions catalysed by *Pf*HGXPRT (Keough *et al*., 2010).

Where: PP_i = pyrophosphate.

ANPs appear to be promising antimalarial agents, as currently ANPs and immucillin-5' phosphates are the only known inhibitors of *Pf*HGXPRT; however, ANPs are the only inhibitors capable of discriminating between *Pf*HGXPRT and human HGPRT (Hocková *et al*., 2009; Keough *et al*., 2010).

Nucleoside and nucleobase analogues have been shown to be inhibitors of numerous other parasitic enzymes of DNA synthesis and replication, including *Plasmodium falciparum* adenosine deaminase, adenylyl cyclase, guanylyl cyclase, ribonucleotide reductase (the rate-limiting enzyme in DNA replication responsible for converting ribonucleotides to deoxyribonucleotides), as well as cyclin-dependant kinases (CDKs) (Harmse *et al*., 2001; Biagini *et al*., 2003; Hyde, 2007).

5.1.4.1 The parasitic cell division cycle as a drug target

In mammalian cells the transition through the G_1, S, G_2 and M phases of the cell division cycle is highly regulated by CDKs, which in their active forms are composed of a catalytic unit (CDK) and a regulatory cyclin (Harmse *et al*., 2001; Doerig *et al*., 2002; Knockaert *et al*., 2002). CDKs are serine/threonine kinases that, upon binding of a cyclin, shift into an active conformation, which then facilitates configuration of the active site and ATP positioning (Geyer *et al*., 2005). CDK/cyclin deregulation in diseases such as cancer has fuelled the search for kinase inhibitors to be evaluated for the treatment of neurological and cardiovascular disorders, as well as viral and parasitic infections (Harmse *et al*., 2001; Knockaert *et al*., 2002).

The cell division cycle of *P. falciparum* differs greatly from that of mammalian cells in that during schizogony the parasite undergoes multiple rounds of division to produce 8-32 merozoites, in contrast to the two daughter cells produced in mammalian cell division (Harmse *et al*., 2001; Geyer *et al*., 2005). In this regard, parasitic cell division is regulated differently to that of mammalian cells, with identified CDKs or CDK-related kinases exhibiting 40-60% homology to human CDKs (Knockaert *et al*., 2002; Geyer *et al*., 2005). Several genes encoding for CDKs and cyclins have been identified in *P. falciparum* and have shown to be inhibited by human CDK inhibitors (Doerig *et al*., 2002; Geyer *et al*., 2005). CDK-like sequences include; *Plasmodium falciparum* protein kinase 5, *Pf*mrk, *Plasmodium falciparum* protein kinase 6, and the *Plasmodium falciparum* cyclin-related kinases-1,-3,-4

and -5 (Doerig *et al*., 2002; Geyer *et al*., 2005). *Plasmodium falciparum* protein kinase 5 is related to the human CDK1 and CDK5; however unlike its mammalian counterparts, it possesses *in vitro* autophosphorylation activity (Doerig *et al*., 2002; Geyer *et al*., 2005). *Pf*mrk, expressed throughout the trophozoite- and schizont-stages, is related to the human CDK7, which in mammalian cells is responsible for activating other CDK/cyclin complexes (Doerig *et al*., 2002). *Plasmodium falciparum* protein kinase 6, also expressed in the trophozoite- and schizont-stages, exhibits limited homology to human CDK2 and the p38 mitogen-activated protein kinase and interestingly, does not require activation by cyclins (Doerig *et al*., 2002; Geyer *et al*., 2005). *Plasmodium falciparum* cyclin-related kinase-1 is expressed mainly in the non-dividing gametocyte and exhibits homologies to a group of kinases mainly found to be involved in apoptosis induction and cellular differentiation. *Plasmodium falciparum* cyclin-related kinases-3 and -4 are expressed in both the asexual and gametocyte stages of the parasitic life cycle, with *Plasmodium falciparum* cyclin-related kinase-3 exhibiting homology to CDK1 and *Plasmodium falciparum* cyclin-related kinase-4 exhibing homology to CDKs and p38 mitogen-activated protein kinases (Harmse *et al*., 2001; Doerig *et al*., 2002; Geyer *et al*., 2005); whilst *Plasmodium falciparum* cyclin-related kinase -5 is predicted to be a CDK/p38 mitogen-activated protein kinase protein hybrid (Geyer *et al*., 2005). Purine analogues have shown strong CDK inhibitory effects, by competing with ATP for binding in the ATP-kinase binding site (Harmse *et al*., 2001; Knockaert *et al*., 2002; Geyer *et al*., 2005).

It is evident that nucleoside phosphonates, phosphonic acids and purine/pyrimidine derivatives are a promising class of novel antimalarial agents and warrant further investigation.

5.2 Materials and methods

5.2.1 Test compounds

A total of 90 nucleoside phosphonates, phosphonic acids, and purine/pyrimidine derivatives were received from Professors Ivan Rosenberg and Dominik Rejman of the Academy of Sciences of the Czech Republic, Prague, Czech Republic. The compounds were synthesised according to the methodology laid out by Roudeau *et al*. (2006), Suk *et al*. (2007), Rejman *et al*. (2009), and Vaněk *et al*. (2009), and grouped according to structural

similarities. The 90 compounds were classified into 11 structural groups, namely; Phosphonoxins (Table 5.1), Nucleoside Lipophosphonates (Table 5.2), Lipophosphonoxins (Table 5.3), PyrroPME (Table 5.4), Mickey Mouse (Table 5.5), Pyrrolidine nucleotides (Table 5.6), Piperidine nucleosides and nucleotides (Table 5.7), and Aza sugars, U/T miscellaneous nucleosides and miscellaneous (Table 5.8).

Table 5.1: The chemical names and codes of the Phosphonoxin group, as well as the (nucleo)base present. Chemical structures are represented in Table 5.17. Abbreviations: U, uracil; G, guanine.

Chemical Code	Chemical name	Base
DR-3128	Uridin-5'-yl ([3*R*,4*R*]-3,4-dihydroxypyrrolidin-1-*N*-yl)methyl-phosphonate	U
DR-3129	Uridin-5'-yl ([3*RS*]-3-hydroxypyrrolidin-1-*N*-yl)thiocarbonyl-phosphonate	U
DR-3122	Uridin-5'-yl ([3*RS*]-3-hydroxypyrrolidin-1-*N*-yl)carbonylphosphonate	U
DR-3573	Uridin-5'-yl 2-([3*R*,4*R*]-3,4-dihydroxypyrrolidin-1-*N*-yl)ethyl-phosphonate	U
DR-3510	Uridin-5'-yl-2-([3S, 4S]-3,4-dihydroxypyrrolidin-1-N-yl)ethyl-phosphonate	U
DR-4066	Guanosin-5'-yl 2-([3*S*,4*S*]-3,4-dihydroxypyrrolidin-1-*N*-yl)ethyl-phosphonate	G
DR-4165	Guanosin-5'-yl 2-([3*R*,4*R*]-3,4-dihydroxypyrrolidin-1-*N*-yl)ethyl-phosphonate	G
DR-3095	Uridin-5'-yl 2-([3*R*,4*R*]-3,4-dihydroxy-2,5-dioxopyrrolidin-1-*N*-yl)ethyl-phosphonate	U
DR-3096	Uridin-5'-yl 2-([3*R*,4*R*]-3,4-dihydroxy-2,5-dioxopyrrolidin-1-*N*-yl)ethyl-phosphonate	U
DR-3111	Uridin-5'-yl 3-([3*R*,4*R*]-3,4-dihydroxypyrrolidin-1-*N*-yl)propyl-phosphonate	U
DR-3112	Uridin-5'-yl 2-([3*R*,4*R*]-3,4-dihydroxypyrrolidin-1-*N*-yl)ethoxymethyl-phosphonate	U
DR-3502-C	Uridin-5'-yl 2-([3*RS*]-3-hydroxypiperidin-1-*N*-yl)ethylphosphonate	U
DR-3679	Uridin-5'-yl 2-([3*S*,4*R*]-3,4-dihydroxypiperidin-1-*N*-yl)ethyl-phosphonate	U
DR-3707	Uridin-5'-yl 2-([3*R*,4*S, 5S*]-3,4,5-trihydroxypiperidin-1-*N*-yl)ethyl-phosphonate	U

Table 5.2: The chemical names and codes of the Nucleoside Lipophosphonate group, as well as the (nucleo)base present. Chemical structures are represented in Table 5.10. Abbreviations: A, adenine; U, uracil; G, guanine.

Chemical Code	Chemical name	Base
DR-3641	Hexadecyloxypropyl (adenosin-5'-yl)methanphosphonate	A
DR-3621	Hexadecyloxypropyl (uridin-5'-yl)methanphosphonate	U
DR-3960	Hexadecyloxypropyl (guanosin-5'-yl)methanphosphonate	G

Table 5.3: The chemical names and codes of the Lipophosphonoxin group, as well as the (nucleo)base present. Chemical structures are represented in Table 5.11. Abbreviations: U, uracil; G, guanine.

Chemical Code	Chemical name	Base
DR-4658	Ethyl uridin-5'-yl 2-([3*R*,4*R*]-3,4-dihydroxypyrrolidin-1-*N*-yl)ethyl-phosphonate	U
DR-4695	2-Pivaloylthioethyl uridin-5'-yl 2-([3*R*,4*R*]-3,4-dihydroxypyrrolidin-1-*N*-yl)ethylphosphonate	U
DR-4696	2-Pivaloylthioethyl uridin-5'-yl 2-([3*R*,4*R*]-3,4-dihydroxypyrrolidin-1-*N*-yl)ethylphosphonate	U
DR-4137	Hexadecyloxypropyl uridin-5'-yl 2-([3*R*,4*R*]-3,4-dihydroxypyrrolidin-1-*N*-yl)ethylphosphonate	U
DR-4878	Hexadecyloxypropyl cytidin-5'-yl 2-([3*R*,4*R*]-3,4-dihydroxypyrrolidin-1-*N*-yl)ethylphosphonate	C
DR-4850	Under patent	G
DR-4914B	Under patent	G
DR-4848	Hexadecyloxypropyl ((2*R*,3*S*,4*R*,5*R*)-5-(4-((3*r*,4*s*)-3,4-dihydroxypyrrolidin-1-yl)-2-oxopyrimidin-1(2H)-yl)-3,4-dihydroxytetrahydrofuran-2-yl)methyl ([3*r*,4*s*]-3,4-dihydroxypyrrolidin-1-*N*-yl)ethylphosphonate	C
DR-4463	Hexadecyloxypropyl uridin-5'-yl 2-([3*S*,4*S*]-3,4-dihydroxypyrrolidin-1-*N*-yl)ethylphosphonate	U
DR-4458	Hexadecyloxypropyl uridin-5'-yl 2-([3*R*,5*R*]-3,4-dihydroxypiperidin-1-*N*-yl)ethylphosphonate	U
DR-4459	Hexadecyloxypropyl uridin-5'-yl 2-([3*R*,4*S,5S*]-3,4-trihydroxypiperidin-1-*N*-yl)ethylphosphonate	U

Table 5.4: The chemical names and codes of the PyrroPME group, as well as the (nucleo)base present. Chemical structures are represented in Table 5.12. Abbreviations: A, adenine; T, thymine; U, uracil; C, cytosine.

Chemical Code	Chemical name	Base
DR-3919	[3*S*,4*R*]-4-(Adenin-9-yl)-3-phosphonomethoxypyrrolidine	A
DR-3953	[3*S*,4*R*]-4-(Adenin-9-yl)-3-cyclohexyloxypropylphosphono-methoxypyrrolidine	A
DR-3945	[3*S*,4*R*] 3-Phosphonomethoxy -4-(thymin-1-yl)- pyrrolidine	T
DR-3769	[3*R*,4*S*] 3-Phosphonomethoxy -4-(thymin-1-yl)- pyrrolidine	T
DR-4140	3-(Hexadecyloxy)propyl ((((3*S*,4*R*)-4-(5-methyl-2,4-dioxo-3,4-dihydropyrimidin-1(2*H*)-yl)pyrrolidin-3-yl)oxy)methyl)phosphinate	T
DR-4001	[3*S*,4*S*] -3-Phosphonomethoxy-4-(uracil-1-yl)- pyrrolidine	U
DR-4255A	[3*R*,4*S*]-4-(Cytosin-2-*O*-yl)- 3-phosphonomethoxypyrrolidine-1-carbaldehyde	C

Table 5.5: The chemical names and codes of the Mickey Mouse group, as well as the (nucleo)base present. Chemical structures are represented in Table 5.13. Abbreviations: Pu, purine ring structure; /, no (nucleo)base present.

Chemical Code	Chemical name	Base
$Bn_2NH.HCl$	Dibenzylamine hydrochloride	/
D1293-S	*N*^{6},*N*^{6}-Dibenzyl-9*H*-purine-2,6-diamine	Pu
DR-4461	2-Amino-6- dibenzylaminopurine	Pu
DR-4523	6-(*N*-Benzyl-*N*-3-trifluoromethylphenylmethylamino)purine	Pu
DR-4541	2-(6-(*N*-Benzyl-*N*-3-trifluoromethylphenylmethylamino)purin-9-yl)ethyloxymethylphosphonic acid	Pu
DR-4651	2-(2-Amino-6- dibenzylaminopurin-9-yl)ethyloxymethyl-phosphonic acid	Pu
DR-3896	2-(6-Dibenzylaminopurin-9-yl)ethyloxymethylphosphonic acid	Pu
DR-4598A	3-(6-Dibenzylaminopurin-9-yl)propylphosphonic acid	Pu
DR-4640	4-(6-Dibenzylaminopurin-9-yl)butylphosphonic acid	Pu
DR-4599A	5-(6-Dibenzylaminopurin-9-yl)pentylphosphonic acid	Pu
DR-3892	4-((*R*)-3-(2-Amino-6-(dibenzylamino)-9H-purin-9-yl)pyrrolidin-1-yl)-2-hydroxy-4-oxobutanoic acid	Pu
DR-3898	(R)-(2-(3-(2-Amino-6-(dibenzylamino)-9H-purin-9-yl)pyrrolidin-1-yl)-2-oxoethyl)phosphonic acid	Pu
DR-4251	[3*S*,4*R*]-4-(6-*N*-Dibenzylaminopurin-9-yl)-3-phosphonomethoxy-pyrrolidine-1-carbaldehyde	Pu
DR-4558	(2*S*,3*S*)-4-(3-(6-(Dibenzylamino)-9H-purin-9-yl)piperidin-1-yl)-2,3-dihydroxy-4-oxobutanoic acid	Pu

Table 5.6: The chemical names and codes of the Pyrrolidine nucleotide group, as well as the (nucleo)base present. Chemical structures are represented in Table 5.14. Abbreviations: U, uracil; T, thymine; A, adenine; G, guanine.

Chemical Code	Chemical name	Base
K584	1-(Uracil-1-yl)-1,2,3-trideoxy-3-aza-4a-carba-α-L-glyceropentofuranos-3-ylmethylphosphonic acid	U
K578	1-(Thymin-1-yl)-1,2,3-trideoxy-3-aza-4a-carba-α-L-glyceropento-furanos-3-ylmethylphosphonic acid	T
DR-4028	[3*S,4R*]-[4-(4-Bromouracil-9-yl)-3-hydroxypyrrolidin-1-*N*-yl]carbonyl-phosphonic acid	U
DR-3616	[3*S,4R*]-[4-(Adenin-9-yl)-3-hydroxypyrrolidin-1-*N*-yl]carbonyl-phosphonic acid	A
Pe141	[3S,4S]-[4-(Guanin-9-yl)-3-hydroxypyrrolidin-1-N-yl]carbonylphosphonic acid	A
DR-3876	Under patent	G

Table 5.7: The chemical names and codes of the Piperidine nucleoside (K366-DR-4290B) and nucleotide (K423-K416) groups, as well as the (nucleo)base present. Chemical structures are represented in Table 5.15. Abbreviations: A, adenine; U, uracil; T, thymine; C, cytosine; G, guanine.

Chemical Code	Chemical name	Base
K366	4-(Adenin-9-yl)piperidine	A
DR-3994	(RS)-3-(Uracil-1-yl)piperidine	U
PipT	4-(Thymin-1-yl)piperidine	T
K349_B	(RS)-3-(Adenin-9-yl)piperidine	A
K370_B	(RS)-3-(Thymin-1-yl)piperidine	T
K351	(RS)-3-(Cytosin-2-O-yl)piperidine	C
K371_B	(RS)-3-(Guanin-9-yl)piperidine	G
K523	(3S,5R)-5-Hydroxy-3-(uracil-1-yl)piperidine	U
K524	(3S,5R)-5-Hydroxy-3-(thymin-1-yl)piperidine	T
DR-4377	[3*S*,4*R*,5*R*]-1-(3,5-Dihydroxypiperidin-4-yl)uracil	U
DR-4380	[3*S*,4*R*,5*S*]-1-(4,5-Dihydroxypiperidin-5-yl)uracil	U
DR-4513	[3*S*,4*R*,5*R*]-9-(3,5-Dihydroxypiperidin-4-yl)adenine	A
DR-4290B	[3*S*,4*R*,5*R*]-1-(4,5-Dihydroxypiperidin-5-yl)uracil	U
K423	(*RS*)-(3-(Thymine-1-yl)piperidin-1-yl)thiocarbonylphosphonic acid	T
K418	(*RS*)-(3-(Thymine-1-yl)piperidin-1-yl)methylphosphonic acid	T
K422	(*RS*)-(3-(Thymine-1-yl)piperidin-1-yl)ethylphosphonic acid	T
K414_A	(*RS*)-(3-(Thymine-1-yl)piperidin-1-yl)carbonylphosphonic acid	T
K416	(*RS*)-(3-(Thymine-1-yl)piperidin-1-yl)carbonylmethylphosphonic acid	T

5.2.2 Pharmacological evaluation

5.2.2.1 General methodology

The methodology used was that as described in Sections 2.2, 2.3 and 2.4, with some modifications. Additional experimentation included the assessment of antimalarial activity over a double parasitic life cycle (Section 5.2.2.2), and combination studies with the nucleoside transport inhibitor, dipyridamole (Section 5.2.2.3). All compounds were assessed for antimalarial activity using the [^{3}H]-hypoxanthine incorporation assay (Section 2.2.2.1), as well as for toxicity against red blood cells (Section 2.4.2). From the results obtained, four compounds with IC_{50} values of less than 100 μM and twenty one inactive compounds (IC_{50} values > 100 μM), representative of all the chemical groups, were selected for flow cytometric analysis (Section 2.2.3.3). A lead compound was selected for a combination study with quinine (Section 2.2.2.3), as well as for stage sensitivity and

parasite morphology studies (Section 2.2.3.4). Due to the fact that only small amounts of the test compounds were received, some antimalarial mechanisms of action studies could not be completed on all of the active compounds, and in the case of combination, stage sensitivity and parasite morphology studies, the next most active compound was investigated. In order to examine the structure-activity relationships of the compounds, a selection of inactive compounds were also assessed for DPPH$^{\bullet}$ free-radical scavenging (Section 2.3.2.1.2), iron chelating (Section 2.3.2.2.2) and β-haematin formation inhibitory activity (Section 2.3.1.2).

Table 5.8: The chemical names and codes of the Aza sugars (K568 and K537), U/T miscellaneous nucleosides (K469-K545) and Miscellaneous (DR-3227-K580) groups, as well as the (nucleo)base present. Chemical structures are represented in Table 5.16. Abbreviations: T, thymine; U, uracil; G, guanine; Py, pyrimidine ring structure; /, no (nucleo)base present.

Chemical Code	Chemical name	Base
K568	(3*R*,5*R*)-piperidine-3,5-diol	/
K537	(3*R*,5*R*)-1-benzylpiperidine-3,5-diol	/
K469	1-Cyclopropyluracil	U
DR-4034	1-Cyclopropylthymine	T
K470	1-(1-(Hydroxymethyl)cyclopentyl)uracil	U
DR-4031	1-(*cis*-2-Hydroxycyclopentyl)uracil	U
K479	1-Cyclohexyluracil	U
DR-4030	1-(*trans*-2-Hydroxycyclohexyl)uracil	U
DR-4037	1-(*trans*-4-Hydroxycyclohexyl)uracil	U
DR-4011	Methyl 2-(1-uracilyl)acetate	U
K480	1-(2,3-Dihydroxypropyl)uracil	U
K545	1-(2,3-Dihydroxypropyl)thymine	T
DR-3227	9-((3S,4R)-4-Hydroxypyrrolidin-3-yl)guanine	G
DR-3845	5-Methyl-1-((3R,4R,5S,6R)-2,3,5-trihydroxy-6-(hydroxymethyl)-tetrahydro-2H-pyran-4-yl)pyrimidine-2,4(1H,3H) –dione	Py
DA-IX-158	Under patent	A
OP35	9-(Tetrahydrothiophen-3-yl)-adenine	A
K580	[3S,5S]-1-(5-(Hydroxymethyl)pyrrolidin-3-yl)uracil	U

5.2.2.2 Modified tritiated hypoxanthine incorporation assay

A total of seven active and four inactive compounds were selected from the various chemical groups, with quinine included for comparison purposes, in order to assess

whether there was any improvement in the antimalarial activity of the compounds over two cycles of DNA synthesis and division, or two parasitic life cycles. Duplicate 96-well plates were prepared so that single (SC) and double cycle (DC) results could be compared. The methodology was that as described in Section 2.2.2.1, with the exception of the double cycle plate to which the [^{3}H]-hypoxanthine isotope was added after a 72 hour incubation period, as opposed to 24 hour incubation period as in the single cycle plate. The optimal gaseous atmosphere was maintained by re-lighting the candle within the glass dessicator on a 24 hourly basis and blood smears prepared at 48 and 96 hours to monitor parasite viability over the elongated incubation period.

5.2.2.3 Combination studies with dipyridamole

Dipyridamole is a highly lipophilic pyrimidopyrimidine analogue that interacts with the lipid phase of cell membranes, thereby modifying membrane lipids and membrane-bound proteins with the resultant inhibition of both human ENT1 and malarial *Pf*ENT1 (Gupte and Buolamwini, 2004; Lin and Buolamwini, 2007).

Due to the fact that dipyridamole acts as a nucleoside transport inhibitor, and could interfere with the uptake of the [^{3}H]-hypoxanthine isotope, combination studies were carried out using the flow cytometric methodology. Dipyridamole itself possesses fluorescent properties. However, its excitation and emission spectra (Ex = 280 nm, Em = 490 nm) (Lin and Buolamwini, 2007) is different from that of dihydroethidium (Ex = 488 nm, Em = 610 nm), and would, therefore, not interfere with the detection of dihydroethidium in the FL2 channel of the BD FACSCalibur™. The antimalarial activity of dipyridamole and compounds DR-4463 and D1293-S were assessed utilising the flow cytometric methodology (Section 2.2.3.3); from which log sigmoid dose-response curves were constructed, and individual IC_{90}, IC_{50} and IC_{10} values obtained using Enzfitter® (version 1.05) software (Section 2.2.3.5). The test compounds and dipyridamole were prepared at concentrations 20 times higher than the IC_{90}, IC_{50} and IC_{10} values obtained, in order to account for the dilution factor of the experiment. Dipyridamole was combined with each test compound at different inhibitory concentration ratios (Table 5.9). Following a 24 hour incubation period, 25 µl of incomplete culture media was added to each well, in the place of the [^{3}H]-hypoxanthine isotope, before the plates were re-incubated for a further 24 hours, under

optimal conditions. Flow cytometric analysis was then performed according to the methodology described in Section 2.2.3.3.

Table 5.9: Ratios of dipyridamole to the test compounds used to determine pharmacological interactions in the combination study.

Dipyridamole	Test compound(s)
IC_{90}	0
IC_{50}	0
IC_{10}	0
IC_{90}	IC_{90}
IC_{90}	IC_{50}
IC_{90}	IC_{10}
IC_{50}	IC_{50}
IC_{50}	IC_{90}
IC_{50}	IC_{10}
IC_{10}	IC_{10}
IC_{10}	IC_{50}
IC_{10}	IC_{90}
0	IC_{90}
0	IC_{50}
0	IC_{10}

Following acquisition of the % parasite growth for each sample, as described in Section 2.2.3.3, relative ratios for each combination were calculated (Section 2.2.2.3). From the relative ratios obtained, isobolograms were constructed and the degree of the interaction determined (Section 2.2.2.3).

5.3 Results

5.3.1 *In vitro* antimalarial activity

Of the 90 compounds screened for antimalarial activity, 21.11% or 19 compounds inhibited parasite growth in a dose-dependent manner, with IC_{50} values below 100 µM (Figure 5.5); whilst the remaining compounds were incapable of inhibiting parasite growth below 100 µM. Of the 19 compounds, 14 exhibited moderate antimalarial activity (10 µM ≤ IC_{50} value ≤ 50 µM) and 5 exhibited low antimalarial activity (50 µM ≤ IC_{50} value ≤ 100 µM). Compounds DR-4850, DR-4878 and DR-4463 exhibited the most promising antimalarial activity (IC_{50} values: 13.35 ± 0.38 µM, 17.76 ± 1.72 µM and 19.81 ± 0.80 µM, respectively); however they

proved to be 89-, 118- and 132-fold less active than quinine (IC_{50} value: 0.15 ± 0.01 µM) (Table 5.11).

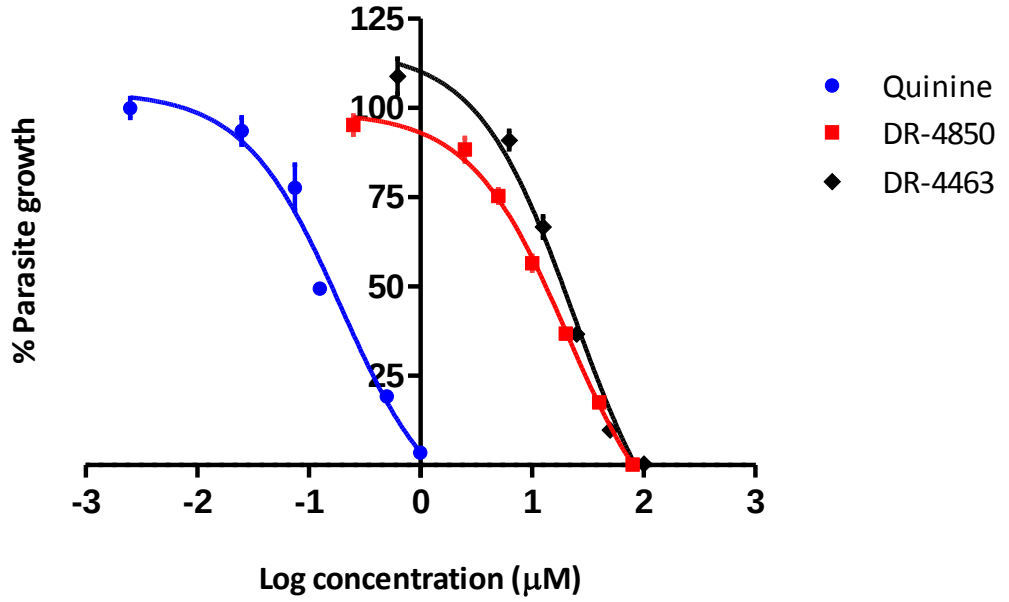


Figure 5.5: Antimalarial activity of compounds DR-4850 and DR-4463 compared to quinine.

The Nucleoside Lipophosphonate, Lipophosphonoxin, PyrroPME, Mickey Mouse and Pyrrolidine nucleotide groups all produced active compounds (Tables 5.10, 5.11, 5.12, 5.13 and 5.14). Whereas, the Piperidine nucleoside and nucleotide, Aza sugar, U/T Miscellaneous nucleoside and Miscellaneous, and Phosphonoxin structural groups produced no compounds with IC_{50} values < 100 µM (Tables 5.15-5.17).

The three compounds comprising the Nucleoside Lipophosphonate group were all active (Table 5.10), followed by the Lipophosphonoxin (Table 5.11), Mickey Mouse (Table 5.13), PyrroPME (Table 5.12) and Pyrrolidine nucleotide (Table 5.14) groups, of which 73%, 33%, 25% and 17% of the compounds within each respective group were active. The base composition of the active compounds varied, 58% of the active compounds possessed a guanine or adenine base or the basic purine ring structure, whereas 42% of the active compounds possessed a cytosine, thymine or uracil base.

Table 5.10: The *in vitro* antimalarial (1% haematocrit, 0.5% parasitaemia) and haemolytic activity of the Nucleoside Lipophosphonate group of compounds (n = 4). Where: SC = single cycle; DC = double cycle

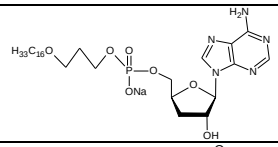
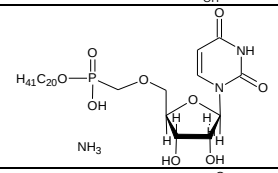
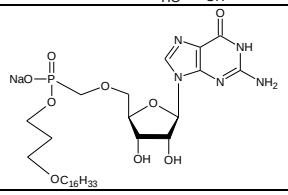
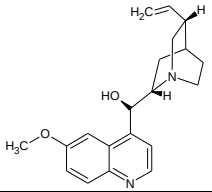
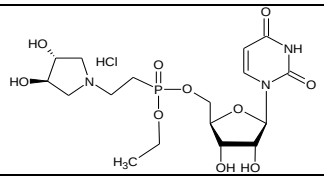
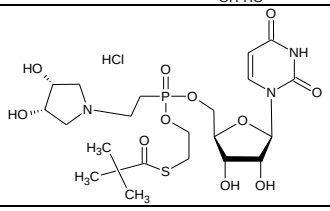
Chemical Code	Chemical structure	Antimalarial activity	Haemolytic activity
		IC_{50} value µM ± s.d.	**% 100 µM ± s.d.**
DR-3641		43.14 ± 1.67	0.61 ± 0.04
DR-3621		30.01 ± 1.65 S.C. 27.67 ± 2.21 D.C.	1.41 ± 0.85
DR-3960		33.13 ± 2.10 S.C. 33.30 ± 1.69 D.C.	9.32 ± 3.50
Quinine		0.15 ± 0.01 S.C. 0.18 ± 0.00 D.C.	1.22 ± 0.98

Table 5.11: The *in vitro* antimalarial (1% haematocrit, 0.5% parasitaemia) and haemolytic activity of the Lipophosphonoxin group of compounds. Values in parenthesis indicate the % inhibition of parasite growth at 100 µM (n = 4).

Chemical Code	Chemical structure	Antimalarial activity	Haemolytic activity
		IC_{50} value µM ± s.d.	**% 100 µM ± s.d.**
DR-4658		> 100 (0.01 ± 2.61)	0.38 ± 0.08
DR-4695		> 100 (0.01 ± 1.62)	0.37 ± 0.12

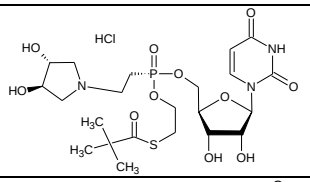
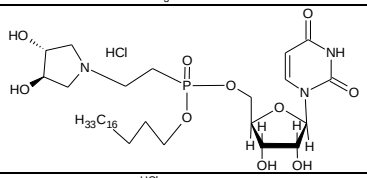
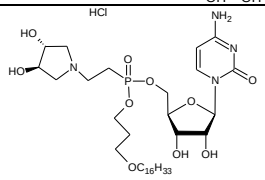
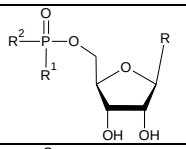
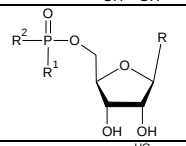
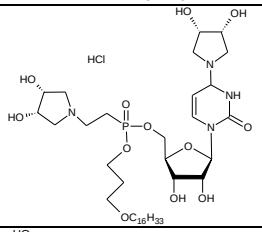
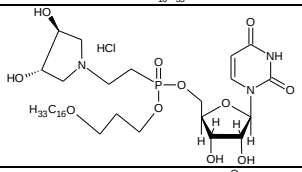
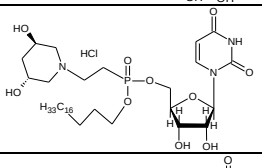
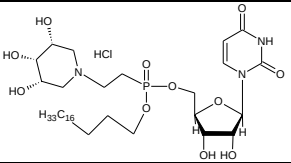
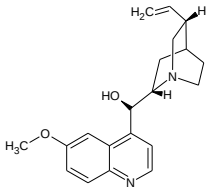
Chemical Code	Chemical structure	Antimalarial activity	Haemolytic activity
		IC_{50} value µM ± s.d.	% 100 µM ± s.d.
DR-4696		> 100 (2.16 ± 1.61)	0.39 ± 0.13
DR-4137		49.18 ± 0.79	4.56 ± 1.00
DR-4878		17.76 ± 1.72	5.17 ± 3.62
DR-4850		13.35 ± 0.38	9.25 ± 2.08
DR-4914B		21.05 ± 0.71	50.20 ± 3.35
DR-4848		30.46 ± 3.54	1.07 ± 0.34
DR-4463		19.81 ± 0.80 S.C. 6.04 ± 0.31 D.C.	7.85 ± 1.41
DR-4458		29.98 ± 0.70	6.32 ± 2.33
DR-4459		49.11 ± 4.11	1.14 ± 1.41
Quinine		0.15 ± 0.01 S.C. 0.18 ± 0.00 D.C.	1.22 ± 0.98

Table 5.12: The *in vitro* antimalarial (1% haematocrit, 0.5% parasitaemia) and haemolytic activity of the PyrroPME group of compounds. Values in parenthesis indicate the % inhibition of parasite growth at 100 µM (n = 4).

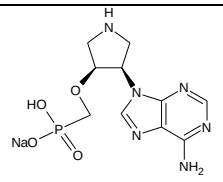
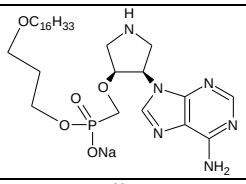
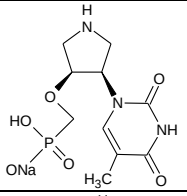
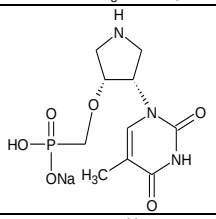
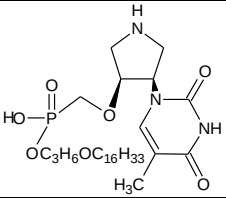
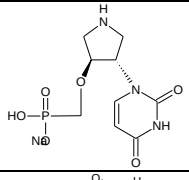
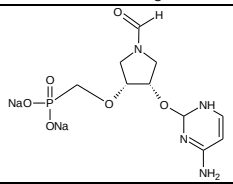
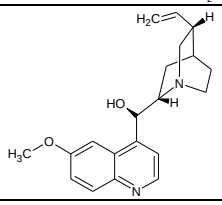
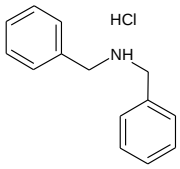
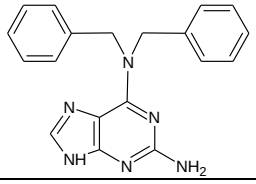
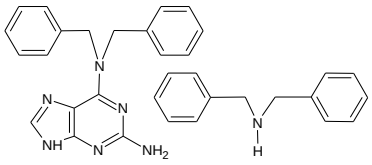
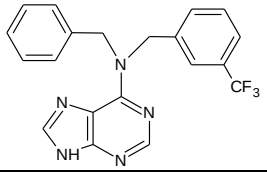
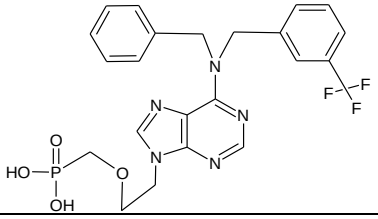
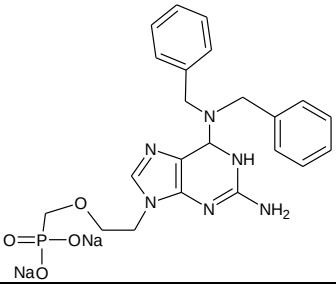
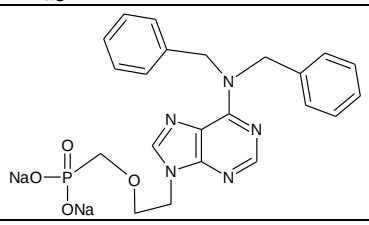
Chemical Code	Chemical structure	Antimalarial activity	Haemolytic activity
		IC_{50} value µM ± s.d.	**% 100 µM ± s.d.**
DR-3919		> 100 (0.01 ± 10.46) S.C. (0.01 ± 2.10) D.C.	0.27 ± 0.10
DR-3953		39.34 ± 2.77	5.64 ± 0.72
DR-3945		> 100 (0.01 ± 3.47) S.C. (2.20 ± 3.35) D.C.	0.36 ± 0.15
DR-3769		> 100 (0.01 ± 5.17)	0.44 ± 0.21
DR-4140		63.51 ± 5.60	0.93 ± 0.33
DR-4001		> 100 (2.26 ± 3.66)	0.39 ± 0.19
DR-4255A		> 100 (6.41 ± 2.78)	0.39 ± 0.16
Quinine		0.15 ± 0.01 S.C. 0.18 ± 0.00 D.C.	1.22 ± 0.98

Table 5.13: The *in vitro* antimalarial (1% haematocrit, 0.5% parasitaemia) and haemolytic activity of the Mickey Mouse group of compounds. Values in parenthesis indicate the % inhibition of parasite growth at 100 µM (n = 5).

Chemical Code	Chemical structure	Antimalarial activity	Haemolytic activity
		IC_{50} value µM ± s.d.	**% 100 µM ± s.d.**
$Bn_2NH.HCl$		> 100 (12.57 ± 4.88)	0.31 ± 0.13
D1293-S		52.63 ± 3.79	0.39 ± 0.10
DR-4461	 cca **1 : 10**	> 100 (33.87 ± 6.76)	0.22 ± 0.05
DR-4523		77.48 ± 8.57 S.C. 73.93 ± 1.03 D.C.	8.95 ± 5.70
DR-4541		> 100 (14.26 ± 4.63)	0.64 ± 0.31
DR-4651		79.66 ± 2.11	0.39 ± 0.15
DR-3896		> 100 (27.05 ± 10.99)	0.51 ± 0.05

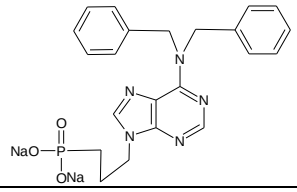
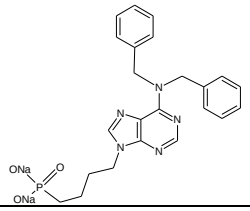
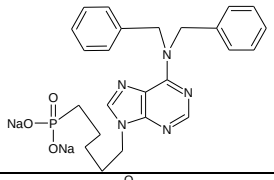
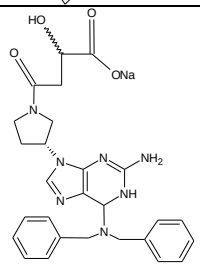
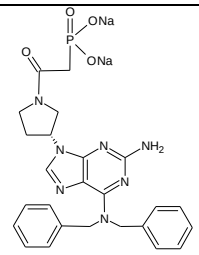
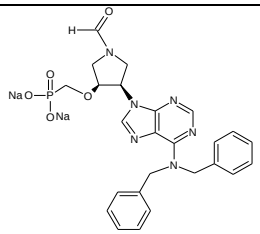
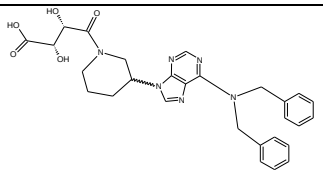
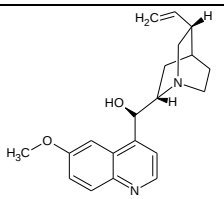
Chemical Code	Chemical structure	Antimalarial activity	Haemolytic activity
		IC_{50} value µM ± s.d.	**% 100 µM ± s.d.**
DR-4598A		> 100 (34.61 ± 3.17)	0.46 ± 0.13
DR-4640		> 100 (44.10 ± 3.07)	0.47 ± 0.21
DR-4599A		> 100 (25.38 ± 6.03)	0.44 ± 0.23
DR-3892		57.11 ± 1.49 S.C. 47.73 ± 1.07 D.C.	0.38 ± 0.15
DR-3898		> 100 (2.50 ± 3.32) S.C. (0.01 ± 1.12) D.C.	0.38 ± .17
DR-4251		> 100 (7.45 ± 5.10)	0.40 ± 0.17
DR-4558		23.85 ± 1.76 S.C. 16.71 ± 0.77 D.C.	0.32 ± 0.09
Quinine		0.15 ± 0.01 S.C. 0.18 ± 0.00 D.C.	1.22 ± 0.98

Table 5.14: The *in vitro* antimalarial (1% haematocrit, 0.5% parasitaemia) and haemolytic activity of the Pyrrolidine nucleotide group of compounds. Values in parenthesis indicate the % inhibition of parasite growth at 100 µM (n = 3).

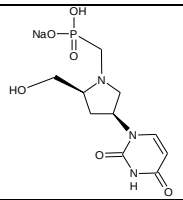
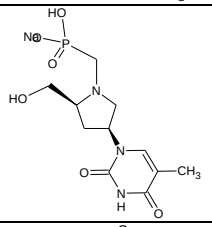
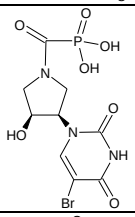
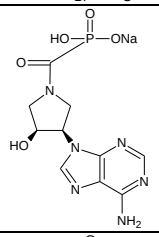
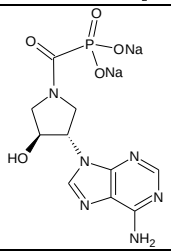
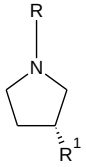
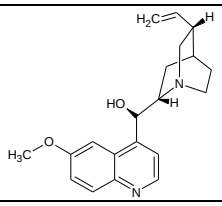
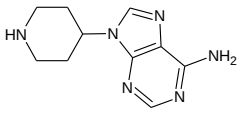
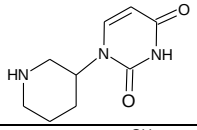
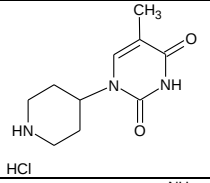
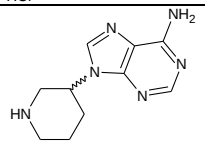
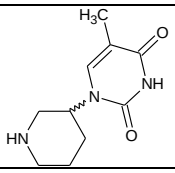
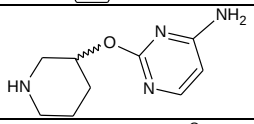
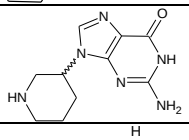
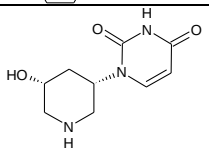
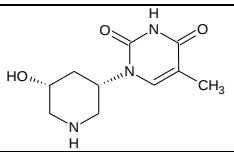
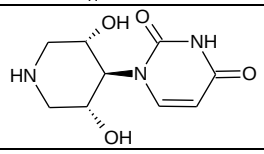
Chemical Code	Chemical structure	Antimalarial activity	Haemolytic activity
		IC_{50} value µM ± s.d.	**% 100 µM ± s.d.**
K584		> 100 (1.93 ± 0.76)	0.41 ± 0.17
K578		> 100 (7.60 ± 3.00)	0.93 ± 1.24
DR-4028		> 100 (0.64 ± 6.74)	0.47 ± 0.24
DR-3616		> 100 (7.42 ± 8.39)	0.31 ± 0.03
Pe141		> 100 (0.01 ± 2.17)	0.52 ± 0.16
DR-3876		31.08 ± 2.33 S.C. 20.01 ± 0.88 D.C.	0.40 ± 0.11
Quinine		0.15 ± 0.01 S.C. 0.18 ± 0.00 D.C.	1.22 ± 0.98

Table 5.15: The *in vitro* antimalarial (1% haematocrit, 0.5% parasitaemia) and haemolytic activity of the Piperidine nucleoside (K366-DR-4290B) and nucleotide (K423-K416) group of compounds. Values in parenthesis indicate the % inhibition of parasite growth at 100 µM (n = 3).

Chemical Code	Chemical structure	Antimalarial activity	Haemolytic activity
		IC_{50} value µM ± s.d.	% 100 µM ± s.d.
K366		> 100 (6.15 ± 1.22)	0.41 ± 0.08
DR-3994		> 100 (0.01 ± 7.30)	0.40 ± 0.17
PipT		> 100 (5.04 ± 3.79)	0.49 ± 0.21
K349_B		> 100 (13.55 ± 9.85)	0.41 ± 0.25
K370_B		> 100 (0.01 ± 0.07)	0.39 ± 0.20
K351		> 100 (4.00 ± 9.78)	0.33 ± 0.17
K371_B		> 100 (19.40 ± 3.76)	0.58 ± 0.31
K523		> 100 (6.24 ± 0.12)	0.30 ± 0.13
K524		> 100 (0.01 ± 3.68)	0.36 ± 0.18
DR-4377		> 100 (0.01 ± 1.31)	0.38 ± 0.18

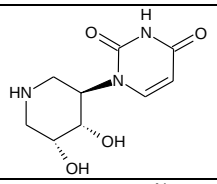
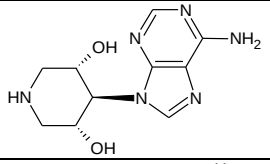
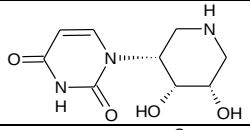
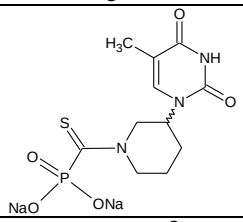
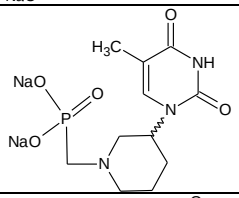
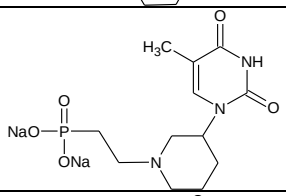
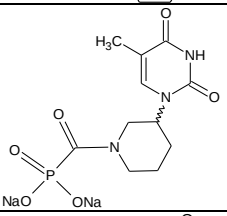
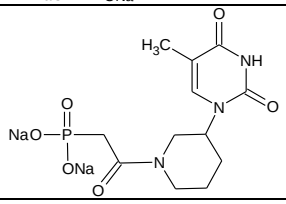
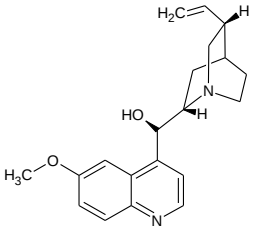
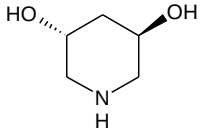
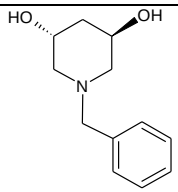
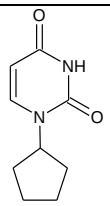
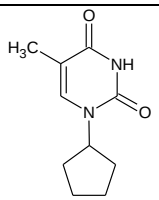
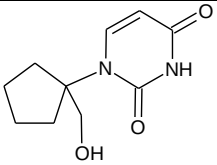
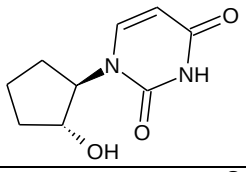
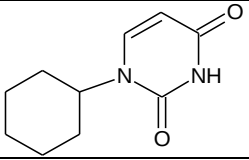
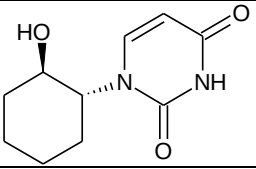
Chemical Code	Chemical structure	Antimalarial activity	Haemolytic activity
		IC_{50} value µM ± s.d.	**% 100 µM ± s.d.**
DR-4380		> 100 (4.35 ± 1.80)	0.35 ± 0.17
DR-4513		> 100 (43.57 ± 0.48)	0.49 ± 0.26
DR-4290B		> 100 (0.01 ± 4.84)	0.39 ± 0.12
K423		> 100 (0.01 ± 3.18)	0.31 ± 0.13
K418		> 100 (0.01 ± 3.96)	0.42 ± 0.22
K422		> 100 (0.01 ± 5.20)	0.36 ± 0.14
K414_A		> 100 (0.01 ± 10.66)	0.27 ± 0.11
K416		> 100 (2.19 ± 5.42)	0.40 ± 0.21
Quinine		0.15 ± 0.01 S.C. 0.18 ± 0.00 D.C.	1.22 ± 0.98

Table 5.16: The *in vitro* antimalarial (1% haematocrit, 0.5% parasitaemia) and haemolytic activity of the Aza sugars (K568 and K537), U/T miscellaneous nucleosides (K469-K545) and Miscellaneous (DR-3227-K580) groups of compounds. Values in parenthesis indicate the % inhibition of parasite growth at 100 µM (n = 3).

Chemical Code	Chemical structure	Antimalarial activity	Haemolytic activity
		IC_{50} value µM ± s.d.	% 100 µM ± s.d.
K568		> 100 (2.57 ± 0.98)	0.24 ± 0.18
K537		> 100 (5.87 ± 1.54)	0.38 ± 0.16
K469		> 100 (0.01 ± 0.64)	0.31 ± 0.15
DR-4034		> 100 (0.01 ± 7.21)	0.42 ± 0.23
K470		> 100 (4.81 ± 4.02)	0.26 ± 0.13
DR-4031		> 100 (0.85 ± 1.48)	0.38 ± 0.24
K479		> 100 (4.75 ± 2.90)	0.21 ± 0.12
DR-4030		> 100 (3.22 ± 3.15)	0.28 ± 0.16

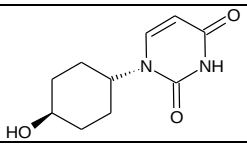
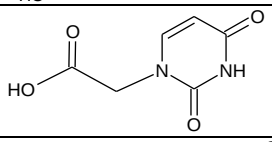
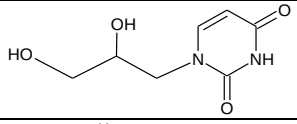
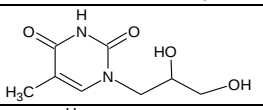
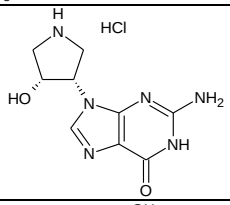
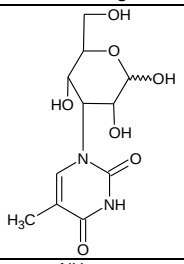
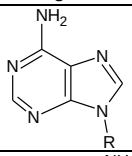
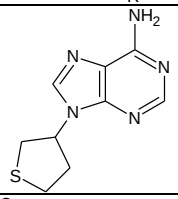
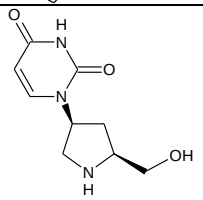
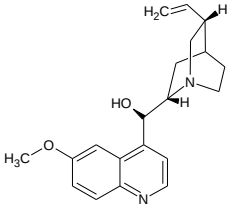
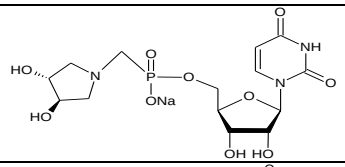
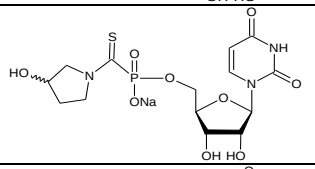
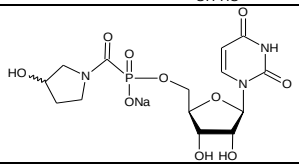
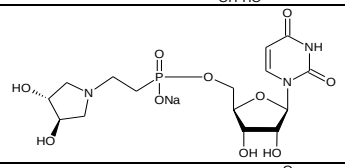
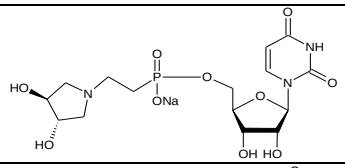
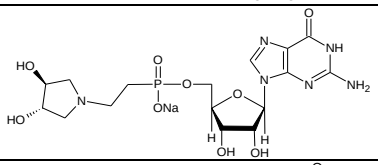
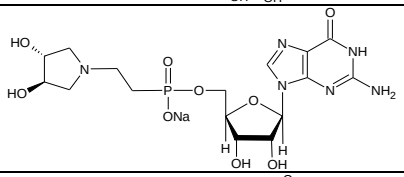
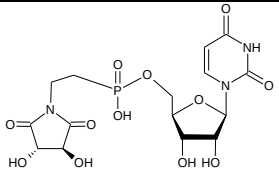
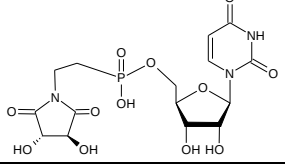
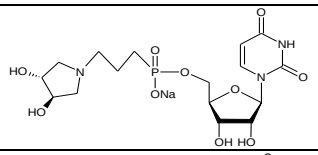
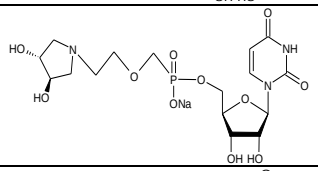
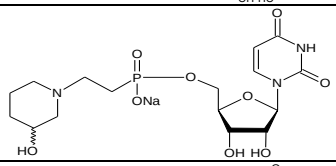
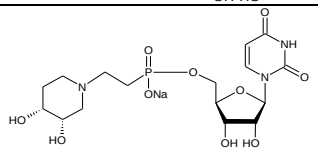
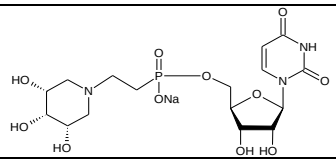
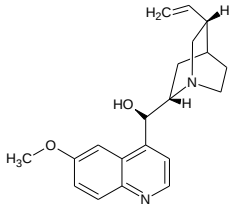
Chemical Code	Chemical structure	Antimalarial activity	Haemolytic activity
		IC_{50} value µM ± s.d.	% 100 µM ± s.d.
DR-4037		> 100 (7.20 ± 3.10)	0.41 ± 0.23
DR-4011		> 100 (2.45 ± 16.76)	0.55 ± 0.26
K480		> 100 (0.01 ± 8.49)	0.25 ± 0.08
K545		> 100 (5.13 ± 2.17)	0.25 ± 0.14
DR-3227		> 100 (5.36 ± 7.40)	0.29 ± 0.18
DR-3845		> 100 (5.77 ± 1.03)	0.36 ± 0.16
DA-IX-158		> 100 (13.53 ± 8.97)	0.25 ± 0.12
OP 35		> 100 (0.75 ± 4.67)	0.39 ± 0.11
K580		> 100 (2.25 ± 3.81)	0.42 ± 0.15
Quinine		0.15 ± 0.01 S.C. 0.18 ± 0.00 D.C.	1.22 ± 0.98

Table 5.17: The *in vitro* antimalarial (1% haematocrit, 0.5% parasitaemia) and haemolytic activity of the Phosphonoxin group of compounds. Values in parenthesis indicate the % inhibition of parasite growth at 100 µM (n = 3).

Chemical Code	Chemical structure	Antimalarial activity	Haemolytic activity
		IC_{50} value µM ± s.d.	% 100 µM ± s.d.
DR-3128		> 100 (0.01 ± 4.03)	0.31 ± 0.14
DR-3129		> 100 (0.01 ± 1.20)	0.37 ± 0.25
DR-3122		> 100 (6.97 ± 0.18)	0.36 ± 0.08
DR-3573		> 100 (12.54 ± 3.37)	0.41 ± 0.23
DR-3510		> 100 (0.01 ± 2.52)	0.39 ± 0.16
DR-4066		> 100 (36.84 ± 2.62)	0.38 ± 0.09
DR-4165		> 100 (23.65 ± 8.24)	0.39 ± 0.19
DR-3095		> 100 (6.32 ± 2.41)	0.43 ± 0.19
DR-3096		> 100 (10.15 ± 4.75)	0.48 ± 0.21

Chemical Code	Chemical structure	Antimalarial activity	Haemolytic activity
		IC_{50} value µM ± s.d.	% 100 µM ± s.d.
DR-3111		> 100 (9.59 ± 4.45)	0.29 ± 0.10
DR-3112		> 100 (3.54 ± 4.34)	0.43 ± 0.14
DR-3502-C		> 100 (0.01 ± 4.81)	0.40 ± 0.43
DR-3679		> 100 (15.20 ± 0.26) S.C. (0.01 ± 1.60) D.C.	0.34 ± 0.20
DR-3707		> 100 (6.06 ± 2.21)	0.35 ± 0.16
Quinine		0.15 ± 0.01 S.C. 0.18 ± 0.00 D.C.	1.22 ± 0.98

5.3.1.1 Antimalarial activity over a double parasitic life cycle

Of the seven active compounds assessed for improvement in antimalarial activity over a double parasitic life cycle, four exhibited statistically significant reductions ($p < 0.05$) in their IC_{50} values.

The greatest improvement was that of compound DR-4463, where a 3.3-fold reduction in its IC_{50} value occurred over a double cycle (Figure 5.6). A 1.6-, 1.4- and 1.2-fold decrease occurred in the IC_{50} values of compounds DR-3876, DR-4558 and DR-3892, respectively, over a double cycle (Figure 5.6).

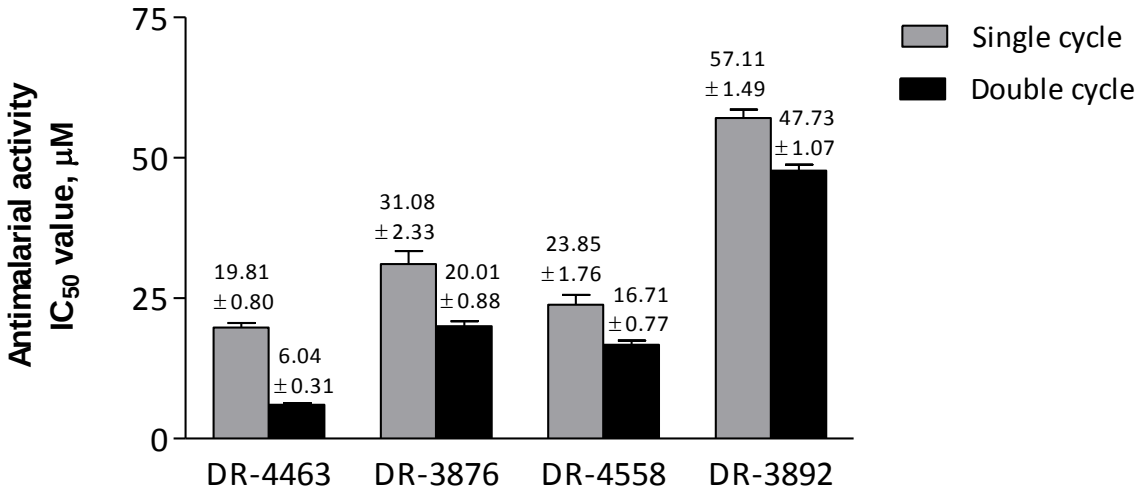


Figure 5.6: The improved antimalarial activity of compounds DR-4463, DR-3876, DR-4558 and DR-3892 over a double parasitic life cycle (n = 4).

Compound DR-3960 showed no improvement in antimalarial activity over a double cycle (Table 5.10), and compounds DR-4523 (Table 5.13) and DR-3621 (Table 5.10) exhibited minimal reductions in their IC_{50} values. None of the four inactive compounds selected showed any improvement in antimalarial activity, with compound DR-3679 exhibiting a slight decrease in activity over a double cycle (Table 5.17). Similarly, quinine exhibited no statistically significant improvement in antimalarial activity over a double cycle, showing a slight increase in its IC_{50} value over a double cycle (IC_{50} value: 0.18 ± 0.00 µM) as opposed to a single cycle (IC_{50} value: 0.15 ± 0.01 µM).

5.3.1.2 The effect of methodology on antimalarial evaluation

Of the four active compounds selected for comparison in the two methodologies, only DR-4878 showed a statistically significant difference ($p < 0.05$) in its IC_{50} value as determined by the tritiated hypoxanthine assay (24.77 ± 0.26 µM) and flow cytometric analysis (16.72 ± 0.73 µM) (Table 5.18). Of the 21 inactive compounds selected from the various structural groups for re-screening using the flow cytometric methodology, six compounds, namely DR-4598A, DR-4066, DR-4461, DR-3227, OP 35 and DR-4034, showed discrepancies between the two methodologies (Table 5.18).

Table 5.18: A comparison of the IC_{50} values and % parasite growth inhibitions, at a 2% haematocrit and 2% parasitaemia, obtained from the [^{3}H]-hypoxanthine incorporation assay and flow cytometry (n = 6). N.D. = not determined.

Compound	Antimalarial activity			
	[^{3}H]-hypoxanthine incorporation assay		Flow cytometric analysis	
	IC_{50} value (µM)	% Inhibition at 100µM	IC_{50} value (µM)	% Inhibition at 100µM
DR-4878	24.77 ± 0.26		16.72 ± 0.73	
DR-4463	28.09 ± 3.26		20.49 ± 1.41	
DR-4850	30.04 ± 2.75		29.91 ± 1.88	
D1293-S	57.29 ± 2.84		57.72 ± 3.54	
DR-4598A	> 100	30.58 ± 0.16	> 100	14.01 ± 9.70
DR-4066	> 100	16.47 ± 4.04	> 100	0.01 ± 6.29
DR-4461	> 100	12.16 ± 6.18	> 100	66.94 ± 4.35
DR-3111	> 100	9.47 ± 3.71	> 100	9.20 ± 4.20
DR-4695	> 100	9.39 ± 2.04	> 100	0.01 ± 3.47
K414A	> 100	8.61 ± 3.63	> 100	11.80 ± 3.52
DR-4028	> 100	7.95 ± 1.53	> 100	11.02 ± 5.74
K480	> 100	7.89 ± 3.02	> 100	6.93 ± 2.69
K523	> 100	7.38 ± 3.31	> 100	4.32 ± 6.75
DR-4255A	> 100	7.34 ± 0.38	> 100	0.01 ± 3.82
DR-3227	> 100	7.27 ± 4.92	> 100	28.33 ± 3.84
DR-4034	> 100	7.17 ± 5.50	> 100	21.70 ± 4.80
PipT	> 100	6.82 ± 3.95	> 100	5.68 ± 0.20
K545	> 100	6.33 ± 0.80	> 100	5.31 ± 4.45
K580	> 100	5.52 ± 2.62	> 100	1.08 ± 3.27
DR-3707	> 100	4.72 ± 2.79	> 100	9.99 ± 6.00
Pe141	> 100	4.17 ± 2.17	> 100	6.89 ± 2.09
OP 35	> 100	3.90 ± 6.25	> 100	23.44 ± 4.18
DR-3919	> 100	3.60 ± 4.08	> 100	8.46 ± 6.16
DR-4377	> 100	3.04 ± 2.49	> 100	4.48 ± 4.89
DR-4001	> 100	2.63 ± 0.56	> 100	1.46 ± 4.35
Chloroquine	0.012 ± 0.0013		0.014 ± 0.00068	
Quinine	0.15 ± 0.0014		0.058 ± 0.0026	
Dipyridamole	N.D.		35.41 ± 7.31	

5.3.2 *In vitro* haemolytic activity

The haemolytic activity of the compounds was generally low, with 78 compounds resulting in less than 1% haemolysis at 100 µM. Eleven compounds, namely DR-4137, DR-4878, DR-4850, DR-4848, DR-4463, DR-4458, DR-4459 (Table 5.11), DR-3621, DR-3960 (Table 5.10), DR-3953 (Table 5.12) and DR-4523 (Table 5.13), resulted in less than 10% haemolysis at 100

µM. Compound DR-4914B possessed the highest haemolytic activity of the compounds (50.20 ± 3.35% haemolysis at 100 µM) (Table 5.11). However, it did not appear to correlate with its antimalarial activity, as at a concentration of 50 µM, corresponding to the IC_{90} value of DR-4914B (51.67 ± 4.16 µM), the haemolytic activity was greatly reduced to 0.71 ± 0.16%.

5.3.3 Combination studies

The isobolograms depict the variable pharmacological interactions between compound DR-4463 in combination with quinine, as well as compounds DR-4463 and D1293-S in combination with the nucleoside transport inhibitor, dipyridamole (Figure 5.7).

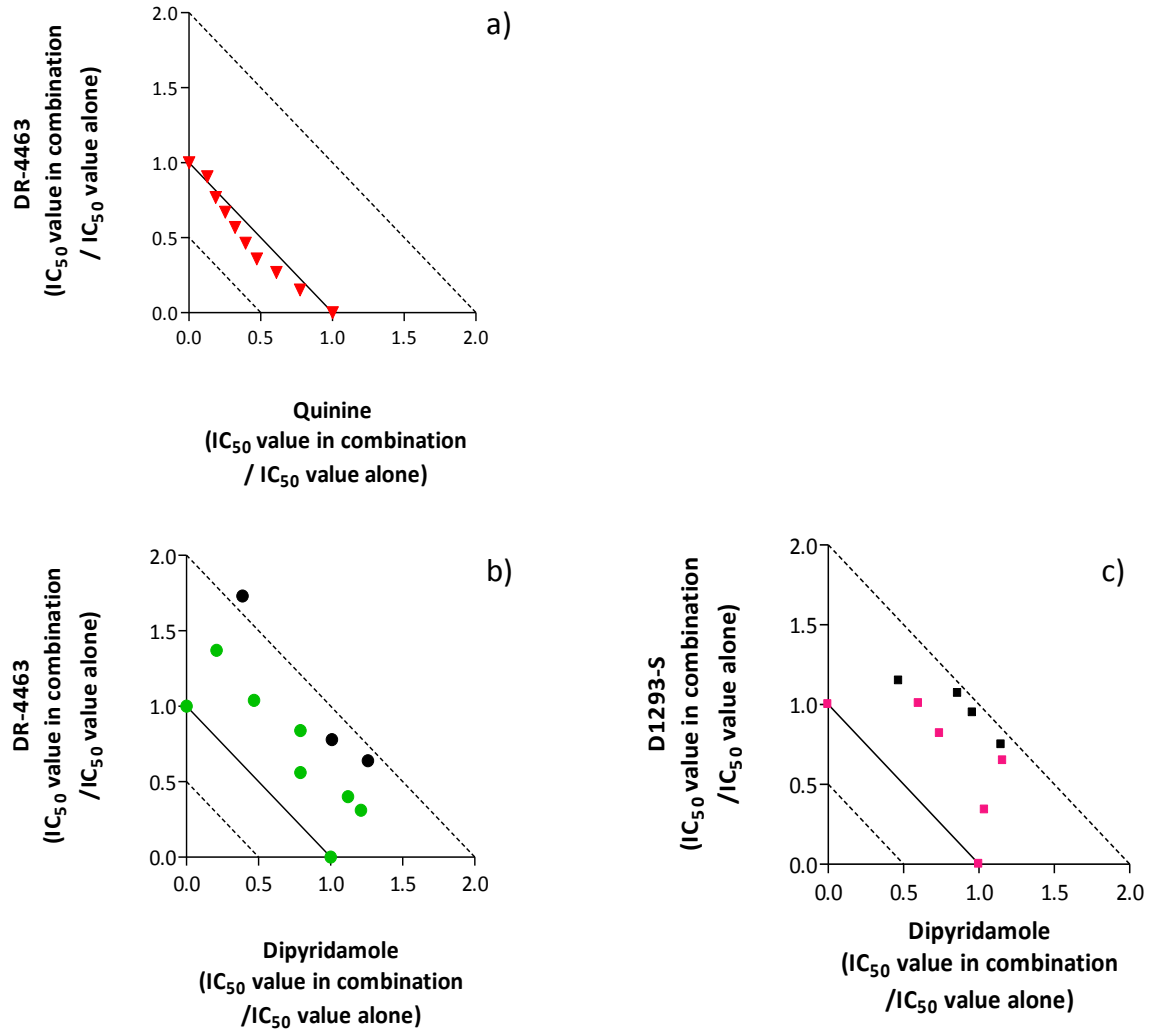


Figure 5.7: Isobolograms depicting the pharmacological interactions of compound DR-4463 in combination with quinine (a) (n = 3), as well as compounds DR-4463 (b) (n = 4) and D1293-S (c) in combination with dipyridamole (n = 3).

The ΣFIC for each experiment was calculated from FIC values generated for each data point (Appendix E). Compound DR-4463, when combined with quinine, exhibited an additive interaction (ΣFIC = 0.89 ± 0.12) (Figure 5.7a), and when combined with dipyridamole exhibited an additive-antagonistic to antagonistic relationship (ΣFIC = 1.83 ± 0.17), with the greatest antagonism observed in combination ratios of dipyridamole to DR-4463 of IC_{50}:IC_{90}, IC_{50}:IC_{10}, as well as IC_{10}:IC_{10} (Figure 5.7b). Similarly, combinations of compound D1293-S and dipyridamole also exhibited an additive-antagonistic to antagonistic interaction (ΣFIC = 1.87 ± 0.34), with the greatest antagonism observed at the ratios of IC_{50}:IC_{90} , IC_{50}:IC_{10}, IC_{90}:IC_{90}, as well as IC_{10}:IC_{10} (Figure 5.7c).

5.3.4 Morphological and stage-specific effects of compound DR-4463

The morphological and stage-specific effects of compound DR-4463 at its IC_{50} value (20 µM), when compared to an untreated control, are depicted in Figures 5.8 and 5.9. No notable changes in parasite morphology occurred during the ring-stage, with the treated parasites progressing into the early trophozoite-stage (Figure 5.9A), where haemozoin crystals were evident (Figure 5.8A). Thereafter, treated parasites progressed through the mid to late trophozoite-stage (Figure 5.9B) with no distinct morphological changes (Figure 5.8B). However, upon progression into the schizont-stage, development of the treated parasites appeared to be slightly stalled, with most parasites appearing to be in the late trophozoite- and early schizont-stages instead of the early to mid schizont-stage as in the untreated control (Figure 5.9C), and with no distinct merozoite formation as noted in the untreated control (Figure 5.8C).

Thereafter, the untreated parasites progressed into the late schizont- and early ring-stages (Figure 5.9D), with 71% of parasites in the ring-stage and 29% of parasites in the late schizont-stage (Figure 5.8D), to produce an overall parasitaemia of 4.81%. In contrast, the total parasitaemia of the treated parasites was 2.4%, and appeared to be stalled predominantly in the late trophozoite- (40%) and mixed early to late schizont-stages (32%) (Figure 5.9D), with late trophozoite-staged parasites exhibiting signs of possible cytoplasmic vacuolation (Hamzah *et al*., 2004; Totino *et al*., 2008) (Figure 5.8D).

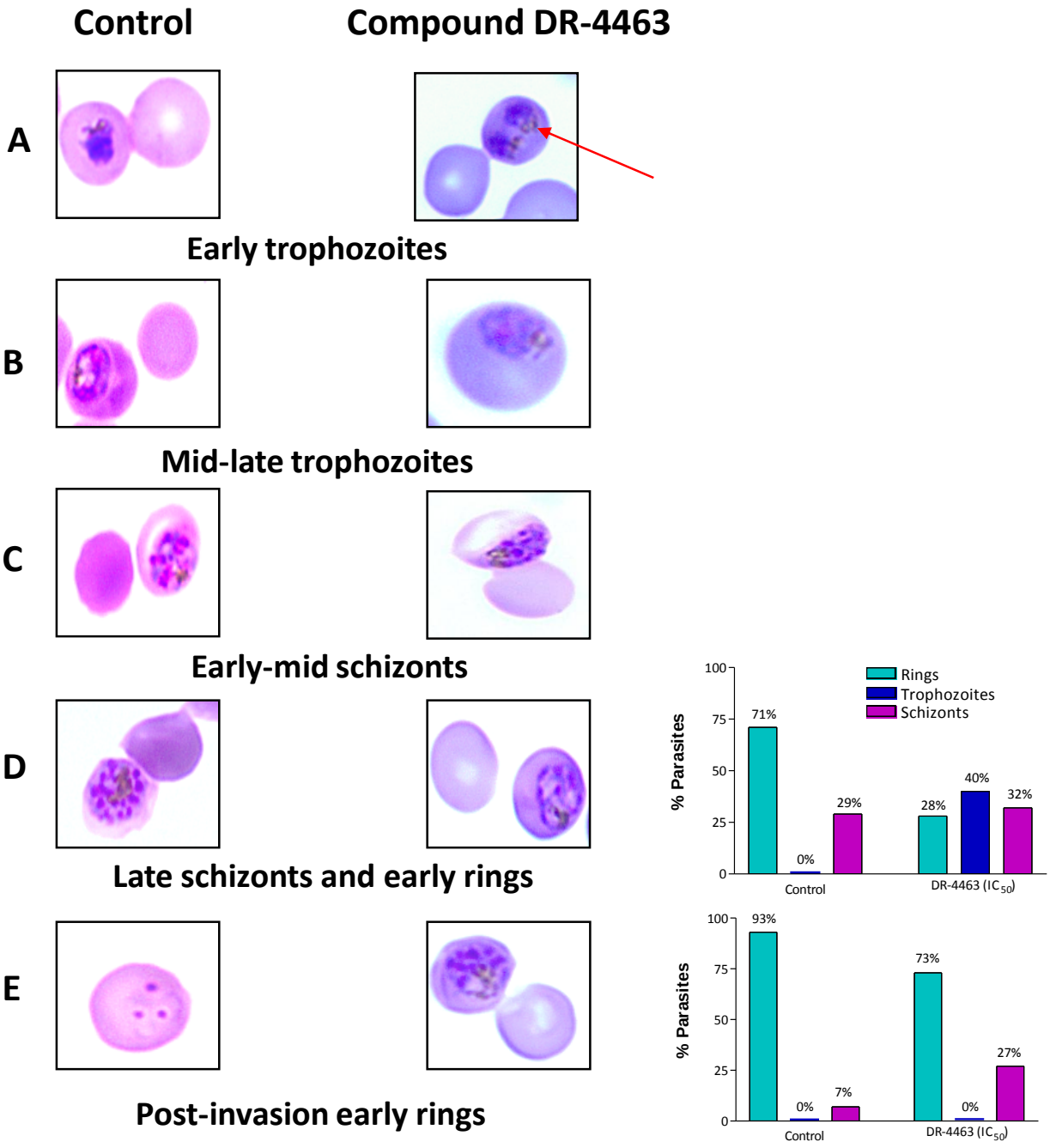


Figure 5.8: The effects of compound DR-4463 at the IC_{50} value (20µM) on parasite morphology and development. Red arrows indicate parasitic haemozoin (n = 1).

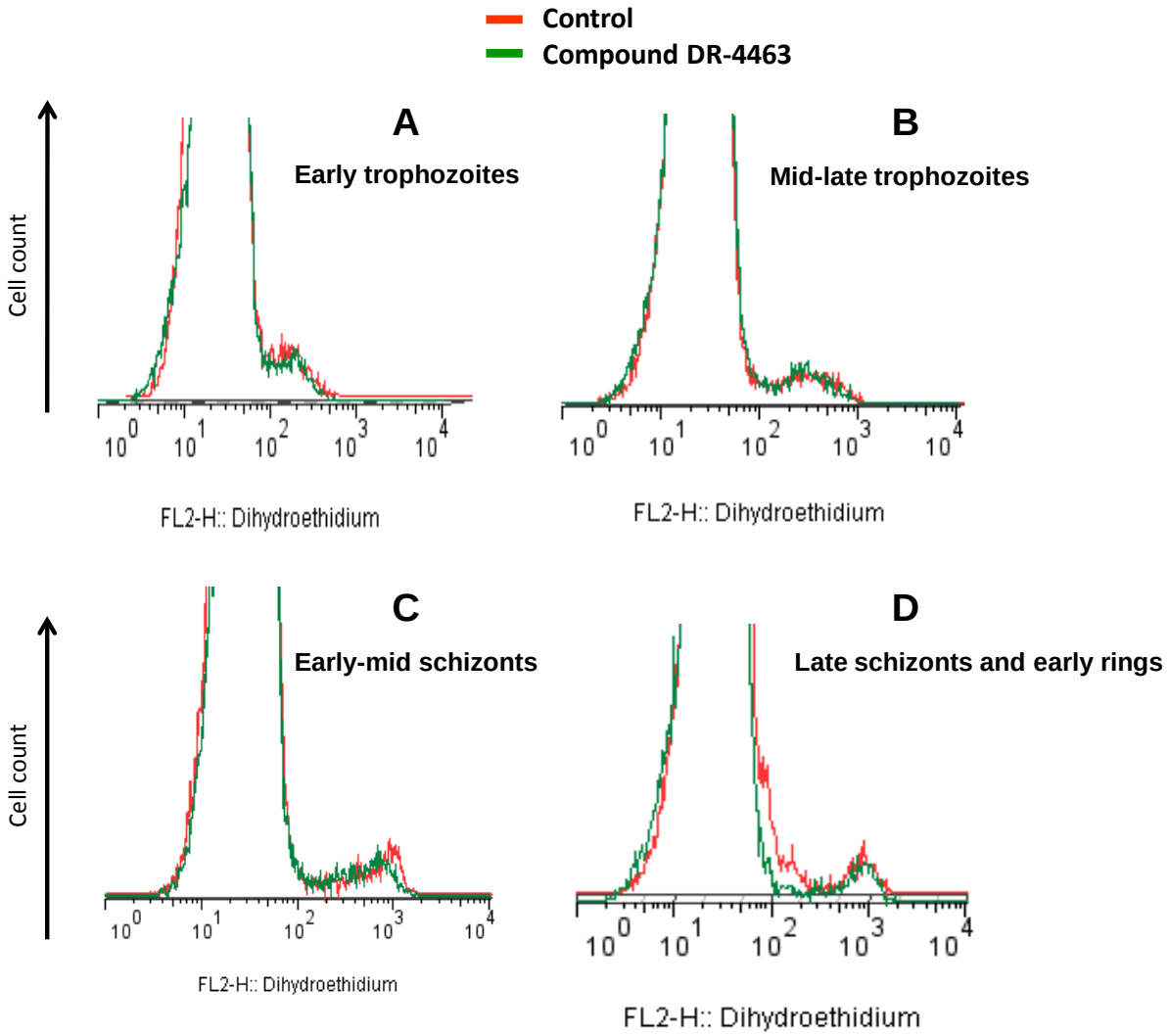


Figure 5.9: Flow cytometric analysis depicting the effects of compound DR-4463, at the IC_{50} value (20 µM), on parasite development. Where: FL2-H represents the maximum fluorescent intensity of dihydroethidium, the green line represents parasites treated with compound DR-4463 and the red line represents the parasite control (n = 1).

Examination of the blood smears four hours post-invasion, or four hours into the next cycle showed the overall parasitaemia of the treated parasites to be 3.51%, as opposed to the parasitaemia of 7.45% of the untreated control. The majority of the parasites were in the ring-stage (73%), with the remainder in the schizont-stage (27%), as opposed to the untreated control, where 93% of parasites were in the ring-stage, and 7% were in the late schizont-stage (Figures 5.8E). Of the schizonts present in the treated parasite

sample, distinct merozoite formation was noticeable (Figure 5.8E), however the number of merozoites formed appeared to be greatly reduced from the untreated control of Figure 5.8D. The increase in the percentage of ring-staged parasites indicated that the schizonts (Figure 5.8D) had progressed through the cycle, and were capable of reinvading red blood cells.

Parasites treated with compound DR-4463 at the IC_{25} value (10 µM) exhibited similar developmental abnormalities as those treated with compound DR-4463 at the IC_{50} value. However, an examination of blood smears prepared four hours post-invasion showed that the number of merozoites formed by treated parasites appeared similar to that of the parasite control of Figure 5.8D.

5.3.5 Antimalarial mechanisms of action

The effects of select compounds on β-haematin formation, as well as anti-oxidant and metal chelating activity were determined (Table 5.19). A total of 35 compounds were selected from the various structural groups, in order to examine structure-activity relationships. Of the 14 compounds possessing antimalarial activity, five were potent inhibitors of β-haematin formation, and showed significant differences ($p < 0.05$) in their activity when compared to chloroquine (IC_{50} value: 29.64 ± 3.35 µM) (Table 5.19). Compound DR-4137 proved to be the most potent (IC_{50} value: 8.29 ± 1.11 µM), and was 3.6-fold more active than chloroquine. Compounds DR-4458, DR-4459, DR-4463 and DR-3621 proved to be on average twice as active as chloroquine. Compounds DR-4523, DR-4878 and DR-4914B were capable of inhibiting more than 75% of β-haematin formation at 400 µM; however their IC_{50} values were well above 100 µM (Table 5.19). The remaining six compounds inhibited β-haematin formation by between 13% and 53% at 400 µM. Of the 21 compounds which lacked antimalarial activity, compound DR-4598A was noted to be a strong inhibitor of β-haematin formation (IC_{50} value: 9.19 ± 0.39 µM), and was 3.2-fold more potent than chloroquine. The remaining 20 compounds, as well as dipyridamole, were only capable of between 0.01% and 46% inhibitory activity at 400 µM (Table 5.19).

Table 5.19: The β-haematin inhibitory, free-radical scavenging, and iron chelating activity of select compounds. Values in parenthesis indicate where IC_{50} values (< 100 μM) were obtained (n = 5). N.D. = not determined.

Compound	% Inhibition of β-haematin formation at 400 μM (± s.d.)	% DPPH$^{\bullet}$ free-radical scavenging activity at 240 μM (± s.d.)	% Fe(II) chelation at 200 μM (± s.d.)
DR-4137	(8.29 ± 1.11)	5.55 ± 2.30	N.D.
DR-4598A	(9.19 ± 0.39)	0.01 ± 2.16	12.00 ± 3.35
DR-4458	(10.77 ± 1.12)	25.26 ± 3.16	1.51 ± 0.34
DR-4459	(11.39 ± 1.71)	29.62 ± 2.47	N.D.
DR-4463	(13.39 ± 2.16)	13.85 ± 1.03	N.D.
DR-3621	(13.95 ± 0.65)	5.03 ± 1.95	4.67 ± 1.24
DR-4523	97.30 ± 2.78	4.89 ± 2.53	0.01 ± 6.53
DR-4878	75.74 ± 4.80	0.01 ± 4.53	1.33 ± 0.83
DR-4914B	75.57 ± 7.68	23.43 ± 2.06	3.64 ± 2.90
DR-4850	53.31 ± 9.15	31.60 ± 5.34	4.80 ± 1.05
DR-3876	47.72 ± 7.27	N.D.	N.D.
DR-4461	46.10 ± 7.91	6.32 ± 1.72	2.43 ± 2.00
DR-4001	42.70 ± 10.01	0.01 ± 4.25	6.72 ± 3.14
DR-3919	38.42 ± 10.10	0.01 ± 2.13	3.69 ± 3.43
DR-4848	34.43 ± 5.43	N.D.	N.D.
K414_A	31.99 ± 8.76	12.47 ± 1.64	34.86 ± 8.44
DR-4558	27.27 ± 4.20	N.D.	N.D.
D1293-S	15.49 ± 5.17	N.D.	N.D.
DR-4028	14.38 ± 3.53	0.01 ± 4.51	7.19 ± 2.18
DR-3641	13.22 ± 5.33	N.D.	N.D.
DR-3111	11.94 ± 2.62	0.01 ± 4.35	5.37 ± 2.62
OP 35	11.81 ± 0.64	7.66 ± 5.78	1.02 ± 1.06
DR-4695	10.50 ± 2.42	21.13 ± 2.76	3.77 ± 2.15
K580	9.56 ± 2.86	0.01 ± 3.16	2.20 ± 1.52
K545	6.93 ± 2.76	3.60 ± 1.09	2.36 ± 2.04
PipT	6.75 ± 4.52	4.03 ± 2.69	2.40 ± 1.05
K523	6.25 ± 4.06	0.01 ± 2.29	0.01 ± 1.71
DR-3227	6.15 ± 2.43	11.07 ± 0.87	0.01 ± 4.30
DR-4034	5.25 ± 4.89	3.48 ± 1.50	2.34 ± 0.94
DR-3707	3.13 ± 2.14	0.01 ± 3.70	12.85 ± 2.69
Pe141	1.17 ± 0.23	0.01 ± 4.04	2.20 ± 1.94
DR-4377	0.01 ± 12.81	3.25 ± 0.80	1.35 ± 1.05
DR-4255A	0.01 ± 10.54	9.35 ± 1.44	7.50 ± 3.03
K480	0.01 ± 7.14	2.50 ± 1.09	0.01 ± 1.50
DR-4066	0.01 ± 5.75	0.01 ± 3.59	3.01 ± 2.00
Dipyridamole	21.75 ± 9.92	2.30 ± 0.75	0.01 ± 3.26
Chloroquine	(29.64 ± 3.35 μM)	0.31 ± 3.28	70.68 ± 0.97
Quinine	(63.00 ± 3.27 μM)	2.53 ± 1.17	0.01 ± 6.08
EDTA	N.D.	N.D.	(23.90 ± 1.83 μM)
Ascorbic acid	N.D.	(19.31 ± 2.62 μM)	N.D.

None of the 35 compounds, as well as dipyridamole, exhibited free-radical scavenging or iron chelating activity comparable to the respective controls, ascorbic acid (IC_{50} value: 19.31 ± 2.62 µM) and EDTA (IC_{50} value: 23.90 ± 1.83 µM). With free-radical scavenging activity ranging from 0.01% to 32% at 240 µM and iron chelating activity ranging from 0.01% and 35% at 200 µM (Table 5.19).

5.4 Discussion

The antimalarial activity of the nucleoside phosphonates, phosphonic acids and purine/pyrimidine derivatives tested in this study exhibited variable antimalarial activity, not only between the various structural groups, but also within the groups (Tables 5.10-5.17; Figure 5.10).

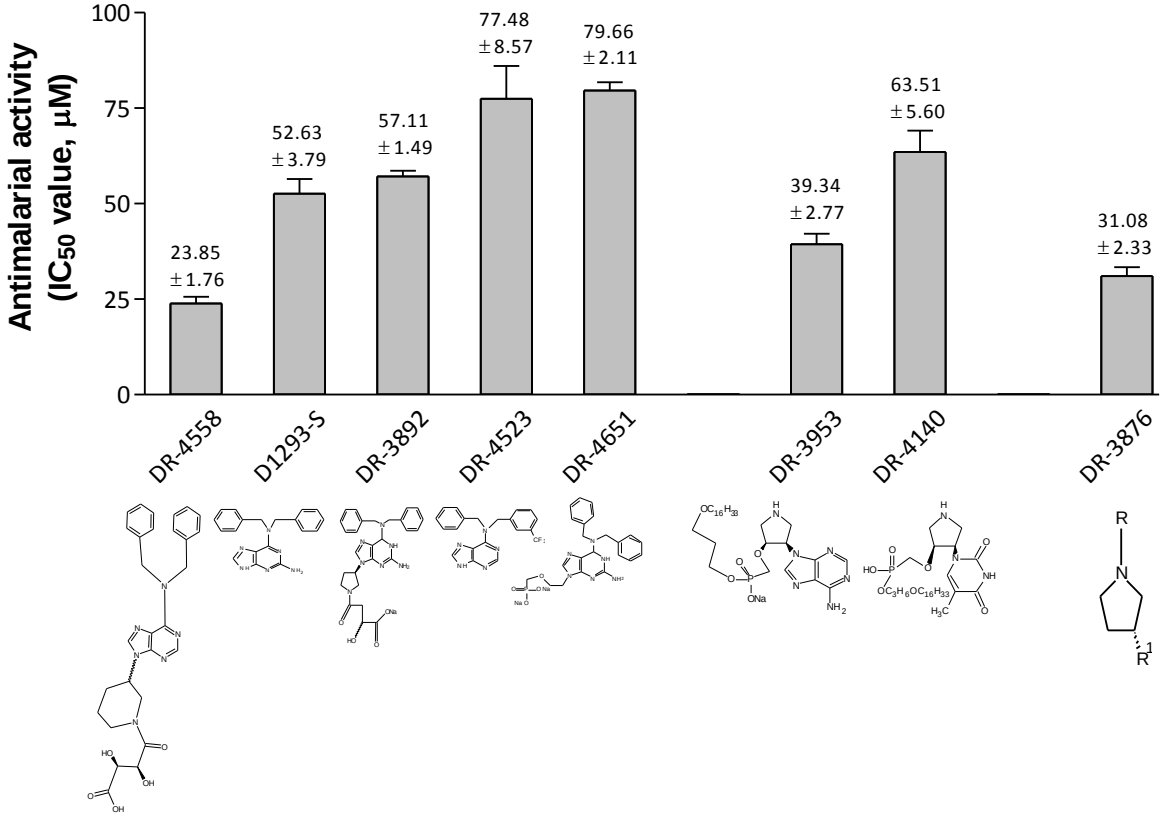


Figure 5.10: Active antimalarial compounds of the Mickey Mouse, PyrroPME and pyrrolidine nucleotide groups.

When examining the general antimalarial activity of the various structural groups, it can be seen that the Lipophosphonoxin and Nucleoside lipophosphonate groups had the best antimalarial activity, producing 11 of the active compounds, with IC_{50} values ranging between 10 µM and 50 µM (Tables 5.13 and 5.14). Followed by the Mickey Mouse, PyrroPME, and Pyrrolidine nucleotide groups which had five, two, and one active compound(s), all producing one drug with an IC_{50} value of less than 50 µM (Figure 5.10).

The Piperidine nucleoside and nucleotide, Aza sugar, U/T Miscellaneous, Miscellaneous, and Phosphonoxin groups exhibited disappointing antimalarial activity; with compounds of these groups only capable of inhibiting parasite growth at 100 µM by a maximum of 43.57 ± 0.48%, 2.19 ± 5.42%, 5.87 ± 1.54%, 7.20 ± 3.10%, 13.53 ± 8.97% and 36.84 ± 2.62%,respectively (Tables 5.15-5.17).

In contrast, an examination of the antiprotozoal effects of Phosphonoxins against *Giardia*, the protozoa responsible for the majority of reported waterborne-associated cases of diarrhoea in the United States, showed that compound DR-3510 was as active as existing therapeutics against the WB-6 strain of *Giardia lamblia* (Suk *et al*., 2007). The activity of this Phosphonoxin was attributed to the chelation of metal ions, most likely calcium, which are proposed to be at the active site of the cyst wall synthase enzyme, thereby inhibiting trophozoite cyst wall formation (Suk *et al*., 2007). The metal chelating activity was attributed to donor groups in the aminoalkylphosphonate moiety, speculating that the 2-carbon linker between the amino and phosphonate moieties allowed for the correct conformation for chelation of the metal ion (Suk *et al*., 2007). However, in this study, the linker between the amino and phosphonate moieties appeared to play no role in antimalarial activity, with compounds of the Phosphonoxin group possessing the 2C linker displaying no antimalarial activity (Table 5.17). Additionally, when tested for their ability to chelate Fe(II), none of the Phosphonoxins displayed any metal chelating activity (Table 5.19).

What did appear to play a role in antimalarial activity was the attachment of a bulky ($C_{16}H_{33}$) aliphatic side chain to the phosphonate group, with a comparison of the Phosphonoxin (Table 5.17) and Lipophosphonoxin (Table 5.11) groups showing that they exhibited strong structural similarities, with the only difference lying in the addition of

this side chain. A study conducted by Rejman *et al*. (2011) showed that the addition of the aliphatic side chain to the Phosphonoxin group, to produce Lipophosphonoxins (Figure 5.11), resulted in substantially increased antibacterial activity (Rejman *et al*., 2011). It was concluded that the negative charge of the phosphonate group of Phosphonoxins hampered cellular uptake, whilst the addition of the aliphatic side chain facilitated cellular uptake (Rejman *et al*., 2011).

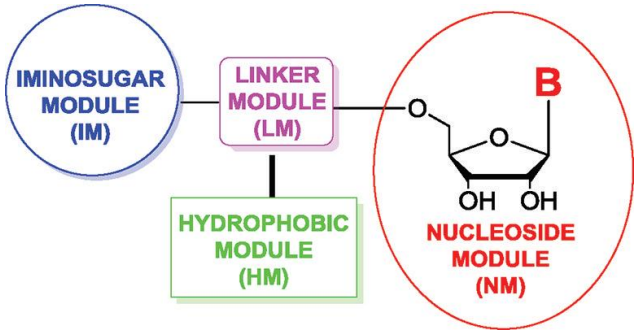


Figure 5.11: The general structure of the Lipophosphonoxin group of compounds (Rejman *et al*., 2011).

This substitution appeared to confer antimalarial activity to the Lipophosphonoxin group of compounds, with IC_{50} values ranging from 13 µM to 49 µM, as when the side chain was shortened, or substituted with other moieties, the antimalarial activity was lost. This was observed with compounds DR-4658, DR-4695 and DR-4696 (0.01 ± 2.61%, 0.01 ± 1.62% and 2.16 ± 1.61% inhibition of parasite growth at 100 µM, respectively) (Table 5.11). Similarly, Rejman *et al*. (2011) found that when the aliphatic side chain was shortened, as was the case with compound DR-4658, antibacterial activity was abolished. They also found that compounds DR-4878 and DR-4463, both having the bulky side chain substitution, showed some of the most significant antibacterial activity, with these compounds also exhibiting some of the best antimalarial activity in this study.

The heterocyclic substitution attached to the Phosphonate group appeared to not play a role in the antimalarial activity of the compounds, as the Nucleoside Lipophosphonoxin group (Table 5.10) lacked this substitution, yet still retained antimalarial activity similar to that of the Lipophosphonoxins. The substitution that did appear to play a role in antimalarial activity was the hydroxyl group on the heterocyclic ring. A comparison of

the structures of compounds DR-4458 and DR-4459 showed that the addition of an extra hydroxyl group on the heterocyclic ring resulted in a 1.6-fold decrease in the IC_{50} value (Table 5.11). The orientation of the hydroxyl groups also appeared to play a role, with compounds DR-4850 (IC_{50} value: 13.35 ± 0.38 µM) and DR-4914B (IC_{50} value: 21.07 ± 0.71 µM) having identical chemical structures with the exception of the orientation of these groups on the heterocyclic ring (Table 5.11). The bond orientation of the hydroxyl groups on the pyrrolidine ring also appeared to play a role in the haemolytic activity of the compounds, with compound DR-4850 exhibiting 9.25 ± 2.08% haemolysis at 100 µM compared to 50.20 ± 3.35% for compound DR-4914B (Table 5.11).

The base composition of the compounds appeared to play a role in the antimalarial activity of the Lipophosphonoxins. Although the structures of compounds DR-4137 and DR-4850 were almost identical, the base attached to the ribose moiety was uracil in compound DR-4137 and guanine in compound DR-4850. This resulted in the 3.7-fold decrease in antimalarial activity observed in compound DR-4137 (Table 5.11). Similarly, the only difference between compounds DR-4914B and DR-4848 was that compound DR-4914B had a guanine base, and compound DR-4848 a modified cytosine base, resulting in compound DR-4914B being 1.5-fold more active than compound DR-4848 (Table 5.11).

Overall, the base composition of the compounds did not appear to be the determinant of antimalarial activity, with the three most active compounds (DR-4850, DR-4878 and DR-4463) having guanine, cytosine and uracil bases, respectively (Table 5.11). Similarly, the base composition of the Nucleoside Lipophosphonates was not a determinant of antimalarial activity, with compounds DR-3641, DR-3621 and DR-3960 having adenine, uracil and guanine bases, respectively (Table 5.10). When examining the structure of compound DR-3641, which had the highest IC_{50} value (43.14 ± 1.67 µM) of the three Nucleoside Lipophosphonates, the ribose moiety was dehydroxylated at the 3’ position of the ribose moiety (Table 5.10).

An examination of the PyrroPME group showed that the only two active compounds in this group possessed the same bulky aliphatic side chain attachment to the phosphonate group (Figure 5.10; Table 5.12). The base composition did not play a role in the

antimalarial activity of the compounds in this group. Compounds DR-3919 and DR-3945 were identical, except that DR-3919 had an adenine base and DR-3945 a thymine base, yet both displayed no antimalarial activity (Table 5.12). However, upon replacement of the hydroxyl group of compound DR-3919 with a bulky aliphatic side chain to produce compound DR-3953, the antimalarial activity was greatly improved (IC_{50} value: 39.34 ± 2.77 µM). A similar trend was observed when comparing compound DR-3945 to compound DR-4140 (IC_{50} value: 63.51 ± 5.60 µM) (Table 5.12).

Structural analysis of the Mickey Mouse group (Table 5.13) showed that the phosphonic acid derivatives exhibited no antimalarial activity; with the exception of compound DR-4651, which exhibited poor antimalarial activity (IC_{50} value: 79.66 ± 2.11 µM) (Figure 5.10; Table 5.13). When comparing the structures of compounds DR-4651, DR-4598A, DR-4640 and DR-4599A, all exhibit structural similarities, with the exception that compound DR-4651 had an amino group at the C^2 position on the purine ring and contained an ethyloxymethyl linker between the purine ring and phosphonic acid moiety. Whereas compounds DR-4598A and DR-4640 contained propyl and butyl linkers, respectively (Table 5.13). A comparison of compounds DR-4541 and DR-4523 showed that the attachment of a trifluoromethyl group at the C^3 position of the purine ring conferred weak antimalarial activity to compound DR-4523 (IC_{50} value: 77.48 ± 8.57 µM). However, upon addition of a phosphonic acid group via an ethyloxymethyl linker, the antimalarial activity was abolished, as observed in compound DR-4541 (14.26 ± 4.63% inhibition at 100 µM) (Table 5.13). A comparison of the chemical structures of compounds DR-3892 (IC_{50} value: 57.11 ± 1.49 µM) and DR-3898 (2.50 ± 3.32% inhibition at 100 µM), which were the same except DR-3892 was an oxobutanoic acid derivative and DR-3898 a phosphonic acid derivative. This indicates that the oxobutanoic acid moiety appeared to confer antimalarial activity, whereas the phosphonic acid moiety abolished it (Table 5.13).

Compounds D1293-S, Bn_2.NH.HCl and DR-4461 are closely related to each other, where compound DR-4461 is a composition of compounds D1293-S and Bn_2.NH.HCl in a 1:10 ratio. It can be seen that the dibenzylamine (Bn_2.NH.HCl) component exhibits no antimalarial activity on its own (12.57 ± 4.88% inhibition of parasite growth at 100 µM);

whilst the addition of compound D1293-S to produce compound DR-4461 slightly increased the antimalarial activity (33.87 ± 6.76% inhibition of parasite growth at 100 µM) (Table 5.13). Which was expected since compound D1293-S on its own exhibited moderate antimalarial activity (IC_{50} value: 52.63 ± 3.79 µM) (Table 5.13).

Of the Pyrrolidine nucleotide group, only compound DR-3876 exhibited antimalarial activity (IC_{50} value: 31.08 ± 2.33 µM) (Figure 5.10). When comparing compounds DR-3616, Pe141 and DR-3876, the latter differed from the other two in that it contained a guanine base, whilst the others contained an adenine base, with no hydroxyl group on the pyrrolidine ring, and it possessed a methyl linker between the phosphonic acid and carbonyl groups (Table 5.14). However, these structural modifications did not greatly improve its activity over a double parasitic life cycle, only contributing to a 1.6-fold decrease in the IC_{50} value (Figure 5.6). When tested for activity against human purine nucleoside phosphorylase, the enzyme responsible for catalysing the formation of hypoxanthine from inosine and the cleavage of guanine and hypoxanthine nucleosides to form the corresponding base and sugar phosphate, D. Rejman and co-workers found that two compounds were potent inhibitors of this enzyme, one of which was structurally similar to compound DR-3876 (D. Rejman; unpublished observations). In this respect, compound DR-3876 may have acted to inhibit human purine nucleoside phosphorylase present in the erythrocyte cytosol. However, inosine metabolism would still occur, following its transport into the parasite cytosol by *Pf*ENT1, and then via the *P. falciparum* purine nucleoside phosphorylase enzymes (Hyde, 2007; Downie *et al*., 2008; Riegelhaupt *et al*., 2010).

When comparing compounds K584, K578 and DR-4028, the latter compound was hydroxylated on the pyrrolidine ring and contained a bromo-substitution on its uracil base (Table 5.14). However, the bromo-substitution did not improve antimalarial activity, with compound DR-4028 exhibiting a similar lack of antimalarial activity as seen for compounds K584 and K578 (Table 5.14).

In contrast, the Piperidine nucleoside and nucleotide group produced no active compounds, regardless of the various structural differences between the compounds (Table 5.15). However, when comparing the Piperidine nucleosides, compounds DR-

4377 and DR-4513, which are identical, except for the adenine base of compound DR-4513 and uracil base of DR-4377. It was observed that compound DR-4513 exhibited slightly better inhibitory activity (43.57 ± 0.48 % growth inhibition at 100 µM) when compared to compound DR-4377 (0.01 ± 1.31% growth inhibition at 100 µM) (Table 5.15). Similarly, the Aza sugar, U/T miscellaneous and Miscellaneous group of compounds displayed no antimalarial activity despite structural variations, such as the hydroxylation of piperidine/pyridine rings and attachment of sulphur-containing heterocyclic groups (Table 5.16).

Derivatives of acyclic nucleoside phosphonates, prodrugs of the triphosphate inhibitors of DNA replication, have previously been shown to exhibit potent antimalarial activity. The most active of which, an adenine derivative, exhibited antimalarial activity in the low micromolar concentration range (IC_{50} value: 0.18 ± 0.07 µM) against the K1 strain of *Plasmodium falciparum* (Smeijsters *et al*., 1999). The antimalarial activity of these compounds was attributed to the inhibition of plasmodial DNA polymerases, thereby acting as DNA chain terminators (Smeijsters *et al*., 1999). It does not appear as if the compounds tested in this study acted in a similar manner, due to the fact that the activity of nucleoside phosphonate/phosphonic acid derivatives containing pyrimidine bases (Tables 5.10-5.15, 5.17) were comparable to those containing the purine ring structure (Table 5.13) or purine base (Tables 5.10-5.17). With Smeijsters *et al*. (1999) reporting that pyrimidine analogues of acyclic nucleoside phosphonates were inactive at concentrations exceeding 250 µM, which is validated by the fact that the parasite does not incorporate exogenous pyrimidines into its DNA (Parker *et al*., 2000; Hyde, 2007). Moreover, if the compounds acted by incorporation into parasitic DNA, a much lower IC_{50} value would be expected (< 1 µM), together with a greater difference between IC_{50} values in the double versus single cycle of parasite growth (Figure 5.6).

Select compounds from the Phosphonoxin, Piperidine nucleoside and nucleotide, Aza sugar, U/T Miscellaneous, Miscellaneous, Nucleoside Lipophosphonate, PyrroPME, Mickey Mouse and Pyrrolidine nucleotide groups (Table 5.20) were screened against the cancerous white blood cell lines, L1210 (murine lymphocytic leukaemia), HL60 (human acute promyelocytic leukaemia), CCRF-CEM (human acute lymphoblastic leukaemia); as

well as an epithelial cancer cell line HeLa S3 (human adenocarcinoma), by a collaborative laboratory.

Table 5.20: The compounds tested for cytotoxicity (D. Rejman; personal communication).

Group name	Compounds
Phosphonoxin	DR-3573, DR 3679, DR3707
Piperidine nucleoside and nucleotide	DR-3994, PipT
Aza sugars, U/T Miscellaneous and Miscellaneous	K469, DR-4034, K470 DR-4031, K479, DR-4030 DR-4037, DR-4011, K480 DR-3227, DR-3845
Lipophosphonate	DR-4696, DR-4878, DR-4463
Nucleoside Lipophosphonate	DR-3641, DR-3621, DR-3960
PyrroPME	DR-3953, DR-3919, DR-3945 DR-3769, DR-4001
Mickey Mouse	DR-3892, DR-3896, DR-3898
Pyrrolidine Nucleotide	DR-3876, DR-4028, DR-3616

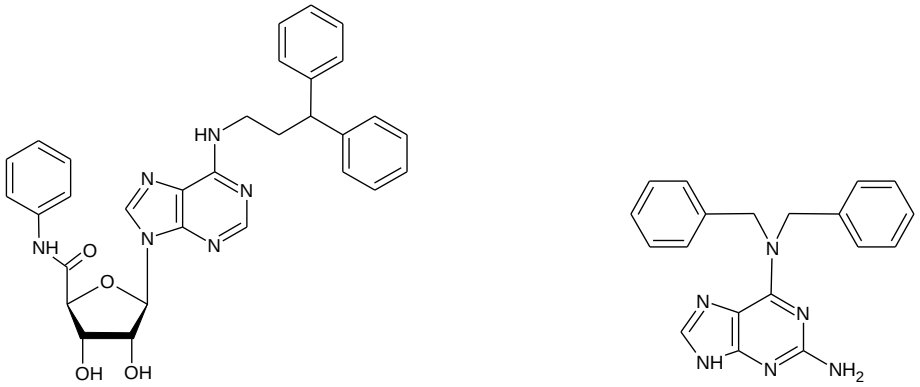
Of the compounds screened for cytotoxicity that possessed antimalarial activity (DR-3641, DR-3621, DR-3960, DR-3953, DR-3892 and DR-3876), only compound DR-3621 exhibited any cytotoxicity when screened at a concentration of 10 µM, inhibiting cell growth at IC_{50} values of 15.72 ± 0.87 µM, 14.10 ± 0.77 µM, 14.44 ± 0.14 µM and 13.90 ± 0.19 µM against the L1210, HL60, CCRF-CEM and HeLa S3 cell lines, respectively (D. Rejman; personal communication).

Similarly, none of the Lipophosphonates tested for cytotoxicity against erythroid progenitor cells (Table 5.20), derived from human umbilical cord blood, exhibited potent effects on cell viability, but did induce low levels of apoptosis (Rejman *et al*., 2011). The lack of appreciable anticancer activity or effects on cell viability on normal cells would then indicate that these compounds, with the possible exception of compound DR-3621, do not act to inhibit DNA replication even in mammalian cells. Unlike the triphosphate forms of 6-mercaptopurine and 6-thioguanine that are incorporated into RNA or DNA, thereby acting as chain terminators, that have IC_{50} values in the low micromolar range against the HEK293 (transformed human embryonic kidney) cell line (Wielinga *et al*., 2002). However, none of the compounds, with the exception of compound DR-4914B

(50.20 ± 3.35 % haemolysis at 100 µM; Table 5.11), displayed toxicity against the host red blood cell (Tables 5.10-5.17). Possibly indicating that the activity of the compounds was as a result of a direct effect on the parasite by mechanisms other than inhibition of DNA polymerase enzymes.

Thirteen (Tables 5.10-5.12) of the nineteen active compounds exhibited amphipathic properties and may have been capable of permeating cell membranes, in a similar manner to dipyridamole and amantadine. Amantadine is a primary amine used to treat and prevent Influenza A, but displays antimalarial activity in the micromolar concentration range against the chloroquine-resistant (FCR-3) strain of *P. falciparum* (Evans and Havlik, 1993).

Whilst the remaining six active compounds (Tables 5.16 and 5.17) were modified purine bases, which may have inhibited nucleoside transport by *Pf*ENT1 in a manner similar to NBMPR, which inhibits human equilibrative nucleoside transporters in mammalian cells (Akaki *et al*., 2002; Lin and Buolamwini, 2007). In this respect, the mechanism of action of these compounds may lie in their ability to inhibit the transport of nucleosides. N^6-Diphenylethyl-5'-phenyl-carboxamidoadenosine (Figure 5.12a), a nucleoside derivative bearing a similar modified purine base to that of compound D1293-S (IC_{50} value: 52.63 ± 3.79 µM; Table 5.13), has been shown to inhibit the growth of a chloroquine-resistant strain of *P. falciparum* (IC_{50} value: 1.8 µM), with its mechanism of action attributed to the inhibition of *Pf*ENT1 (Rodenko *et al*., 2006). However, the 25-fold difference in activity between N^6-Diphenylethyl-5'-phenyl-carboxamidoadenosine and compound D1293-S pointed to the fact that D1293-S may not have acted to inhibit *Pf*ENT1.



a) b)

Figure 5.12: The chemical structures of a) N^6-diphenylethyl-5'-phenyl-carboxamidoadenosine (Rodenko *et al*., 2006) and b) compound D1293-S.

In order to determine whether compound D1293-S did in fact act to inhibit *Pf*ENT1, it was selected, together with the amphipathic uridine phosphonate derivative, compound DR-4463 (Table 5.11), for combination studies with dipyridamole, a known *Pf*ENT1 inhibitor (Section 5.3.3). In both cases, an additive-antagonistic to antagonistic interaction was observed (Figure 5.7 b and c; Appendix E). An antagonistic interaction between two drugs may point to the fact that both drugs were competing for activity on the same target, or that binding of one drug to the transporter was inhibiting the uptake of the other (Bell, 2005).

However, in this case, the noted antagonism did not appear to be due to compounds DR-4463 and D1293-S acting on the same target as dipyridamole. Examination of blood smears of parasites treated with compounds DR-4463 and D1293-S showed that parasite development was affected primarily in the schizont-stage, whereas examination of dipyridamole-treated parasites showed that parasite development was halted in the early trophozoite-stage, which is similar to parasites carrying a disrupted *Pf*ENT1 gene (El Bissati *et al*., 2006). This interference in stage progression by dipyridamole would be expected, since the gene expression of nucleoside transporters begins in the ring-stage with maximal expression at 32 hours into the parasitic cycle (Martin *et al*., 2005; El Bissati *et al*., 2006). The poor antimalarial activity of compound D1293-S (IC_{50} value:

52.63 ± 3.79 µM) (Table 5.13) compared to that of N^6-diphenylethyl-5'-phenyl-carboxamidoadenosine may possibly have been due to the fact that Rodenko *et al*. (2006) attributed the *Pf*ENT1 inhibitory activity of the 5'-carboxamidoadenosine derivatives to a combination of the N^6-diphenylethyl group on the adenine base and an aromatic residue on the 5' position of the ribose moiety, with replacement of the aromatic residue with a methyl group resulting in IC_{50} values greater than 10 µM.

In addition, if these compounds acted as *Pf*ENT1 inhibitors, a discrepancy between their IC_{50} values as determined by the [^{3}H]-hypoxanthine incorporation assay and flow cytometric analysis would have occurred, since they would have inhibited the uptake of the radiolabelled isotope (Table 5.18).

However, some authors suggest that *Pf*ENT1 is insensitive to dipyridamole. Parker *et al*. (2000) cloned *Pf*ENT1 from the 3D7 strain of *P. falciparum* and expressed it in *Xenopus* oocytes and found that 10 µM dipyridamole had no effect on *Pf*ENT1-mediated transport of adenosine. In contrast, Carter *et al*. (2000), reported that *Pf*ENT1 cloned form the 3D7 (chloroquine-sensitive) and W2 (chloroquine-resistant) strains and expressed in *Xenopus* oocytes, was sensitive to 10 µM dipyridamole which inhibited adenosine uptake by 85%.

In this study, dipyridamole exhibited a direct effect on the parasite, inhibiting parasite growth in the micromolar concentration range (Table 5.18). However, the concentration of dipyridamole used in the combination study may have resulted in the inhibition of human ENT1, found in the red blood cell membrane. This could possibly result in the decreased transport of both purine and pyrimidine nucleosides and base analogues into the red blood cell, which may also be the cause of the noted antagonism (Figure 5.7) (Downie *et al*., 2008). There is also the possibility that compound D1293-S inhibited a non-*Pf*ENT1 purine nucleoside transporter (Figure 5.1), however in that case an additive or synergistic interaction with dipyridamole would be expected.

Examination of the stage-specific and morphological effects of compound DR-4463 showed some cytoplasmic vacuolisation in the late trophozoite-stage and a lag in schizont development and merozoite formation (Figure 5.8C,D and E). There was also a possible reduction in the number of merozoites formed or inability of merozoites to

invade red blood cells; with schizonts that had progressed through the cycle to form early rings only resulting in an increased parasitaemia of 3.51% (Section 5.3.4). In the latter case, it is possible that compound DR-4463 may have inhibited the sialic acid-dependant binding of the merozoite to the red blood cell in a manner similar to that of polyanionic compounds, such as oligodeoxynucleotides (Ramasamy *et al*., 1996; Kanagaratnam *et al*., 1998).

The process of merozoite invasion begins with the attachment of the merozoite to the red blood cell via merozoite membrane proteins, which potentially act as erythrocyte ligands (Figure 5.13A).

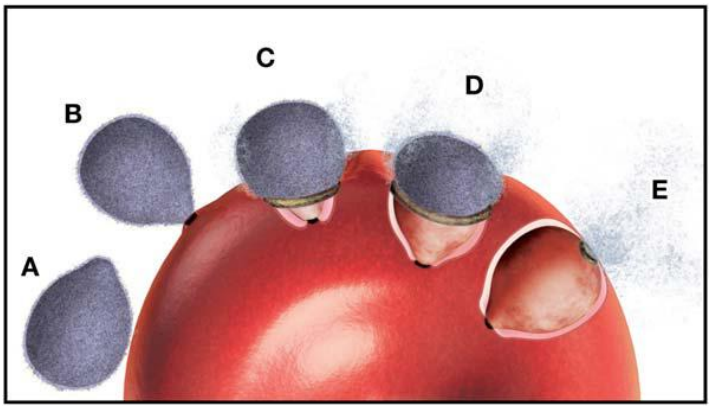


Figure 5.13: The invasion of a red blood cell by a merozoite (Cowman *et al*., 2006).

Following merozoite attachment, merozoite reorientation occurs (Figure 5.13B) so that the apical end of the merozoite is adjacent to the red blood cell; thereby facilitating the secretion of substances from merozoite organelles that are vital to the attachment of the apical end of the merozoite to the red blood cell and pit formation. Thereafter, the merozoite is propelled into the red blood cell (Figure 5.13C and D) by the action of the actin-myosin pump and finally, upon entry into the red blood cell, the merozoite protein surface coat is removed by parasitic proteases (Figure 5.13E) (Bozdech *et al*., 2003; Soni *et al*., 2005; Cowman *et al*., 2006).

In addition, the amphipathic nature of compound DR-4463 may have facilitated its incorporation into the lipid bilayer of the red blood cell membrane, where it altered membrane shape and composition (Evans and Havlik, 1993; Ziegler *et al*., 2002).

Resulting in altered fluidity of the membrane and affecting parasite-induced modification of the red blood cell membrane, such as transport channels, exo- and endocytosis, as well as adhesion, making the membrane unfavourable for invasion by merozoites (Evans and Havlik, 1993; Ziegler *et al*., 2002). In addition, receptor-mediated processes may have been disrupted by compound DR-4463 resulting in the noted cytoplasmic vacuolisation, possibly due to the induction of autophagy (Evans and Havlik, 1993; López *et al*., 2010). Amphiphiles have displayed growth inhibitory properties in the range of 7-28 µM in the 3D7 strain of *P. falciparum*, using [^{3}H]-phenylalanine as a growth indicator. This activity was slightly lower than the IC_{50} value range observed with the amphiles in this study (13-64 µM) using [^{3}H]-hypoxanthine as a growth indicator (Ziegler *et al*., 2002, 2004).

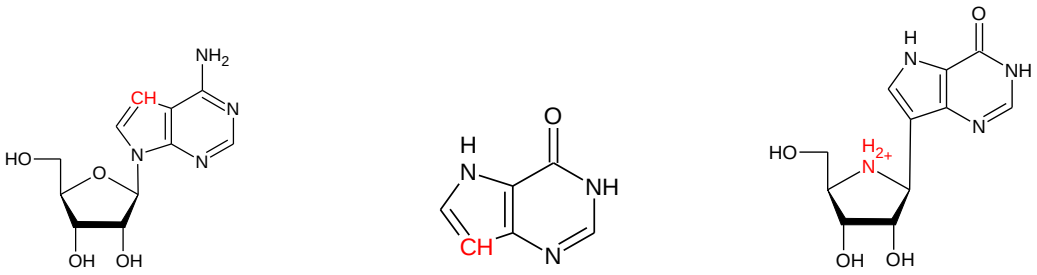
Alternatively, the aliphatic side chains may have conferred the lipophilicity needed to facilitate the entry of the compounds into the red blood cell, and may have been cleaved off following entry. In this manner, the side chain may not have contributed to the inhibition of parasite growth. In all of the amphipathic compounds, the side chain was linked to the phosphonate/phosphonic acid group by a phosphoester bond (Table 5.10-5.12), which is prone to attack by esterase enzymes present in the red blood cell cytosol (De Clercq, 2007; Vaněk *et al*., 2009). Similarly, nucleoside phosphonates and phosphonic acid derivatives containing a phosphoester linkage to the ribose moiety are also prone to attack by 5'-nucleotidases (Hyde, 2007; Mehrotra *et al*., 2010). Nucleotidases are capable of cleaving the phosphoester bond of both purine and pyrimidine nucleoside monophosphates to form the corresponding nucleoside, and are involved in the catabolism of ATP to form adenosine, providing a key source of hypoxanthine for the parasite (Hyde, 2007; Mehrotra *et al*., 2010). In contrast, a phosphate-carbon linkage between the ribose and phosphonate/phosphonic acid moieties provides metabolic stability against attack by catabolic enzymes (De Clercq, 2007; Vaněk *et al*., 2009). However, it did not appear as if the possible cleavage of the phosphate group from the Lipophosphonoxin group of compounds (Table 5.11) had a detrimental effect on antimalarial activity. A comparison of the antimalarial activity of compounds which had a phosphoester linkage between the ribose and phosphonate

moieties, such as compound DR-4850 (IC_{50} value: 13.35 ± 0.38 µM; Table 5.11), and those with a phosphate-carbon linkage, such as compound DR-3960 (IC_{50} value: 33.13 ± 2.10 µM; Table 5.10) highlights this. Following possible modification by enzymes in the red blood cell cytosol, the (nucleo)base derivatives and nucleoside analogues may then have been transported into the parasite by *Pf*ENT1 and in the case of some purine derivatives, possibly non-*Pf*ENT1 mechanisms (Downie *et al*., 2008; Riegelhaupt *et al*., 2010).

Following the entry of the pyrimidine (nucleo)base and nucleoside derivatives into the parasite, the lag in schizont development and possible reduction in merozoite formation may have been due to the pyrimidine analogues and pyrimidine-containing nucleoside phosphonates/phosphonic acids acting as substrate analogues, thereby weakly inhibiting critical enzymes of DNA synthesis and division (Baragaña *et al*., 2011). One such enzyme is deoxyuridine 5'-triphosphate nucleotidohydrolase, and is responsible for catalysing the hydrolysis of deoxyuridine 5'-triphosphate (dUTP) to dUMP, thereby providing the dUMP necessary for dTTP synthesis in the thymidylate cycle. It is also responsible for the low dUTP:dTTP ratio necessary to prevent the inclusion of uracil into DNA by plasmodial DNA polymerases. The enzyme has been shown to be inhibited by both cyclic and acyclic deoxyuridine analogues, with some inhibiting enzyme activity at sub-micromolar concentrations (K_i range: 0.5-98 µM) (Baragaña *et al*., 2011).

Similarly, orotidine-5'-monophosphate decarboxylase, responsible for the carboxylation of OMP to UMP (Figure 5.2), has been shown to be inhibited by pyrimidine nucleotide derivatives (Meza-Avina *et al*., 2010). Enzyme inhibition results from the interaction of the phosphoribosyl moiety of the derivative with the enzyme, through hydrogen bonding of the hydroxyl and phosphoryl moieties (Meza-Avina *et al*., 2010). Furthermore, the plasticity of orotidine-5'-monophosphate decarboxylase enables it to accept various nucleotide derivatives as ligands, including purine derivatives (Meza-Avina *et al*., 2010). Taking into account the low affinity transport of thymine and uracil bases and nucleosides derivatives, along with the relatively high IC_{50} values of the compounds (Tables 5.10-5.12), it seems unlikely that this enzyme was inhibited.

However, purine bases and nucleosides are transported by *Pf*ENT1 at a higher affinity than pyrimidine derivatives, due to the reliance of *P. falciparum* on purine salvage from the host (El Bissati *et al*., 2006; Downie *et al*., 2008; Riegelhaupt *et al*., 2010). The increased transport of purine base and nucleoside derivatives, together with the fact that *Pf*ENT1 is capable of accommodating a wide variety of alterations on natural substrates, makes purine metabolism an excellent drug target (Riegelhaupt *et al*., 2010). *Pf*ENT1 has been shown to transport tubercidin (Figure 5.14a), a 7-deazaadenosine analogue, and 9-deazahypoxanthine (Figure 5.14b), with an affinity similar to the natural substrates, adenosine and hypoxanthine, respectively. Indicating that alterations on the N^7 and N^9 positions on the purine ring did not inhibit substrate recognition. However, alteration of the ribose moiety in immucillins (Figure 5.14c), which are 9-deaza purines containing a cationic nitrogen in the place of oxygen in the ribose moiety, appeared to decrease or inhibit transportation of the nucleoside derivatives, possibly due to the altered charge of the moiety (Riegelhaupt *et al*., 2010).



a) b) c)

Figure 5.14: The chemical structures of tubercidin (a) 9-deazahypoxanthine (b) and immucillin-H (c), showing where the base was modified (Riegelhaupt *et al*., 2010).

The metabolism of adenosine into inosine and then hypoxanthine by *P. falciparum* adenosine deaminase and *P. falciparum* purine nucleoside phosphorylase enzymes, respectively (Figure 5.1), maintains a low internal adenosine concentration which drives the uptake of adenosine into the parasite until equilibrium is reached (Riegelhaupt *et al*., 2010). In addition, parasite-induced new permeation pathways within the red blood cell membrane are not saturable for concentrations in the millimolar range (Gero *et al*.,

2003), possibly creating a situation where adenosine derivatives hyper-concentrate within the parasite, exerting toxic effects.

P. falciparum has been shown to proliferate under conditions where adenine, adenosine, guanine, guanosine or xanthine was present as the sole purine source, at concentrations as low as 2 µM (Downie *et al*., 2008; El Bissati *et al*., 2008). It may then seem possible that the parasite utilised the adenine/guanine derivatives or nucleosides as an alternate purine source, incorporating them into its DNA, resulting in their antimalarial activity. However, a lower IC_{50} value would be expected due to DNA chain termination, and IC_{50} results as obtained by the [^{3}H]-hypoxanthine assay and flow cytometric analysis would show large discrepancies due to the lack of incorporation of the hypoxanthine isotope into parasitic DNA, which was not the case (Table 5.18).

Guanine/guanosine derivatives are also taken up via *Pf*ENT1, which may also result in a hyper-concentration of the derivatives within the parasite, with reports that guanine and guanosine are toxic to the parasite at concentrations above 50 µM (El Bissati *et al*., 2008). Alternatively, both guanine and hypoxanthine are phosphoribosylated by the *Pf*HGXPRT enzyme, which exhibits similar affinities for hypoxanthine and guanine (Km values = 0.46 µM and 0.30 µM, respectively). In this manner, the guanine/guanosine derivatives may have competed with hypoxanthine for phosphoribosylation, which ultimately would have lead to decreased ATP levels for nucleic acid synthesis and cell signalling (Downie *et al*., 2008). Alternatively, adenine nucleoside derivatives may act as structural analogues for enzyme substrates, and thereby inhibit enzymes involved in the sequential conversion of IMP to adenylsuccinate and finally to AMP (Bulusu *et al*., 2011). One such nucleoside derivative, 5-aminoimidazole-4-carboxamide ribonucleoside, has been shown to inhibit *Plasmodium falciparum* adenylosuccinate lyase, thereby inhibiting the conversion of adenylsuccinate to AMP. Although, it only exerted its antimalarial effect at very high concentrations (IC_{50} value: 167 ± 5µM) (Bulusu *et al*., 2011). Notwithstanding possible enzymatic inhibition, any minor disturbance of purine uptake, the salvage pathway, or purine nucleotide synthesis in *P. falciparum* would result in growth arrest in the schizont stage (Bulusu *et al*., 2011).

The structural diversity of the compounds and the presence of reactive functional groups' on the side chains, could contribute to the compounds having mechanisms of action other than those proposed above. These could include inhibition of β-haematin formation, free-radical scavenging or metal chelation (Table 5.19).

Aminoalkylphosphonates contain donor groups capable of chelating metals, thereby inactivating metalloenzymes (Kiss *et al*., 1994). However, none of the compounds in this study exhibited any Fe(II) chelating activity, with the Fe(II) chelating activity of the 27 compounds tested ranging from 0.01 ± 1.50% to 34.86 ± 8.44% at 200 µM (Table 5.19). The lack of activity of the compounds could be due to the fact that a higher drug concentration was needed, with 2,2'-bipyridyl, a nitrogen-containing heterocyclic bidentate Fe(II) chelator, only capable of chelating iron in a ratio of 3:1 of drug to Fe(II) (Elandalloussi *et al*., 2003). Therefore, as is the case with 2,2'-bipyridyl, a 3:1 ratio of drug to Fe(II) may have been needed to chelate the free Fe(II) concentration of 200 µM used in this assay.

In a similar manner, none of the 30 compounds tested exhibited any $DPPH^{\bullet}$ free-radical scavenging activity, with free-radical scavenging activity ranging from 0.01 ± 2.13% to 31.60 ± 5.34% at 240 µM (Table 5.19). Despite the fact that the compounds contained amine groups and were hydroxylated; with these groups conferring anti-oxidant activity (Saito and Ishihara, 1997; von Gadow *et al*., 1997; Nishiyama *et al*., 2002). Spanou *et al*. (2007) also found that pyrano-nucleoside analogues of N^4-benzoyl cytosine and N^6-benzoyl adenine did not exhibit any $DPPH^{\bullet}$ free-radical scavenging activity, attributing their inactivity to the size of the analogues, resulting in steric hindrance and preventing their accessibility to the radical site of $DPPH^{\bullet}$.

In contrast, of the 35 compounds screened for β-haematin formation inhibitory activity, six exhibited potent activity (Figure 5.15), with some compounds proving to be over 3.6-fold more active than chloroquine. Of the six compounds, five belonged to the Lipophosphonoxin (Table 5.11) and Nucleoside Lipophosphonate groups (Table 5.10), whereas one belonged to the Mickey Mouse group (Table 5.13).

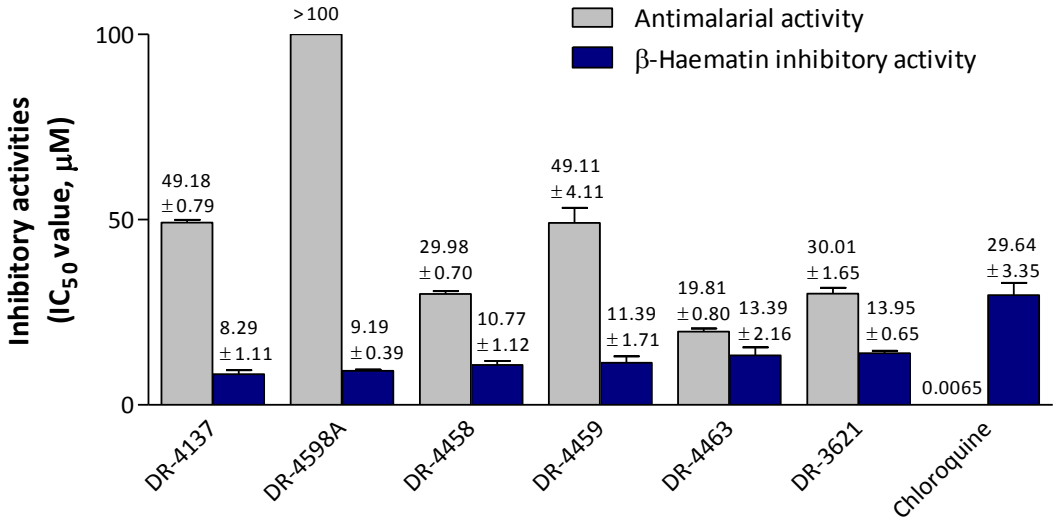


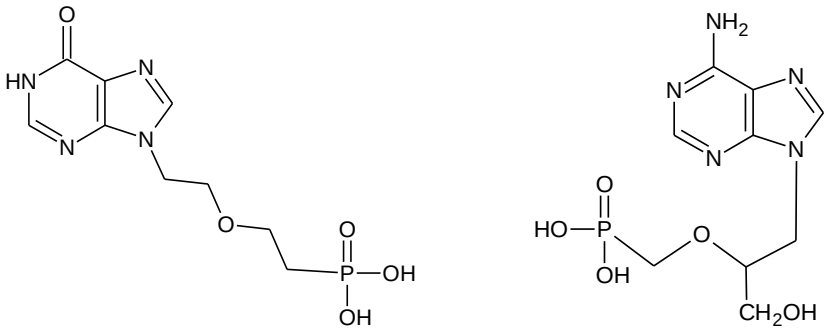
Figure 5.15: The inhibitory activities of compounds from the Lipophosphonate (DR-4137, DR-4458, DR-4459, DR-4463) Nucleoside Lipophosphonate (DR-3621) and Mickey Mouse groups (DR-4598A).

The β-haematin inhibitory activity of the aliphatic side chain of the Lipophosphonoxin and Nucleoside Lipophosphonate groups appeared to parallel the antimalarial activity of the compounds. The Phosphonoxin, compound DR-3707 (Table 5.17) is similar to the Lipophosphonoxin, compound DR-4459 (Table 5.11), except for the aliphatic side chain. This structural difference resulted in an increase in β-haematin formation inhibitory activity from 3.13 ± 2.14% at 400 μM (compound DR-3707) to an IC_{50} value of 11.39 ± 1.71 μM (compound DR-4459) (Table 5.19). The activity of the Lipophosphonoxins and Nucleoside Lipophosphonates may be attributed to the increased lipophilicity and affinity for haematin conferred by the aliphatic side chain, which itself may also have interacted with the porphyrin ring of the Fe(III)-protoporphyrin-IX (Egan *et al*., 2000). Similarly, the side chain may have provided the correct conformation for complexing of the heterocyclic moiety to the porphyrin ring, thereby preventing the interaction of a carboxylate group of one porphyrin ring to the Fe(III) of another porphyrin ring (Chemaly *et al*., 2007). Alternatively, it may have allowed for the hydroxyl groups present on the piperidine and pyrrolidine ring systems to interfere with hydrogen bonding between the dimers (Chemaly *et al*., 2007; Kouznetsov and Gomez-Barrio, 2009), thereby preventing dimerisation and/or chain formation.

Compound DR-4598A exhibited no antimalarial activity (34.61 ± 3.17% growth inhibition at 100 μM) (Table 5.13), however proved to be a potent inhibitor of β-haematin formation, being 3.2-fold more active than chloroquine (Figure 5.15; Table 5.19). The structure of DR-4598A (Table 5.13) is vastly different from those of the Lipophosphonoxins and Nucleoside Lipophosphonate inhibitors of β-haematin formation. It is not a nucleoside derivative and does not have an aliphatic side substitution; but rather contains a purine ring system substituted with dibenzylamino and propylphosphonic acid groups (Table 5.13). Compounds DR-4598A and DR-4523 exhibit some structural similarities, with the exceptions that DR-4523 lacks the propylphosphonic acid substitution on the purine ring, and has a trifluoromethyl substitution on one of its benzene rings (Table 5.13). These differences accounted for a 19-fold decrease in β-haematin inhibitory activity in compound DR-4523 (IC_{50} value: 174.90 ± 4.28 μM). The trifluoro-methyl substitution of DR-4523 may have conferred weak β-haematin inhibitory activity and antimalarial activity in a similar fashion to the 7-chloro group on the aminoquinolines (Egan *et al*., 2000). However, compound DR-4598A lacks this substitution and yet retains potent β-haematin inhibitory activity. Pointing to the propylphosphonic acid substitution as a contributing factor in its activity. Possibly by competing with the carboxylate of the propionic acid groups of a porphyrin ring for coordination to the Fe(III) of another porphyrin ring. The lack of antimalarial activity and strong β-haematin inhibitory activity of compound DR-4598A indicates that the phosphonic acid group contributed to its β-haematin inhibitory activity, but also hampered its ability to move through membranes. With most of the phosphonic acid derivatives tested in this study exhibiting no antimalarial activity (Tables 5.12-5.15).

Although some of the analogues exhibited both antimalarial and β-haematin inhibitory activity, there appeared to be no correlation between the two activities ($r^2 = 0.43$). This is highlighted by the fact that compound DR-4463 exhibited potent *ex vivo* β-haematin inhibitory activity (IC_{50} value: 13.39 ± 2.16 μM) (Table 5.19). However, haemozoin crystals were clearly visible when examining its effect on parasite morphology (Figure 5.8A-D), indicating that perhaps the compound did not concentrate in the food vacuole or that inhibition of haemozoin formation is not its primary mechanism of action.

It can be concluded from the results that the compounds exhibit fairly poor specificity for DNA synthetic and replication processes of *P. falciparum*. However, certain structural modifications could greatly enhance the activity of the compounds. One such example is compound DA-IX-158, an adenine derivative which exhibited poor antimalarial activity (13.53 ± 8.97% inhibition at 100 µM) (Table 5.16). A study conducted by Hocková *et al*. (2009), found that an acyclic nucleoside phosphonate derivative with a similar structure to that of DA-IX-158 exhibited poor inhibition of the *Pf*HGXPRT. However, upon modification of the base from an adenine to a guanine or hypoxanthine (Figure 5.16a), enzyme inhibition was greatly enhanced (Hocková *et al*., 2009). Similarly, DA-IX-158 closely resembles (S)-(3-hydroxy-2-phosphonylmethoxy-propyl)adenine ((S)-HPMPA) (Figure 5.16b), but it lacks the 3'-hydroxyl moiety attributed to the antimalarial activity of ((S)-HPMPA) (0.18 ± 0.07 µM against the K1 chloroquine-resistant strain of *P. falciparum*) (Smeijsters *et al*., 1999).



a) b)

Figure 5.16: Nucleoside phosphonic acids previously assessed for antimalarial activity. Where: a = phosphonoethoxyethyl hypoxanthine (Hocková *et al*., 2009) and b = 3-hydroxy-2-phosphonylmethoxypropyl adenine (HPMPA) (Smeijsters *et al*., 1999).

ANP derivatives provide an excellent drug scaffold in that they do not contain the classic glycosidic linkage, nor do they contain the phosphoester bond prone to hydrolysis. However, ANPs would need to be delivered in the form of a pro-drug due to their inability to cross membranes (Hocková *et al*., 2009).

Similarly, ideal drug scaffolds have been proposed for CDK inhibitors of *Pf*mrk based on structure-activity relationships of *Pf*mrk inhibitors active in sub-micromolar concentrations; with these *Pf*mrk inhibitors also exhibiting no activity against human CDKs. In this manner, the ideal pharmacophore should contain two hydrogen bond acceptors and two hydrophobic sites, one of which should be an aromatic ring (Figure 5.17) (Geyer *et al*., 2005). In addition, Harmse *et al*. (2001) found that substitution on the purine ring at C^2 appeared to play a role in the ability of purine derivatives to inhibit parasite growth through the inhibition of plasmodial CDKs, with bulky aromatic rings in the R orientation abolishing antimalarial activity.

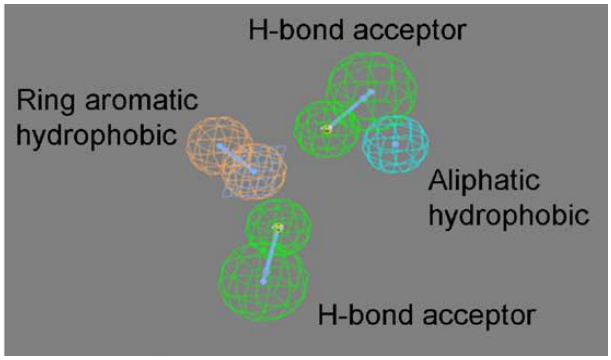


Figure 5.17: The ideal pharmacophore for inhibition of *Pf*mrk (Geyer *et al*., 2005).

Inhibition of the pyrimidine synthesis has typically involved inhibition of enzymes of the folate pathway, due to the necessity of folate cofactors in the conversion of dUMP to dTMP, making this pathway a susceptible antimalarial target (Hyde, 2007; Nzila, 2006). The parasite transports pyrimidines with a low affinity; however it readily takes up orotate derivatives (Baldwin *et al*., 2007; Hyde, 2007; Muregi *et al*., 2009). In this manner, orotic acid derivatives or active metabolites could be capable of inhibiting enzymes such as thymidylate synthase and would warrant further investigation. However, a pyrimidine such as uridine

would need to be co-administered to protect the host from toxicity (Baldwin *et al*., 2007; Hyde, 2007; Muregi *et al*., 2009).

Alternatively, an ideal pharmacophore has been proposed as an inhibitor of the orotidine-5'-monophosphate decarboxylase enzyme, that is required for conversion of OMP to UMP (Meza-Avina *et al*., 2010). The ideal pharmacophore has various components contributing to its activity (Figure 5.18). Component A is involved in the orientation of the nucleobase and substitutions of iodo, azido or nitrile on component B influence the inhibitory activity of the ligand. Whereas, component C, the phosphoribosyl moiety, forms hydrogen bonds with the enzyme via the 2'- and 3'-hydroxyl moieties of the ribose group, as well as the 5' phosphoryl moiety (Meza-Avina *et al*., 2010). In addition, various modifications of the nitrogen-containing heterocyclic are accommodated without affecting the inhibitory activity. These include the substitution of a pyrazole ring structure or even a purine base, with XMP also acting as a strong inhibitor of orotidine-5'-monophosphate decarboxylase. Additionally, the substitution of a purine base for a pyrimidine base may be beneficial in order to improve the transport of the inhibitor into the parasite (Meza-Avina *et al*., 2010).

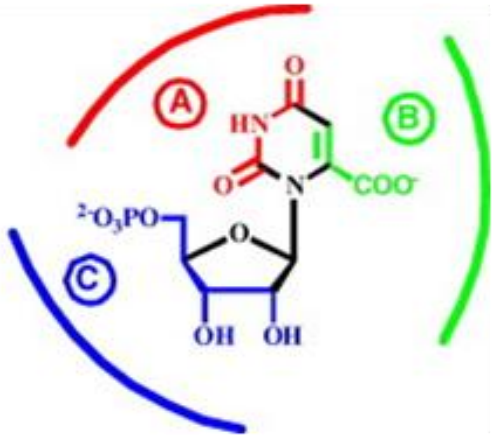


Figure 5.18: The ideal pharmacophore of an orotidine-5'-monophosphate decarboxylase inhibitor (Meza-Avina *et al*., 2010).

When combined with quinine, compound DR-4463, a uridine phosphonate derivative, exhibited an additive interaction (Figure 5.7a; Appendix E), with the two compounds inhibiting parasite growth at different stages of the asexual life cycle. Although these nucleoside phosphonates, phosphonic acids and purine/pyrimidine derivatives did not

warrant further investigation, structural modifications to improve the lipophilicity and specificity of the compounds; whilst maintaining or improving the ability of the compounds to act in an additive or synergistic manner with quinine, may provide a new generation of derivatives worth investigating.

CHAPTER 6: CONCLUSIONS AND RECOMMENDATIONS

6.1 Conclusions

The metronidazole-thiosemicarbazone analogues were most active of the three classes of novel compounds tested, with six of the eight compounds possessing IC_{50} values below 10 µM (Table 3.2). The activity of this group of compounds appeared to be attributed to the presence of a thioamine moiety on the R-group, as when this moiety was replaced with a nitrogen-containing heterocyclic (compounds Y-5 and Y-6) (Figure 3.7) the antimalarial activity decreased to 51.91 ± 6.03% growth inhibition at 100 µM and an IC_{50} value of 71.07 ± 8.97 µM, respectively (Table 3.2). Although, the presence of a quinoline ring structure at the R-group also conferred antimalarial activity, as observed in compound Y-7 (IC_{50} value: 3.79 ± 0.72 µM; Table 3.2), which lacked the thioamine moiety. Metronidazole exhibited no antimalarial activity (22.94 ± 5.61% growth inhibition at 100 µM; Table 3.2), which may have been attributed to the lack of activation and subsequent accumulation of the drug in the parasite. In addition, the metronidazole moiety may have hindered the rotation of the compounds, resulting in their poor Fe(II) chelating activity (Table 3.4).

In addition to the numerous mechanisms of action attributed to the thiosemicarbazone group, the set of analogues in this study were potent inhibitors of β-haematin formation (Figure 3.7), with a strong correlation ($r^2 = 0.87$) noted between antimalarial and β-haematin inhibitory activity. Side chains wherein the R-group was a 2-chloro-benzyl amine (compound Y-3), a cyclooctyl amine (compound Y-1), or a 1,2,3,4-tetrahydroquinoline (compound Y-7) were the most potent inhibitors of β-haematin formation (Figure 3.7). The additive pharmacological interaction with quinine and dihydroartemisinin (Figure 3.4), the lack of toxicity towards the host red blood cells (Table 3.2), as well as the strong anti-oxidant activity (Table 3.4) of the compounds would all prove beneficial in the treatment of malaria.

The antimalarial activity of the chloroquine-chalcones was disappointing when compared to chloroquine (IC_{50} value: 0.0065 ± 0.0002 µM) or quinine (IC_{50} value: 0.14 ± 0.0007 µM), with the most active, compound F-13, possessing an IC_{50} value of 31.31 ± 0.87 µM (Table 4.2). Hybridisation of the chloroquinoline and chalcone moieties abolished the strong β-haematin inhibitory activity of the chloroquinoline moiety, with compounds F-14, F-8 and F-3

inhibiting β-haematin formation by between 89% and 93% at 400 µM (2:1 ratio of drug:haem) (Table 4.3). However, at 100 µM they only inhibited β-haematin formation by between 10% and 23% (Section 4.3.4.1), which may have been attributed to the placement of the chloro- group on the C^2 position and not the C^7 position of the quinoline ring.

Structure-activity relationships showed that compounds with a pyridine ring at R^4 were the most active, possibly due to an interaction with the malarial protease, falcipain-2 (Mishra *et al*., 2008). In the case of the compounds which had a bromo- or chloro-substituted phenyl ring at R^4, the positioning of the methyl and hydrogen substitutions at R^1, R^2 and R^3 were the main determinant in antimalarial activity, and not the position of the chloro- or bromo-group (Table 4.2). Chalcones have previously been shown to alkylate proteins, which would be a concern in that it may induce host cell toxicity, although, none of the compounds exhibited any haemolytic effects in this study. Despite this, future derivatives should be screened against a normal cell line for cytotoxicity. Compound F-13 exhibited a favourable interaction with quinine (Figure 4.5), which is promising for the development of second generation compounds as the WHO advocates the use of combination therapies for the treatment of malaria (WHO, 2010b).

The antimalarial activity of the nucleoside phosphonates, phosphonic acids and purine/pyrimidine derivatives were weak, with only 19 of the 90 compounds tested exhibiting antimalarial activity below 100 µM, and no compounds exhibiting activity below 10 µM (Tables 5.10-5.17). The compounds showed variable activity, not only between the 11 structural groups, but also within each group. Overall, all compounds with an aliphatic side chain possessed antimalarial activity, with compounds DR-4850, DR-4878 and DR-4463 possessing the best IC_{50} values of these compounds (IC_{50} values: 13.35 ± 0.38 µM, 17.76 ± 1.72 µM, 19.81 ± 0.80 µM, respectively) (Tables 5.11). This could possibly be attributed to the increased lipophilicity of the compounds, or the facilitation of the incorporation of these compounds into lipid membranes, where they could have acted to inhibit merozoite invasion of the red blood cell or disrupt transport channels in the membrane (Evans and Havlik, 1993; Ramasamy *et al*., 1996; Kanagaratnam *et al*., 1998). Some compounds lacking the aliphatic side chain substitution, such as compounds DR-4558 and DR-3876 (IC_{50} values: 23.85 ± 1.76 µM, 31.08 ± 2.33 µM, respectively) (Tables 5.13-5.14) also displayed

antimalarial activity, which may have been due to weak inhibition of enzymes involved in DNA synthesis and division. However, no particular base appeared to confer antimalarial activity, nor did antimalarial activity significantly improve over a double parasitic life cycle (Section 5.3.1.1, Figure 5.6), indicating the lack of selectivity of the compounds for the inhibition of DNA/RNA synthesis and replication.

Interestingly, some compounds such as compound DR-4137 exhibited strong β-haematin inhibitory activity (IC_{50} value: 8.29 ± 1.11 μM; Table 5.19), however, β-haematin inhibitory activity did not correspond to the antimalarial activity of the compounds. This was highlighted in morphological studies with compound DR-4463, which was a potent *ex vivo* inhibitor of β-haematin formation in the β-haematin inhibitory activity assay (IC_{50} value: 13.39 ± 2.16 μM; Table 5.19), yet haemozoin crystals were clearly visible *in vitro* (Figure 5.8), indicating that these compounds work outside of the food vacuole or are incapable of entering the food vacuole. Generally the compounds caused no red blood cell lysis (Tables 5.10-5.17), with the exception of compound DR-4914B (50.20 ± 3.35% haemolysis at 100 μM; Table 5.11). When tested for cytotoxicity against cancer cell lines and erythroid progenitor cells, a selection of 33 compounds (Table 5.20) did not exhibit toxicity, with the exception of compound DR-3621 which inhibited growth of the cancer lines at IC_{50} values ranging from 14 μM to 16 μM.

A comparison of the results obtained by the [^{3}H]-hypoxanthine incorporation assay and flow cytometric analysis revealed some statistically significant differences ($p < 0.05$). Results obtained by flow cytometry correlated to blood smear analysis in which both non-viable and viable parasites were counted, indicating a lack of specificity for viable parasites only. The fluorochrome used in this study was selected due to the fact that it is oxidised into its DNA intercalating form in only viable parasites; however, it would appear as if the fluorochrome was spontaneous oxidised in non-viable parasites. The methodology provided a means in which the stage-specific activity of compounds could be quantitated, however due to the overlap in stages, the preparation of duplicate samples for assessment by blood smear analysis is crucial.

6.2 Recommendations

6.2.1 Metronidazole-thiosemicarbazone analogues

- Thiosemicarbazones have numerous proposed mechanisms of action, in this respect it would be worthwhile to further examine this class of compounds, such as testing their ability to chelate transition metals other than Fe(II), generate reactive oxygen species, and inhibit *Plasmodial* cysteine protease enzymes, from which additional structure-activity data could be generated and a potent second generation of compounds synthesised.
- In addition, replacement of the metronidazole moiety with other nitrogen-containing heterocyclics or an aliphatic amine side chain may facilitate the metal chelation activity of the compounds.
- It would also be worthwhile to test the activity of the compounds against the sexual stages of the parasitic life cycle, as a compound that is active against both asexual and sexual stages would be highly beneficial as it would not only treat the disease, but also block transmission of the disease.

6.2.2 Chloroquinoline-chalcones

- The chalcone structure provides an ideal drug scaffold, thereby providing opportunities for structural improvements to increase the lipophilicity of the compounds, and facilitate the accumulation of the compounds in the food vacuole, via the substitution of nitrogen-containing groups at R^4.
- In addition, the chloroquinoline moiety can be modified to improve β-haematin inhibitory activity, whilst also circumventing drug resistance which is proposed to be conferred by the aminoalkyl side chain of chloroquine (Vangapandu *et al*., 2007; van Schalkwyk and Egan, 2006).
- Further experimentation into the antimalarial mechanisms of action attributed to chalcones, such as an examination of their direct effect on the falcipain-2 enzyme, ability to form complexes with GSH, and inhibitory activities on parasite-induced new permeation pathways and plasmodial CDKs would be worthwhile examining, in order to provide structure-activity information for the further development of derivatives.

6.2.3 Nucleoside phosphonates, phosphonic acids and purine/pyrimidine derivatives

- Derivatives of nucleosides and nucleobases to increase their specificity for parasitic enzymes of DNA synthesis would also be worthwhile investigating; such as, a series of acyclic nucleoside phosphonates, with a hypoxanthine or a guanine base and a 3' hydroxyl moiety. However, these compounds would need to be delivered in the form of a pro-drug to facilitate their entry into the parasite.
- Similarly, an orotic acid or orotidine derivative which may act to inhibit *de novo* pyrimidine synthesis or the conversion of orotidine monophosphate to uridine monophosphate would also be worth investigating.
- Additionally, it would be interesting to examine other pyrimidine derivatives based on the structure and inhibitory activity of pyrimethamine against dihydrofolate reductase.

6.2.4 Flow cytometry

- The development of a double staining technique, wherein an RNA-specific fluorochrome is used together with dihydrethidium so that both DNA and RNA could be quantified would be beneficial, as it may provide a more accurate assessment of parasite viability and life cycle progression. However, fluorochromes are also costly, and dihydroethidium requires three washing steps, making the methodology time consuming and not necessarily suitable for IC_{50} value determination.
- Additionally, any compound that could alter the intracellular pH, thereby affecting the binding of the probe to parasitic DNA, or result in fluorescent interference due to a similar emission spectra to that of the fluorochrome, or cause clumping of red blood cells would skew the results obtained using this methodology. In this respect, duplicate samples for microscopic analysis would need to be prepared to validate the results, negating this method as a high-throughput screening method.

In the case of the metronidazole-thiosemicarbazone analogues the effects of the compounds on the parasitic targets examined were clear. The mechanisms of action of the chloroquinoline-chalcones and nucleoside phosphonates, phosphonic acids and purine/pyrimidine derivatives were not as evident. However, their effects on parasite morphology, parasitic life cycle progression and pharmacological interactions with standard

antimalarial drugs provided some insight into their antimalarial mechanisms of action. The results of the assays used in this study provided valuable structure-activity relationships for the rational drug design of second generations of the compounds. Priorority should be given to the further development of the metronidazole-thiosemicarbazone analogues since they were the most active class of compounds against *P. falciparum,* had additive pharmacological interactions when combined with standard antimalarials, and that phase I clinical trials of the thiosemicarbazone-derivative Triapine® showed that the drug was generally well-tolerated by patients (Giles *et al*., 2003).

REFERENCES

Abdalla, H., Matambo, T.S., Koekemoer, L.L., *et al*. 2008. Insecticide susceptibility and vector status of natural populations of *Anopheles arabiensis* from Sudan. Trans R Soc Trop Med Hyg 102, 263-271.

Abid, M. & Azam, A. 2005. 1-*N*-substituted thiocarbamoyl-3-phenyl-2-pyrazolines: synthesis and *in vitro* antiamoebic activities. Eur J Med Chem 40, 935-942.

Abid, M., Agarwal, S.M., Azam, A. 2008. Synthesis and antiamoebic activity of metronidazole thiosemicarbazone analogues. Eur J Med Chem 43, 2035-2039.

Abid, M., Bhat, A.R., Athar, F., *et al*. 2009. Synthesis, spectral studies and antiamoebic activity of new 1-*N*-substituted thiocarbamoyl-3-phenyl-2-pyrazolines. Eur J Med Chem 44, 417-425.

Akaki, M., Nakano, Y., Ito, Y., *et al*. 2002. Effects of dipyridamole on *Plasmodium falciparum*-infected erythrocytes. Parasitol Res 88, 1044-1050.

Aki, H. & Yamamoto, M. 1991. Drug binding to human erythrocytes in the process of ionic drug-induced hemolysis. Biochem Pharmacol 41(1), 133-138.

Alonso, P.L. 2006. Malaria: deploying a candidate vaccine (RTS,S/AS02A) for an old scourge of humankind. Int Microbiol 9, 83-93.

Amador, R., Moreno, A., Valero, V., et al. 1992. The first field trials of the chemically synthesised malaria vaccine Spf66: safety, immunogenicity and protectivity. Vaccine 10(3), 179-184.

Apte, S.H., Groves, P.L., Rodick, J.S., *et al*. 2011. High-throughput multi-parameter flow-cytometric analysis from micro-quantities of *Plasmodium*-infected blood. Int J Parasitol 41(12), 1285-1294.

Arnot, D.E., Ronander, E., Bengtsson, D.C. 2011. The progression of the intra-erythrocytic cell cycle of *Plasmodium falciparum* and the role of the centriolar plaques in asynchronous mitotic division during schizogony. Int J Parasitol 41, 71-80.

Athar, F., Husain, K., Abid, M., *et al*. 2005. Synthesis and anti-amoebic activity of gold(I), ruthenium(II), and copper(II) complexes of metronidazole. Chem Biodivers 2, 1320-1330.

Auffret, G., Labaied, M., Frappier, F., *et al*. 2007. Synthesis and antimalarial evaluation of a series of piperazinyl flavones. Bioorg Med Chem Lett 17, 959-963.

Balconi, E., Pennati, A., Crobu, D., *et al*. 2009. The ferrodoxin-$NADP^+$ reductase/ferrodoxin electron transfer system of *Plasmodium falciparum*. FEBS J 276, 4249-4260.

Baldwin, S.A., McConkey, G.A., Cass, C.E., *et al*. 2007. Nucleoside transport as a potential target for chemotherapy in malaria. Curr Pharm Des 13, 569-580.

Bandgar, B.P., Gawande, S.S., Bodade, R.G., *et al*. 2010. Synthesis and biological evaluation of simple methoxylated chalcones as anticancer, anti-inflammatory and antioxidant agents. Bioorg Med Chem Lett 18, 1364-1370.

Banerjee, R., Liu, J., Beatty, W., *et al*. 2002. Four plasmepsins are active in the *Plasmodium falciparum* food vacuole, including a protease with an active-site histidine. Proc Natl Acad Sci U S A 99(2), 990-995.

Bannister, L.H., Hopkins, J.M., Fowler, R.E., *et al*. 2000. A brief illustrated guide to the ultrastructure of *Plasmodium falciparum* asexual blood stages. Parasitol Today 16(10), 427-433.

Baragaña, B., McCarthy, O., Sánchez, P., *et al*. 2011. β-Branched acyclic nucleoside analogues as inhibitors of *Plasmodium falciparum* dUTPase. Bioorg Med Chem 19, 2378-2391.

Basilico, N., Pagani, E., Monti, D., *et al*. 1998. A microtitre-based method for measuring the haem polymerization inhibitory activity (HPIA) of antimalarial drugs. J Antimicrob Chemother 42, 55-60.

Basso, L.G.M., Rodrigues, R.Z., Naal, R.M.Z.G., *et al.* 2011. Effects of the antimalarial drug primaquine on the dynamic structure of lipid model membranes. Biochim Biophys Acta 1808, 55-64.

BD Biosciences, 2011. Updated 2011. <http://www.bdbiosciences.com> [Accessed 1 May 2011].

Becker, K. & Kirk, K. 2004. Of malaria, metabolism and membrane transport. Trends Parasitol 20(12), 590-596.

Bell, A. 2005. Antimalarial drug synergism and antagonism: Mechanistic and clinical significance. FEMS Microbiol Lett 253, 171-184.

Bennett, T.N., Paguio, M., Gligorijevic, B., *et al*. 2004. Novel, rapid, and inexpensive cell-based quantification of antimalarial drug efficacy. Antimicrob Agents Chemother 48(5), 1807-1810.

Berenbaum, M.C. 1978. A method for testing for synergy with any number of agents. J Infect Dis 137(2), 122-131.

Bhattacharya, A., Mishra, L.C., Sharma, M., *et al*. 2009. Antimalarial pharmacodynamics of chalcone derivatives in combination with artemisinin against *Plasmodium falciparum in vitro*. Eur J Med Chem 44, 3388-3393.

Biagini, G.A., O' Neill, P.M., Nzila, A., *et al*. 2003. Antimalarial chemotherapy: young guns or back to the future? Trends Parasitol 19(11), 479-487.

Biagini, G.A., Ward, S.A., Bray, P.G. 2005. Malaria parasite transporters as a drug-delivery strategy. Trends Parasitol 21(7), 299-301.

Biot, C. & Chibale, K. 2006. Novel approaches to antimalarial drug discovery. Infect Disord Drug Targets 6, 173-204.

Bozdech, Z., Llinás, M., Pulliam, B.L., *et al*. 2003. The transcriptome of the intraerythrocytic developmental cycle of *Plasmodium falciparum*. PLoS Biol 1(1), 85-100.

Bulusu, V., Thakur, S.S., Venkatachala, R., *et al*. 2011. Mechanism of growth inhibition of intraerythrocytic stages of *Plasmodium falciparum* by 5-aminoimidazole-4-carboxamide ribonucleoside (AICAR). Mol Biochem Parasitol 177, 1-11.

Butcher, G.A. 1997. Antimalarial drugs and the mosquito transmission of *Plasmodium*. Int J Parasitol 27(9), 975-987.

Carter, N.S., Mamoun, C.B., Liu, W., *et al*. 2000. Isolation and functional characterization of the *Pf*NT1 nucleoside transporter gene from *Plasmodium falciparum.* J Biol Chem 275(14), 10683-10691.

Carter, N.S., Landfear, S.M., Ullman, B. 2001. Nucleoside transporters of parasitic protozoa. Trends Parasitol 17(3), 142-145.

Centres for disease control and prevention. 2009. Updated: 20-07-2009. <http://www.dpd.cdc.gov/dpdx/hTML/Frames/MR/Malaria/falciparum/bodymalariadffalciparum.htm> [Accessed 8 March 2011].

Chango, A. & Abdennebi-Najar, L. 2011. Folate metabolism pathway and *Plasmodium falciparum* malaria infection in pregnancy. Nutr Rev 69(1), 34-40.

Chellan, P., Nasser, S., Vivas, L., *et al*. 2010. Cyclopalladated complexes containing tridentate thiosemicarbazone ligands of biological significance: Synthesis, structure and antimalarial activity. J Organomet Chem 695, 2225-2232.

Chemaly, S.M., Chen, C-T., van Zyl, R.L. 2007. Naturally occurring cobalamins have antimalarial activity. J Inorg Biochem 101, 764-773.

Chen, M., Theander, T.G., Christensen, S.B., *et al*. 1994. Licochalcone A, a new antimalarial agent, inhibits *in vitro* growth of the human malaria parasite *Plasmodium falciparum* and protects mice from *P. yoelii* infection. Antimicrob Agents Chemother 38(7), 1470-1475.

Chen, M., Zhai, L., Christensen, S.B., *et al*. 2001. Inhibition of fumarate reductase in *Leishmania major* and *L. donovani* by chalcones. Antimicrob Agents Chemother 45(7), 2023-2029.

Chen, R.F. 1967. Some characteristics of the fluorescence of quinine. Anal Biochem 19, 374-387.

Cheng, Z-J., Kuo, S-C., Chan, S-C., *et al*. 1998. Antioxidant properties of butein isolated from *Dalbergia odorifera*. Biochim Biophys Acta 1392, 291-299.

Chipeleme, A., Gut, J., Rosenthal, P.J., *et al*. 2007. Synthesis and biological evaluation of phenolic Mannich bases of banzaldehyde and (thio)semicarbazone derivatives against he cysteine protease falcipain-2 and a chloroquine resistant strain of *Plasmodium falciparum*. Bioorg Med Chem Lett 15, 273-282.

Chulay, J.D., Haynes, J.D., Diggs, C.L. 1983. *Plasmodium falciparum*: assessment of *in vitro* growth by [^{3}H]hypoxanthine incorporation. Exp Parasitol 55, 138-146.

Clark, I.A. & Cowden, W.B. 2003. The pathophysiology of *falciparum* malaria. Pharmacol Therapeut 99, 221-260.

Coetzee, M. & Fontenille, D. 2004. Advances in the study of *Anopheles fenestus*, a major vector of malaria in Africa. Insec Biochem Mol Biol 34, 599-605.

Cooke, B.M., Lingelbach, K., Bannister, L.H., *et al*. 2004. Protein trafficking in *Plasmodium falciparum*-infected red blood cells. Trends Parasitol 20(12), 581-589.

Coppens, I., Sullivan, D.J., Prigge, S.T. 2010. An update on the rapid advances on malaria parasite cell biology. Trends Parasitol 26, 305-310.

Cowman, A.F. & Crabb, B.S. 2006. Invasion of red blood cells by malaria parasites. Cell 124, 755-766.

Cui, H., Ruiz-Pérez, L.M., González-Pacanowska, D., *et al*. 2010. Potential application of thymidylate kinase in nucleoside analogue activation in *Plasmodium falciparum*. Bioorg Med Chem 18, 7302-7309.

d'Onofrio, G., Chirillo, R., Zini, G., *et al*. 1995. Simultaneous measurement of reticulocyte and the red blood cell indices in healthy subjects and patients with microcytic and macrocytic anemia. Blood 85(3), 819-823.

Dahl, E.L. & Rosenthal, P.J. 2005. Biosynthesis, localization, and processing of falcipain cysteine proteases of *Plasmodium falciparum.* Mol Biochem Parasitol 139, 205-212.

Dahl, E.L., Shock, J.L., Shenai, B.R., *et al*. 2006. Tetracyclines specifically target the apicoplast of the malaria parasite *Plasmodium falciparum.* Antimicrob Agents Chemother 50(9), 3124-3131.

Dasaradhi, P.V.N., Mohmmed, A., Kumar, A., *et al*. 2005. A role of falcipain-2, principal cysteine proteases of *Plasmodiun falciparum* in merozoite egression. Biochem Biophys Res Commun 336, 1062-1068.

De Clercq, E. 2007. The acyclic nucleoside phosphonates from inception to clinical use: Historical perspective. Antiviral Res 75, 1-13.

de Dios, A.C., Tycko, R., Ursos, L.M.B., *et al*. 2003. NMR studies of chloroquine-ferriprotoporphyrin IX complex. J Phys Chem A 107, 5821-5825.

de Oliveira, R.B., de Souza-Fagundes, E.M., Soares, R.P.P., *et al*. 2008. Synthesis and antimalarial activity of semicarbazone and thiosemicarbazone derivatives. Eur J Med Chem 43, 1983-1988.

de Rojas, M.O. & Wasserman, M. 1985. Temporal relationships on macromolecular synthesis during the asexual cell cycle of *Plasmodium falciparum*. Trans R Soc Trop Med Hyg 79, 792-796.

Deitch, A.D., Law, H., deVere White, R. 1982. A stable propidium iodide staining procedure for flow cytometry. J Histochem Cytochem 30(9), 967-972.

Delmas-Beauvieux, M.C., Peuchant, E., Dumon, M.F., *et al*. 1995. Relationship between red blood cell antioxidant enzymatic system status and lipoperoxidation during the acute phase of malaria. Clin Biochem 28(2), 163-169.

Deponte, M. & Becker, K. 2004. *Plasmodium falciparum*- do killers commit suicide? Trends Parasitol 20(4), 165-169.

Desjardins, R.E., Canfield, C.J., Haynes, J.D., *et al*. 1979. Quantatative assessment of antimalarial activity *in vitro* by a semiautomated microdilution technique. Antimicrob Agents Chemother 16(6), 710-718.

Dilović, I., Rubčić, M., Vrdoljak, V., *et al*. 2008. Novel thiosemicarbazone derivatives as potential antitumour agents: Synthesis, physicochemical and structural properties, DNA interactions and antiproliferative activity. Bioorg Med Chem 16, 5189-5198.

Ding, X., Xie, H., Kang, Y.J. 2011. The significance of copper chelators in clinical and experimental application. J Nutr Biochem 22, 301-310.

Doerig, C., Endicott, J., Chakrabarti, D. 2002. Cyclin-dependant kinase homologues of *Plasmodium falciparum*. Int J Parasitol 32, 1575-1585.

Domínguez, J.N., López, S., Charris, J., *et al*. 1997. Synthesis and antimalarial effects of phenothiazine inhibitors of a *Plasmodium falciparum* cysteine protease. J Med Chem 40, 2726-2732.

Domínguez, J.N., Charris, J.E., Lobo, G., *et al*. 2001. Synthesis of quinolinyl chalcones and evaluation of their antimalarial activity. Eur J Med Chem 36, 555-560.

Downie, M.J., Kirk, K., Mamoun, C.B. 2008. Purine salvage pathways in the intraerythrocytic malaria parasite *Plasmodium falciparum*. Eukaryot Cell 7(8), 1231-1237.

Edwards, D.I. 1979. Mechanism of antimicrobial action of metronidazole. J Antimicrob Chemother, 499-502.

Edwards, D.I. 1993. Nitroimidazole drugs-action and resistance mechanisms. J Antimicrob Chemother 31, 9-20.

Egan, T.J., Hunter, R., Kaschula, C.H., *et al*. 2000. Structure-function relationships in aminoquinolines: Effect of amino and chloro groups on quinoline-hematin complex formation, inhibition of β-haematin formation, and antiplasmodial activity. J Med Chem 43(2), 283-291.

Egan, T.J. 2003. Haemozoin (malaria pigment): a unique crystalline drug target. Targets 2(3), 115-124.

Egan, T.J. 2008. Haemozoin formation. Mol Biochem Parasitol 157, 127-136.

El Bissati, K., Zufferey, R., Witola, W.H., *et al*. 2006. The plasma membrane permease PfNT1 is essential for purine salvage in the human malaria parasite *Plasmodium falciparum*. Proc Natl Acad Sci U S A 103(4), 9286-9291.

El Bissati, K., Downie, M.J., Kim, S-K., *et al*. 2008. Genetic evidence for the essential role of *Pf*NT1 in the transport and utilization of xanthine, guanine, guanosine and adenine by *Plasmodium falciparum.* Mol Biochem Parasitol 161, 130-139.

Elandalloussi, L.M., Afonso, R., Nunes, A., *et al.* 2003. Effect of desferrioxamine and 2,2'-bipyridyl on the proliferation of *Perkinsus atlanticus.* Biomol Eng 20, 349-354.

Evans, S.G. & Havlik, I. 1993. *Plasmodium falciparum*: effects of amantadine, an antiviral, on chloroquine-resistant and -sensitive parasites *in vitro* and its influence on chloroquine activity. Biochem Pharmacol 45(5), 1168-1170.

Fanello, C.I., Karema, C., Ngamije, D., *et al*. 2008. A randomised trial to assess the efficacy and safety of chlorproguanil/dapsone + artesunate for the treatment of uncomplicated *Plasmodium falciparum* malaria. Trans R Soc Trop Med Hyg 102, 412-420.

Feng, T-S., Guantai, E.M., Nell, M., *et al*. 2011. Effects of highly active novel artemisinin-chloroquinoline hybrid compounds in β-haematin formation, parasite morphology and endocytosis in *Plasmodium falciparum*. Biochem Pharmacol 82, 236-247.

Ferrer, R., Lobo, G., Gamboa, N., *et al*. 2009. Synthesis of [(7-Chloroquinolin-4-yl)amino]chalcones: potential antimalarial and anticancer agents. Sci Pharm 77, 725-741.

Fidock, D.A., Rosenthal, P.J., Croft, S.L., *et al*. 2004. Antimalarial drug discovery: Efficacy models for compound screening. Nat Rev Drug Discov 3, 509-520.

Fidock, D.A., Eastman, R.T., Ward, S.A., *et al*. 2008. Recent highlights in antimalarial drug resistance and chemotherapy research. Trends Parasitol 24(12), 537-544.

Fletcher, B.L., Dillard, C.J., Tappel, A.L. 1973. Measurement of fluorescent lipid peroxidation products in biological systems and tissues. Anal Biochem 52, 1-9.

Florenta, I., Mouray, E., Ali, F.D., *et al*. 2000. Cloning of *Plasmodium falciparum* protein disulfide isomerise homologue by affinity purification using the antiplasmodial inhibitor 1,4-bis {3-[*N*-(cyclohexyl methyl)amino]propyl} piperazine. FEBS Lett 484, 246-252.

Frayha, G.J., Smyth, J.D., Gobert, J.G., *et al*. 1997. The mechanisms of action of antiprotozoal and antihelmintic drugs in man. Gen Pharmac 29(2), 273-299.

Freese, J.A., Sharp, B.L., Ridl, F.C., *et al*. 1988. *In vitro* cultivation of southern African strains of *Plasmodium falciparum* and gametocytogenesis. S Afr Med J 73, 720-722

Friesen, J. & Matuschewski, K. 2011. Comparative efficacy of pre-erythrocytic whole organism vaccine strategies against the malaria parasite. Vaccine 29, 7002-7008.

Frölich, S., Schubert, C., Bienzle, U., *et al*. 2005. *In vitro* antiplasmodial activity of prenylated chalcone derivatives of hops (*Humulus lupulus*) and their interaction with haemin. J Antimicrob Chemother 55, 883-887.

Garavito, G., Monje, M-C., Maurel, S., *et al*. 2007. A non-radiolabeled heme-GSH interaction test for the screening of antimalarial compounds. Exp Parasitol 116, 311-313.

Gardiner, D.L., Dixon, M.W.A., Spielmann, T., *et al*. 2005. Implication of a *Plasmodium falciparum* gene in the switch between asexual reproduction and gametocytogenesis. Mol Biochem Parasitol 140, 153-160.

Gavigan, C.S., Dalton, J.P., Bell, A. 2001. The role of aminopeptidases in haemoglobin degradation in *Plasmodium falciparum*-infected erythrocytes. Mol Biochem Parasitol 117, 37-48.

Gero, A.M., Dunn, C.G., Brown, D.M., *et al*. 2003. New malaria chemotherapy developed by utilization of a unique parasite transport system. Curr Pharm Des 9, 867-877.

Geyer, J.A., Prigge, S.T., Waters, N.C. 2005. Targeting malaria with specific CDK inhibitors. Biochim Biophys Acta 1754, 160-170.

Geyer, J.A., Keenan, S.M., Woodard, C.L., *et al*. 2009. Selective inhibition of *Pf*mrk, a *Plasmodium falciparum* CDK, by antimalarial 1,3-diaryl-2-propenones. Bioorg Med Chem Lett 19, 1982-1985.

Giles, F.J., Fracasso, P.M., Kantarjian, H.M., *et al*. 2003. Phase I and pharmacodynamic study of Triapine®, a novel ribonucleotide reductase inhibitor, in patients with advanced leukemia. Leuk Res 27, 1077-1083.

Ginsburg, H. 1988. Effects of calcium antagonists on malaria susceptibility to chloroquine. Parasitol Today 4(8), 209-211.

Ginsburg, H. "Malaria parasite metabolic pathways". Updated 24-03-2011. <http://sites.huji.ac.il/malaria/> [Accessed May-September 2011].

Go, M-L. 2003. Novel antiplasmodial agents. Med Res Rev 23(4), 456-487.

Go, M-L., Liu, M., Wilairat, P., *et al*. 2004. Antiplasmodial chalcones inhibit sorbitol-induced hemolysis of *Plasmodium falciparum*-infected erythrocytes. Antimicrob Agents Chemother 48(9), 3241-3245.

Goodman, C.D., Su, V., McFadden, G.I. 2007. The effects of anti-bacterials on the malaria parasite *Plasmodium falciparum.* Mol Biochem Parasitol 152, 181-191.

Grazul, M. & Budzisz, E. 2009. Biological activity of metal ions complexes of chromones, coumarins and flavones. Coord Chem Rev 253, 2588-2598.

Greenbaum, D.C., Mackey, Z., Hansell, E., *et al*. 2004. Synthesis and structure-activity relationships of parasiticidal thiosemicarbazone cysteine protease inhibitors against *Plasmodium falciparum*, *Trypanosoma brucei*, and *Trypanosoma cruzi*. J Med Chem 47, 3212-3219.

Greenwood, B.M., Fidock, D.A., Kyle, D.E., *et al*. 2008. Malaria: progress, perils, and prospects for eradication. J Clin Invest 118(4), 1266-1276.

Greenwood, B. & Targett, G. 2009. Do we still need a malaria vaccine? Parasite Immunol 31, 582-586.

Grellier, P., Šarlauskas, J., Anusevičius, Ž., *et al*. 2001. Antiplasmodial activity of nitroaromatic and quinoidal compounds: redox potential vs inhibition of erythrocyte glutathione reductase. Arch Biochem Biophys 393(2), 199-206.

Griffiths, M.J., Ndungu, F., Baird, K.L., *et al*. 2001. Oxidative stress and erythrocyte damage in Kenyan children with severe *Plasmodium falciparum* malaria. Br J Haematol 113, 486-491.

Grimberg, B.T., Erickson, J.J., Sramkoski, R.M., *et al*. 2008. Monitoring *Plasmodium falciparum* growth and development by UV flow cytometry using an optimized Hoechst-thiazole orange staining strategy. Cytometry A 73A, 546-554.

Grimberg, B.T. 2011. Methodology and application of flow cytometry for investigation of human malaria parasites. J Immunol Methods 367, 1-16.

Gronowicz, G., Swift, H., Steck, T.L. 1984. Maturation of the reticulocyte *in vitro*. J Cell Sci 71, 177-197.

Guantai, E.M., Ncokazi, K., Egan, T.J., *et al*. 2010. Design, synthesis and *in vitro* antimalarial evaluation of triazole-linked chalcone and dienone hybrid compounds. Bioorg Med Chem 18, 8243-8256.

Gülçin, I., Küfrevioglu, I., Oktay, M., *et al*. 2004. Antioxidant, antimicrobial, antiulcer and analgesic activities of nettle (*Urtica dioica* L.). J Ethnopharmacol 90, 205-215.

Gupte, A. & Buolamwini, J.K. 2004. Novel halogenated nitrobenzylthioinosine analogs as es nucleoside transporter inhibitors. Bioorg Med Chem Lett 14, 2257-2260.

Hamzah, J., Davis, T.M.E., Skinner-Adams, T.S., *et al*. 2004. Characterization of the effect of retinol on *Plasmodium falciparum in vitro*. Exp Parasitol 107, 136-144.

Hancock, C.N., Stockwin, L.H., Han, B., *et al*. 2011. A copper chelate of thiosemicarbazone NSC 689534 induces oxidative/ER stress and inhibits tumor growth *in vitro* and *in vivo*. Free Radic Biol Med 50, 110-121.

Hanssen, E., McMillan, P.J., Tilley, L. 2010. Cellular architecture of *Plasmodium falciparum*-infected erythrocytes. Int J Parasitol 40, 1127-1135.

Hare, J.D & Bahler, D.W. 1986. Analysis of *Plasmodium falciparum* growth in culture using acridine orange and flow cytometry. J Histochem Cytochem 34(2), 215-220.

Harmse, L., van Zyl, R., Gray, N., *et al*. 2001. Structure-activity relationships and inhibitory effects of various purine derivatives on the *in vitro* growth of *Plasmodium falciparum*. Biochem Pharmacol 62, 341-348.

Hayat, F., Moseley, E., Salahuddin, A., *et al*. 2011. Antiprotozoal activity of chloroquinolone based chalcones. Eur J Med Chem 46(5), 1897-1905.

Haynes, R.K., Monti, D., Taramelli, D., *et al*. 2003. Artemisinin antimalarials do not inhibit haemozoin formation. Antimicrob Agents Chemother 47(3), 1175.

Hocková, D., Holý, A., Masojídková, M., *et al*. 2009. Synthesis of branched 9-[2-(2-phosphonoethoxy)ethyl]purines as a new class of acyclic nucleoside phosphonates which inhibit *Plasmodium falciparum* hypoxanthine-guanine-xanthine phosphoribosyltransferase. Bioorg Med Chem 17, 6218-6232.

Hoffman, P.S., Goodwin, A., Johnsen, J., *et al*. 1996. Metabolic activities of metronidazole-sensitive and -resistant strains of *Helicobacter pylori*: respression of pyruvate oxidoreductase and expression of isocitrate lyase activity correlate with resistance. J Bacteriol 178(16), 4822-4829.

Hoffman, S.L., Subramanian, G.M., Collins, F.H., *et al.* 2002. *Plasmodium,* human and *Anopheles* genomics and malaria. Nature 415, 702-709.

Hughes, L.M., Lanteri, C.A., O'Neil, M.T., *et al*. 2011. Design of anti-parasitic and anti-fungal hydroxy-naphthoquinones that are less susceptible to drug resistance. Mol Biochem Parasitol 177, 12-19.

Hyde, J.E. 2005. Exploring the folate pathway in *Plasmodium falciparum*. Acta Trop 94(3), 191-206.

Hyde, J.E. 2007. Targeting purine and pyrimidine metabolism in human apicomplexan parasites. Curr Drug Targets 8(1), 31-47.

Jagetia, G. C., Venkatesha, V.A., Reddy, T.K. 2003. Naringin, a citrus flavonone, protects against radiation-induced chromosome damage in mouse bone marrow. Mutagenesis 18(4), 337-343.

Jana, S. & Paliwal, J. 2007. Novel molecular targets for antimalarial chemotherapy. Int J Antimicrob Agents 30, 4-10.

Jefford, C.W. 2007. New developments in synthetic peroxidic drugs as artemisinin mimics. Drug Discov Today 12(11/12), 487-495.

Jenks, P.J. & Edwards, D.I. 2002. Metronidazole resistance in *Helicobacter pylori*. Int J Antimicrob Agents 19, 1-7.

Jensen, J.B. & Trager, W. 1978. *Plasmodium falciparum* in culture: establishment of additional strains. Am J Trop Med Hyg 27(4), 743-746.

Johnson, D.J., Owen, A., Plant, N., *et al*. 2008. Drug-related expression *of Plasmodium falciparum* P-glycoprotein homologue 1: a putative role for nuclear receptors. Antimicrob Agents Chemother 52(4), 1438-1445.

Jouin, H., Daher, W., Khalife, J., *et al*. 2003. Double staining of *Plasmodium falciparum* nucleic acids with hydroethidine and thiazole orange for cell cycle analysis by flow cytometry. 2004. Cytometry A 57A, 34-38.

Jullian, V., Bonduelle, C., Valentin, A., *et al*. 2005. New clerodane diterpenoids from *Laetia procera* (Poepp.) Eichler (Flacourtiaceae), with antiplasmodial and antileishmanial activities. Bioorg Med Chem Lett 15, 5065-5070.

Kanagaratnam, R., Misiura, K., Rebowski, G., *et al*. 1998. Malaria merozoite surface protein antisense oligodeoxynucleotides lack antisense activity but function as polyanions to inhibit red cell invasion. Int J Biochem Cell Biol 30, 979-985.

Kannan, R., Kumar, K., Sahal, D., *et al*. 2005. Reaction of artemisinin with haemoglobin: implications for antimalarial activity. Biochem J 385, 409-418.

Kaur, K., Jain, M., Kaur, T., *et al*. 2009. Antimalarials from nature. Bioorg Med Chem 17, 3229-3256.

Keenan, S.M., Geyer, J.A., Welsh, W.J., *et al*. 2005. Rational inhibitor design and iterative screening in the identification of selective plasmodial cyclin dependant kinase inhibitors. Comb Chem High Throughput Screen 8, 27-38.

Keough, D.T., Hocková, D., Krečmerová, M., *et al*. 2010. *Plasmodium vivax* hypoxanthine-guanine phosphoribosyltransferase: A target for anti-malarial chemotherapy. Mol Biochem Parasitol 173, 165-169.

Kerb, R., Fux, R., Mörike, K., *et al*. 2009. Pharmacogenetics of antimalarial drugs: effect on metabolism and transport. Lancet Infect Dis 9, 760-774.

Khan, S.A., Kumar, P., Joshi, R., *et al*. 2008. Synthesis and *in vitro* antibacterial activity of new steroidal thiosemicarbazone derivatives. Eur J Med Chem 43, 2029-2034.

Khan, S.M., Franke-Fayard, B., Mair, G.R., *et al*. 2005. Proteome analysis of separated male and female gametocytes reveals novel sex-specific *Plasmodium* biology. Cell 121, 675-687.

Kiss, T., Lázár, I., Kafarski, P. 1994. Chelating tendencies of bioactive aminophosphonates. Met Based Drugs 1(2-3), 247-264.

Klayman, D.L., Bartosevich, J.F., Griffin, T.S., *et al*. 1979. 2-Acetylpyridine thiosemicarbazones. 1. A new class of potential antimalarial agents. J Med Chem 22(7), 855-862.

Knockaert, M., Greengard, P., Meijer, L. 2002. Pharmacological inhibitors of cyclin-dependant kinases. Trends Pharmacol Sci 23(9), 417-425.

Kolbe, L., Immeyer, J., Batzer, J., *et al*. 2006. Anti-inflammatory efficacy of Licochalcone A: correlation of clinical potency and *in vitro* effects. Arch Dermatol Res 298, 23-30.

Koury, M.J., Koury, S.T., Kopsombut, P., *et al*. 2005. *In vitro* maturation of nascent reticulocytes to erythrocytes. Blood 105(5), 2168-2174.

Kouznetsov, V.V. & Gómez-Barrio, A. 2009. Recent developments in the design and synthesis of hybrid molecules based on aminoquinoline ring and their antiplasmodial evaluation. Eur J Med Chem 44, 3091-3113.

Kremsner, P.G & Krishna, S. 2004. Antimalarial combinations. Lancet 364, 285-294.

Krishna, S., Bustamante, L., Haynes, R.K., *et al*. 2008. Artemisinins: their growing importance in medicine. Trends Pharmacol Sci 29(10), 520-527.

Krishna, S., Pulcini, S., Fatih, F., *et al*. 2010. Artemisinins and the biological basis for the *Pf*ATP6/SERCA hypothesis. Trends Parasitol 26(11), 517-523.

Kulda, J. 1999. Trichomonads, hydrogenosomes and drug resistance. Int J Parasitol 29, 199-212.

Kumar, S., Guha, M., Choubey, V., *et al*. 2007. Antimalarial drugs inhibiting hemozoin (β-hematin) formation: a mechanistic update. Life Sci 80, 813-828.

Lambros, C. & Vanderberg, J.P. 1979. Synchronization of *Plasmodium falciparum* erythrocytic stages in culture. J Parasitol 65(3), 418-420.

Land, K.M., Gelgadillo, M.G., Johnson, P.J. 2002. *In vivo* expression of ferredoxin in a drug resistance trichomonad increases metronidazole susceptibility. Mol Biochem Parasitol 121, 153-157.

Lazarus, M.D., Schneider, T.G., Taraschi, T.F. 2008. A new model for haemoglobin ingestion and transport by the human malaria parasite *Plasmodium falciparum.* J Cell Sci 121(11), 1937-1949.

Lehane, A.D., Hayward, R., Saliba, K.J., *et al*. 2008. A verapamil-sensitive chloroquine-associated H^+ leak from the digestive vacuole in chloroquine-resistant malaria parasites. J Cell Sci 121, 1624-1632.

LePecq, J.B. & Paoletti, C. 1967. A fluorescent complex between ethidium bromide and nucleic acids. J Mol Biol 27, 87-106.

Liberta, A.E. & West, D.X. 1992. Antifungal and antitumour activity of heterocyclic thiosemicarbazones and their metal complexes: current status. Biometals 5, 121-126.

Lim, L. & McFadden, G.I. 2010. The evolution, metabolism and functions of the apicoplast. Phil Trans R Soc B 365, 749-763.

Lin, W. & Buolamwini, J.K. 2007. Synthesis, flow cytometric evaluation, and identification of highly potent dipyridamole analogues as equilibrative nucleoside transporter 1 inhibitors. J Med Chem 50, 3906-3920.

Liu, M., Wilairat, P., Go, M-L. 2001. Antimalarial alkoxylated and hydroxylated chalcones: structure-activity relationship analysis. J Med Chem 44, 4443-4452.

López, M.L., Vommario, R., Zalis, M., *et al*. 2010. Induction of cell death on *Plasmodium falciparum* asexual blood stages by *Solanum nudum* steroids. Parasitol Int 59, 217-225.

Mabeza, G.F., Loyevsky, M., Gordeuk, V.R., *et al*. 1999. Iron chelation therapy for malaria: A review. Pharmacol Ther 81(1), 53-75.

Mackenzie, M.J., Saltman, D., Hirte, H., *et al*. 2007. A Phase II study of 3-aminopyridine-2-carboxaldehyde thiosemicarbazone (3-AP) and gemcitabine in advanced pancreatic carcinoma. A trial at the Princess Margaret Hospital Phase II consortium. Invest New Drugs 25, 553-558.

Makler, M.T., Lee, L.G., Recktenwald, D. 1987. Thiazole orange: a new dye for *Plasmodium* species analysis. Cytometry 8, 568-570.

Malkin, E.M., Diemert, D.J., McArthur, J.H., *et al*. 2005. Phase 1 clinical trial of apical membrane antigen 1: an asexual blood-stage vaccine for *Plasmodium falciparum* malaria. Infect Immun 73(6), 3677-3685.

Marti, M., Baum, J., Rug, M., *et al*. 2005. Signal-mediated export of proteins from the malaria parasite to the host erythrocyte. J Cell Biol 171(4), 587-592.

Martin, R.E., Henry, R.I., Abbey, J.L., *et al*. 2005. The 'permeome' of the malaria parasite: an overview of the membrane transport proteins of *Plasmodium falciparum*. Genome Biol 6(3), R26.1-R26.22.

Martirosyan, A.R., Rahim-Bata, R., Freeman, A.B., *et al*. 2004. Differentiation-inducing quinolines as experimental breast cancer agents in the MCF-7 human breast cancer model. Biochem Pharmacol 68, 1729-1738.

Mehrotra, S., Bopanna, M.P., Bulusu, V., *et al*. 2010. Adenine metabolism in *Plasmodium falciparum.* Exp Parasitol 125, 147-151.

Mendz, G.L. & Mégraud, F. 2002. Is the molecular basis of metronidazole resistance in microaerophilic organisms understood? Trends Microbiol 10(8), 370-375.

Meshnick, S.R. 2002. Artemisinin: mechanism of action, resistance and toxicity. Int J Parasitol 32, 1655-1660.

Meza-Avina, M.E., Wei, L., Liu, Y., *et al*. 2010. Structural determinants for the inhibitory ligands of orotidine-5'-monophosphate decarboxylase. Bioorg Med Chem 18, 4032-4041.

Miller, L.H., Baruch, D.I., Marsh, K., *et al*. 2002. The pathogenic basis of malaria. Nature 415, 673-679.

Mills, J.P., Diez-Silva, M., Quinn, D.J., *et al*. 2007. Effect of plasmodial RESA on deformability of human red blood cells harbouring *Plasmodium falciparum*. Proc Natl Acad Sci U S A 104(22), 9213-9217.

Mishra, N., Arora, P., Kumar, B., *et al*. 2008. Synthesis of novel substituted 1,3-diaryl propenone derivatives and their antimalarial activity *in vitro*. Eur J Med Chem 43, 1530-1535.

Müller, I.B., Hyde, J.E., Wrenger, C. 2010. Vitamin B metabolism in *Plasmodium falciparum* as a source of drug targets. Trends Parasitol 26(1), 35-43.

Müller, S. 2004. Redox and antioxidant systems of the malaria parasite *Plasmodium falciparum*. Mol Microbiol 53(5), 1291-1305.

Muregi, F.W., Kano, S., Kino, H., *et al*. 2009. *Plasmodium berghei*: Efficacy of 5-fluoroorotate in combination with commonly used antimalarial drugs in a mouse model. Exp Parasitol 121, 376-380.

Muregi, F.W. & Ishih, A. 2010. Next-generation antimalarial drugs: hybrid molecules as a new strategy in drug design. Drug Dev Res 71, 20-32.

Murren, J., Modiana, M., Clairmont, C., *et al*. 2003. Phase I and pharmacokinetic study of Triapine, a potent ribonucleotide reductase inhibitor, administered daily for five days in patients with advanced solid tumors. Clin Cancer Res 9, 4092-4100.

Musonda, C.C., Whitlock, G.A., Witty, M.J., *et al*. 2009. Synthesis and evaluation of 2-pyridyl pyrimidines with *in vitro* antiplasmodial and antileishmanial activity. Bioorg Med Chem Lett 19, 401-405.

Nadelmann, L., Tjørnelund, J., Hansen, S.H., *et al*. 1997. Synthesis, isolation and identification of glucuronides and mercapturic acids of a novel antiparasitic agent, licochalcone A. Xenobiotica 27(7), 667-680.

National Department of Health. 2009. Guidelines for the prevention of malaria in South Africa. www.doh.gov.za, accessed on the 11th Febraury 2011.

National Department of Health. 2010. Guidelines for the treatment of malaria in South Africa. www.doh.gov.za, accessed on the 11th Febraury 2011.

Naughton, J.A., Nasizadeh, S., Bell, A. 2010. Downstream effects of haemoglobinase inhibition in *Plasmodium falciparum*-infected erythrocytes. Mol Biochem Parasitol 173, 81-87.

Nishiyama, T., Suzuli, T., Hashiguchi, Y., *et al*. 2002. Antioxidant activity of aromatic and cyclic amine derivatives. Polym Degrad Stabil 75, 549-554.

Nolan, J.P., Lauer, S., Prossnitz, E.R., *et al*. 1999. Flow cytometry: a versatile tool for all phases of drug discovery. Drug Discov Today DDT 4(4), 173-180.

Nosten, F. & Brasseur, P. 2002. Combination therapy for malaria: the way forward? Drugs 62(9), 1315-1329.

Nowakowska, Z. 2007. A review of anti-infective and anti-infammatory chalcones. Eur J Med Chem 42, 125-137.

Nzila, A. 2006. Inhibitors of *de novo* folate enzymes in *Plasmodium falciparum*. Drug Discov Today 11(19/20), 939-943.

O'Neill, P.M & Posner, G.H. 2004. A medicinal chemistry perspective on artemisinin and related endoperoxides. J Med Chem 47(12), 2945-2964.

Olive, P.L. 1989. Hydroethidine: a fluorescent redox probe for locating hypoxic cells in spheroids and murine tumours. Br J Cancer 60, 332-338.

Olliaro, P. 2001. Mode of action and mechanisms of resistance for antimalarial drugs. Pharmacol Therapeut 89, 207-219.

Olszewski, K.L., Mather, M.W., Morrisey, J.M., *et al*. 2010. Branched tricarboxylic acid metabolism in *Plasmodium falciparum*. Nature 466, 774-778.

Padmanaban, G., Nagaraj, V.A., Rangarajan, P.N. 2007. Drugs and drug targets in malaria. Curr Sci 92(11), 1545-1555.

Pandey, A.V., Tekwani, B.L., Singh, R.L., *et al*. 1999. Artemisinin, an endoperoxide antimalarial, disrupts the haemoglobin catabolism and heme detoxification systems in malarial parasite. J Biol Chem 274(27), 19383-19388.

Papalexis, V., Siomos, M-A., Campanale, N.M., *et al*. 2001. Histidine-rich protein 2 of the malaria parasite, *Plasmodium falciparum*, is involved in detoxification of the by-products of haemoglobin degradation. Mol Biochem Parasitol 115, 77-86.

Papapostolou, I., Patsoukis, N., Georgiou, C.D. 2004. The fluorescence detection of superoxide radical using hydroethidine could be complicated by the presence of heme proteins. Anal Biochem 332, 290-298.

Parker, M.D., Hyde, R.J., Yao, S.Y.M., *et al*. 2000. Identification of a nucleoside/nucleobase transporter from *Plasmodium falciparum*, a novel target for anti-malarial chemotherapy. Biochem J 349, 67-75.

Pattanapanyasat, K., Thaithong, S., Kyle, D.E., *et al*. 1997. Flow cytometric assessment of hydroxypyridinone iron chelators on the *in vitro* growth of drug-resistant malaria. Cytometry 27, 84-91.

Postma, N.S., Mommers, E.C., Eling, W.M.C., *et al*. 1996. Oxidative stress in malaria; implications for prevention and therapy. Pharm World Sci, 121-129.

Pradines, B., Rogier, C., Fusai, T., *et al*. 2001. *In vitro* activities of antibiotics against *Plasmodium falciparum* are inhibited by iron. Antimicrob Agents Chemother 45(6), 1746-1750.

Pradines, B., Rolain, J.M., Ramiandrasoa, F., *et al*. 2002. Iron chelators as antimalarial agents: *in vitro* activity of dicatecholate against *Plasmodium falciparum*. J Antimicrob Chemother 50, 177-187.

Prathima, B., Rao, Y.S., Ramesh, G.N., *et al*. 2011. Synthesis, spectral characterisation and biological activities of Mn(II) and Co(II) complexes with benzyloxybenzaldehyde-4-phenyl-3-thiosemicarbazone. Spectrochim Acta A Mol Biomol Spectrosc 79, 39-44.

Quaye, I.K. 2008. Haptoglobin, inflammation and disease. Trans R Soc Trop Med Hyg 102, 735-742.

Ramasamy, R., Kanagaratnam, R., Misiura, K., *et al*. 1996. Anti-sense oligodeoxynucleoside phosphorothioates nonspecifically inhibit invasion of red blood cells by malaria parasites. Biochem Biophys Res Commun 218, 930-933.

Rasoloson, D., Shi, L., Chong, C.R., *et al*. 2004. Copper pathways in *Plasmodium falciparum* infected erythrocytes indicate an efflux role for the copper P-ATPase. Biochem J 381, 803-811.

Rejman, D., Kovačková, S., Pohl, R., *et al*. 2009. A convenient, high-yield synthesis of 1-substituted uracil and thymine derivatives. Tetrahedron 65, 8513-8523.

Rejman, D., Rabatinová, A., Pombinho, A.R., *et al*. 2011. Lipophosphonoxins: new modular molecular structures with significant antibacterial properties. J Med Chem 54(22), 7884-7898.

Ren, W., Qiao, Z., Wang, H., *et al*. 2003. Flavonoids: promising anticancer agents. Med Res Rev 23(4), 519-534.

Riegelhaupt, P.M., Cassera, M.B., Fröhlich, R.F.G., *et al*. 2010. Transport of purines and purine salvage pathway inhibitors by the *Plasmodium falciparum* equilibrative nucleoside transporter *Pf*ENT1. Mol Biochem Parasitol 169, 40-49.

Rodenko, B., Detz, R.J., Pinas, V.A., *et al*. 2006. Solid phase synthesis and antiprotozoal evaluation of di- and trisubstituted 5'-carboxamidoadenosine analogues. Bioorg Med Chem 14, 1618-1629.

Rodriguez-Lucena, D., Schalk, I.J., Mislin, G.L.A. 2011. Synthesis of triethylene-tetramine bridged bis-tridentate iron(III) chelators. Tetrahedron 67, 2149-2154.

Rosenthal, P.J. 1995. *Plasmodium falciparum*: effects of proteinase inhibitors on globin hydrolysis by cultured malaria parasites. Exp Parasitol 80, 272-281.

Rosenthal, P.J & Meshnick, S.R. 1996. Hemoglobin catabolism and iron utilization by malaria parasites. Mol Biochem Parasitol 83, 131-139.

Rosenthal, P.J. 2009. Chapter 52: antiprotozoal drugs. In: Katzung, B.G., Masters, S.B., Trevor, A.J., editors. Basic and Clinical Pharmacology, 11th edition <http://0-www.accesspharmacy.com.innopac.wits.ac.za/content.aspx?aID=4516313> [Accessed 17 December 2011]

Rossiter, D. 2010. South African Medicines Formulary. Ninth edition. Barnes, K.I., Cohen, K., Decloedt, E., Gounden, R., Kredo, T., Maartens, G., McIlleron, H., Orrell, C., Sinxadi, P.Z., van der Walt, J-S, editors. Health and Medical Publishing Group. South Africa. 196, 216, 500-510.

Roudeau, R., Gomez Pardo, D., Cossy, J. 2006. Enantioselective diethylzinc addition to aromatic and aliphatic aldehydes using (3*R*,5*R*)-dihydroxypiperidine derivatives catalyst. Tetrahedron 62, 2388-2394.

Saito, H. & Ishihara, K. 1997. Antioxidant activity and active sites of phospholipids as antioxidants. J Am Oil Chem Soc 74(12), 1531-1536.

Saito-Ito, A., Akai, Y., He, S., *et al*. 2001. A rapid, simple and sensitive flow cytometric system for detection of *Plasmodium falciparum*. Parasitol Int 50, 249-257.

Samuelson, J. 1999. Why metronidazole is active against both bacteria and parasites. Antimicrob Agents Chemother 43(7), 1533-1541.

Sanchez, C.P., Dave, A., Stein, W.D., *et al*. 2010. Transporters as mediators of drug resistance in *Plasmodium falciparum*. Int J Parasitol 40, 1109-1118.

Sauerwein, R.W. 2009. Clinical malaria vaccine development. Immunol Lett 122, 115-117.

Schulze, D.L.C., Makgatho, E.M., Coetzer, T.L., *et al*. 1997. Development and application of a modified flow cytometric procedure for rapid *in vitro* quantification of malaria parasitaemia. S Afr J Sci 93, 156-158.

Scott, C.S., van Zyl, D., Ho, E., *et al*. 2002. Patterns of pseudo-reticulocytosis in malaria: fluorescent analysis with the Cell-Dyn® CD4000. Clin Lab Haem 24, 15-20.

Sharma, M., Chaturvedi, V., Manju, Y.K., *et al*. 2009. Substituted quinolinyl chalcones and quinolinyl pyrimidines as a new class of anti-infective agents. Eur J Med Chem 44(5), 2081-2091.

Sharma, P. & Sharma, J.D. 2001. *In vitro* hemolysis of human erythrocytes- by plant extracts with antiplasmodial activity. J Ethnopharmacol 74, 239-243.

Sharma, V. 2005. Therapeutic drugs for targeting chloroquine resistance in malaria. Mini Rev Med Chem 5, 337-351.

Skinner-Adams, T.S., Stack, C.M., Trenholme, K.R., *et al*. 2009. *Plasmodium falciparum* neutral aminopeptidases: new targets for anti-malarials. Trends Biochem Sci 35(1), 53-61.

Sklar, L.A., Carter, M.B., Edwards, B.S. 2007. Flow cytometry for drug discovery, receptor pharmacology and high-throughput screening. Curr Opin Pharmacol 7, 527-534.

Smeijsters, L.J.J.W., Franssen, F.F.J., Naesens, L., *et al*. 1999. Inhibition of the *in vitro* growth of *Plasmodium falciparum* by acyclic nucleoside phosphonates. Int J Antimicrob Agents 12, 53-61.

Solomon, V.R. & Lee, H. 2009. Chloroquine and its analogs: a new promise of an old drug for effective and safe cancer therapies. Eur J Pharmacol 625, 220-233.

Solyakov, L., Halbert, J., Alam, M.M., *et al*. 2011. Global kinomic and phospho-proteomic analyses of the human malaria parasite *Plasmodium falciparum.* Nat Commun. DOI: 10.1038/ncomms1558.

Soni, S., Dhawan, S., Rosen, K.M., *et al*. 2005. Characterization of events preceding the release of malaria parasite from the host red blood cell. Blood Cells Mol Dis 35, 201-211.

Spanou, C., Manta, S., Komiotis, D., *et al*. 2007. Antioxidant activity of a series of fluorinated pyrano-nucleoside analogues of N^4-benzoyl cytosine and N^6-benzoyl adenine. Int J Mol Sci 8, 695-704.

Spielmann, T., Fergusen, D.J.P., Beck, H-P. 2003. *etramps*, a new *Plasmodium falciparum* gene family coding for developmentally regulated and highly charged membrane proteins located at the parasite-host cell interface. Mol Biol Cell 14, 1529-1544.

Spielmann, T., Hawthorne, P.L., Dixon, M.W.A., *et al*. 2006. A cluster of ring stage-specific genes linked to a locus implicated in cytoadherence in *Plasmodium falciparum* codes for PEXEL-negative and PEXEL-positive proteins exported into the host cell. Mol Biol Cell 17, 3613-3624.

Spycher, C., Rug, M., Klonis, N., *et al*. 2006. Genesis of and trafficking to the maurer's clefts of *Plasmodium falciparum*-infected erythrocytes. Mol Cell Biol 26(11), 4074-4084.

Suk, D-H., Rejman, D., Dykstra, C.C., *et al*. 2007. Phosphonoxins: rational design and discovery of a potent nucleotide anti-*Giardia* agent. Bioorg Med Chem Lett 17, 2811-2816.

Sullivan, D.J. 2002. Theories on malarial pigment formation and quinoline action. Int J Parasitol 32, 1645-1653.

Takahashi, T., Takasuka, N., Ligo, M., *et al*. 2004. Isoliquiritigenin, a flavonoid from licorice, reduces prostaglandin E_2 and nitric oxide, causes apoptosis, and suppresses aberrant crypt foci development. Cancer Sci 95(5), 448-453.

The RTS,S Clinical Trials Partnership. 2011. First results of phase 3 trial of RTS,S/AS01 malaria vaccine in African children. N Engl J Med 365(20), 1863-1875.

Tilley, L., Dixon, M.W.A., Kirk, K. 2011. The *Plasmodium falciparum*-infected red blood cell. Int J Biochem Cell Biol 43, 839-842.

Totino, P.R.R., Daniel-Ribeiro, C.T., Corte-Real, S., *et al*. 2008. *Plasmodium falciparum*: Erythrocytic stages die by autophagic-like cell death under drug pressure. Exp Parasitol 118, 478-486.

Trager, W. & Jensen, J.B. 1976. Human malaria parasites in continuous culture. Science 193(4254), 673-675.

van der Heyde, H.C., Elloso, M.M., vande Waa, J., *et al*. 1995. Use of hydroethidine and flow cytometry to assess the effects of leukocytes on the malarial parasite *Plasmodium falciparum*. Clin Diagn Lab Immunol 2(4), 417-425.

van Dooren, G.G., Marti, M., Tonkin, C.J., *et al*. 2005. Development of the endoplasmic reticulum, mitochondrion and apicoplast during the asexual life cycle of *Plasmodium falciparum*. Mol Microbiol 57(2), 405-419.

van Schalkwyk, D.A & Egan, T.J. 2006. Quinoline-resistance reversing agents for the malaria parasite *Plasmodium falciparum*. Drug Resist Updat 9, 211-226.

van Vianen, P.H., van Engen, A., Thaithong, S., *et al*. 1993. Flow cytometric screening of blood samples for malaria parasites. Cytometry 14, 276-280.

Vanderberg, J.P. 2009. Reflections on early malaria vaccine studies, the first successful human malaria vaccination, and beyond. Vaccine 27, 2-9.

Vanék, V., Buděšínsky, M., Rinnová, M., *et al*. 2009. Prolinol-based nucleoside phosphonic acids: new isoteric conformationally flexible nucleotide analogues. Tetrahedron 65, 862-876.

Vangapandu, S., Jain, M., Kaur, K., *et al*. 2007. Recent advances in antimalarial drug development. Med Res Rev 27(1), 65-107.

Verhaeghe, P., Azaz, N., Hutter, S., *et al*. 2009. Synthesis and *in vitro* antiplasmodial evaluation of 4-anilino-2-trichloromethylquinazolines. Bioorg Med Chem 17(13), 4313-4322.

Vinetz, J.M., Clain, J., Bounkeua, V., *et al*. 2011. Chapter 49: Chemotherapy of malaria. In: Vinetz, J.M., Clain, J., Bounkeua, V., Eastman, R.T., Fidock, D., editors. Goodman & Gilman's the Pharmacological Basis of Therapeutics, 12th edition <http://0-www.accesspharmacy.com.innopac.wits.ac.za/content.aspx?aID=16676038> [Accessed 17 December 2011]

von Gadow, A., Joubert, E., Hansmann, C.F. 1997. Comparison of the antioxidant activity of aspalathin with that of other plant phenols of rooibos tea (*Aspalathus linearis*), α-tocopherol, BHT, and BHA. J Agric Food Chem 45, 632-638.

Wagner, M.A., Andemariam, B., Desai, S.A. 2003. A two-compartment model of osmotic lysis in *Plasmodium falciparum*-infected erythrocytes. Biophys J 84, 116-123.

Waki, S., Tamura, J., Jingu, M., *et al*. 1986. A new technique for drug susceptibility tests for *Plasmodium falciparum* by ethidium bromide fluoroassay. Trans R Soc Trop Med Hyg 80, 47-49.

Waller, A., Simons, P.C., Biggs, S.M., *et al*. 2004. Techniques: GPCR assembly, pharmacology and screening by flow cytometry. Trends Pharmacol Sci 25(12), 663-669.

Walsh, J.J. & Bell, A. 2009. Hybrid drugs for malaria. Curr Pharm Des 15, 2970-2985.

Wegener, J.W. & Nawrath, H. 1997. Cardiac effects of isoliquiritigenin. Eur J Pharmacol 326, 37-44.

Whaun, J.M., Rittershaus, C., Ip, S.H.C. 1983. Rapid identification and detection of parasitized human red cells by automated flow cytometry. Cytometry 4, 117-122.

White, N.J. 2004. Antimalarial drug resistance. J Clin Invest 113(8), 1084-1092.

Wielinga, P.R., Reid, G., Challa, E.E., *et al*. 2002. Thiopurine metabolism and identification of the thiopurine metabolites transported by MRP4 and MRP5 overexpressed in human embryonic kidney cells. Mol Pharmacol 62(6), 1321-1331.

Wilairatana, P., Krudsood, S., Treeprasertsuk, S., *et al*. 2002. The future outlook of antimalarial drugs and recent work on the treatment of malaria. Arch Med Res 33, 416-421.

Wirth, D.F. 2002. The parasite genome: biological revelations. Nature 419, 495-496.

Wissing, F., Sanchez, C.P., Rohrbach, P., *et al*. 2002. Illumination of the malaria parasite *Plasmodium falciparum* alters intracellular pH. J Biol Chem 277(40), 37747-37755.

World Health Organisation (WHO). 2010a. Basic Malaria Microscopy Part I. Learner's guide, Second Edition. WHO Geneva. www.who.int, accessed 10th Febraury 2011.

World Health Organisation (WHO) 2010b. Guidelines for the treatment of malaria, second edition. WHO Geneva. www.who.int, accessed on 10th Febraury 2011.

World Health Organisation (WHO). 2010c. World malaria report. WHO Geneva. www.who.int, accessed 10th Febraury 2011.

World Health Organisation (WHO). 2011. World malaria report. WHO Geneva. www.who.int, accessed 23rd December 2011.

Wozniacka, A., Carter, A., McCauliffe, DP. 2002. Antimalarials in cutaneous lupus erythromatosus: mechanisms of therapeutic benefit. Lupus 11, 71-81.

www.rollbackmalaria.com, accessed 20th December 2011.

Wyatt, C.R., Goff, W., Davis, W.C. 1991. A flow cytometric method for assessing viability of intraerythrocytic hemoparasites. J Immunol Methods 140, 23-30.

Zhan, Y., Dong, C-H., Yao, Y-J. 2006. Antioxidant activities of aqueous extract from cultivated fruit-bodies of *Cordyceps militaris* (L.) link *in vitro*. J Integr Plant Biol 48(11), 1365-1370.

Zhao, H., Kalivendi, S., Zhang, H., *et al*. 2003. Superoxide reacts with hydroethidine but forms a fluorescent product that is distinctly different from ethidium: potential implications in intracellular fluorescence detection of superoxide. Free Radic Biol Med 34(11), 1359-1368.

Zhong, Z., Zhong, Z., Xing, R., *et al*. 2010. The preparation and antioxidant activity of 2-[phenylhydrazine (or hydrazine)-thiosemicarbazone]-chitosan. Int J Biol Macromol 47, 93-97.

Ziegler, H.L., Stærk, D., Christensen, J., *et al*. 2002. *In vitro Plasmodium falciparum* drug sensitivity assay: inhibition of parasite growth by incorporation of stomatocytogenic amphiphiles into the erythrocytic membrane. Antimicrob Agents Chemother 46(5), 1442-1446.

Ziegler, H.L., Franzyk, H., Sairafianpour, M., *et al*. 2004. Erythrocyte membrane modifying agents and the inhibition of *Plasmodium falciparum* growth: structure-activity relationships for betulinic acid analogues. Bioorg Med Chem 12, 119-127.

Zielonka, J. & Kalyanaraman, B. 2010. Hydroethidine- and MitoSOX-derived red fluorescence is not a reliable indicator of intracellular superoxide formation: Another inconvenient truth. Free Radic Biol Med 48, 983-1001.

APPENDIX A: CONFERENCE PRESENTATIONS AND PUBLICATIONS

Appendix A1: (Poster presentation: The 5th International Conference on Pharmaceutical and Pharmacological Sciences, Potchefstroom, 2009)

The Antimalarial Properties of Metronidazole Thiosemicarbazone Analogues

Emma J. Moseley[1], Robyn L. van Zyl[1*], Mohammad Abid[2], Ivan Havlik[1], Amir Azam[2]
[1]Pharmacology Division, Department of Pharmacy and Pharmacology, University of the Witwatersrand, Johannesburg, South Africa.
[2]Department of Chemistry, Jamia Millia Islamia, Delhi, India.
*Corresponding author: Robyn.vanZyl@wits.ac.za

Introduction:
Ninety percent of malaria cases reported in sub-Saharan Africa are due to the *Plasmodium falciparum* parasite. For decades malaria chemotherapy has hinged on a limited range of drugs, with the parasite developing resistance to some. This has initiated an urgent search for novel compounds with unique mechanisms of action against plasmodia species. Metronidazole is commonly used against bacterial and protozoal infections by causing DNA damage through free-radical damage. Thiosemicarbazones are a small class of compounds which have shown to have profound antiviral, antifungal, antitumour and antimalarial effects.

Aims:
To examine the effects of a series of metronidazole-thiosemicarbazone analogues on the *in vitro* growth of *P. falciparum*, elucidate a possible mechanism of action, as well as assess the toxicity of these compounds.

Methods:
Metronidazole thiosemicarbazone analogues were synthesized wherein the thioamide moiety was substituted by different cyclic and aromatic amines. The *P. falciparum* chloroquine-sensitive strain (3D7) was maintained continuously in culture. For assessment of antimalarial activity, the tritiated hypoxanthine incorporation assay was employed. From the data generated the concentration required to inhibit parasite growth by 50% (IC_{50} value) was obtained. To determine a possible mechanism of action, the effects of the compounds on β-haematin formation was examined. To assess the toxicity of these compounds a red blood cell toxicity assay was performed.

Results:
The results obtained showed that all but one of the compounds inhibited parasite growth, with IC_{50} values below 10µM. Results from the β-haematin assay indicated that all but two of the compounds were able to completely inhibit β-haematin formation by an average of 95% at a mole:mole ratio of less than one for drug:haemin. Some of the compounds inhibited β-haematin formation as effectively as quinine. Red blood cell toxicity results indicated negligible amounts of red blood cell lysis and were comparable to those of quinine and metronidazole alone.
Overall, (1E)-1-(4-((E)-2-(1-(2-hydroxyethyl)-5-nitro-1H-imidazol-2-yl)vinyl)benzylidene)-4-cyclooctylthiosemicarbazide (**Y1**) and (1E)-4-(2-chlorobenzyl)-1-(4-((E)-2-(1-(2-hydroxyethyl)-

5-nitro-1H-imidazol-2-yl)vinyl)benzylidene)thiosemicarbazide (**Y3**) were the most active, with IC_{50} values of 2.99 ± 0.10µM and 2.89 ± 0.09µM respectively, as well as possessing the best safety profile.

Conclusion:

The above results indicate that these compounds show promising antimalarial activity, but require further attention to determine their combined interaction when used with classic antimalarials.

Appendix A2: (Poster presentation: WorldPharma 2010, the 16th World Congress of Basic and Clinical Pharmacology, Copenhagen, 2010)

The Antimalarial Properties of Metronidazole Thiosemicarbazone Analogues

Emma J. Moseley[1], Robyn L. van Zyl[1*], Mohammad Abid[2], Ivan Havlik[1], Amir Azam[2]
[1]Pharmacology Division, Department of Pharmacy and Pharmacology, University of the Witwatersrand, Johannesburg, South Africa.
[2]Department of Chemistry, Jamia Millia Islamia, Delhi, India.
*Corresponding author: Robyn.vanZyl@wits.ac.za

Ninety percent of malaria cases reported in sub-Saharan Africa are due to the *Plasmodium* falciparum parasite. For decades malaria chemotherapy has hinged on a limited range of drugs, with the parasite developing resistance to some. This has initiated a search for novel compounds with unique mechanisms of action against plasmodia species. Thiosemicarbazones are a small class of compounds with reported antifungal and antimalarial effects; while metronidazole is a commonly used broad spectrum antiprotozoal agent. The properties of these two groups of compounds were combined by synthesizing metronidazole thiosemicarbazone analogues, wherein the thioamide moiety of the thiosemicarbazone backbone was substituted by different cyclic and aromatic amines. The sensitivity of the chloroquine-sensitive *P. falciparum* strain (3D7) to the compounds was assessed using the tritiated hypoxanthine incorporation assay. The compounds were evaluated for their ability to inhibit β-haematin formation as well as their haemolytic properties. All but one of the compounds inhibited parasite growth, with IC_{50} values below 10µM. Results from the β-haematin assay indicated that, with the exception of two compounds, all compounds inhibited β-haematin formation as effectively as quinine. Red blood cell toxicity results indicated negligible amounts of haemolysis and were comparable to those of quinine and metronidazole. Overall, (1E)-1-(4-((E)-2-(1-(2-hydroxyethyl)-5-nitro-1Himidazol-2-yl)vinyl)benzylidene)-4-cyclooctylthiosemicarbazide (Y1) and (1E)-4-(2-chlorobenzyl)-1-(4-((E)-2-(1-(2-hydroxyethyl)-5-nitro-1H-imidazol-2yl)vinyl)benzylidene)-thiosemi-carbazide (Y3) were the mostactive, with IC_{50} values of 2.99±0.10µM and 2.89±0.09µM respectively, as well as possessing the best safety profile. When combined with quinine Y3 exhibited an additive relationship. These results indicate that metronidazole thiosemicarbazones show promising antimalarial activity and necessatate further investigation.

Appendix A3: (Poster presentation: The University of the Witwatersrand Faculty of Health Sciences Research Day, 2010)

The Antimalarial Properties of Metronidazole Thiosemicarbazone Analogues II

Emma J. Moseley[1], Robyn L. van Zyl[1*], Mohammad Abid[2], Ivan Havlik[1], Amir Azam[2]

[1]Pharmacology Division, Department of Pharmacy and Pharmacology, Faculty of Health Sciences, University of the Witwatersrand, Johannesburg, South Africa. [2]Department of Chemistry, Faculty of Natural Sciences, Jamia Millia Islamia, Delhi, India.

*Corresponding author: Robyn.vanZyl@wits.ac.za

Introduction:

Ninety percent of malaria cases reported in sub-Saharan Africa are attributed to the *Plasmodium falciparum* parasite. For decades malaria chemotherapy has hinged on a limited range of drugs, with the parasite developing resistance to some. This has initiated an urgent search for novel compounds with unique mechanisms of action against plasmodia species. Thiosemicarbazones are a small class of compounds with reported antifungal and antimalarial effects; whilst metronidazole is a commonly used broad spectrum antiprotozoal agent. The properties of these two groups were combined by synthesizing metronidazole-thiosemicarbazone analogues, wherein the thioamide moiety of the thiosemicarbazone backbone was substituted with different cyclic and aromatic amines. These compounds were then tested against the *in vitro* growth of *P. falciparum*. Possible mechanisms of action and drug interactions were examined as well as the toxicity of these compounds.

Methods:

The *P. falciparum* chloroquine-sensitive strain (3D7) was maintained continuously in culture. For assessment of antimalarial activity and possible drug interactions the tritiated hypoxanthine incorporation assay was employed. From the data generated the concentration required to inhibit parasite growth by 50% (IC_{50} value) was obtained. To determine a possible mechanism of action, the effects of the compounds on β-haematin formation was examined. To assess the toxicity of these compounds a red blood cell lysis assay was performed.

Results:

The results obtained showed that all but one of the compounds inhibited parasite growth with IC_{50} values below 10µM. Results from the β-haematin assay indicated that, with the exception of two compounds, all compounds inhibited β-haematin formation as effectively as quinine. Red blood cell toxicity results indicated negligible amounts of red blood cell lysis and were comparable to those of quinine and metronidazole alone.

Overall, (1E)-1-(4-((E)-2-(1-(2-hydroxyethyl)-5-nitro-1H-imidazol-2-yl)vinyl)benzylidene)-4-cyclooctylthiosemicarbazide (**Y1**) and (1E)-4-(2-chlorobenzyl)-1-(4-((E)-2-(1-(2-hydroxyethyl)-5-nitro-1H-imidazol-2-yl)vinyl)benzylidene)thiosemicarbazide (**Y3**) were the most active, with IC_{50} values of 2.99 ± 0.10µM and 2.89 ± 0.09µM respectively, as well as possessing the best safety profile. In combined studies utilizing quinine and dihydroartemisinin **Y3** exhibited an additive relationship.

Conclusion:

The above results indicate that these compounds show promising antimalarial activity combined with a good safety profile and necessitate further investigation

Appendix A4: (Poster presentation: The 3rd Cross Faculty Postgraduate Symposium, University of the Witwatersrand, 2010)

The Antimalarial Properties of Metronidazole Thiosemicarbazone Analogues II

Emma J. Moseley[1], Robyn L. van Zyl[1*], Mohammad Abid[2], Ivan Havlik[1], Amir Azam[2]

[1]Pharmacology Division, Department of Pharmacy and Pharmacology, Faculty of Health Sciences, University of the Witwatersrand, Johannesburg, South Africa. [2]Department of Chemistry, Faculty of Natural Sciences, Jamia Millia Islamia, Delhi, India.

*Corresponding author: Robyn.vanZyl@wits.ac.za

Ninety percent of malaria cases reported in sub-Saharan Africa are due to the *Plasmodium falciparum* parasite. For decades malaria chemotherapy has hinged on a limited range of drugs, with the parasite developing resistance to some. This has initiated an urgent search for novel compounds with unique mechanisms of action against plasmodia species. Thiosemicarbazones are a small class of compounds with reported antifungal and antimalarial effects; while metronidazole is a commonly used broad spectrum antiprotozoal agent. The properties of these two groups of compounds were combined by synthesizing metronidazole-thiosemicarbazone analogues, wherein the thioamide moiety of the thiosemicarbazone backbone was substituted by different cyclic and aromatic amines. The sensitivity of the chloroquine-sensitive *P. falciparum* strain (3D7) to the compounds was assessed using the tritiated hypoxanthine incorporation assay. The compounds were evaluated for their ability to inhibit β-haematin formation, as well as their haemolytic properties. All but one of the compounds inhibited parasite growth, with IC_{50} values below 10µM. Results from the β-haematin assay indicated that, with the exception of two compounds, all compounds inhibited β-haematin formation as effectively as quinine. Red blood cell toxicity results indicated negligible amounts of haemolysis and were comparable to those of quinine and metronidazole. Overall, (1E)-1-(4-((E)-2-(1-(2-hydroxyethyl)-5-nitro-1H-imidazol-2-yl)vinyl)benzylidene)-4-cyclooctylthiosemicarbazide (**Y1**) and (1E)-4-(2-chlorobenzyl)-1-(4-((E)-2-(1-(2-hydroxyethyl)-5-nitro-1H-imidazol-2-yl)vinyl)benzylidene)thiosemi-carbazide (**Y3**) were the most active, with IC_{50} values of 2.99 ± 0.10µM and 2.89 ± 0.09µM respectively, as well as possessing the best safety profile. In combined studies utilizing quinine and dihydroartemisinin **Y3** exhibited an additive relationship.These results indicate that metronidazole thiosemicarbazone show promising antimalarial activity and necessatate further investigation.

Appendix A5: (Publication: Antiprotozoal activity of chloroquinoline based chalcones)

European Journal of Medicinal Chemistry 46 (2011) 1897–1905

Contents lists available at ScienceDirect

European Journal of Medicinal Chemistry

journal homepage: http://www.elsevier.com/locate/ejmech

Short communication

Antiprotozoal activity of chloroquinoline based chalcones

Faisal Hayat [a], Emma Moseley [b], Attar Salahuddin [a], Robyn L. Van Zyl [b], Amir Azam [a,*]

[a] Department of Chemistry, Jamia Millia Islamia, Jamia Nagar, New Delhi 110025, India
[b] Pharmacology Division, Department of Pharmacy and Pharmacology, Faculty of Health Sciences, University of Witwatersrand, Johannesburg 2193, South Africa

ARTICLE INFO

Article history:
Received 7 September 2010
Received in revised form
28 January 2011
Accepted 3 February 2011
Available online 5 March 2011

Keywords:
2-Chloro-3-formylquinolines
Aromatic ketones
Chalcones
Entamoeba histolytica
Cytotoxicity
Plasmodium falciparum
β-Haematin
Anti-oxidant
Haemolysis

ABSTRACT

A new series of chloroquinoline based chalcones were synthesized and evaluated for *in vitro* antiamoebic and antimalarial activities. The results showed that out of fifteen compounds, four were found to be more active against the *Entamoeba histolytica*; while one compound was moderatively active compared to the standard drug metronidazole (IC_{50} = 1.46 μM). In contrast, *in vitro* antimalarial activity against the chloroquine-sensitive (3D7) strain of *P. falciparum* indicated relatively low activity when compared to controls such as chloroquine and quinine (IC_{50} = 0.0065 μM and 0.14 μM, respectively). The toxicological studies of these compounds on human breast cancer MCF-7 cell line showed that all the compounds were non-toxic at the concentration range of 1.56–50 μM.

© 2011 Elsevier Masson SAS. All rights reserved.

1. Introduction

Parasitic protozoa are the causative agents of numerous diseases and affect an immense proportion of the world's population [1]. Two such protozoa are *Entamoeba histolytica* and *Plasmodium falciparum*, the causative agents of amoebiasis and malaria, respectively. Amoebiasis continues to be a major problem in developing countries partly due to a lack of adequate sanitation and health education [2]. Countries where *E. histolytica* remains endemic include India, South Africa and Mexico to name a few [2]. Invasive amoebiasis is the second most common cause of mortality due to parasitic infections worldwide [3] killing one in 30 children in Bangladesh alone [4]. It results primarily in an infection of the colon, but may also be spread via the haematogenous path to other organs, especially the liver [5] and is characterized by its high capacity to destroy host tissues, leading to potentially life-threatening diseases such as ulcerative colitis or liver abscess. Metronidazole (1-(2-hydroxyethyl)-2-methyl-5-nitroimidazole) is the drug of choice for the treatment of amoebiasis and giardiasis [6] and is reported to cause several toxic effects such as genotoxicity, gastric mucus irritation and spermatozoid damage [7,8]. Furthermore, failures in the treatment of several intestinal protozoan parasites may result from drug resistant by parasites [9,10] A similar trend has been observed in the treatment of malaria, a haematoprotozoan parasite of the *Plasmodium* species, carried by certain types of the *Anopheles* mosquito [11]. It is one of the most prevalent diseases of the developing world, affecting over a hundred countries and resulting in an estimated 300–500 million cases annually [12]. In sub-Saharan Africa alone over 90% of reported malaria cases are attributed to the *P. falciparum* parasite [13–15]. Epidemiological models have suggested that *P. falciparum* infections outside of Africa, specifically in Southeast Asia, are expected to be 200% higher than figures originally published by the World Health Organization, with 76% of the total cases originating from India [12]. The widespread resistance of the parasite to chloroquine, the backbone of malaria chemotherapy, has highlighted the fact that the investigation of new chemotherapeutics with similar mechanisms of action and toxicity profile to that of chloroquine is highly desired. The mechanism of action of chloroquine lies in the fact that, once haemoglobin has been degraded by

Abbreviations: μg, microgram; μL, microliter; μM, micromole; mL, milliliter; mg, milligram; mmol, millimole; nm, nanometer; MTT, 3-(4,5-dimethylthiazol-2-yl)-2,5-diphenyl tetrazolium bromide; DMSO, dimethyl sulfoxide; DPPH, 2,2-diphenyl-1-picrylhydrazyl; IC_{50}, the drug concentration at which 50% growth inhibition occurs.

* Corresponding author. Tel.: +91 11 2698 1717/3254; fax: +91 11 2698 0229.
E-mail address: amir_sumbul@yahoo.co.in (A. Azam).

0223-5234/$ – see front matter © 2011 Elsevier Masson SAS. All rights reserved.
doi:10.1016/j.ejmech.2011.02.004

plasmodial cysteine proteases, the toxic haem intermediate cannot be detoxified into haemozoin, resulting in oxidative stress and death of the parasite [16]. A therapeutic agent capable of acting in a similar manner as well as interacting favourably with other established antimalarials would be invaluable.

It is well known that chalcones and quinoline incorporating heterocycles play an important role in medicinal chemistry and possess various biological activities such as antimicrobial, anti-inflammatory, analgesic, antimalarial, anticancer, antiviral, anti-leishmanial and antitubercular [17–22]. According to the literature iodoquinol is currently used as antiamoebic drug in medical practice [23] and quinoline based hydrazones have shown antimalarial and antitubercular activity [24–26]. Many natural products bearing a quinoline nucleus such as quinidine, quinidinone, and quinine from the plant *Cinchona ledgeriana* were also found to be antiamoebic [27]. In recent years it is reported that the incorporation of a quinoline nucleus could alter the course of reaction, as well as the biological properties of the molecules [28,29].

Since chalcones and quinoline incorporating heterocycles are biologically active and as a part of our continuous efforts towards the development of more potent antiprotozoal agents, we herein report the synthesis, characterization, antiamoebic, antiplasmodial and cytotoxic properties of a new series of chloroquinoline based chalcones (**4**–**18**) in an attempt to improve upon the efficacy of current antiamoebic and antimalarial agents.

2. Chemistry

The synthesis of the chloroquinoline based chalcones (**4**–**18**) was performed in a manner as outlined in Scheme 1. The reaction of 2-chloro-3-formylquinolines (**1**–**3**) with different commercially available aromatic ketones in presence of aqueous sodium hydroxide in ethanol gave the quinolinyl chalcones. All the compounds are insoluble in water, but soluble in most of the organic solvents. Melting points were recorded on KSW melting point apparatus and are uncorrected.

3. Pharmacology

All quinolinyl chalcones (**4**–**18**) were screened *in vitro* against HM1:IMSS strain of *E. histolytica* by microdilution method [30]. All the experiments were carried out in triplicate at each concentration level and repeated thrice. Cytotoxicity of active compounds has been studied using the MTT cell viability assay on the breast cancer MCF-7 cell line. The results of antiamoebic activity and cytotoxicity are summarized in Table 1. *In vitro* antimalarial activity was carried out on the chloroquine-sensitive (3D7) strain of *P. falciparum* by use of the [^{3}H]-hypoxanthine-incorporation assay. All experiments were repeated, at least, in triplicate. To determine a possible mechanism of antimalarial action the inhibition of β-haematin formation, as well as free radical scavenging activity were determined. Drug toxicity was determined by examining the haemolytic effects of the compounds on healthy erythrocytes. Out of the **14** compounds, one lead compound was selected and combined with quinine to determine possible drug interactions. The results of the above are summarized in Table 2 and Fig. 2.

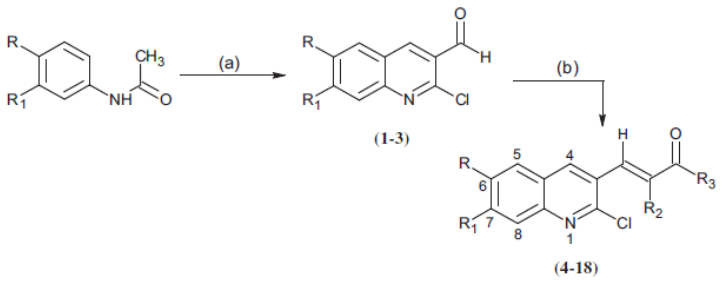
4. Results and discussion

4.1. Synthesis

The chloroquinoline based chalcones were prepared by one-step Claisen–Schmidt condensation [31] of substituted 2-chloro-3-formylquinolines with different aromatic ketones using the reaction sequence as shown in Scheme 1. For this purpose a series of 2-chloro-3-formylquinolines (**1**–**3**) were prepared from different acetanilides [32]. The required acetanilides were prepared by direct condensation of substituted anilines with acetic acid in presence of acetic anhydride [33]. The prepared 2-chloro-3-formylquinolines were condensed with different commercially available aromatic ketones in presence of aqueous sodium hydroxide (2 mL, 40%) in 50 mL ethanol to yield the quinolinyl chalcones (**4**–**18**) in good yield. All the compounds were characterized by IR, ^{1}H and ^{13}C NMR and mass spectra. The purity of the compounds was confirmed by elemental analysis and the data was found in accordance with ±0.3%.

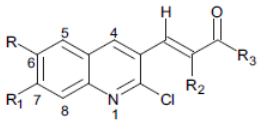
4.2. Antiamoebic activity

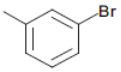
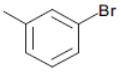
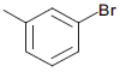
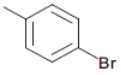
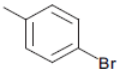
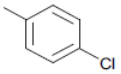
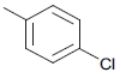
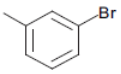
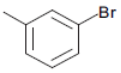
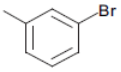
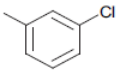
Preliminary experiments were carried out to determine the *in vitro* antiamoebic activity of all the compounds (**4**–**18**) by microdilution method using the HM1:IMSS strain of *E. histolytica*. The antiamoebic effect was compared with the most widely used antiamoebic medication, namely metronidazole which had a 50% inhibitory concentration (IC_{50}) of 1.46 μM (Table 1). SAR showed that compounds (**4**–**10**) which contained chloro and bromo groups as substituent's at **C-3** and **C-4** position of the phenyl ring; while compounds (**4**, **5**, **7** and **9**) with a methyl group as a substituent at **C-6** and **C-7** position of the chloroquinoline ring (excluding compounds **6**, **8** and **10**) showed IC_{50} value in the range of 0.05–7.53 μM. Compounds (**11**–**15**) besides containing the same substitution of chloro and bromo groups at **C-3** and **C-4** position of the phenyl and methyl group at **C-6** and **C-7** position of the chloroquinoline ring except the compound (**13**), contain a methyl group at the α-β unsaturated carbonyl position showed IC_{50} value in the range of 0.06–7.03 μM. Compounds (**16**–**18**) having the same chloroquinoline ring in their structure contain a pyrimidine ring



Scheme 1. Synthesis of chloroquinoline based chalcone (**4**–**18**). Reagent and conditions: (a) DMF/$POCl_3$, 75 °C reflux 17 h, (b) aq. NaOH, C_2H_5OH, different aromatic ketones, where **R**, **R$_1$**, **R$_2$** and **R$_3$** are the different substituted groups.

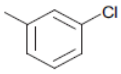
Table 1
In vitro antiamoebic activity of chloroquinoline based chalcones (**4–18**) against HM1:IMSS strain of *E. histolytica* and cytotoxicity profile of compounds **5**, **10**, **11**, **15**, **17** and metronidazole.



Compound	R	R_1	R_2	R_3	Antiamoebic activity		Cytotoxicity profile (MCF-7)	
					IC_{50} (μM) SD[a]		IC_{50} (μM) SD[a]	
4	H	CH_3	H		7.53	0.14	N.D.	N.D.
5	CH_3	H	H		**1.03**	0.22	>100	0.18
6	H	H	H		3.45	0.16	N.D.	N.D.
7	CH_3	H	H		4.09	0.12	N.D.	N.D.
8	H	H	H		3.38	0.23	N.D.	N.D.
9	H	CH_3	H		6.91	0.19	N.D.	N.D.
10	H	H	H		**0.05**	0.12	>100	0.14
11	H	CH_3	CH_3		**0.09**	0.22	>100	0.14
12	CH_3	H	CH_3		2.79	0.11	N.D.	N.D.
13	H	H	CH_3		3.65	0.32	N.D.	N.D.
14	H	CH_3	CH_3		7.03	0.11	N.D.	N.D.

(*continued on next page*)

Table 1 (*continued*).

Compound	R	R_1	R_2	R_3	Antiamoebic activity		Cytotoxicity profile (MCF-7)	
					IC_{50} (μM) SD[a]		IC_{50} (μM) SD[a]	
15	CH_3	H	CH_3		**0.06**	0.14	>100	0.28
16	CH_3	H	H		1.45	0.17	N.D.	N.D.
17	H	CH_3	H		**0.05**	0.10	75.7	0.16
18	H	H	H		5.30	0.22	N.D.	N.D.
				Metronidazole	**1.46**	0.17	>100	0.11

[a] Standard deviation, N.D. = Not determined.
The compounds with bold IC_{50} values are more active than metronidazole.

instead of the phenyl ring. The compounds (**16**) and (**17**) except (**18**) having the chloroquinoline ring being substituted by methyl group at **C-6** and **C-7** position showed IC_{50} value in the range of 0.05–5.30 μM. From these 15 compounds, five (**5**, **10**, **11**, **15** and **17**) were found to be more active against *.E. histolytica* than the reference drug, metronidazole (IC_{50} = 1.46 μM). Out of these five compounds, four compounds **10** (IC_{50} = 0.05 μM), **11** (IC_{50} = 0.09 μM), **15** (IC_{50} = 0.06 μM) and **17** (IC_{50} = 0.05 μM) showed excellent antiamoebic activity being 16–29 times more active than metronidazole. While compound **5** (IC_{50} = 1.03 μM) was moderately active compare to metronidazole.

4.3. Antimalarial activity

A series of chloroquinoline based chalcones (**4–18**) were examined for their *in vitro* antimalarial activity, their interactions with classic antimalarials, as well as their ability to inhibit the formation of β-heamatin and scavenge free radicals. The results have been summarized in Table 2. The hypoxanthine incorporation assay indicated that, although not comparable to the reference agents chloroquine and quinine (IC_{50} values = 0.0065 μM and 0.14 μM, respectively), compounds **10**, **16**, **17** and **18** (IC_{50} values = 39.17 μM, 31.54 μM, 31.31 μM and 31.98 μM, respectively) showed the most promising antimalarial activity. Compounds **16–18** were the only compounds to have a pyridine ring substitutions at R_3 and a hydrogen group at R_2, with either hydrogen or methyl groups at R and R_1. Compound **10**, which had the highest IC_{50} value out of the 4, has hydrogen groups at R, R_1 and R_2 with a 4-chloro phenyl ring at R_3. It appears as if the substitution of the hydrogen group, instead of a methyl group, at R_2 positively influences the activity of compounds **4** and **5** when compared to compounds **11–13**, all of which have a bromophenyl ring. However, when all methyl groups are replaced with hydrogen groups, as seen in compound **6**, activity diminishes. The positioning of the bromo

Table 2
The *in vitro* antimalarial and haemolytic activity of chloroquinoline based chalcones (**4–18**) and reference agents along with their effect on β-haematin formation.

Compound	Antimalarial activity		Haemolytic activity	Inhibition Of β-haematin formation	
	IC_{50} ± S.D. (μM)	Maximum inhibition at 100 μM (%)	% Lysis at 100 μM	IC_{50} ± S.D. (μM)	Maximum inhibition at 100 μM (%)
4	59.73 ± 1.19		1.09 ± 0.55	>100	27.50 ± 4.80
5	50.11 ± 3.85		1.68 ± 0.66	>100	14.88 ± 6.86
6	>100	61.22 ± 13.09	1.38 ± 0.67	>100	16.03 ± 4.81
7	74.84 ± 3.39		1.40 ± 0.96	>100	55.38 ± 19.1
8	44.56 ± 1.75		2.20 ± 0.54	>100	13.55 ± 2.61
9	N.D.	N.D.	N.D.	N.D.	N.D.
10	39.17 ± 2.05		1.74 ± 0.67	>100	19.49 ± 5.35
11	47.06 ± 2.76		1.04 ± 0.64	>100	10.54 ± 0.88
12	>100	51.15 ± 8.1	1.53 ± 0.34	>100	13.30 ± 5.38
13	>100	34.3 ± 8.93	2.17 ± 0.59	>100	9.35 ± 5.76
14	50.44 ± 3.22		1.44 ± 0.66	>100	5.64 ± 3.72
15	>100	8.74 ± 13.66	1.24 ± 0.78	>100	14.42 ± 4.21
16	31.54 ± 3.03		1.55 ± 1.15	>100	11.52 ± 5.20
17	31.31 ± 0.87		0.47 ± 0.77	>100	15.00 ± 0.99
18	31.98 ± 1.27		1.10 ± 1.04	>100	12.29 ± 4.35
Chloroquine	0.0065 ± 0.0002		0.72 ± 0.32	24.97 ± 5.3	
Quinine	0.14 ± 0.007		1.22 ± 0.98	65.80 ± 1.77	

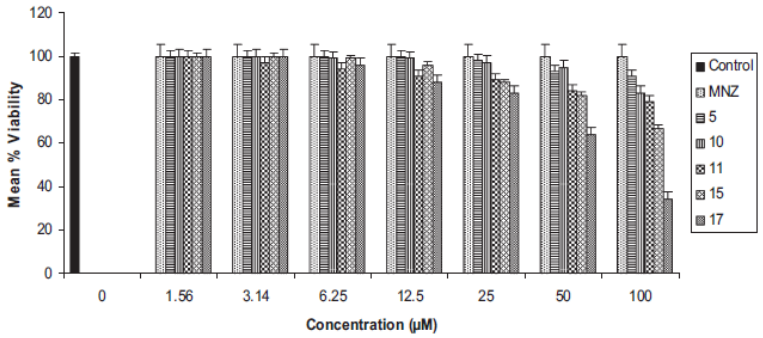


Fig. 1. Percentage of viable cells after 48 h pre-treatment of human breast cancer MCF-7 cells with compounds **5**, **10**, **11**, **15**, **17** and metronidazole (MNZ), evaluated by the MTT assay.

group on the phenyl ring appeared not to influence antimalarial activity. A study conducted against the FCB1 chloroquine-resistant strain of *P. falciparum* indicated that quinolinyl chalcones with a single chloro substitution at position 4 on the phenyl ring displayed no antimalarial activity (>200 μM). However, once di-substituted at positions 2, 4 and 2, 5, the IC_{50} values decreased to 19 μM and 48.6 μM, respectively, whilst di-substitutions at positions 3 and 4 diminished the antimalarial activity [34]. The same study also indicated that the addition of bromo, methoxy or hydrogen groups to the phenyl ring diminished antimalarial activity. The above results indicate differences in drug sensitivity between chloroquine-sensitive and -resistant strains, but also highlight the significant role that not only the various substitutions, but also the positioning of the substitutions, play. None of the compounds were capable of inhibiting the formation of β-haematin, the synthetic molecule with the same chemical structure as haemozoin, as effectively as chloroquine or quinine (IC_{50} = 24.9 μM and 65.8 μM, respectively). Compound **7** exhibited the greatest activity with 55.38% inhibition at 100 μM, however this was not well correlated with antimalarial activity. None of the compounds were capable of scavenging the free electron of DPPH• as effectively as ascorbic acid (IC_{50} = 20.10 μM), compounds **1**, **2**, **10**, **11**, **13** and **14** showed some anti-oxidant activity at 80 μM, or a ratio of drug to DPPH• of 1:1 (% scavenging activity = 7.79, 2.06,3.69, 2.27, 1.43, and 0.78%, respectively) and were comparable to the anti-oxidant activity of chloroquine and quinine (% scavenging activity = 4.06 and 2.65%, respectively). The mechanism of action of this class of compounds remains unclear, when tested against the *P. falciparum* cysteine protease, falcipain, the quinolinyl chalcones showed weak activity that was not correlated with antimalarial activity [34]. In an examination of the interaction of compound **17** and quinine, an additive interaction was noted. This is possibly due, to the different complementary mechanisms of actions of these two compounds.

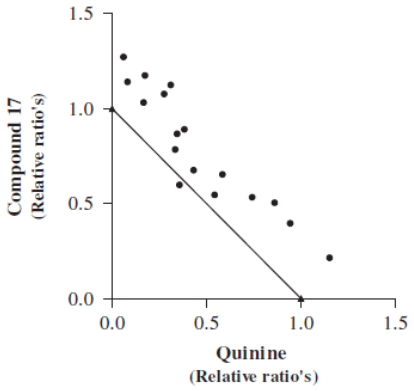


Fig. 2. Isobologram depicting the additive interaction between compound **17** and quinine.

4.4. Cytotoxicity profile

Since compounds **5**, **10**, **11**, **15** and **17** were more potent than metronidazole, they were screened for cytotoxicity against the human breast cancer MCF-7 cell line. Compounds **5**, **10**, **11** and metronidazole inhibited <20% cell growth. Whilst compound **17** inhibited cell growth in a dose dependant manner, where 50 μM inhibited 36% and 100 μM, inhibited 66% cell growth (Fig. 1). To ensure the antimalarial activity noted for these compounds were due to a direct inhibitory effect on the intra-erythrocytic parasite, all the compounds were screened against healthy red blood cells for any haemolytic effects (Table 2). None of the compounds showed any notable haemolytic effects when compared to antimalarials such as chloroquine or quinine (% haemolysis of 0.72 and 1.22%, respectively). The greatest haemolytic activity was noted for compounds **8** and **13** (% haemolysis of 2.2 and 2.17%, respectively).

5. Conclusion

The 15 chloroquinoline based chalcones (**4**–**18**) were synthesized by condensation of substituted 2-chloro-3-formylquinolines with different aromatic ketones. *In vitro* antiamoebic and antimalarial activities were determined against the HM1:IMSS strain of *E. histolytica* and 3D7 strain of *P. falciparum*, respectively. Anti-amoebic activity indicated that out of the 15 compounds, 5 compounds exhibited more potent activity than the reference drug metronidazole (IC_{50} = 1.46 μM). Antimalarial activity was not as promising, none of the chloroquinoline based chalcones were capable of inhibiting parasite growth as effectively as the reference drugs chloroquine and quinine (IC_{50} values = 0.0065 μM and 0.14 μM, respectively). When combined with quinine, compound **17** interacted in a favourable additive manner. Both the inhibition of β-haematin formation and DPPH• free radical scavenging assays indicated that the antimalarial mechanisms of action of the compounds do not lie in their ability to inhibit haemozoin formation or act as anti-oxidants. The MTT assay revealed that compounds **5**, **10**, **11**, **15** and metronidazole were non-toxic, however compound **17** was found to inhibit 66% cell growth at 100 μM. Whilst, the red blood cell toxicity assay showed negligible

amounts of haemolysis when compared to that of chloroquine and quinine. The results obtained indicate that these compounds show excellent antiamoebic activity, with 16–29 times the activity of the standard treatment, metronidazole. No correlation was noted between the antiamoebic and antimalarial activity with the above compounds exhibiting only moderate antimalarial activity when compared to standard treatments. Generally the compounds proved to be non-toxic. Investigation into derivatives of this class of compounds is essential, to examine the exact nature of their antimalarial activity, as well as the effect of structural changes on antiamoebal and antiplasmodial activities.

6. Experimental protocol

All the required chemicals were purchased from Merck and Aldrich Chemical Company (USA). 2-Chloro-3-formylquinolines were synthesized by using the methods reported in literature [32]. Precoated aluminium sheets (silica gel 60 F_{254}, Merck Germany) were used for thin-layer chromatography (TLC) and spots were visualized under UV light. Elemental analysis was carried out on CHNS Elementar (Vario EL-III) and the results were within ±0.3% of the theoretical values. IR spectra were recorded on Perkin–Elmer model 1600 FT-IR RX1 spectrophotometer as KBr discs. ^{1}H NMR and ^{13}C NMR spectra were recorded on Bruker Spectrospin DPX 300 MHz and Bruker Spectrospin DPX 75 MHz spectrometer respectively using $CDCl_3$ as a solvent and trimethylsilane (TMS) as an internal standard. Splitting patterns are designated as follows; s, singlet; d, doublet; m, multiplet. Chemical shift values are given in ppm. The FAB mass spectra of the compounds were recorded on JEOL SX 102/DA-6000 mass spectrometer using Argon/Xenon (6 KV, 10 mA) as the FAB gas and *m*-nitrobenzyl alcohol (NBA) was used as the matrix.

6.1. Preparation of 2-chloro-3-formylquinolines (**1**–**3**)

Substituted 2-chloro-3-formylquinolines were prepared by a reported method [32].

6.2. General procedure for the synthesis of chloroquinoline based chalcones (**4**–**18**)

A mixture of substituted 2-chloro-3-formylquinolines (0.01 mol), the respective aromatic ketones (0.01 mol), and sodium hydroxide (2 mL, 40% aqueous) in 50 mL ethanol was stirred at room temperature for 24 h. The resulting precipitate was collected by filtration, washed with water and recrystallized from ethyl acetate.

6.2.1. (E)-1-(3-Bromophenyl)-3-(2-chloro-7-methylquinoline-3yl) prop-2-en-1-one (**4**)

Yield 88% (Ethyl acetate); mp: 276 °C; Anal. calc. for $C_{19}H_{13}NOClBr$: C 59.02, H 3.39, N 3.62%; found: C 59.04, H 3.33, N 3.58%; IR ν_{max} (cm^{-1}): 1652 (C=O), 1579 (C=C); ^{1}H NMR ($CDCl_3$) δ (ppm): 8.46 (s,1H, H_4 quinoline), 8.24 (s,1H, phenyl), 8.19 (d,1H, J = 15.6 Hz, H_β), 7.99 (d,1H, J = 7.5 Hz, phenyl), 7.80–7.73 (m, 2H, H_5 H_8 quinoline), 7.56 (d,1H, J = 15.6 Hz, H_α), 7.46–7.39 [m, 3H, (2H phenyl, H_6 quinoline)], 2.58 (s, 3H, CH_3 quinoline); ^{13}C NMR ($CDCl_3$) δ (ppm): 188.3 (C=O), 150.3 (C–Cl), 148.2 (C-β), 142.8, 140.4, 139.4, 135.9, 131.6, 130.4, 127.5, 127.1, 126.7 (Ar–C), 123.0 (C-α), 22.1 (CH_3 quinoline). FAB-MS (*m*/*z*): [M^++1] 387.34.

6.2.2. (E)-1-(3-Bromophenyl)-3-(2-chloro-6-methylquinolin-3-yl) prop-2-en-1-one (**5**)

Yield 74% (Ethyl acetate); mp: 142–144 °C; Anal. calc. for $C_{19}H_{13}NOClBr$: C 59.02, H 3.39, N 3.62%; found: C 59.03, H 3.32, N 3.56%. IR ν_{max} (cm^{-1}): 1662 (C=O), 1581 (C=C); ^{1}H NMR ($CDCl_3$) δ (ppm): 8.39 (s, 1H, H_4 quinoline), 8.22 (s, 1H, phenyl), 8.16 (d, 1H, J = 15.6 Hz, H_β), 7.98 (d, 1H, J = 7.5 Hz, phenyl), 7.69 (s, 1H, H_5 quinoline) 7.66–7.60 [m, 2H, (1H phenyl, H_8 quinoline)], 7.57 (d, 1H, J = 15.6 Hz, H_α), 7.49–7.39 [m, 2H, (1H phenyl, H_7 quinoline)], 2.55 (s, 3H, CH_3 quinoline); ^{13}C NMR ($CDCl_3$) δ (ppm): 188.8 (C=O), 149.4 (C–Cl), 146.5 (C-β), 140.1, 137.9, 136.3, 135.6, 134.0, 132.0, 130.01, 128.1, 127.6, 126.8 (Ar–C), 122.5 (C-α), 21.6 (CH_3 quinoline); FAB-MS (*m*/*z*): [M^++1] 387.25.

6.2.3. (E)-1-(3-Bromophenyl)-3-(2-chloroquinoline-3yl) prop-2-en-1-one (**6**)

Yield 78% (Ethyl acetate); mp: 173 °C; Anal. calc. for $C_{18}H_{11}NOClBr$: C 59.95, H 3.77, N 3.50%; found: C 59.89, H 3.71, N 3.44%. IR ν_{max} (cm^{-1}): 1659 (C=O), 1583 (C=C); ^{1}H NMR ($CDCl_3$) δ (ppm): 8.41 (s, 1H, H_4 quinoline), 8.24 (s, 1H, phenyl), 8.21 (d, 1H, J = 15.6 Hz, H_β), 7.97 (d, 1H, J = 7.5 Hz, phenyl), 7.94–7.78 (m, 3H, H_5 H_7 H_8 quinoline), 7.54 (d, 1H, J = 15.6 Hz, H_α), 7.46–7.35 [m, 3H, (2H phenyl, H_6 quinoline)]; ^{13}C NMR ($CDCl_3$) δ (ppm): 188.9 (C=O), 148.9 (C–Cl), 145.6 (C-β), 139.0, 137.7, 134.6, 133.4, 129.6, 127.6 (Ar–C), 126.6 (C-α); FAB-MS (*m*/*z*): [M^++1] 373.11.

6.2.4. (E)-1-(4-Bromophenyl)-3-(2-chloro-6-methylquinoline-3yl) prop-2-en-1-one (**7**)

Yield 84% (Ethyl acetate); mp: 276 °C; Anal. calc. for $C_{19}H_{13}NOClBr$: C 59.02, H 3.39, N 3.62%; found: C 59.03, H 3.33, N 3.56%. IR ν_{max} (cm^{-1}): 1651 (C=O), 1578 (C=C); ^{1}H NMR ($CDCl_3$) δ (ppm): 8.41 (s, 1H, H_4 quinoline), 8.22 (d, 1H, J = 15.6 Hz, H_β), 8.05–7.91 [m, 3H, (2H phenyl, H_8 quinoline)], 7.64 (s,1H, H_5 quinoline), 7.63–7.52 [m, 3H, (1H phenyl, H_α, H_7 quinoline)], 2.56 (s, 3H, CH_3 quinoline); ^{13}C NMR ($CDCl_3$) δ (ppm): 189.4 (C=O), 149.4 (C–Cl), 146.4 (C-β),139.5, 137.5, 135.5, 133.1, 128.6, 127.6 (Ar–C), 122.7 (C-α), 22.5 (CH_3 quinoline); FAB-MS (*m*/*z*): [M^++1] 387.39.

6.2.5. (E)-1-(4-Bromophenyl)-3-(2-chloroquinoline-3yl)prop-2-en-1-one (**8**)

Yield 88% (Ethyl acetate); mp: 223 °C; Anal. calc. for $C_{18}H_{11}NOClBr$: C 58.02, H 2.98, N 3.76%; found: C 58.05, H 2.94, N 3.70%. IR ν_{max} (cm^{-1}): 1651 (C=O), 1586 (C=C); ^{1}H NMR ($CDCl_3$) δ (ppm): 8.50 (s, 1H, H_4 quinoline), 8.24 (d,1H, J = 15.6 Hz, H_β), 8.05 (d, 1H, J = 8.4 Hz, H_5 quinoline), 7.95–7.77 [m, 4H, (2H phenyl, H_6 H_8 quinoline)], 7.69–7.60 [m, 3H, (2H phenyl, H_7 quinoline)], 7.55 (d, 1H, J = 15.6 Hz, Hα); ^{13}C NMR ($CDCl_3$) δ (ppm): 188.86 (C=O), 150.3 (C–Cl), 147.9 (C-β), 139.9, 136.2, 131.7, 130.1, 129.4, 128.4 (Ar–C), 125.7 (C-α). FAB-MS (*m*/*z*): [M^++1] 373.44.

6.2.6. (E)-3-(2-Chloro-7-methylquinolin-3-yl)-1-(4-chlorophenyl) prop-2-en-1-one (**9**)

Yield 78% (Ethyl acetate); mp: 158 °C; Anal. calc. for $C_{19}H_{13}NOCl_2$: C 66.68, H 3.83, N 4.09%; found: C 66.63, H 3.77, N 4.11%. IR ν_{max} (cm^{-1}): 1650 (C=O), 1563 (C=C); ^{1}H NMR ($CDCl_3$) δ (ppm): 8.47 (s, 1H, H_4 quinoline), 8.19 (d, 1H, J = 15.7 Hz, H_β), 8.06 (d, 1H, J = 7.6 Hz, phenyl), 7.89 (d, 1H, J = 7.5 Hz, phenyl), 7.87–7.76 (m, 2H, H_5 H_8 quinoline), 7.56 (d, 1H, J = 15.6 Hz, H_α),7.48–7.33 [m, 3H, (2H phenyl, H_6 quinoline), 2.55 (s, 3H, CH_3 quinoline); ^{13}C NMR ($CDCl_3$) δ (ppm): 189.9 (C=O), 149.9 (C–Cl), 147.1 (C-β), 139.2, 138.4, 136.8, 134.6, 132.2, 131.2, 129.7, 128.0, 127.6 (Ar–C), 124.6 (C-α), 21.25 (CH_3 quinoline); FAB-MS (*m*/*z*): [M^++1] 343.03.

6.2.7. (E)-1-(4-Chlorophenyl)-3-(2-chloroquinoline-3yl)prop-2-en-1-one (**10**)

Yield 86% (Ethyl acetate); mp: 167 °C; Anal. calc. for $C_{18}H_{11}NOCl_2$: C 65.87, H 3.38, N 4.27%; found: C 65.82, H 3.31, N 4.22%. IR ν_{max} (cm^{-1}): 1662 (C=O),1580 (C=C); ^{1}H NMR ($CDCl_3$) δ (ppm): 8.50 (s, 1H, H_4 quinoline), 8.24 (d, 1H, J = 15.6 Hz, H_β), 8.05 (d, 1H, J = 8.2 Hz, H_5 quinoline), 8.01–7.77 [m, 4H, (2H phenyl, H_6 H_8

quinoline), 7.65–7.60 [m, 3H, (2H phenyl, H_7 quinoline)], 7.56 (s, 1H, J = 15.6 Hz, H_α); ^{13}C NMR ($CDCl_3$) δ (ppm): 188.6 (C=O), 150.6 (C–Cl), 147.7 (C-β), 139.4, 136.2, 135.2, 131.2, 130.0, 128.3, 127.5, 126.3 (Ar–C), 125.2 (C-α); FAB-MS (m/z): [M^++1] 329.24.

*6.2.8. (E)-1-(3-Bromophenyl)- 3-(2-chloro-7-methylquinoline-3yl)-2-methylprop-2-en-1-one (**11**)*

Yield 82% (Ethyl acetate); mp: 275 °C; Anal. calc. for $C_{20}H_{15}NOClBr$: C 59.95, H 3.77, N 3.50%; found: C 59.89, H 3.73, N 3.46%; IR ν_{max} (cm^{-1}): 1657 (C=O), 1580 (C=C); ^{1}H NMR ($CDCl_3$) δ (ppm): 8.11 (s, 1H, H_4 quinoline), 8.01 (s, 1H, phenyl), 7.79–7.74 [m, 3H, (1H phenyl, H_5 H_8 quinoline)], 7.72 (s, 1H, H_β, **CH$_\beta$**=CMe), 7.44–7.36 [m, 3H, (2H phenyl, H_6 quinoline)], 2.57 (s, 3H, CH_3 quinoline), 2.20 (s, 3H, CH_β=**CMe**); ^{13}C NMR ($CDCl_3$) δ (ppm): 196.8 (C=O), 149.2 (C–Cl), 147.2 (C-β), 141.9, 139.2, 138.7, 138.0, 137.1, 129.8, 129.7, 128.0, 127.3, 126.9 (Ar–C), 124.5 (C-α), 21.9 (CH_3 quinoline), 14.1 [CH_3 (CH_β=**CMe**)]; FAB-MS (m/z): [M^++1] 401.22.

*6.2.9. (E)-1-(3-Bromophenyl)-3-(2-chloro-6-methylquinolin-3-yl)-2-methylprop-2-en-1-one (**12**)*

Yield 84% (Ethyl acetate); mp: 181–183 °C; Anal. calc. for $C_{20}H_{15}NOClBr$: C 59.95, H 3.77, N 3.50%; found: C 59.87, H 3.71, N 3.44%; IR ν_{max} (cm^{-1}): 1645 (C=O), 1577 (C=C); ^{1}H NMR ($CDCl_3$) δ (ppm): 8.17 (s, 1H, H_4 quinoline), 8.02 (s, 1H, phenyl), 7.94 (d, 1H, J = 8.3 Hz, phenyl), 7.81 (d, 1H, J = 7.5 Hz, H_8 quinoline), 7.73 (s, 1H, H_β **CH$_\beta$**=CMe),7.63 (s, 1H, H_5 quinoline), 7.42–7.37 (m, 2H, phenyl), 7.33 (d, 1H, J = 7.8 Hz, H_7 quinoline), 2.55 (s, 3H, CH_3 quinoline), 2.19 (s, 3H, CH_3 CH_β=**CMe**); ^{13}C NMR ($CDCl_3$) δ (ppm): 196.3 (C=O), 148.0 (C–Cl), 147.2 (C-β), 141.3, 138.7, 137.6, 135.5, 133.6, 132.3, 129.1, 128.1, 127.6 (Ar–C), 126.4 (C-α), 21.3 (CH_3 quinoline), 14.5 [CH_3 (CH_β = **CMe**)]; FAB-MS (m/z): [M^++1] 401.32.

*6.2.10. (E)-1-(3-Bromophenyl)-3-(2-chloroquinoline-3yl)-2-methylprop-2-en-1-one (**13**)*

Yield 89% (Ethyl acetate); mp: 217 °C; Anal. calc. for $C_{19}H_{13}NOClBr$: C 59.02, H 3.39, N 3.62%; found: C 59.03, H 3.32, N 3.58%. IR ν_{max} (cm^{-1}): 1644 (C=O), 1579 (C=C); ^{1}H NMR ($CDCl_3$) δ (ppm): 8.17 (s, 1H, H_4 quinoline), 8.05 (s, 1H, phenyl), 7.89 (d, 1H, J = 8.4 Hz, phenyl), 7.82 (d, 1H, J = 7.8 Hz, H_8 quinoline), 7.79–7.73 (m,2H, H_5 H_6 quinoline), 7.71(s, 1H, **CH$_\beta$** = CMe), 7.64–7.59 (1H, t, J = 7.2 Hz, H_7 quinoline), 7.42–7.33 (m, 2H, phenyl), 2.21 (s, 3H, CH_β=**CMe**); ^{13}C NMR ($CDCl_3$) δ (ppm): 196.5 (C=O), 149.5 (C–Cl), 147.3 (C-β), 139.2, 138.5, 136.1, 135.4, 132.4, 128.6, 127.5 (Ar–C), 124.2 (C-α), 14.3[CH_3 (CH_β=**CMe**)]. FAB-MS (m/z): [M^++1] 387.16.

*6.2.11. (E)-3-(2-Chloro-7-methylquinoline-3yl)-1-(3-chlorophenyl)-2-methylprop-2-en-1-one (**14**)*

Yield 84% (Ethyl acetate); mp: 236 °C; Anal. calc. for $C_{20}H_{15}NOCl_2$: C 67.43, H 4.24, N 3.93%; found: C 67.38, H 4.18, N 3.86%. IR ν_{max} (cm^{-1}): 1655 (C=O), 1576 (C=C); ^{1}H NMR ($CDCl_3$) δ (ppm): 8.12 (s, 1H, H_4 quinoline), 7.86 (s, 1H, phenyl), 7.81 (s, 1H, H_8 quinoline), 7.77–7.74 [m, 2H, (1H phenyl, H_5 quinoline)], 7.73 (s, 1H, **CH$_\beta$**=CMe), 7.47–7.33 [m, 3H, (2H phenyl, H_6 quinoline)] 2.55 (s, 3H, CH_3 quinoline), 2.20 (s, 3H, CH_β=**CMe**); ^{13}C NMR ($CDCl_3$) δ (ppm): 197.0 (C=O), 149.8 (C–Cl), 145.0 (C-β), 139.1, 137.1, 134.6, 132.1, 129.8, 127.6 (Ar–C), 124.5 (C-α), 22.0 (CH_3 quinoline), 14.2 [CH_3 (CH_β=**CMe**)]; FAB-MS (m/z): [M^++1] 357.08.

*6.2.12. (E)-3-(2-Chloro-6-methylquinolin-3-yl)-1-(3-chlorophenyl)-2-methylprop-2-en-1-one (**15**)*

Yield 88% (Ethyl acetate); mp: 178 °C Anal. calc. for $C_{20}H_{15}NOCl_2$: C 67.43, H 4.24, N 3.93%; found: C 67.39 H 4.19, N 3.88%. IR ν_{max} (cm^{-1}): 1651 (C=O), 1578 (C=C); ^{1}H NMR ($CDCl_3$) δ (ppm): 8.16 (s, 1H, H_4 quinoline), 8.07 (s, 1H, phenyl), 7.94 (d, 1H, J = 8.4 Hz, phenyl), 7.82 (d, 1H, J = 7.5 Hz, H_8 quinoline), 7.74 (s, 1H, **CH$_\beta$**=CMe), 7.63 (s, 1H, H_5 quinoline) 7.48–7.32 [m, 3H, (2H phenyl, H_7 quinoline)], 2.56 (s, 3H, CH_3 quinoline), 2.20 (s, 3H, CH_β=**CMe**); ^{13}C NMR ($CDCl_3$) δ (ppm): 196.3 (C=O), 148.7 (C–Cl), 145.9 (C-β), 138.5, 137.4, 136.3, 134.1, 133.4, 132.2, 129.1, 127.6 (Ar–C), 124.3 (C-α) 21.3, (CH_3 quinoline), 14.5 [CH_3 (CH_β=**CMe**)]; FAB-MS (m/z): [M^++1] 357.41.

*6.2.13. (E)-3-(2-Chloro-6-methylquinoline-3yl)-1-(pyridine-2yl) prop-2-en-1-one (**16**)*

Yield 78% (Ethyl acetate); mp: 188 °C; Anal. calc. for $C_{18}H_{13}N_2OCl$: C 70.02, H 4.24, N 9.07%; found: C 70.03, H 4.19, N 9.02%. IR ν_{max} (cm^{-1}): 1651 (C=O), 1560 (C=C); ^{1}H NMR ($CDCl_3$) δ (ppm): 8.78 (d, 1H, J = 4.2 Hz, pyridine), 8.58 (s,1H, H_4 quinoline), 8.46 (d, 1H, J = 15.9 Hz, H_β), 8.39 (d, 1H, J = 2.4 Hz, pyridine), 8.26 (d, 1H, J = 7.8 Hz, H_8 quinoline), 7.95–7.90 [m, 2H, (1H pyridine, H_5 quinoline)] 7.66–7.59 [m, 2H, (1H pyridine, H_7 quinoline)], 7.56 (d, 1H, J = 15.6 Hz, H_α), 2.56 (s, 3H, CH_3 quinoline); ^{13}C NMR ($CDCl_3$) δ (ppm): 188.5 (C=O), 149.7 (C–Cl), 148.8 (C-β), 146.5, 139.1, 137.6, 135.6, 133.8, 128.0, 127.1, 126.8 (Ar–C), 124.5 (C-α), 21.5 (CH_3 quinoline). FAB-MS (m/z): [M^++1] 309.37.

*6.2.14. (E)-3-(2-Chloro-7-methylquinoline-3yl)-1-(pyridine-2yl) prop-2-en-1-one (**17**)*

Yield 88% (Ethyl acetate); mp: 235 °C; Anal. calc. for $C_{18}H_{13}N_2OCl$: C 70.02, H 4.24, N 9.07%; found: C 70.05, H 4.18, N 9.03%; IR ν_{max} (cm^{-1}): 1658 (C=O), 1578 (C=C); ^{1}H NMR ($CDCl_3$) δ (ppm): 8.76 (d, 1H, J = 4.2 Hz, pyridine), 8.63 (s,1H, H_4 quinoline), 8.40 (d, 1H, J = 15.9 Hz, H_β), 8.38 (d, 1H, J = 2.3 Hz, pyridine), 8.26 (d, 1H, J = 7.5 Hz, H_5 quinoline), 7.95–7.81 [m, 2H (1H pyridine, H_8 quinoline)], 7.67–7.57 [m, 2H (1H pyridine, H_6 quinoline)], 7.54 (d, 1H, J = 15.9 Hz, H_α), 2.56 (s, 3H, CH_3 quinoline); ^{13}C NMR ($CDCl_3$) δ (ppm): 188.4 (C=O), 150.3 (C–Cl), 148.4 (C-β), 142.7, 140.4, 139.9, 137.6, 129.1, 127.2, 127.9, 125.3 (Ar–C), 124.2 (C-α), 22.4 (CH_3 quinoline); FAB-MS (m/z): [M^++1] 309.41.

*6.2.15. (E)-3-(2-Chloroquinoline-3yl)-1 (pyridine-2yl)prop-2-en-1-one (**18**)*

Yield 89% (Ethyl acetate); mp: 248 °C; Anal. calc. for $C_{17}H_{11}N_2OCl$: C 69.28, H 3.76, N 9.50%; found: C 69.24, H 3.72, N 9.47%. IR ν_{max} (cm^{-1}): 1653 (C=O), 1566 (C=C); ^{1}H NMR ($CDCl_3$) δ (ppm): 8.78 (d, 1H, J = 4.2 Hz, pyridine), 8.67 (s, 1H, H_4 quinoline), 8.42 (d, 1H, J = 15.9 Hz, H_β), 8.35 (d, 1H, J = 2.4 Hz, pyridine), 8.26 (d, 1H, J = 7.5 Hz, H_5 quinoline), 8.05–7.76 [m, 3H, (1H pyridine, H_6 H_8 quinoline)], 7.63–7.58 [m, 2H, (1H pyridine, H_7 quinoline)], 7.55 (d, 1H, J = 15.9 Hz, H_α), ^{13}C NMR ($CDCl_3$) δ (ppm): 188.6 (C=O), 150.9 (C–Cl), 148.1 (C-β), 139.9, 137.3, 128.2, 127.8, 125.3 (Ar–C), 124.4 (C-α); FAB-MS (m/z): [M^++1] 295.13.

6.3. In vitro antiamoebic assay

All the compounds (**4**–**18**) were screened *in vitro* for anti-amoebic activity against HM1:IMSS strain of *E. histolytica* by microdilution method [30]. *E. histolytica* trophozoites were cultured in a 96-well microtiter plate suspended in Diamond TYIS-33 growth medium [35]. The test compounds (1 mg) were dissolved in DMSO (40 μL, concentration at which no inhibition of amoeba growth occurred) [27,36]. The stock solutions (1 mg/mL) of the compounds were freshly prepared and twofold serial dilutions were made in the wells of a 96-well microtiter plate. The following controls were included in each plate: metronidazole as a standard amoebicidal drug, control wells (culture medium plus amoebae) and a blank (culture medium only). All the experiments were carried out in triplicate at each concentration and repeated thrice. The amoeba suspension was prepared from a confluent culture by

pouring off the medium at 37 °C and adding 5 mL of fresh medium, chilling the culture tube on ice to detach the organisms from the side of the flask. The number of amoeba/mL was estimated with a haemocytometer, using the Trypan blue exclusion assay to confirm viability. The suspension was diluted to 10^5 organism per mL in fresh medium and 170 μL of this suspension was added to the test and control wells in the plate such that an inoculum of 1.7×10^4 organisms/well was achieved to ensure confluency but no excessive growth in control wells. Plates were sealed and gassed for 10 min with nitrogen before incubation at 37 °C for 72 h. After incubation, the growth of amoeba in the plate was checked with a low power microscope. The culture medium was removed by inverting the plate and shaking gently. The plate was then immediately washed with prewarmed (37 °C) 0.9% (w/v) sodium chloride solution. This procedure was completed as quickly as possible to ensure the plate did not cool, in order to prevent the detachment of amoebae. The plate was allowed to dry at room temperature and the amoebae were fixed with chilled (−20 °C) 100% methanol and when dried, stained with 0.5% aqueous eosin for 15 min. The stained plate was washed 3 times with distilled water and allowed to dry before 200 μL 0.1 N sodium hydroxide was added to each well to dissolve the protein and release the dye. The optical density of the resulting solution was determined at 490 nm with a microplate reader. The % inhibition of amoebal growth was calculated taking into account the controls and then plotted against the logarithm of the compound concentration. Linear regression analysis was used to determine the best fitting line from which the IC_{50} value was found (Table 1).

6.3.1. In vitro antimalarial assay

Antimalarial activity of the compounds, against the chloroquine-sensitive (3D7) strain of *P. falciparum*, was performed using the [^{3}H]-hypoxanthine-incorporation assay [37]. The 3D7 strain was continuously maintained *in vitro* in supplemented RPMI-1640 culture media and at a haematocrit of 5%. The culture was incubated at 37 °C in a gaseous atmosphere of 5% CO_2, 3% O_2, 92% N_2 [38] and synchronized at the ring stage with 5% D-sorbitol [39] before being adjusted to a final parasitemia of 0.5% and haematocrit of 1%. This suspension (200 μL) was added to each well of the 96-well plate with the exception of some wells which received non-parasitized red blood cells. Stock solutions of the test compounds were made up in DMSO and serially diluted in a 96-well microtiter plate [37]. The microtiter plate was then incubated for 24 h. Following the incubation period, 25 μL of the radiolabeled [^{3}H]-hypoxanthine isotope (Amersham) at a concentration of 0.5 μCi/well was added to each well. The microtiter plate was then incubated for a further 24 h. The parasitic DNA was harvested onto glass fibre filter mats by use of a Titertek™ semi-automatic cell harvester. The mats were then transferred to sample bags containing scintillation fluid (Perkin–Elmer) and the β-radioactivity counted on the Wallac 1205 Betaplate scintillation counter. The counts per minute (cpm) were generated and the parasite survival rate calculated. The concentration required to inhibit parasite growth by 50% (IC_{50} value) was determined from log sigmoid dose-response curves using the Enzfitter® software. Chloroquine and quinine were used as reference agents. Each experiment was repeated, at least, in triplicate.

6.3.2. Combination study

The antagonistic, synergistic or additive effect of the compound exhibiting the most promising antimalarial activity and quinine were determined by using the tritiated hypoxanthine incorporation assay and constructing isobolograms. This involved preparing various ratios of the two drugs (9:1, 8:2, 7:3, 6:4, 5:5, 4:6, 3:7, 2:8 and 1:9) from which serial dilutions were prepared and from each combination, an IC_{50} value was obtained. The IC_{50} values were used to construct an isobologram from which the type of interaction could be determined [40,41]. Each experiment was repeated, at least, in triplicate.

6.4. Inhibition of β-haemozoin formation assay

To determine whether the compounds had a similar mechanism of action to that of chloroquine, the following were combined in a 96-well microtiter plate: 12.5 μL of the test compound, 12.5 μL of a 1 mg/mL haemin (Sigma) solubilised in DMSO, 25 μL H_2O and finally 50 μl of a 0.5M acetate buffer. The acetate buffer was utilized to simulate the acidic conditions (pH 4.7) of the parasitic food vacuole. The plates were then incubated for 24 h and 100 μL of the solution removed and the same volume substituted with DMSO, the plates were then centrifuged at 1500 g for 10 min. This was repeated 3 times to remove any unreacted haemin. Following this, 100 μL was removed and substituted with a 2M NaOH solution to dissolve the β-haematin crystals. The solution was diluted twofold and the absorbance read at 405 nm [42]. From the data obtained the concentration at which β-haematin formation was inhibited by 50% (IC_{50} value) was determined by use of Enzfitter® software. Classic antimalarials, such as quinine and chloroquine, were used as positive control. Each experiment was repeated, at least, in triplicate.

6.5. DPPH• assay

The 2,2-diphenyl-1-picrylhydrazyl (DPPH•) assay was used to measure the ability of the compounds to scavenge the stable free radical of DPPH• in comparison to ascorbic acid. DPPH• (100 μL) dissolved in HPLC grade methanol, was added along with 25 μL of the compounds to a 96-well microtiter plate. Controls included a drug-free DPPH• control and a background control consisting of MeOH and DMSO. The plate was then incubated in the dark at room temperature for 30 min before the absorbance read at 540 nm. The DPPH• scavenging activity of the compounds were expressed as the percentage decrease in the absorbance compared with the drug-free DPPH• control. Each experiment was triplicated.

6.6. Cytotoxicity assays

6.6.1. MTT assay

MCF-7 cells were cultured and maintained as a monolayer in Dulbecco's modified Eagle's medium (DMEM, Sigma) supplemented with 10% of fetal calf serum (Sigma) and antibiotics (100 IU/mL of penicillin and 100 μg/mL of streptomycin, Sigma). All cells were cultured at 37 °C in a 100% humidity atmosphere and 5% CO_2 [43]. Exponentially growing viable cells were plated at 1.2×10^4 cells per well into 96-well plates and incubated for 48 h before the addition of the compounds/metronidazole. Stock solutions of compounds were initially dissolved in 20% (v/v) DMSO and further diluted with fresh complete medium. The growth-inhibitory effects of the compounds were measured using standard tetrazolium MTT assay. After 48 h of incubation at 37 °C, the medium was removed and 25 μL of MTT (5 mg/mL) in serum free medium was added to each well. The plates were incubated at 37 °C for 4 h. At the end of the incubation period, the medium was removed and 100 μL DMSO added to all wells. The metabolized MTT product dissolved in DMSO was quantified by reading the absorbance at 570 nm with a reference wavelength of 655 nm in an ELISA plate reader (Labsystems Multiskan RC, Helsinki, Finland). All assays were performed in triplicate. Percent viability was defined as the relative absorbance of treated versus untreated control cells.

6.6.2. Red blood cell toxicity assay

The haemolytic activities of the compounds were evaluated in comparison to the standard antimalarial agents, chloroquine and quinine as well as metronidazole [44]. A suspension of fresh human red blood cells was adjusted to a 1% haematocrit in culture media and plated together with each test compound (100 μM).This suspension was incubated for 48 h before the absorbance was read at 412 nm. The % haemolysis was calculated using a 0.5% Triton X100 solution as the 100% haemolytic control. These results were used to generate a log sigmoid dose-response curve to calculate IC_{50} values and the mean ± s.d. were calculated from at least triplicate values.

Acknowledgements

This work was supported by Council of Scientific and Industrial Research (grant # 01(2278)/08/EMR-II New Delhi, India) and the Medical Faculty Research Endowment Fund of the University of the Witwatersrand, South Africa. We would like to acknowledge the financial support for F. Hayat from the University Grant Commission (UGC), India and E. Moseley from the National Research Fund (South Africa), Belgium Technical Cooperation and the University of the Witwatersrand.

References

[1] J.F. Turrens, Mol. Apects. Med. 25 (2004) 211–220.
[2] C. Ximenez, P. Moran, L. Rojas, A. Valadez, A. Gomez, Infect. Genet. Evol. 9 (2009) 1023–1032.
[3] S.L. Stanley Jr., Lancet. 361 (2003) 1025–1034.
[4] R. Haque, C.D. Huston, M. Hughes, E. Houpt, W.A. Petri Jr., New Engl. J. Med. 348 (2003) 1565–1573.
[5] O. Hecht, N.A. van Nuland, K. Schleinkofer, A.J. Dingley, H. Bruhn, M. Leippe, J.G. Rotzinger, J. Biol. Chem. 279 (2004) 17834–17841.
[6] M. Rustia, P. Shubik, J. Natl. Cancer Inst. 48 (1972) 721–729.
[7] F.A. el-Nahas, M.I. el-Ashmawy, Basic Clin. Pharmacol. Toxicol. 94 (2004) 226–231.
[8] V. Purohit, K.A. Basu, Chem. Res. Toxicol. 13 (2000) 673–692.
[9] P. Abboud, V. Lemee, G. Gargala, P. Brasseur, J.J. Ballet, F. Borsa-Lebas, F. Caron, L. Favennec, Clin. Infect. Dis. 32 (2001) 1792–1794.
[10] W. Petri, Trends Parasitol. 19 (2003) 523–526.
[11] W. White, J. Clin. Invest. 113 (2004) 1084–1092.
[12] A. Kumar, N. Valecha, T. Jain, A.P. Dash, Am. J. Trop. Med. Hyg. 77 (2007) 69–78.
[13] E.M. Malkin, D.J. Diemert, J.H. McArthur, P.R. Perreault, Infect. Immun. 73 (2005) 3677–3685.
[14] N. Mishra, P. Arora, B. Kumar, Eur. J. Med. Chem. 43 (2008) 1530–1535.
[15] J.N. Dominguez, C. Leon, J. Rodrigues, N.G. de Dominguez, J. Gut, P.J. Rosenthal, Eur. J. Med. Chem. (2008) 1–6.
[16] J.P. Mallari, W.A. Guigemde, R.K. Guy, Bioorg. Med. Chem. Lett. 19 (2009) 3546–3549.
[17] P. Venkatesan, S. Sumathi, J. Heterocycl. Chem. 47 (2009) 81–84.
[18] B.P. Bandgar, S.S. Gawande, R.G. Bodade, J.V. Totre, C.N. Khobragade, Bioorg. Med. Chem. 18 (2010) 1364–1370.
[19] R.H. Hans, E.M. Guantai, C. Lategan, P.J. Smith, B. Wan, S.G. Franzblau, J. Gut, P.J. Rosenthal, K. Chibale, Bioorg. Med. Chem. Lett. 20 (2010) 942–944.
[20] V. Tomar, G. Bhattacharjee, Kamaluddin, S. Rajakumar, K. Srivastava, S.K. Puri, Eur. J. Med. Chem. 45 (2010) 745–751.
[21] S.N. Suryawanshi, N. Chandra, P. Kumar, J. Porwal, S. Gupta, Eur. J. Med. Chem. 43 (2008) 2473–2478.
[22] P.M.S. Chauhan, S.K. Srivastava, Curr. Med. Chem. 8 (2001) 1535–1542.
[23] S. Singh, N. Bharti, P.P. Mohapatra, Chem. Rev. 109 (2009) 1900–1947.
[24] S. Gemma, G. Kukreja, C. Fattorusso, M. Persico, M. Romano, M. Altarelli, L. Savini, G. Campiani, E. Fattorusso, N. Basilico, Bioorg. Med. Chem. Lett. 16 (2006) 5384–5388.
[25] L. Savini, L. Chiasserini, A. Gaeta, C. Pellerano, Bioorg. Med. Chem. 10 (2002) 2193–2198.
[26] A. Nayyar, A. Malde, E. Coutinho, R. Jain, Bioorg. Med. Chem. 14 (2006) 7302–7310.
[27] A.T. Keene, A. Harris, J.D. Phillipson, D.C. Warhurst, Planta Med. 52 (1986) 278–284.
[28] K.H. Chikhalia, M.J. Patel, D.B. Vashi, Arkivoc xiii (2008) 189–197.
[29] M. Azad, M.A. Munawar, H.L. Siddiqui, J. Appl. Sci. 7 (2007) 2485–2489.
[30] C.W. Wright, M.J. O'Neill, J.D. Phillipson, D.C. Warhurst, Antimicrobial. Agents Chemother. 32 (1988) 1725–1729.
[31] J.N. Dominguez, C. Leon, J. Rodrigues, N.G. Dominguez, J. Gut, P.J. Rosenthal, Eur. J. Med. Chem. 44 (2009) 1457–1462.
[32] O. Meth–Cohn, B. Narine, Tetrahedron Lett. 23 (1978) 2045–2048.
[33] B.S. Furnis, A.J. Hannaford, P.W.G. Smith, A.R. Tatchell, Textbook of Practical Organic Chemistry (Vogel's), fifth ed. (1989) Great Britain916–917.
[34] J.N. Dominguez, J.E. Charris, G. Lobo, N.G. de Dominguez, M.M. Moreno, F. Riggione, E. Sanchez, J. Olson, P.J. Rosenthal, Eur. J. Med. Chem. 36 (2001) 555–560.
[35] L.S. Diamond, D.R. Harlow, C.C.R. Cunnick, Trans. R. Soc. Trop. Med. Hyg. 72 (1978) 431–432.
[36] F.D. Gillin, D.S. Reiner, M. Suffness, Antimicrob. Agents Chemother. 22 (1982) 342–345.
[37] R.E. Desjardins, C.J. Canfield, J.D. Haynes, J.D. Chulay, Antimicrob. Agents Chemother. 16 (1979) 710–718.
[38] J.A. Freese, B.L. Sharp, F.C. Ridl, M.B. Markus, S. Afr. Med. J. 73 (1988) 720–722.
[39] C. Lambros, J.P. Vanderberg, J. Parasitol. 65 (1979) 418–420.
[40] A. Bell, FEMS Microbiol. Lett. 253 (2005) 171–184.
[41] M.C. Berenbaum, J. Infect. Dis. 137 (1978) 122–130.
[42] S.M. Chemaly, C.-T. Chen, R.L. van Zyl, J. Inorg. Biochem. 101 (2007) 764–773.
[43] F. Gümüş Ö, G. AlgülEren, H. Eroğlu, N. Diril, S. Gür, A.Ö zkul, Eur. J. Med. Chem. 38 (2003) 473–480.
[44] P. Sharma, J.D. Sharma, J. Ethnopharmacol. 74 (2001) 239–243.

APPENDIX B: BIOSAFETY AND ETHICAL CLEARANCES

APPENDIX B1:

PARASITE BIOSAFETY CLEARANCE

UNIVERSITY OF THE WITWATERSRAND, JOHANNESBURG
Research Office

INSTITUTIONAL BIOSAFETY COMMITTEE
(R 14/16)

CLEARANCE CERTIFICATE - RENEWAL **PROTOCOL NUMBER: 20090503**

BRIEF DESCRIPTION OF APPLICATION:

Chemotherapeutic properties of novel synthetic and natural compounds

APPLICANT: Dr R van Zyl

SCHOOL/DEPARTMENT : Pharmacy/Pharmacology

DATE CONSIDERED: 20090528

DECISION OF COMMITTEE:

Renewal approved

This clearance certificate expires on 20110501 and may be renewed on presentation of a progress report.

DATE: 20100504 **CHAIRPERSON:** _____
(Professor C Tiemessen)

DECLARATION BY APPLICANT:

To be completed in duplicate and **one copy** returned to the Secretary, Room 10004, 10th floor, Senate House, University.

1. I have read, understood and accepted the approval conditions above
2. I agree to submit a yearly progress report to the Committee and to submit an interim report in the event of any significant unforeseen event, e.g. suspension of a drug trial, temporary closure or relocation of my laboratory, etc
3. I note that the University Safety Officer, or his/her representative, may at any reasonable time inspect my laboratory or trial site to ensure compliance with current Health and Safety legislation. I undertake to offer my full co-operation in any such inspection.
4. I have read, understood and will comply with the *recommended standard operating procedures for the handling of biohazardous materials* posted at http://web.wits.ac.za/Academic/Research/Biosafety.htm
5. I declare (delete as appropriate) that:
   a. I have all the approvals required by statute or regulation and by the funding agencies supporting this work, or
   b. that I will not begin work until such approvals are obtained

Signed: _____ Date: _____

MSWorks2000/Iain0015/IBCClearRenew.wps

PLEASE QUOTE THE PROTOCOL NUMBER IN ALL ENQUIRIES

***Ethical clearance was renewed in 2011 for a further five years.

APPENDIX B2:

ETHICAL CLEARANCE FOR THE DRAWING OF BLOOD FROM VOLUNTEERS

UNIVERSITY OF THE WITWATERSRAND, JOHANNESBURG

Division of the Deputy Registrar (Research)

HUMAN RESEARCH ETHICS COMMITTEE (MEDICAL)
R14/49 Dr Robyn L van Zyl

CLEARANCE CERTIFICATE	**M090532**
PROJECT	The Chemotherapeutic Properties of Novel Synthetic and natural Compounds (Blanket Approval)
INVESTIGATORS	Dr Robyn L van Zyl.
DEPARTMENT	Department of Pharmacy & Pharmacology
DATE CONSIDERED	09.05.29
DECISION OF THE COMMITTEE*	Approved unconditionally

Unless otherwise specified this ethical clearance is valid for 5 years and may be renewed upon application.

DATE 09.05.29 **CHAIRPERSON** .....
(Professor P E Cleaton Jones)

*Guidelines for written 'informed consent' attached where applicable

cc: Supervisor : Dr RL van Zyl

DECLARATION OF INVESTIGATOR(S)

To be completed in duplicate and **ONE COPY** returned to the Secretary at Room 10004, 10th Floor, Senate House, University.
I/We fully understand the conditions under which I am/we are authorized to carry out the abovementioned research and I/we guarantee to ensure compliance with these conditions. Should any departure to be contemplated from the research procedure as approved I/we undertake to resubmit the protocol to the Committee. **I agree to a completion of a yearly progress report.**

PLEASE QUOTE THE PROTOCOL NUMBER IN ALL ENQUIRIES...
.....

APPENDIX C: SUM OF THE FRACTIONAL INHIBITORY CONCENTRATIONS (FIC_{50}) FOR COMBINATION STUDIES WITH COMPOUNDS Y-3 AND Y-7

Table C1: Sum of FIC_{50} values for compound Y-3 in combination with quinine. Experiment 1.

Combination ratio's		IC_{50} values				FIC_{50} values		ΣFIC_{50} values
Y-3	**Quinine**	**Y-3**	**s.d.**	**Quinine**	**s.d.**	**Y-3**	**Quinine**	
10	0	3.14	0.26	0	-	1	0	
9	1	3.65	0.16	0.02	-	1.16	0.13	1.29
8	2	3.16	0.04	0.04	-	1.01	0.26	1.27
7	3	2.12	0.19	0.046	-	0.68	0.30	0.98
6	4	1.83	0.10	0.06	-	0.58	0.41	0.99
5	5	1.25	0.09	0.062	-	0.40	0.41	0.81
4	6	1.39	0.20	0.10	-	0.44	0.69	1.13
3	7	0.98	0.13	0.11	-	0.31	0.76	1.07
2	8	0.55	0.19	0.11	-	0.18	0.73	0.91
1	9	0.30	0.10	0.13	-	0.095	0.89	0.99
0	10	0	-	0.15	0.033	0	1	
			SUM	**9.44**	**AVE**	**1.05**	**s.d.**	**0.16**

Table C2: Sum of FIC_{50} values for compound Y-3 in combination with quinine. Experiment 2.

Combination ratio's		IC_{50} values				FIC_{50} values		ΣFIC_{50} values
Y-3	**Quinine**	**Y-3**	**s.d.**	**Quinine**	**s.d.**	**Y-3**	**Quinine**	
10	0	1.33	0.10	0	-	1	0	
9	1	1.33	0.03	0.0074	-	1	0.13	1.13
8	2	1.17	0.017	0.015	-	0.88	0.26	1.14
7	3	0.88	0.02	0.019	-	0.67	0.34	1.01
6	4	0.89	0.04	0.030	-	0.67	0.53	1.2
5	5	0.69	0.03	0.034	-	0.52	0.61	1.13
4	6	0.54	0.07	0.041	-	0.41	0.72	1.13
3	7	0.39	0.02	0.046	-	0.29	0.81	1.1
2	8	0.28	0.02	0.055	-	0.21	0.98	1.19
1	9	0.14	0.01	0.062	-	0.10	1.10	1.2
0	10	0	-	0.056	0.0046	0	1	
			SUM	**10.23**	**AVE**	**1.14**	**s.d.**	**0.06**

Table C3: Sum of FIC_{50} values for compound Y-3 in combination with quinine. Experiment 3.

Combination ratio's		IC_{50} values				FIC_{50} values		ΣFIC_{50} values
Y-3	**Quinine**	**Y-3**	**s.d.**	**Quinine**	**s.d.**	**Y-3**	**Quinine**	
10	0	0.98	0.041	0	-	1	0	
9	1	0.83	0.013	0.0046	-	0.85	0.15	1
8	2	0.81	0.015	0.010	-	0.82	0.33	1.15
7	3	0.69	0.012	0.015	-	0.70	0.48	1.19
6	4	0.62	0.016	0.021	-	0.64	0.68	1.32
5	5	0.46	0.011	0.023	-	0.47	0.76	1.23
4	6	0.37	0.035	0.028	-	0.37	0.90	1.27
3	7	0.26	0.019	0.030	-	0.26	0.99	1.25
2	8	0.17	0.013	0.033	-	0.17	1.08	1.25
1	9	0.084	0.0074	0.038	-	0.09	1.23	1.31
0	10	0	-	0.031	0.0018	0.00	1.00	
			SUM	**10.98**	**AVE**	**1.22**	**s.d.**	**0.098**

Table C4: Sum of FIC_{50} values for compound Y-7 in combination with quinine. Experiment 1.

Combination ratio's		IC_{50} values				FIC_{50} values		ΣFIC_{50} values
Y-7	**Quinine**	**Y-7**	**s.d.**	**Quinine**	**s.d.**	**Y-7**	**Quinine**	
10	0	4.44	0.46	0	-	1	0	
9	1	3.42	0.101	0.011	-	0.77	0.26	1.03
8	2	2.69	0.057	0.017	-	0.61	0.41	1.02
7	3	2.54	0.15	0.027	-	0.57	0.67	1.24
6	4	1.99	0.075	0.033	-	0.45	0.82	1.27
5	5	1.61	0.11	0.040	-	0.36	0.99	1.36
4	6	0.92	0.14	0.034	-	0.21	0.85	1.05
3	7	0.62	0.018	0.036	-	0.14	0.89	1.03
2	8	0.45	0.031	0.045	-	0.10	1.11	1.22
1	9	0.21	0.011	0.048	-	0.05	1.18	1.22
0	10	0	-	0.0406	0.0027	0	1	
			SUM	**10.44**	**AVE**	**1.16**	**s.d.**	**0.13**

Table C5: Sum of FIC_{50} values for compound Y-7 in combination with quinine. Experiment 2.

Combination ratio's		IC_{50} values				FIC_{50} values		ΣFIC_{50} values
Y-7	**Quinine**	**Y-7**	**s.d.**	**Quinine**	**s.d.**	**Y-7**	**Quinine**	
10	0	3.54	0.12	0	-	1	0	
9	1	3.33	0.095	0.0093	-	0.94	0.33	1.27
8	2	2.90	0.14	0.018	-	0.82	0.64	1.47
7	3	1.85	0.083	0.020	-	0.52	0.70	1.22
6	4	1.45	0.065	0.024	-	0.41	0.86	1.27
5	5	1.15	0.035	0.029	-	0.32	1.02	1.34
4	6	0.83	0.051	0.031	-	0.24	1.11	1.35
3	7	0.61	0.031	0.036	-	0.17	1.27	1.44
2	8	0.39	0.021	0.039	-	0.11	1.40	1.51
1	9	0.18	0.015	0.041	-	0.05	1.44	1.49
0	10	0	-	0.028	0.00072	0	1	
			SUM	**12.36**	**AVE**	**1.37**	**s.d.**	**0.11**

Table C6: Sum of FIC_{50} values for compound Y-7 in combination with quinine. Experiment 3.

Combination ratio's		IC_{50} values				FIC_{50} values		ΣFIC_{50} values
Y-7	**Quinine**	**Y-7**	**s.d.**	**Quinine**	**s.d.**	**Y-7**	**Quinine**	
10	0	2.70	0.049	0	-	1	0	
9	1	2.33	0.50	0.0065	-	0.86	0.16	1.02
8	2	2.28	0.031	0.014	-	0.84	0.34	1.19
7	3	1.51	0.073	0.016	-	0.56	0.39	0.95
6	4	1.29	0.057	0.022	-	0.48	0.52	1.00
5	5	0.98	0.044	0.024	-	0.36	0.59	0.95
4	6	0.88	0.074	0.033	-	0.32	0.80	1.12
3	7	0.72	0.024	0.042	-	0.27	1.02	1.28
2	8	0.43	0.02	0.043	-	0.16	1.05	1.21
1	9	0.22	0.017	0.049	-	0.08	1.18	1.26
0	10	0	-	0.041	0.0013	0	1	
			SUM	**9.97**	**AVE**	**1.11**	**s.d.**	**0.13**

Table C7: Sum of FIC_{50} values for compound Y-3 in combination with dihydroartemisinin (DA). Experiment 1.

Combination ratio's		IC_{50} values				FIC_{50} values		ΣFIC_{50} values
Y-3	**DA**	**Y-3**	**s.d.**	**DA**	**s.d.**	**Y-3**	**DA**	
10	0	1.62	0.05	0	-	1	0	
9	1	1.75	0.084	0.00013	-	1.08	0.19	1.27
8	2	1.55	0.068	0.00026	-	0.96	0.37	1.33
7	3	1.11	0.077	0.00032	-	0.69	0.46	1.14
6	4	0.94	0.034	0.00042	-	0.58	0.61	1.19
5	5	0.77	0.045	0.00051	-	0.48	0.74	1.22
4	6	0.66	0.067	0.00066	-	0.41	0.96	1.36
3	7	0.40	0.0073	0.00062	-	0.25	0.90	1.15
2	8	0.24	0.012	0.00064	-	0.15	0.93	1.08
1	9	0.12	0.011	0.00072	-	0.07	1.04	1.12
0	10	0	-	0.00069	0.000033	0	1	
			SUM	**10.86**	**AVE**	**1.21**	**s.d.**	**0.098**

Table C8: Sum of FIC_{50} values for compound Y-3 in combination with dihydroartemisinin (DA). Experiment 2.

Combination ratio's		IC_{50} values				FIC_{50} values		ΣFIC_{50} values
Y-3	**DA**	**Y-3**	**s.d.**	**DA**	**s.d.**	**Y-3**	**DA**	
10	0	3.51	0.1	0	-	1	0	
9	1	3.88	0.24	0.00029	-	1.11	0.18	1.29
8	2	3.48	0.15	0.00058	-	0.99	0.37	1.36
7	3	3.34	0.19	0.00095	-	0.95	0.61	1.56
6	4	2.56	0.029	0.0011	-	0.73	0.73	1.46
5	5	2.16	0.037	0.0014	-	0.62	0.92	1.54
4	6	1.38	0.037	0.0014	-	0.39	0.88	1.28
3	7	0.98	0.0046	0.0015	-	0.28	0.98	1.26
2	8	0.67	0.019	0.0018	-	0.19	1.15	1.34
1	9	0.29	0.0049	0.0017	-	0.08	1.12	1.20
0	10	0	-	0.00156	0.021	0	1	
			SUM	**12.28**	**AVE**	**1.36**	**s.d.**	**0.13**

Table C9: Sum of FIC_{50} values for compound Y-3 in combination with dihydroartemisinin (DA). Experiment 3.

Combination ratio's		IC_{50} values				FIC_{50} values		ΣFIC_{50} values
Y-3	**DA**	**Y-3**	**s.d.**	**DA**	**s.d.**	**Y-3**	**DA**	
10	0	1.69	0.11	0	-	1	0	
9	1	1.96	0.055	0.00022	-	1.16	0.32	1.48
8	2	1.34	0.06	0.00034	-	0.79	0.49	1.28
7	3	1.07	0.042	0.00046	-	0.63	0.67	1.30
6	4	0.86	0.028	0.00057	-	0.51	0.83	1.34
5	5	0.59	0.034	0.00059	-	0.35	0.86	1.20
4	6	0.47	0.0069	0.00071	-	0.28	1.03	1.31
3	7	0.33	0.0052	0.00077	-	0.20	1.12	1.31
2	8	0.20	0.0042	0.00079	-	0.12	1.14	1.26
1	9	0.087	0.001	0.00078	-	0.05	1.13	1.19
0	10	0	-	0.00069	0.000027	0	1	
			SUM	**11.67**	**AVE**	**1.30**	**s.d.**	**0.084**

Table C10: Sum of FIC_{50} values for compound Y-7 in combination with dihydroartemisinin (DA). Experiment 1.

Combination ratio's		IC_{50} values				FIC_{50} values		ΣFIC_{50} values
Y-7	**DA**	**Y-7**	**s.d.**	**DA**	**s.d.**	**Y-7**	**DA**	
10	0	5.98	0.26	0	-	1	0	
9	1	8.68	0.48	0.00022	-	1.45	0.14	1.59
8	2	5.85	0.18	0.00044	-	0.98	0.28	1.26
7	3	5.35	0.17	0.00072	-	0.89	0.46	1.35
6	4	3.68	0.14	0.00085	-	0.62	0.55	1.16
5	5	2.5	0.052	0.0011	-	0.42	0.69	1.11
4	6	2.15	0.074	0.0010	-	0.36	0.66	1.02
3	7	1.53	0.027	0.0011	-	0.26	0.73	0.99
2	8	0.96	0.004	0.0013	-	0.16	0.86	1.02
1	9	0.4	0.005	0.0013	-	0.07	0.84	0.90
0	10	0	-	0.00156	0.000049	0	1	
			SUM	**10.41**	**AVE**	**1.16**	**s.d.**	**0.21**

Table C11: Sum of FIC_{50} values for compound Y-7 in combination with dihydroartemisinin (DA). Experiment 2.

Combination ratio's		IC_{50} values				FIC_{50} values		ΣFIC_{50} values
Y-7	**DA**	**Y-7**	**s.d.**	**DA**	**s.d.**	**Y-7**	**DA**	
10	0	6.77	0.15	0	-	1	0	
9	1	5.93	0.091	0.00033	-	0.88	0.39	1.26
8	2	4.04	0.018	0.00051	-	0.60	0.60	1.19
7	3	2.96	0.049	0.00063	-	0.44	0.75	1.19
6	4	2.1	0.066	0.0007	-	0.31	0.83	1.14
5	5	1.47	0.059	0.00074	-	0.22	0.87	1.09
4	6	0.94	0.052	0.00070	-	0.14	0.83	0.97
3	7	0.61	0.0089	0.00071	-	0.09	0.84	0.93
2	8	0.35	0.012	0.00069	-	0.05	0.82	0.87
1	9	0.20	0.007	0.00088	-	0.03	1.04	1.07
0	10	0	-	0.00085	0.000031	0	1	
			SUM	**9.71**	**AVE**	**1.08**	**s.d.**	**0.13**

Table C12: Sum of FIC_{50} values for compound Y-7 in combination with dihydroartemisinin (DA). Experiment 3.

Combination ratio's		IC_{50} values				FIC_{50} values		ΣFIC_{50} values
Y-7	**DA**	**Y-7**	**s.d.**	**DA**	**s.d.**	**Y-7**	**DA**	
10	0	3.7	0.17	0	-	1	0	
9	1	3.29	0.097	0.00018	-	0.89	0.30	1.19
8	2	2.54	0.16	0.00032	-	0.69	0.52	1.21
7	3	1.59	0.074	0.00034	-	0.43	0.56	0.99
6	4	1.62	0.081	0.00054	-	0.44	0.89	1.32
5	5	1.11	0.043	0.00056	-	0.30	0.91	1.21
4	6	0.79	0.031	0.00059	-	0.21	0.97	1.19
3	7	0.58	0.022	0.00068	-	0.16	1.11	1.27
2	8	0.37	0.031	0.00074	-	0.10	1.21	1.31
1	9	0.14	0.009	0.00063	-	0.04	1.03	1.07
0	10	0	-	0.00061	0.000012	0	1	
			SUM	**10.75**	**AVE**	**1.19**	**s.d.**	**0.11**

APPENDIX D: SUM OF THE FRACTIONAL INHIBITORY CONCENTRATIONS (FIC_{50}) FOR COMBINATION STUDIES WITH COMPOUND F-13 AND QUININE

Table D1: Sum of FIC_{50} values for compound F-13 in combination with quinine. Experiment 1.

Combination ratio's		IC_{50} values				FIC_{50} values		ΣFIC_{50} values
F-13	**Quinine**	**F-13**	**s.d.**	**Quinine**	**s.d.**	**F-13**	**Quinine**	
10	0	37.12	1.71	0	-	1	0	
9	1	42.78	2.48	0.014	-	1.15	0.22	1.37
8	2	35.03	1.2	0.027	-	0.94	0.40	1.34
7	3	27.55	1.72	0.036	-	0.74	0.53	1.28
6	4	21.7	1.03	0.044	-	0.58	0.65	1.24
5	5	13.23	1.55	0.040	-	0.36	0.60	0.96
4	6	12.78	1.43	0.058	-	0.34	0.87	1.21
3	7	10.21	1.49	0.072	--	0.28	1.08	1.35
2	8	6.49	1.17	0.079	-	0.17	1.18	1.35
1	9	3.49	0.73	0.095	-	0.09	1.42	1.52
0	10	0	-	0.067	0.011	0	1	
			SUM	**11.61**	**AVE**	**1.29**	**s.d.**	**0.15**

Table D2: Sum of FIC_{50} values for compound F-13 in combination with quinine. Experiment 2.

Combination ratio's		IC_{50} values				FIC_{50} values		ΣFIC_{50} values
F-13	**Quinine**	**F-13**	**s.d.**	**Quinine**	**s.d.**	**F-13**	**Quinine**	
10	0	33.91	4.38	0	-	1	0	
9	1							
8	2	43.89	3.83	0.033	-	1.29	0.50	1.80
7	3	34.73	1.66	0.045	-	1.02	0.68	1.71
6	4	26.33	0.93	0.053	-	0.78	0.80	1.58
5	5	18.39	1.48	0.056	-	0.54	0.84	1.38
4	6	12.98	2.41	0.059	-	0.38	0.89	1.27
3	7	10.53	2.62	0.074	-	0.31	1.13	1.44
2	8	5.64	1.64	0.068	-	0.17	1.03	1.20
1	9	2.77	0.72	0.076	-	0.08	1.14	1.22
0	10	0	-	0.066	0.013	0	1	
			SUM	**11.60**	**AVE**	**1.45**	**s.d.**	**0.22**

Table D3: Sum of FIC_{50} values for compound F-13 in combination with quinine. Experiment 3.

Combination ratio's		IC_{50} values				FIC_{50} values		ΣFIC_{50} values
F-13	**Quinine**	**F-13**	**s.d.**	**Quinine**	**s.d.**	**F-13**	**Quinine**	
10	0	67.87	2.53	0	-	1	0	
9	1	82.20	2.55	0.028	-	1.21	0.46	1.67
8	2	65.77	1.93	0.050	-	0.97	0.83	1.80
7	3	43.58	2.71	0.057	-	0.64	0.94	1.59
6	4	32.75	2.85	0.066	-	0.48	1.10	1.59
5	5	18.74	2.37	0.057	-	0.28	0.95	1.22
4	6	7.60	3.90	0.035	-	0.11	0.58	0.69
3	7	4.76	1.53	0.034	-	0.07	0.56	0.63
2	8	3.92	1.38	0.048	-	0.06	0.79	0.85
1	9	1.97	0.59	0.054	-	0.03	0.90	0.92
0	10	0	-	0.060	0.0063	0	1	
			SUM	**10.96**	**AVE**	**1.22**	**s.d.**	**0.46**

Table D4: Sum of FIC_{50} values for compound F-13 in combination with quinine. Experiment 4.

Combination ratio's		IC_{50} values				FIC_{50} values		ΣFIC_{50} values
F-13	**Quinine**	**F-13**	**s.d.**	**Quinine**	**s.d.**	**F-13**	**Quinine**	
10	0	46.85	15.87	0	-	1	0	
9	1	36.57	1.82	0.012	-	0.78	0.20	0.98
8	2	40.31	1.49	0.031	-	0.86	0.51	1.37
7	3	25.43	1.44	0.033	-	0.54	0.55	1.09
6	4	20.23	1.05	0.041	-	0.43	0.68	1.11
5	5	15.65	0.88	0.047	-	0.33	0.79	1.12
4	6	19.64	2.06	0.089	-	0.42	1.48	1.90
3	7	15.40	1.93	0.11	-	0.33	1.80	2.13
2	8	8	1.03	0.097	-	0.17	1.61	1.78
1	9	2.82	0.54	0.077	-	0.06	1.27	1.33
0	10	0	-	0.060	0.0088	0	1	
			SUM	**12.80**	**AVE**	**1.42**	**s.d.**	**0.41**

APPENDIX E: SUM OF THE FRACTIONAL INHIBITORY CONCENTRATIONS (FIC_{50}) FOR COMBINATION STUDIES WITH COMPOUNDS DR-4463 AND D1293-S

Table E1: Sum of FIC_{50} values for compound DR-4463 in combination with quinine. Experiment 1.

Combination ratio's		IC_{50} values				FIC_{50} values		ΣFIC_{50} values
DR-4463	Quinine	DR-4463	s.d.	Quinine	s.d.	DR-4463	Quinine	
10	0	33.76	1.45	0	-	1	0	
9	1	25.92	0.18	0.014	-	0.77	0.26	1.03
8	2	19.18	0.38	0.024	-	0.57	0.43	1.00
7	3	13.60	0.44	0.029	-	0.40	0.52	0.93
6	4	11.38	0.37	0.038	-	0.34	0.68	1.02
5	5	8.33	0.40	0.042	-	0.25	0.75	0.99
4	6	5.68	0.24	0.043	-	0.17	0.77	0.93
3	7	3.76	0.19	0.044	-	0.11	0.79	0.90
2	8	2.57	0.18	0.051	-	0.08	0.92	1.00
1	9	1.27	0.12	0.057	-	0.04	1.03	1.06
0	10	0	-	0.056	0.0053	0	1	
			SUM	**8.86**	**AVE**	**0.98**	**s.d.**	**0.054**

Table E2: Sum of FIC_{50} values for compound DR-4463 in combination with quinine. Experiment 2.

Combination ratio's		IC_{50} values				FIC_{50} values		ΣFIC_{50} values
DR-4463	Quinine	DR-4463	s.d.	Quinine	s.d.	DR-4463	Quinine	
10	0	34.67	2.32	0	-	1	0	
9	1	28.59	1.14	0.016	-	0.82	0.10	0.93
8	2	22.08	0.74	0.028	-	0.64	0.18	0.82
7	3	14.15	0.79	0.030	-	0.41	0.20	0.61
6	4	13.27	0.65	0.044	-	0.38	0.29	0.67
5	5	10.63	0.36	0.053	-	0.31	0.35	0.65
4	6	9.36	0.70	0.070	-	0.27	0.46	0.73
3	7	6.66	0.24	0.078	-	0.19	0.51	0.70
2	8	5.30	0.27	0.11	-	0.15	0.69	0.85
1	9	2.87	0.25	0.13	-	0.08	0.85	0.93
0	10	0	-	0.15	0.014	0	1	
			SUM	**6.88**	**AVE**	**0.76**	**s.d.**	**0.12**

Table E3: Sum of FIC_{50} values for compound DR-4463 in combination with quinine. Experiment 3.

Combination ratio's		IC_{50} values				FIC_{50} values		ΣFIC_{50} values
DR-4463	**Quinine**	**DR-4463**	**s.d.**	**Quinine**	**s.d.**	**DR-4463**	**Quinine**	
10	0	33.04	2.11	0	-	1	0	
9	1	25.57	0.8	0.014	-	0.77	0.15	0.93
8	2	20.10	0.29	0.025	-	0.61	0.27	0.88
7	3	15.63	0.92	0.033	-	0.47	0.36	0.83
6	4	13.01	0.33	0.043	-	0.39	0.46	0.86
5	5	10.61	0.41	0.053	-	0.32	0.57	0.89
4	6	8.35	0.42	0.063	-	0.25	0.67	0.92
3	7	6.15	0.16	0.072	-	0.19	0.77	0.96
2	8	4.23	0.18	0.085	-	0.13	0.91	1.04
1	9	2.27	0.16	0.10	-	0.07	1.10	1.16
0	10	0	-	0.093	0.0075	0	1	
			SUM	**8.46**	**AVE**	**0.94**	**s.d.**	**0.10**

Table E4: Sum of FIC_{50} values for compound DR-4463 in combination studies with dipyridamole. Experiment 1.

Concentration ratio's				FIC values		ΣFIC Values
DR-4463	Dipyridamole	DR-4463	Dipyridamole	DR-4463	Dipyridamole	
IC_{90}	-	125 µM	-	1	0	
IC_{50}	-	20 µM	-	1	0	
IC_{10}	-	4 µM	-	1	0	
IC_{90}	IC_{90}			1.07	0.51	1.58
IC_{50}	IC_{90}			0.46	1.14	1.60
IC_{10}	IC_{90}			0.22	0.97	1.19
IC_{90}	IC_{50}			0.79	0.27	1.06
IC_{50}	IC_{50}			1.70	2.96	4.66
IC_{10}	IC_{50}			0.90	2.73	3.63
IC_{90}	IC_{10}			0.85	0.13	0.98
IC_{50}	IC_{10}			1.25	0.97	2.22
IC_{10}	IC_{10}			0.42	0.56	0.98
-	IC_{90}	-	130 µM	0	1	
-	IC_{50}	-	35 µM	0	1	
-	IC_{10}	-	7 µM	0	1	
	SUM	**17.90**	**AVE**	**1.99**	**s.d.**	**1.31**

Table E5: Sum of FIC_{50} values for compound DR-4463 in combination studies with dipyridamole. Experiment 2.

Concentration ratio's				FIC values		ΣFIC Values
DR-4463	Dipyridamole	DR-4463	Dipyridamole	DR-4463	Dipyridamole	
IC_{90}	-	125 µM	-	1	0	
IC_{50}	-	20 µM	-	1	0	
IC_{10}	-	4 µM	-	1	0	
IC_{90}	IC_{90}			1.04	0.47	1.51
IC_{50}	IC_{90}			0.40	1.12	1.52
IC_{10}	IC_{90}			0.31	1.21	1.52
IC_{90}	IC_{50}			1.73	0.39	2.12
IC_{50}	IC_{50}			0.56	0.79	1.35
IC_{10}	IC_{50}			0.64	1.26	1.90
IC_{90}	IC_{10}			1.37	0.21	1.58
IC_{50}	IC_{10}			0.84	0.79	1.63
IC_{10}	IC_{10}			0.78	1.01	1.79
-	IC_{90}	-	130 µM	0	1	
-	IC_{50}	-	35 µM	0	1	
-	IC_{10}	-	7 µM	0	1	
	SUM	**14.92**	**AVE**	**1.66**	**s.d.**	**0.24**

Table E6: Sum of FIC_{50} values for compound DR-4463 in combination studies with dipyridamole. Experiment 3.

Concentration ratio's				FIC values		ΣFIC
DR-4463	Dipyridamole	DR-4463	Dipyridamole	DR-4463	Dipyridamole	Values
IC_{90}	-	125 µM	-	1	0	
IC_{50}	-	20 µM	-	1	0	
IC_{10}	-	4 µM	-	1	0	
IC_{90}	IC_{90}			2.92	1.41	4.33
IC_{50}	IC_{90}			0.27	1.42	1.69
IC_{10}	IC_{90}			0.17	1.31	1.48
IC_{90}	IC_{50}			3.35	0.46	3.81
IC_{50}	IC_{50}			1.22	1.86	3.08
IC_{10}	IC_{50}			1.10	2.43	3.53
IC_{90}	IC_{10}			1.66	0.63	2.29
IC_{50}	IC_{10}			1.01	0.09	1.10
IC_{10}	IC_{10}			1.07	0.98	2.05
-	IC_{90}	-	130 µM	0	1	
-	IC_{50}	-	35 µM	0	1	
-	IC_{10}	-	7 µM	0	1	
	SUM	**23.36**	**AVE**	**2.60**	**s.d.**	**1.13**

Table E7: Sum of FIC_{50} values for compound DR-4463 in combination with dipyridamole. Experiment 4.

Concentration ratio's				FIC values		ΣFIC
DR-4463	Dipyridamole	DR-4463	Dipyridamole	DR-4463	Dipyridamole	Values
IC_{90}	-	125 µM	-	1	0	
IC_{50}	-	20 µM	-	1	0	
IC_{10}	-	4 µM	-	1	0	
IC_{90}	IC_{90}			1.95	0.49	2.44
IC_{50}	IC_{90}			0.75	1.06	1.81
IC_{10}	IC_{90}			0.37	1.05	1.42
IC_{90}	IC_{50}			1.99	0.16	2.15
IC_{50}	IC_{50}			0.90	0.40	1.30
IC_{10}	IC_{50}			1.09	0.97	2.06
IC_{90}	IC_{10}			1.55	0.11	1.66
IC_{50}	IC_{10}			1.21	0.49	1.70
IC_{10}	IC_{10}			1.13	0.90	2.03
-	IC_{90}	-	130 µM	0	1	
-	IC_{50}	-	35 µM	0	1	
-	IC_{10}	-	7 µM	0	1	
	SUM	**16.57**	**AVE**	**1.84**	**s.d.**	**0.36**

Table E8: Sum of FIC_{50} values for compound D1293-S in combination studies with dipyridamole. Experiment 1.

Concentration ratio's				FIC values		ΣFIC
D1293-S	**Dipyridamole**	**D1293-S**	**Dipyridamole**	**D1293-S**	**Dipyridamole**	**Values**
IC_{90}	-	135 µM	-	1	0	
IC_{50}	-	58 µM	-	1	0	
IC_{10}	-	13 µM	-	1	0	
IC_{90}	IC_{90}			0.83	0.73	1.56
IC_{50}	IC_{90}			0.41	1.07	1.48
IC_{10}	IC_{90}			0.28	1.28	1.56
IC_{90}	IC_{50}			0.73	0.46	1.19
IC_{50}	IC_{50}			0.49	0.88	1.37
IC_{10}	IC_{50}			0.42	1.37	1.79
IC_{90}	IC_{10}			0.76	0.21	0.97
IC_{50}	IC_{10}			0.74	0.60	1.34
IC_{10}	IC_{10}			0.83	1.19	2.02
-	IC_{90}	-	130 µM	0	1	
-	IC_{50}	-	35 µM	0	1	
-	IC_{10}	-	7 µM	0	1	
	SUM	**13.28**	**AVE**	**1.48**	**s.d.**	**0.31**

Table E9: Sum of FIC_{50} values for compound D1293-S in combination studies with dipyridamole. Experiment 2.

Concentration ratio's				FIC values		ΣFIC
D1293-S	**Dipyridamole**	**D1293-S**	**Dipyridamole**	**D1293-S**	**Dipyridamole**	**Values**
IC_{90}	-	135 µM	-	1	0	
IC_{50}	-	58 µM	-	1	0	
IC_{10}	-	13 µM	-	1	0	
IC_{90}	IC_{90}			1.07	0.86	1.93
IC_{50}	IC_{90}			0.65	1.16	1.81
IC_{10}	IC_{90}			0.34	1.04	1.38
IC_{90}	IC_{50}			1.15	0.47	1.62
IC_{50}	IC_{50}			0.82	0.74	1.56
IC_{10}	IC_{50}			0.75	1.15	1.9
IC_{90}	IC_{10}			4.29	1.14	5.43
IC_{50}	IC_{10}			1.01	0.60	1.61
IC_{10}	IC_{10}			0.95	0.96	1.91
-	IC_{90}	-	130 µM	0	1	
-	IC_{50}	-	35 µM	0	1	
-	IC_{10}	-	7 µM	0	1	
	SUM	**19.15**	**AVE**	**2.13**	**s.d.**	**1.25**

Table E11: Sum of FIC_{50} values for compound D1293-S in combination studies with dipyridamole. Experiment 3.

Concentration ratio's				FIC values		ΣFIC
D1293-S	**Dipyridamole**	**D1293-S**	**Dipyridamole**	**D1293-**	**Dipyridamole**	**Values**
IC_{90}	-	135 µM	-	1	0	
IC_{50}	-	58 µM	-	1	0	
IC_{10}	-	13 µM	-	1	0	
IC_{90}	IC_{90}			1.33	0.92	2.25
IC_{50}	IC_{90}			0.22	1.08	1.30
IC_{10}	IC_{90}			0.14	1.21	1.35
IC_{90}	IC_{50}			1.89	0.38	2.27
IC_{50}	IC_{50}			1.07	1.52	2.59
IC_{10}	IC_{50}			0.97	2.35	3.32
IC_{90}	IC_{10}			1.20	0.10	1.30
IC_{50}	IC_{10}			1.04	0.61	1.65
IC_{10}	IC_{10}			0.92	0.92	1.84
-	IC_{90}	-	130 µM	0	1	
-	IC_{50}	-	35 µM	0	1	
-	IC_{10}	-	7 µM	0	1	
	SUM	**17.87**	**AVE**	**1.99**	**s.d.**	**0.69**